INFORMATION TO USERS

This manuscript has been reproduced from the microfilm master. UMI films the text directly from the original or copy submitted. Thus, some thesis and dissertation copies are in typewriter face, while others may be from any type of computer printer.

The quality of this reproduction is dependent upon the quality of the copy submitted. Broken or indistinct print, colored or poor quality illustrations and photographs, print bleedthrough, substandard margins, and improper alignment can adversely affect reproduction.

In the unlikely event that the author did not send UMI a complete manuscript and there are missing pages, these will be noted. Also, if unauthorized copyright material had to be removed, a note will indicate the deletion.

Oversize materials (e.g., maps, drawings, charts) are reproduced by sectioning the original, beginning at the upper left-hand corner and continuing from left to right in equal sections with small overlaps.

ProQuest Information and Learning
300 North Zeeb Road, Ann Arbor, MI 48106-1346 USA
800-521-0600

Multi-Dimensional Chromatographic Methods for Polycyclic Aromatic Compounds in Complex Environmental Samples

by

Michael A. Potvin

Submitted in partial fulfillment of the requirements
for the degree of Doctor of Philosophy

Dalhousie University
Halifax, Nova Scotia
August 2002

© Copyright by Michael A. Potvin, 2002

National Library of Canada
Acquisitions and Bibliographic Services
395 Wellington Street
Ottawa ON K1A 0N4
Canada

Bibliothèque nationale du Canada
Acquisitions et services bibliographiques
395, rue Wellington
Ottawa ON K1A 0N4
Canada

Your file Votre référence

Our file Notre référence

The author has granted a non-exclusive licence allowing the National Library of Canada to reproduce, loan, distribute or sell copies of this thesis in microform, paper or electronic formats.

L'auteur a accordé une licence non exclusive permettant à la Bibliothèque nationale du Canada de reproduire, prêter, distribuer ou vendre des copies de cette thèse sous la forme de microfiche/film, de reproduction sur papier ou sur format électronique.

The author retains ownership of the copyright in this thesis. Neither the thesis nor substantial extracts from it may be printed or otherwise reproduced without the author's permission.

L'auteur conserve la propriété du droit d'auteur qui protège cette thèse. Ni la thèse ni des extraits substantiels de celle-ci ne doivent être imprimés ou autrement reproduits sans son autorisation.

0-612-75708-0

Canada

DALHOUSIE UNIVERSITY

FACULTY OF GRADUATE STUDIES

The undersigned hereby certify that they have read and recommend to the Faculty of Graduate Studies for acceptance a thesis entitled "Multi-Dimensional Chromatographic Methods for Polycyclic Aromatic Compounds in Complex Environmental Samples" by Michael Potvin in partial fulfilment for the degree of Doctor of Philosophy.

Dated: September 6, 2002

External Examiner:

Research Supervisor:

Examining Committee:

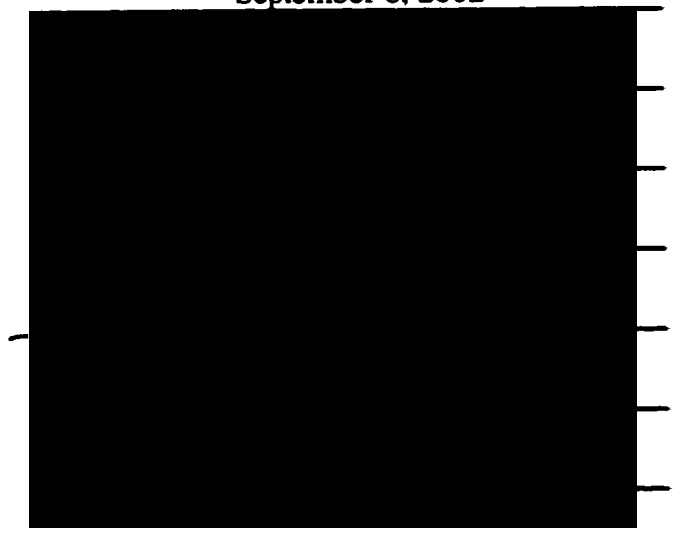

Dalhousie University

Date: Sept 6, 2002

Author: Michael A. Potvin

Title: Multi-Dimensional Chromatographic Methods for Polycyclic Aromatic compounds in Complex Environmental Samples.

Department: Chemistry

Degree: PhD **Convocation:** October **Year:** 2002

Permission is herewith granted to Dalhousie University to circulate and to have copied for non-commercial purposes, at its discretion, the above title upon the request of individual institutions.

[redacted]

Signature of Author

The author reserves other publication rights, and neither the thesis nor extensive extracts from it may be printed or otherwise reproduced without the author's permission.

The author attests that permission has been obtained for the use of any copyrighted material appearing in this thesis (other than brief excerpts requiring only proper acknowledgement in scholarly writing), and that all such use is clearly acknowledged.

Table of Contents

List of Tables

List of Figures

Multi-Dimensional Chromatographic Methods
for Polycyclic Aromatic Compounds in Complex
Environmental Samples

by

Michael A. Potvin

Date of Submission: July12, 2002

Abstract

The research for this thesis was divided into two principal areas. This first area was concerned with the development of multi-dimensional chromatographic methods for the determination of polycyclic aromatic hydrocarbons (PAHs) in light gas oils. A two-dimensional liquid chromatography (LC)-gas chromatography (GC) (LC-GC) and three-dimensional LC procedures were developed. A two-dimensional LC-supercritical fluid chromatography (SFC) procedure was used to investigate the difference between the normal phase LC and SFC modes of operation. LC-GC was able to provide qualitative information about the aromatic class (by ultraviolet and fluorescence spectroscopy) and general levels of aliphatic substitution (by mass spectrometry). Three-dimensional LC was able to further expand on this information and added structural details. A light gas oil was found to contain aromatic species with 1 to 4 rings. There was no evidence for larger aromatic compounds. A series of phenanthrenes and pyrenes were identified that had an aliphatic ring substituent.

The second part of this research was concerned with the development of quantitative methods for the analysis of the priority PAHs and nitro-PAHs in diesel exhaust and air particulates. A two-dimensional procedure using a commercial aminopropyl column derivatized with 2,5-dinitrobenzenesulfonyl (DNBS) chloride was developed to clean-up samples prior to analysis by LC-fluorescence and GC-MS. A SFC separation was used to quantify nitro-PAHs by off-line reduction to the amines and by molecular fluorescence detection. Variable levels of PAHs and nitro-PAHs were found between diesel exhaust samples. The distribution of priority PAHs was found to be consistent for the Environment Canada diesel particulates collected from different buses. A more detailed analysis was not possible because sampling information was not provided with the filters from Environment Canada. The distribution of priority PAHs observed with the diesel exhaust particulates was different from that of an urban dust sample. Diesel particulates contained much larger concentrations of small aromatics while the urban dust showed higher levels of larger PAHs.

List of Abbreviations and Acronyms

ACDA	2-amino-1-cyclopentene-1-dithiocarboxylic acid
APCI	atmospheric pressure chemical ionization
CCD	charge coupled device
CI	chemical ionization
DBE	double bond equivalent
DNBS	2,5-dinitrobenzenesulfonyl
ECD	electron capture detector
EI+	electron ionization (positive)
EMD	evaporative mass detector
FI	flame ionization
GC	gas chromatography
HPLC	high performance liquid chromatography
m/z	mass to charge ratio
MASE	microwave assisted solvent extraction
MS	mass spectrometry
NIAPCI	negative ion atmospheric pressure chemical ionization
NICI	negative ion chemical ionization
NIST	National Institute of Standards and Technology
NP	normal phase
ODS	octadecylsilane
Oxy-PAHs	oxygen containing polycyclic aromatic hydrocarbons
PACs	polycyclic aromatic compounds

PAHs	polycyclic aromatic hydrocarbons
PANHs	nitrogen containing polycyclic aromatic hydrocarbons
PASHs	sulfur containing polycyclic aromatic hydrocarbons
PFE	pressurized fluid extraction
RP	reversed phase
SFC	supercritical fluid chromatography
SFE	supercritical fluid extraction
SPE	solid phase extraction
SRM	standard reference material
TCP	tetrachlorophthalimido
UV	ultraviolet
VIS	visible

Acknowledgments

Thank You to Dalhousie University for this opportunity. I would like to thank the members of my research group for discussions and helpful contributions. A special thanks to Drs. Grossert and Ramaley for providing support and advice. I wish to acknowledge Dr. Jean Cooley of Syncrude Canada Ltd. and Lisa Graham of Environment Canada for providing samples. Most importantly, Dr. Robert Guy whose tireless support and guidance serves as an inspiration. My deepest thanks and admiration to my family whose sacrifice and dedication has allowed me to follow this path.

Chapter 1 Introduction

1.1 Overview

Petroleum oils and air particulate samples are complex materials that contain a mixture of saturated alkanes, naphthenes, aromatic acids, nitro-aromatics, heterocyclic aromatics and polycyclic aromatic compounds. The primary objective of this work was to develop chromatographic methods suitable for the determination of polycyclic aromatic hydrocarbons (PAHs) in oils derived from the Alberta Tar Sands and in typical environmental air particulate and diesel exhaust particulate samples. This introduction consists of a description of the compounds present in oils and air particulates, a review of the chromatographic and analytical methods suitable for their analyses reported in the literature, and a description of the experimental methods used in multi-dimensional chromatography.

1.2 What are PAHs?

Oils are often characterized by fractionation into the following classes: saturates, mono-aromatics, poly-aromatics, and polars [1]. Benzene and its alkyl derivatives make up the simplest of all aromatic structures. Historically, this group of compounds would be defined as the mono-aromatic fraction, typically consisting of such additional compounds as indene, styrene, and tetralin. Naphthalene, biphenyl and their alkyl derivatives are referred to as the di-aromatic compounds. Further to this, all other homocyclic aromatics containing three or more aromatic rings are termed PAHs. Typically, this would consist of compounds like phenanthrene, anthracene, pyrene, benzo[*a*]pyrene, coronene and their alkyl derivatives.

However, compounds that contain at least one benzene ring are often referred to as PAHs. PANHs and PASHs are used to describe the heterocyclic analogs of PAHs containing nitrogen and sulfur, respectively. An example of a nitrogen containing species is acridine. Thiophene is a typical sulfur heterocyclic aromatic species. Several classes of aromatic compound are shown in Figures 1.1 and 1.2. Several other classification systems exist for aromatic compounds. PAHs are grouped into two broad categories consisting of alternate compounds and the non-alternate species. Alternate PAHs contain only fused six-membered benzenoid rings. Examples of such compounds would include pyrene, phenanthrene, and chrysene. Non-alternate PAHs consist of the compounds with benzenoid rings fused with four, five, and seven carbon rings. This class of compounds is typical of fluoranthenes and acenaphthylene. In addition to this classification, polyaromatics are often further grouped as to whether they are peri-condensed or cata-condensed. Cata-condensed PAHs are usually benzenoid rings fused in a linear or angular arrangement. Chrysene and phenanthrene are representative of this classification. Peri-condensed compounds are defined as hydrocarbons that contain third degree vertices. Pyrene represents the smallest peri-condensed polyarene. The type of compounds created depends upon the conditions of combustion and the source of the fuel [2]. In general it was noted that temperature played a critical role in product formation. High temperatures (about 1000 K) and oxygen deficient flames tend to form PAHs with little or no alkylation [3]. These PAHs were typically mixtures containing one to five aromatic rings, consisting of mainly peri- and cata-condensed structures [4]. Reducing the temperature down to 700 K increases the complexity of product formation considerably. In such cases larger condensed ring structures were not favored. Instead, the tendency was

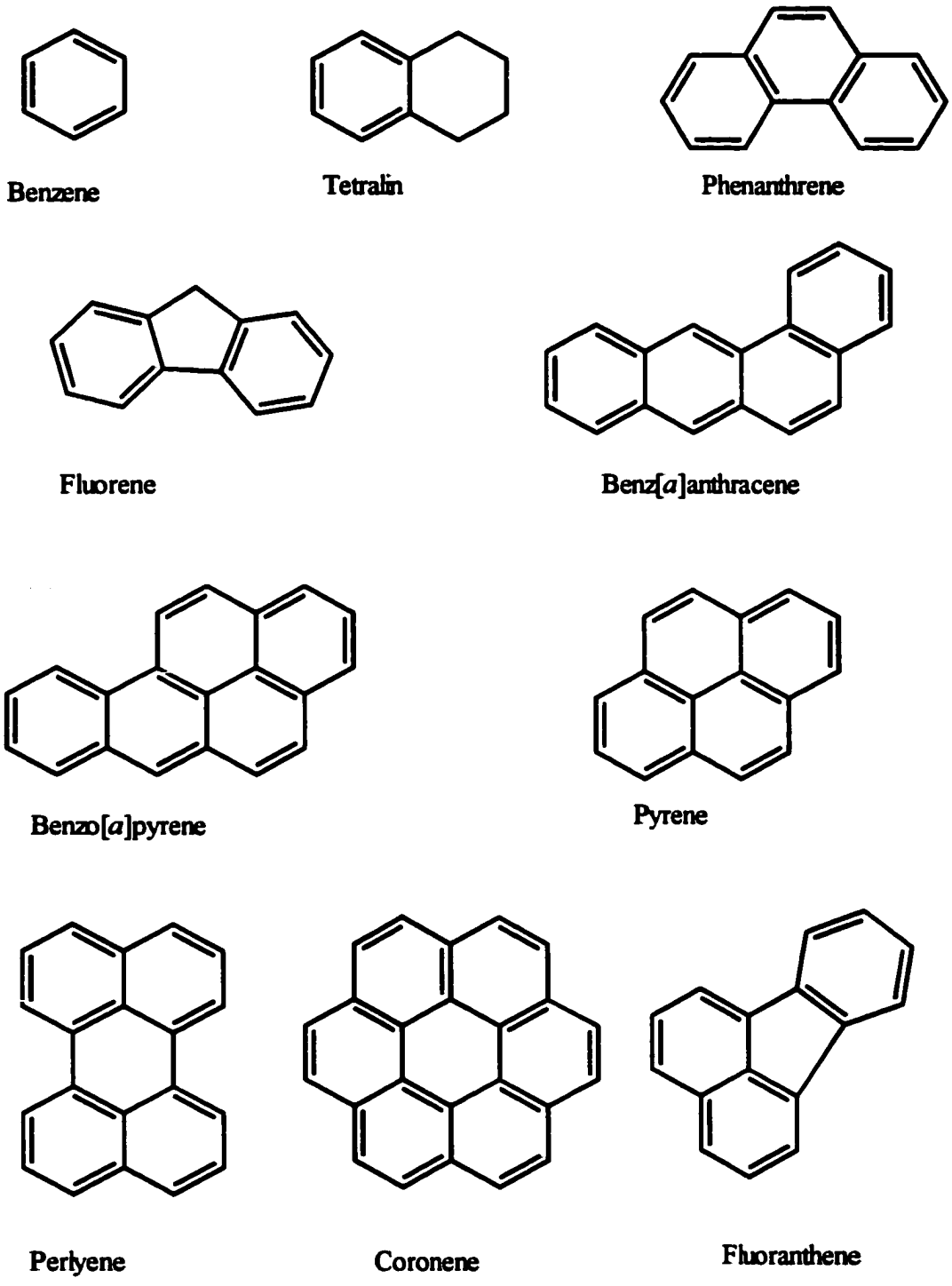

Figure 1.1: Structures of some common aromatic compounds.

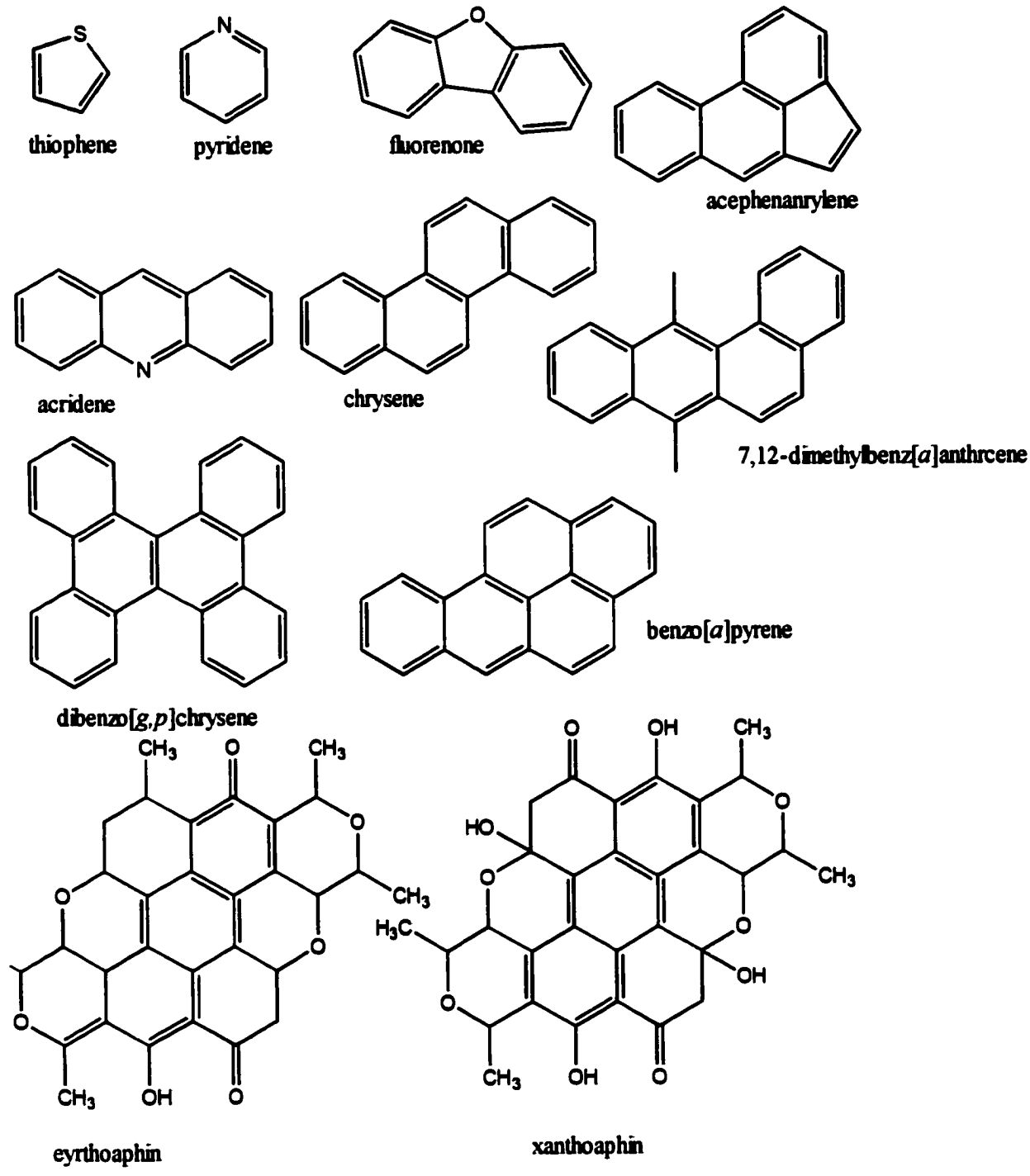

Figure 1.2: Additional structures of PAH species.

towards the formation of methyl-alkylated structures containing fewer rings. At this point it should also be noted that mixed PAHs containing five-membered rings are present in these mixtures [5]. Acephenanthrylene is one such compound represented by this description.

1.3 What are Nitro-Polycyclic Aromatic Hydrocarbons?

Nitro-polycyclic aromatic hydrocarbons (nitro-PAHs) are generally characterized by the substitution of a nitro group for a hydrogen atom on an aromatic ring. Thus, the nitro-aromatic analog is created from the corresponding parent PAH. Figure 1.3 outlines several of the most common nitro-PAHs found in air and diesel exhaust particulate matter. The addition of a nitro substituent alters the photochemical behavior of the compound. For example, PAHs such as pyrene and chrysene fluoresce when excited with ultraviolet light. This fluorescence is quenched by the addition of a nitro substituent. This prevents the direct use of fluorescence to detect this class of aromatic compounds. The highly mutagenic and carcinogenic behavior of nitrated PAHs has increased concern with respect to environmental burden and exposure levels in general. For example, 1,3-, 1,6-, and 1,8-dinitropyrene have been reported to show the highest mutagenic behavior of all PAHs examined thus far [6].

1.4 PAH Formation

Polycyclic aromatic hydrocarbons are naturally occurring compounds ubiquitous to the environment. It is believed that bacterial lipids and terpenoids present in terrestrial plants

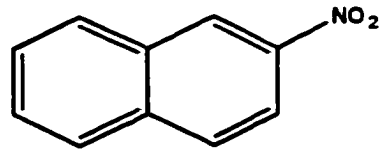

2-nitronaphthalene

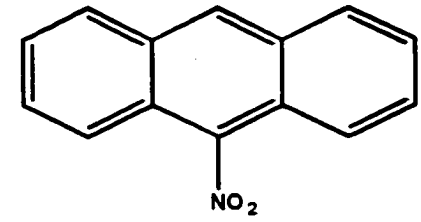

9-nitroanthracene

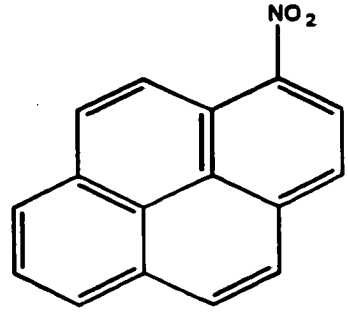

1-nitropyrene

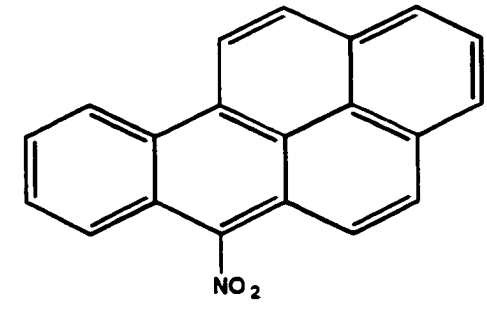

6-nitrobenzo[*a*]pyrene

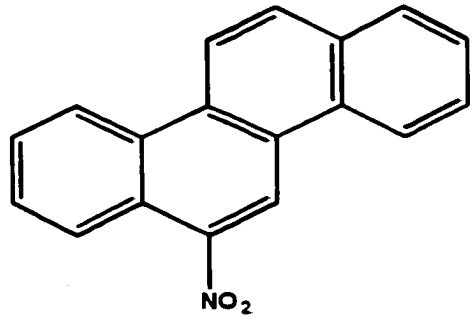

6-nitrochrysene

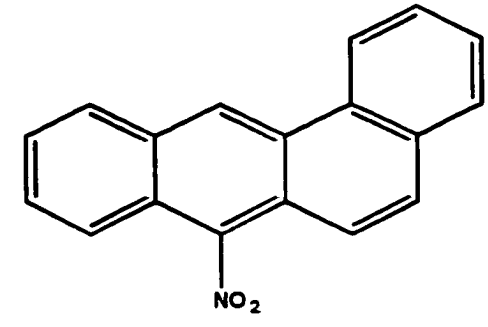

7-nitrobenz[*a*]anthracene

Figure 1.3: Selected structure of nitro-PAHs.

leads to PAH precursors [7]. There has even been some evidence to suggest quinones, such as xanthoaphin and erythroaphin, provide building blocks to larger PAHs such as perylene [8]. Biogenic sources are not believed to contribute to the large-scale distribution of PAHs in the atmosphere. PAHs are created through various combustion processes. Anthropogenic sources contribute significant amount PAHs to the urban atmosphere. These contributions are based on the combustion of various fossil fuels and wood burning operations. In fact, naturally occurring forest fires add to the atmospheric PAH pollution [9]. Fine *et al.* [10] studied the emission rates of small particulate matter and PAHs from the use of wood for household heating. The amount of PAHs observed from combustion was dependent upon the type of wood used as fuel but in some cases 7.6 mg of pyrene was emitted for each kg of wood. Anthropogenic sources of PAHs also include industrial processing. In 1997, for example, it was estimated that Canadian industry emitted 525 tonnes of PAHs into the environment [11]. Alcan, for example, emitted about 400 tonnes, with a further 100 tonnes coming from various steel plants combined. However, the emission of PAHs from home heating has been reported to be larger than the contribution by industry by more than three orders of magnitude [12]. Small barbecue cooking fires result in the formation of PAHs and PANHs that are deposited directly to the food that is then later consumed [13]. The amount of PAHs generated during grilling was found to be proportional to the fat content of the meat [14]. Hamburger meat with a fat content of 21% could generate 0.75mg of pyrene and 0.95 mg of chrysene per kilogram of meat grilled. In cases where lean meats were used such as pork steak (4% fat), the charcoal combustion was found to produce the majority of PAHs observed (0.30 mg total PAHs per kg of charcoal) [15].

1.5 Nitro-Aromatic Compound Formation

The occurrence of nitro-PAHs in the atmosphere is thought to result from two sources: direct emission from combustion engines and through atmospheric radical chemical reactions. Gasoline combustion results in less formation of nitro-PAHs than diesel fuel combustion. In fact, diesel combustion produces 30 times the amount of nitro-aromatics compared to gasoline combustion [16]. The type of nitro-PAH formation dictates the principal isomers created. For example 1-nitropyrene is exclusively formed from the combustion process and all of the 1-nitropyrene condensed on diesel particulate exhaust is the result of direct emission, 2-nitrofluoranthene on the other hand is not created through direct emission processes but results from atmospheric reactions [17]. Another nitro-PAH believed to result from direct emission is 9-nitrobenz[*a*]anthracene.

Atmospheric radical chemistry is believed to account for the majority of nitro-PAHs found on air particulates. Two pathways have been proposed depending upon the amount of daylight available. Atkinson and Arey [18] proposed a daytime pathway that proceeds via a hydroxyl-substituted intermediate:

$$\text{Fluoranthene} + OH \Rightarrow \text{Fluoranthene-OH}$$

$$\text{Fluoranthene-OH} + NO_2 \Rightarrow \text{2-nitrofluoranthene} + H_2O$$

This reaction occurs in the gas phase and the nitrated product rapidly condenses onto the particulate surface. Interestingly, this mechanism is considered to be the only significant source for 2-nitrofluoranthene and 2-nitropyrene. In the evening, when the concentration of hydroxyl radicals in the atmosphere is low, Cecinato *et al.* [19] suggest that the nitration of

aromatic compounds may be achieved through substitution reactions with NO_3 radicals and PAHs. Both of these atmospheric reaction pathways form similar products that are different from the nitro-PAHs formed through direct emission. This allows for the possibility to speculate on the source of the compounds found on the particulates according to the types of nitro-aromatics that may be present. For example, samples that contain 1-nitropyrene and 3-nitrofluoranthene suggest that the primary emission source for these particulates was diesel fuel combustion.

Nitro-PAHs and PAHs are considered to be semi-volatile species. Leotz-Gartziandia *et al.* [20] studied the volatility of PAHs and nitro-PAHs from filter collection devices and found that a significant portion of the polar PAHs were observed in the gas phase. Specifically, PAHs less than or equal to the size of benzo[*a*]pyrene were readily sublimed from the particle surface by drawing air across the filter. Also, nitro compounds with 2 aromatic rings were observed almost completely in the gas phase. Nitro-aromatics such as 9-nitroanthracene with more than 2 aromatic rings but less than 4 rings were found to distribute between the two phases but remained primarily in the gas phase. 1-Nitropyrene and the larger nitro-aromatics rapidly condensed onto the particulate surface with very little partitioning into the gas phase. This may account for the presence of 1-nitropyrene in diesel exhaust particulates.

Nitro-PAHs are generally not considered persistent organic pollutants because processes such as photo-degradation can act as a sink for these compounds. Fielberg and Nielsen [21] studied the photodegradation of nitro-PAHs in organic solvents. Organic solvents were used to model the particulate surface because it has been suggested that the organic section of the particulates are liquid-like and nitro-PAHs such as 1-nitropyrene would

rapidly condense onto the organic layer of the particulate. Fieldberg and Nielsen [21] also investigated the effect that oxy-PAHs had on the photodegradation rates of nitro-PAHs and concluded that these compounds increased the rate of degradation. For example, irradiation for 60 minutes at 366nm resulted in a 28% loss of 1-nitropyrene. This was increased to 76% with the addition of hydroquinone as a co-solute. These findings suggest that the concentration of nitro-PAHs may depend upon the particulate composition. For example, particulates that contain elevated concentrations of oxy-PAHs (PAHs containing oxygen) may show decreased nitro-PAH concentrations due to photodegradation reactions.

1.6 Importance for Study of PAHs and Nitro-PAHs

Initially PAHs were studied due to their importance as intermediates in several industrial processes. The most notable of these processes was the synthesis of commercial dyes and pigments [22]. Interest in PAHs increased when implicated in possible health risks to human and animal life forms. Several PAHs have been proven to be potent mutagens and carcinogens. Benzo[*a*]pyrene and 7,12-dimethylbenz(*a*)anthracene produce tumors in lab mice [23]. It is believed that benzo[*a*]pyrene is a precursor which undergoes hydrolysis and oxidation to the 7,8-diol-9,10-epoxide of benzo[*a*]pyrene which is known to be a potent mutagen [24]. In humans, this process occurs in the liver, facilitated through the enzyme cytochrome P450. However, the mutagenic activity of this compound is less than nitro-PAHs such as 1,3-dinitropyrene [6]. The need to qualitatively examine such species and quantify the levels of dangerous PAHs introduced into the environment becomes readily apparent.

As mentioned previously, PAHs comprise a significant portion of fossil fuels. Notwithstanding the PAHs formed during combustion itself, PAHs are not destroyed as they travel through an automobile engine [25, 26]. Table 1.1 (adapted from Marr *et al.* [26]) lists the emission rates of PAHs from automobile exhausts and the concentrations of several PAHs present in commercial gasoline. This research suggests that several PAHs such dibenz[*a,h*]anthracene were formed during combustion because the concentration in the fuel was low. Vehicle emissions add significantly to the long-range distribution of atmospheric PAHs and the resulting impact upon the environment. For example, Van Metre *et al.* [27] suggested that an increase in vehicle use due to urban sprawl resulted in an increase of the levels of PAHs deposited into the sediments of watersheds for several US cities. In addition, point source emissions for PAHs have been shown to impact locations more than 40 km away from the original source [28]. Historically, aromatics in gasoline fuels have not been a great concern because they increase the octane rating of the fuel and environmental impact was not a primary concern [29]. An opposite effect is noted with diesel fuels and the corresponding cetane number. In either case, the complete speciation of the components present in the aromatic fraction was not performed during industrial processing. The tightening of government legislation with respect to aromatics as priority pollutants now requires a more detailed speciation of the PAHs in both fuels and environmental samples.

1.7 Syncrude Samples

Crude petroleum is a complex mixture of thousands of compounds grouped according to the following classifications by the petroleum industry: paraffin hydrocarbons, naphthene

Table 1.1 Emissions of PAHs from automobiles and the concentrations of PAHs present in commercial gasoline (adapted from Marr *et al.* [26]).

Compound	Emission Rates from Cars (μg/kg of fuel)	Concentration in Gasoline (mg/L)
Fluoranthene	10.3 ± 0.9	2.6
Pyrene	13.8 ± 0.6	3.1
Benz(*a*)anthracene	8.8 ± 0.4	1.4
Chrysene	8.6 ± 0.5	0.82
Benzo(*b*)fluoranthene	8.1 ± 1.4	0.28
Benzo(*k*)fluoranthene	3.0 ± 0.4	0.16
Benzo(*a*)pyrene	8.3 ± 0.8	0.50
Benzo(*g,h,i*)perylene	20.7 ± 2.6	0.55
Indeno(*1,2,3-c,d*)pyrene	7.5 ± 1.1	0.74
Dibenz(*a,h*)anthracene	1.3 ± 0.3	0

hydrocarbons, aromatic hydrocarbons, multi-ring hydrocarbons, olefinic hydrocarbons, sulfur, oxygen, nitrogen compounds, and inorganic salts [30]. A typical crude would consist of 83-87% carbon, 11-15% hydrogen, 0.1-6% sulfur, 0.1-1.5% nitrogen, and 0.3-1.2% oxygen. In general, fuels such as gasoline require enrichment of the hydrocarbon fraction before use. The crude oils must therefore undergo processing and refinement before use as fuels or chemical precursors in the manufacturing of plastics. The crude oil must be de-salted with steam, distilled into fractions by boiling point and then treated with hydrogen (cracking). The

mining of the tar sands is more challenging than the mining of conventional crude oil deposits as the oil must first be extracted as bitumen using steam and hot water. This bitumen is then subjected to processing, typically utilizing a fluid catalytic cracker. The cracked bitumen is generally classified into three categories that include light gas oil, heavy gas oil and vacuum gas oils. The distinction usually comes about due the variation in boiling ranges of each fraction. The boiling range for the light gas oil is 216 to 343 C while that of the heavy gas oil is between 343 to 524 C. Typically, Alberta Tar Sand bitumen contains roughly 20 to 30 percent aromatics by weight [31]. Upgrading processes include hydrotreating with appropriate catalysts to reduce aromatic structures and open aliphatic rings to produce branched alkanes. Mono-aromatics are more stable than di-aromatics and polyaromatics so that during upgrading the tendency is to increase the mono-aromatic fraction in the final product. Quian and Hsu [32] have reported on two possible schemes that characterize this behavior in the processed oils. These schemes are shown in Figure 1.4. The bitumen contains a number of aromatic nitrogen, oxygen and sulfur heterocycles, as well as a considerable contribution of unidentified aromatic species. In general, this fraction should not amount to more than ten percent of the total by weight. The heterocycles tend to be removed during the hydrotreatment with nitrogen being removed as ammonia and the sulfur evolved as hydrogen sulfide before recovery as elemental sulfur. The processed Syncrude Sweet Blend typically contains 0.1 to 0.2 percent sulfur as a final product. Saturated and mono-aromatic compounds tend to lead to gasoline precursors. Aromatic species containing two through four rings generally lead to light gas oils [31].

Scheme 1

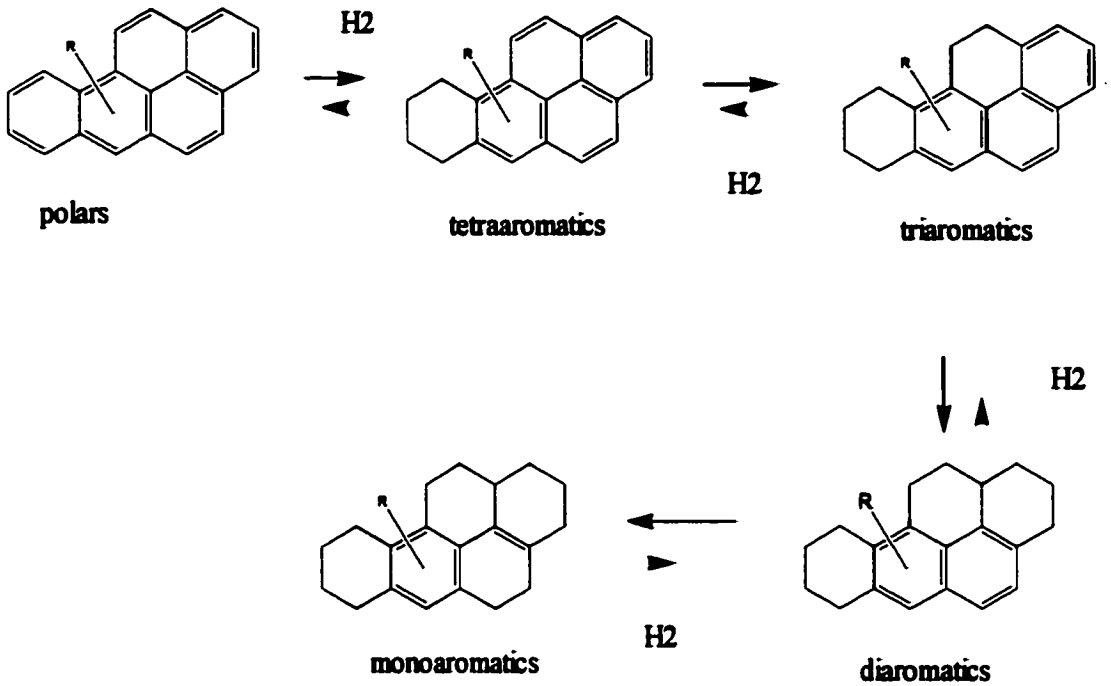

Scheme 2

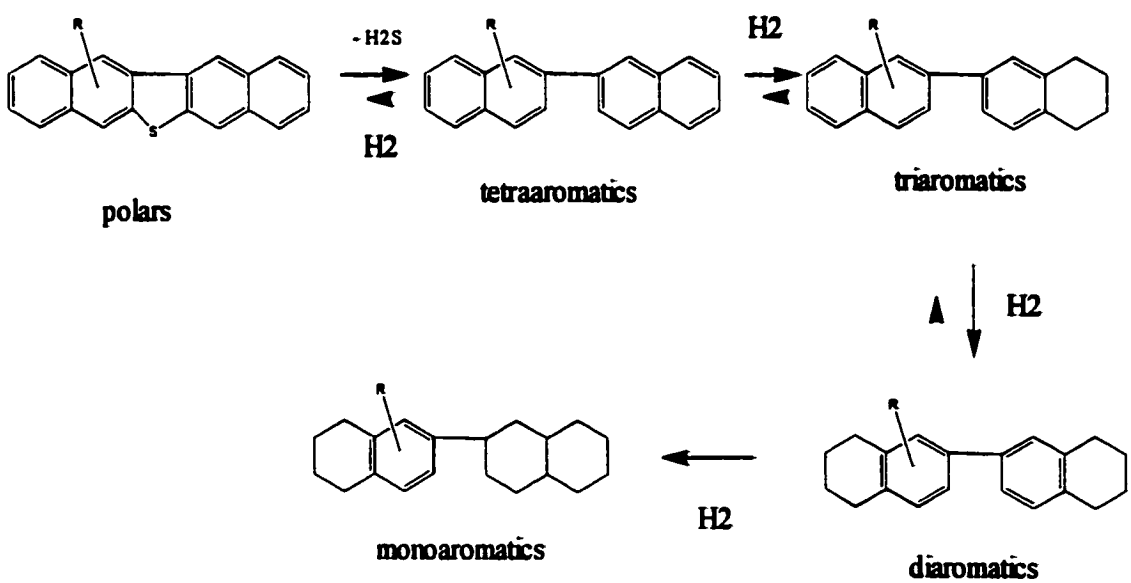

Figure 1.4: Qiann and Hsu catalytic schemes.

1.8 Typical Composition of Air Particulates and Diesel Particulates

The composition of air and diesel exhaust particulate tends to vary according to source emission profiles as well as atmospheric conditions [33]. However, each contains the following groups of compounds: aliphatic hydrocarbons, aromatic hydrocarbons, polar aromatic hydrocarbons, and inorganic species such as calcium, sodium, lead, cadmium, nitrates, sulfates, and ammonium salts [34]. The particle size associated with air particulates ranges from 0.5 – 10 microns with the greatest concern centered on particles smaller than 2.5 micron because of their ability to reach the inner lung during inhalation. Particles that travel to the aveoli are seldom discharged from the lung. This allows the toxic components present on the particulate to be absorbed into the body. Diesel particulates are usually small with particle diameters of 0.2 microns and a relatively high surface area. These small particles may adsorb PAHs and nitro-PAHs from hot combustion gases. Factors such as diesel engine type and fuel source can influence the relative distribution of compounds bound on the particle phase but for the most part distinct similarities are observed. For example, light duty diesel engines used to power passenger cars and trucks were found to emit 30 mg of carbon particulates per kg of fuel burned with an average particulate diameter of 0.12 microns [35]. In the same study heavy diesel engines from transport trucks were observed to produce 1440 mg of carbon per kg of fuel (particulate size 0.12-0.20 microns).

PAHs and nitro-polycyclic aromatic hydrocarbons are the principal compounds of interest in the analysis of both diesel and air particulates. They are not, however, the most abundant components. In fact, nitro-aromatics often represent trace levels with respect to the entire matrix but they may still represent 30 percent of the total mutagenic activity associated

with diesel exhaust particulate extracts [36]. The complex nature of environmental particulate samples often requires complex multi-dimensional analysis to separate nitro-PAHs from other polar PAHs such as heterocyclic aromatics, oxygenated aromatics, and aromatic carboxylic acids. High molecular weight priority PAHs such as benzo[*g,h,i*]perylene are more abundant in urban air particulates but low molecular weight PAHs with increased alkylation are more abundant in diesel exhaust particulates.

1.9 PAH Analysis

Fossil fuels and particulate extracts are incredibly complex mixtures and the analysis of such samples has proved both tedious and time consuming. The similarity of the compounds in these hydrocarbon mixtures and the limited peak capacity associated with a single chromatographic separation suggests that multi-dimensional methods are necessary to obtain more information about sample composition. The peak capacity (the maximum number of resolved compounds) for any chromatographic separation is governed by the following relationship:

$$n = 1 + (N^{1/2})/4 * \ln (V_{max}/V_{min}) \qquad [1\text{-}1]$$

where N is the number of theoretical plates, and V_{max}/V_{min} is a ratio of the volume of mobile phase required to elute the most retained compound (V_{max}) to the least retained compound. Typically this ratio for high pressure liquid chromatography (HPLC) separations is limited to

approximately 10, gas chromatography (GC) separations on the other hand may have ratios around 50. As a result, GC separations often yield larger peak capacities.

Many of the PAHs of interest have high boiling points; gas chromatography is often limited in the scope of analysis by the boiling point of the stationary phase. A standard GC phase for PAH analysis, 5% phenyl/95% methyl polysiloxane has an operating temperature range of 60-350 C. As a result, GC is often selected if the matrix contains smaller PAHs. The selectivity offered with mass spectrometric (MS) detection has proven popular for GC separations of PAHs [26, 37-41]. Flame ionization (FI) detectors have been used but require additional separations to simplify complex samples [42]. A 95% methyl/5% phenyl polysiloxane capillary column has difficulty resolving benzo[*b*]fluoranthene and benzo[*k*]fluoranthene. In addition triphenylene co-elutes with chrysene. This can present problems when detectors are used that are unable to differentiate these compounds such as mass spectrometry or FI. As an alternative, smectic-liquid crystalline polysiloxane columns have been investigated to resolve these co-elution difficulties [43].

Although liquid chromatography (LC) is generally considered a lower resolution technique than capillary GC, the priority PAHs are often better resolved using polymeric reversed phase C18 separations under gradient conditions. Furthermore, HPLC does not suffer from the sample volatility limitations imposed with typical capillary GC separations. Fluorescence detection is typically used for quantitative detection of PAHs [44, 45]. LC-atmospheric pressure chemical ionization (APCI)/MS has also been used to quantify the PAHs in particulate extracts [46]. The sensitivity of this technique for the priority PAHs was less than that for a typical fluorescence detector and therefore less suitable for trace PAH analysis.

Typically, complex mixtures require longer analysis times due to extended solvent gradients and so coupled on-line methods are gaining popularity. A variety of tandem techniques, such as GC/GC [47-51], LC/GC [52-57], supercritical fluid chromatography (SFC)/GC [58, 59], and LC/LC [60-65, 68] have been reported as attempts to develop a robust method for analysis of PAHs. Each technique has met with limited success and none has been established as a universal method. Choice depends on the sample composition. Multi-dimension liquid chromatography is generally explored using a normal phase separation as a first dimension to facilitate a group separation by aromatic ring number or compound class, coupled to a reversed phase separation to classify group isomers or class compounds. Further dimensions are often added to the analysis through the use of selective detection.

1.9.1 Normal Phase Separations

Primarily the goal of the normal phase separation is to fractionate the sample into groups by aromatic classes such as: saturates, mono-aromatics, di-aromatics, polyaromatics, and polars (large PAHs and heterocyclic species). Silica columns have been routinely used to fractionate PAH mixtures and have shown good ability to separate according to aromatic ring number as well as by alkylation [66]. However, silica columns are prone to irreproducible behavior because of variable water content in the mobile phase that can alter the activity of the stationary phase. Typically, chromatographic performance tends to degrade as heavy gas oils are examined. PAHs can act as electron donors or acceptors depending on the nature of the molecule. The exact nature of the interactions are not truly known but stationary phase interactions as a function of the quadrupole moment of the PAH are believed

to be important [67]. This has lead to the investigation of a variety of polar bonded phases to effect better group separations. The aminopropyl stationary phase offers a better separation of the PAHs from polar material compared to a standard silica phase [69]. Boduszynski *et al.* [70] used an amino bonded phase to perform a group separation for compounds in non-distillable coal liquids. The group separation was less definitive if large numbers of isomers exist with the same number of aromatic rings. Alfredson [63] performed a primary separation of various petroleum fractions using a cyanopropyl column coupled with a silica column. The cyanopropyl column offered increased resolution between the mono-aromatics and the saturated hydrocarbon fraction as well as decreasing the sensitivity to impurities. Pyell *et al.* [71, 72] used a 2-amino-1-cyclopentene-1-dithiocarbocyclic acid (ACDA) derivatized silica phase loaded with Ag(I) to fractionate PAHs and sulfur heterocycles. This stationary phase required complex eluents (hexane/isopropanol/methyl-t-butylether), which often lead to poor chromatographic reproducibility. Further to this, diol [73], benzoyl [74], and tetrachlororphthalimidopropyl (TCP) [75] groups have been investigated as bonded stationary phases. Robbins [61] developed a completely automated multi-dimensional chromatographic system that incorporated simultaneous evaporative mass detection (EMD) and ultraviolet (UV) detection for the characterization of aromatics in petroleum distillates. This system used a propylaminocyano column to separate saturates from the mono-aromatic fractions coupled to a dinitroanilidopropyl column through a series of valves that further separated the mixture into the classes: di-aromatic, tri-aromatic, tetra-aromatic and polars. Using the HPLC 2 method Robbins [61] was able to characterize the mass (EMD) and aromatic distribution (UV detector) within a series of process oils.

1.9.2 Reversed Phase Separations

Octadecylsilane (ODS) has been used as the principal bonded phase for reversed phase separations of the priority PAHs and their alkylated derivatives. There are two basic classes of ODS stationary phases, classified as either "monomeric" or "polymeric". Sander and Wise [76] report on the differences in synthetic routes for each stationary phase. Dimethyl-octadecylchlorosilanes are used to prepare the monomeric phases. Methyl-octadecyldichloro- and octadecyltrichlorosilanes are used to prepare both the monomeric or polymeric phases. Anhydrous silica tends to be used for monomeric phases. The addition of water to the silica or silanization solution allows for the substitution of chlorine with a hydroxyl group. The hydroxyl group then crosslinks with an adjacent chlorosilane (with the elimination of HCl) to produce a "polymeric" phase. The stationary phase is classified according to the "alpha scale". Alpha values are defined according to the following relationship:

$$\text{alpha} = k'_{\text{benzo}(a)\text{pyrene}} / k'_{\text{dibenzo}(g,p)\text{chrysene}} \qquad [1\text{-}2]$$

The structure for dibenzo[*g,p*]chrysene is shown in Figure 1.2. These compounds were chosen due their different length to breadth ratios. An alpha value of 1.7 or greater indicates a monomeric phase whereas values below 0.9 signify a polymeric phase. The polymeric phase tends to be much more sensitive to the length/breadth ratios of the PAHs.

Traditionally, most reversed phase separations are performed at ambient temperature. Wise and coworkers have found that the monomeric ODS becomes polymeric in its behavior at lower temperatures (-10 C) [77]. Wise also demonstrated that a selectivity intermediate

of the two phases could be achieved by temperature programming. Through the use of temperature control Wise was able to resolves all six methyl chrysene isomers. The monomeric ODS phase is believed to separate according to the aromaticity of the compound coupled with the degree of alkylation present. The polymeric ODS adds shape selectivity to the separation. Wise *et al.* [78] found that PAH isomers with the same number of aromatic rings and dissimilar patterns of alkyl substitution could be classified according to the overall length to breadth ratio of the molecule and the degree of planarity associated with the molecule. Isomers with higher length to breadth ratios would be retained longer by the polymeric stationary phase, as would those with a higher degree of planarity. This fits the description of a retention slot model suggested by Wise *et al.* [79].

The main factor controlling the retention in the reversed phase is believed to be the solubility of the analyte in the eluent. Chromatographers often report the retention of compounds using the capacity factor, k', defined as follows:

$$k' = (t_r - t_o) / t_o = K (V_s/V_m) \qquad [1\text{-}3]$$

Where t_r and t_o are retention times for the compound and an unretained component, respectively. K is the partition coefficient for the compound distribution between the mobile phase and the stationary phase, V_s and V_m are the phase volumes. It is obvious that retention increases as k' increases. Solvent gradient chromatography is used to separate compounds with large differences in k'. At the end of a chromatogram, a period of time is required to re-equilibrate the stationary and mobile phases. Isocratic elution is used to separate compounds with similar k'. There is no time requirement for re-equilibration of the stationary and mobile

phases, however the eluent strength must be chosen to elute all of the compounds within a reasonable time. Thermal programming affords a new means of controlling eluent strength. Makela and Pye [80] have observed that chromatographic reproducibility is enhanced for isocratic separations when compared to gradient elution. Further to this, Kurganov *et al.* [64] used two ODS columns at different temperatures to perform an isocratic separation of the 16 priority pollutant PAHs.

There has been a resurgence of interest of new non-conventional bonded reverse stationary phases. An example of this is the study by Kohne *et al.* [68]. A safrol based modified silica support was utilized to separate nitro- and amino- aromatics present in explosives. Diphenyl or triphenyl substituted ODS bonded phases have been used as an alternative to polymeric ODS stationary phases. Fetzer and Biggs [81] suggest that the phenyl-substituted phase provides a more uniform surface for solute/phase interactions that in turn generates a more predictable retention pattern. Jinno *et al.* [82] studied a dicoronene stationary phase that displayed a high selectivity towards the planarity of the solute molecule but the column efficiency was poor due to an ineffective packing process. In contrast, Jinno *et al.* [83] produced a 2,4,6-(tri-tert-butylphenoxy)dimethyl silica phase which displayed preferential retention according to the extent of non planarity of the solute. The effect was pronounced for relatively small PAHs only, non-planarity in coronene for instance was not recognized.

1.9.3 SFC Separations of PAHs

The use of SFC has been explored as an intermediate between standard GC and LC methods. Often petroleum samples contain compounds that cannot be analyzed with GC due to volatility limitations. Typically, such compounds would have to be analyzed with LC methods. SFC can be used to separate the heavier compounds with better resolution compared to similar LC separations. In addition, SFC that uses supercritical CO_2 as the mobile phase presents an environmentally friendly option to typical chlorinated organic solvents used for HPLC. High purity HPLC solvents such as hexane and dichloromethane are expensive and present concerns over collection and proper disposal. The solvating power of supercritical CO_2 increases as the density increases. Typical densities of supercritical CO_2 range from 0.45 g/mL to 0.95 g/mL. Even at high densities (0.95 g/mL) the solvating power of CO_2 is generally limited to small, nonpolar compounds [84]. The addition of organic modifiers such as methanol or acetonitrile has been investigated to extend the range of analytes solvated with CO_2 [85]. In principle one of the benefits of SFC is the ability to use the entire range of detectors available to both GC and LC methods. This enhances the versatility of SFC. In practice, however, this is true only for separations done without modifier. For example, flame ionization is a popular detector for both GC and SFC. However, its use with SFC is limited to mobile phases that do not contain organic modifier for the same reasons that the FI detector cannot be used with LC [86]. In addition, the operational parameters of SFC (high pressures) can present additional challenges for interfacing other detectors such as fluorescence.

SFC has been popular in fuel oil analysis [87, 88]. The chromatographic precision of SFC separations can be affected by flow rates and pressure gradients particularly when fixed restrictors are used in place of a variable nozzle restrictor. In fact, up to a six fold increase in precision was reported with the use of a variable restrictor that used specific temperature control [88]. SFC has also been used as a preparative method to fractionate a sample before analysis with GC-MS [89]. The off-line collection of fractions required a pressurized interface to prevent fraction overlap due to peak broadening that occurs during depressurization of the mobile phase. As a result, multi-dimensional chromatographic methods using SFC require that the eluent stream be split before the restrictor while still pressurized or the use of an interface post restrictor that prevents rapid depressurization. This makes multi-dimensional chromatography with SFC much more complex than similar methods involving LC.

Detection methods such as ultraviolet absorption that are commonly used with SFC are not useful for trace analysis. Fluorescence detection offers better sensitivity and selectivity for this purpose. To date, there are no commercially available fluorescence detectors suitable to withstand the pressure demands associated with SFC. Smith *et al.* [90] used a two stage restrictor that facilitated a pressure reduction of the mobile phase without complete depressurization to enable the use of fluorescence detection. Comb *et al.* [91] developed a chemiluminescent detector specific for nitrogen heterocycles. This detector was interfaced post restrictor. Chromatographic broadening due to mobile phase depressurization was offset by the specificity of the detector. Alternatively, SFC coupled to APCI-MS has been used extensively to analyze PAHs [92-96]. Under these circumstances the eluent stream is often heated to high temperatures (~450 C) to offset the problems associated with mobile

phase depressurization. This can result in decomposition of thermally sensitive analytes. However, the use of mass spectrometry with APCI provides good selectivity and reasonable sensitivity.

1.9.4 PAH Detection

Although PAH synthetic methods have undergone dramatic improvements in recent years, a complete line of analytical standards is not yet available. So, even with an effective separation, compound identification still poses a challenge. The role of selective detection methods is evident. Zero order detection offers limited versatility when coupled to complex hydrocarbon samples. There are instances when it may prove convenient. Robbins [61] used an evaporative light scattering (ELD) detector for the detection of large aliphatic compounds in a fractionation separation described earlier (HPLC 2 method). Although not amenable to LC separations, the flame ionization detector has performed a similar task when applied to GC and SFC. The absence of a chromophore in alkanes makes spectroscopic detection impractical, particularly for LC and SFC separations. This underscores the need for general detection methods such as refractive index detectors or ELDs. The most common multi-dimensional detection techniques for PAHs are UV absorption, fluorescence, and mass spectrometry.

Most PAHs absorb ultraviolet radiation and fluoresce provided quenching reagents are not present in solution [97, 98]. Diode Array UV detection has proved to be a very reliable tool for the identification of PAHs. Many PAHs contain absorption bands unique to the parent PAH [99]. Alkyl substitution of the parent PAH causes a bathochromic shift in the

spectrum and the magnitude depends on the number of alkyl substituents. Typical shifts are on the order of one to four nanometers. Also the placement of the substituent can have a significant effect. Often, however, PAHs of interest are present at trace amounts below the detection limits of UV/visual (VIS) absorption spectroscopy.

Fluorescence detection offers a more sensitive and possibly more selective means of PAH detection. The increase in sensitivity is most apparent in Shpol'skii fluorescence [100]. Compounds are trapped in a glass prepared by low temperature solvents, for example, n-octane at 15 K. Reduction of temperature causes decreased mobility of the molecule, which in turn reduces the ability for energy from the excited state to be redistributed throughout the available vibrational modes. This results in fine structure in the fluorescence spectrum. PAHs with less than six aromatic rings can be identified according to alkyl substitution pattern because of the narrow and unique emission lines. Operating temperatures on the order of a few Kelvin, however, does not allow for facile coupling to on-line separation methods. Reproducibility and quantification are significantly impaired by cryogenic processing [101].

Fluorescence spectroscopy at ambient or near ambient temperature has become a significant mode of detection for PAHs in petroleum contaminated samples. Campigila [102] was able to identify six PAHs at trace levels in soil samples using laser-induced phosphorimetry. Solvent properties can play a crucial role in determining the detection of PAHs using fluorescence spectroscopy. The most important factors are solvent polarity, viscosity, and temperature. The polarity of the solvent can affect the intensity of the fluorescence emission of the PAH through selective enhancement of the first vibronic band [103]. Depending on the PAH, a measure of solvent polarity is often judged by the ratio of the first and third or first and fourth vibronic band. An example of a PAH that exhibits this

behavior is pyrene. In polar solvents such as acetonitrile, the first vibronic band is more intense than the second band. This observation is reversed when spectra are recorded in nonpolar solvents such as hexane. Solvent viscosity can also play a role in determining relative emission intensity. PAHs dissolved in high viscosity solvents display a greater relative emission compared to low viscosity solvents. A more viscous solvent limits relaxation of the PAH vibrational energy levels so that a greater quantum yield is observed. PAHs readily undergo reactions with some radical initiators such as chlorinated solvents [104]. An example is the photochemical reaction of anthracene with carbon tetrachloride according the following mechanism [104].

$$A + h\nu \rightarrow {}^1A^*$$

$${}^1A^* + CCl_4 \leftrightarrow {}^1(ACCl_4)^*$$

$${}^1(ACCl_4)^* \rightarrow {}^3(ACCl_4)^* \rightarrow {}^3A^* + CCl_4$$

$${}^1(ACCL_4)^* \rightarrow ACl + CCl_3 \rightarrow \text{Products}$$

The superscripts 1 and 3 denote the singlet and triplet states, respectively. Davidson and Fadiran observed that fluorescence emission intensities could change by as much as 2.5 percent per degree Celsius [105]. Furthermore individual compounds show little predictive behavior as to which bands will be affected and to what extent each band emission may be suppressed. The multiple factors that affect the appearance of the observed spectrum must be carefully controlled to ensure reliable identification and quantification.

As mentioned previously oil samples are complex mixtures containing heterocyclic aromatic species. These heterocycles can act as charge transfer reagents and as a result

quench the fluorescence emission from the PAHs under study [98]. Petroleum mixtures are often not completely separated during chromatographic analysis. As an alternative to additional separations, selective fluorescence detection can be achieved through programming emission and excitation wavelengths [106].

Room temperature fluorescence often offers limited structural information. Depending on the ionization method chosen mass spectrometry can provide fragmentation patterns to assist in structural determination of the compound being investigated. This is most beneficial when coupled to a GC separation [107, 108]. Elizalde-Gonzalez *et al.* [109] reported the identification of over seventy PAH isomers using a methylsilicone capillary GC column and electron impact ionization. PAHs give a high abundance of molecular ions. This, coupled with characteristic fragmentation patterns, allows for isomeric identification of compounds. The separation of PAHs larger than benzo[*a*]pyrene and their alkyl derivatives was limited because their boiling points were higher than the maximum operating temperature of the stationary phase.

Liquid chromatography is a better choice for high molecular weight PAHs but is substantially more complicated to interface. APCI mass spectrometry detection and reversed phase LC separation were used [110, 111] to study PAHs in oil samples with molecular weights from 200-2000 m/z. The protonated molecule of the PAH was readily observed but little structural information can be ascertained from the spectra because of limited fragmentation. A comparison of several less conventional interfacing methods was done by Anacleto *et al.* [112]. In this comparison, a moving belt interface was examined but it proved of limited usefulness because of poor sensitivity for the volatile PAHs. Other limitations of moving belt interfaces have been discussed by Millington *et al.* [113]. It is obvious that a

single detection system will only partially fulfill the requirements of analysis imposed when studying complex samples. A multi-dimensional separation coupled to a multi-dimensional detection system is required to characterize the compounds in complex samples.

1.10 Particulate Extraction Methods

It is a requirement that the sample under investigation be in a form amenable to chromatographic separation. For air or diesel exhaust particulate matter, the compounds of interest must be extracted from the solid matrix into a dissolved form through solvent extraction. The extraction can be avoided if one used thermal vaporization into a GC port [114, 115] or laser desorption [116] followed by direct analysis in a mass spectrometer. Direct particulate analysis has not proven reliable for quantification. Environmental samples are complex matrices and require multiple chromatographic operations to separate overlapping analyte signals before single component quantification can be achieved. By far the most common primary step involves the extraction of the compounds from the particulate surface using solvents. The role of extraction is crucial in quantitative analytical methods because poor extraction recoveries introduce additional uncertainty in the results.

Many different extraction methods have been examined for the removal of PAHs and hydrocarbons from the surface of air particulates, soil, sludge, and waste water. The most prevalent techniques employed are solid phase extraction (SPE), Soxhlet, sonication, supercritical fluid extraction (SFE), microwave assisted solvent extraction (MASE), and pressurized fluid extraction (PFE). Soxhlet extraction is perhaps the benchmark or standard extraction used to assess the accuracy of alternative techniques. The comparison of different

extraction methods can be difficult. For example, Guerin [117] examined the extraction of PAHs from aged clay soil and reported that spiked samples were recovered quantitatively while the native PAHs were not using similar conditions. The author used multiple Soxhlet extractions with acetone/dichloromethane to establish the concentration of native PAHs in the soil. In addition, the rate of extraction for PAHs on aged particulates was much slower than for spiked surrogates. This underlies the danger when validating extraction methods. A validation of extraction methods using spiked samples may give low results when used for a real sample matrix. The need to use real samples to validate extractions becomes evident. However, certified standards still remain relatively unavailable either because of cost or supply and the necessity of careful sampling and storage to maintain certification.

SFE has been extensively investigated as an alternative to Soxhlet extraction. Extraction techniques such as Soxhlet extraction typically require 200-400 mL of chlorinated organic solvents. The recycling of such solvents presents a problem for extraction of trace components and disposal of such solvents continues to increase costs as environmental guidelines become more stringent. SFE coupled with CO_2 presents an attractive alternative. Morselli *et al.* reported on the use of SFE to extract PAHs from contaminated soil [118]. They found that the use of a polar modifier was required to extract PAHs at 75% efficiency. Furthermore, the modifier (acetone) was optimized to 5% of the total volume. Either higher or lower concentrations of modifier resulted in lower extraction yields. Burford *et al.* [119] compared SFE (CO_2/methanol) with sonication (dichloromethane) using an urban dust standard reference material (SRM) from the National Institute of Standards and Technology (NIST) (SRM 1649). Their results indicated that all of the PAHs were quantitatively extracted using SFE with CO_2 and methanol. Most extractions using supercritical CO_2

required some organic modifier. The role of the modifier is to enhance the solubility of larger compounds in the supercritical CO_2 as well as interact with the particulate matrix to increase desorption kinetics [120]. Often, these factors are sample specific which can make method development much more tedious and cumbersome. Both elevated temperatures and pressures are used during SFE operations. Langefeld *et al.* [121] investigated the effect of each of these parameters on the extraction of PAHs from air particulates. The results suggested that quantitative recoveries of PAHs from air particulates could be obtained with pure CO_2 at extreme extraction conditions (200 °C and 650 atm).

Compounds extracted with supercritical CO_2 must be trapped in either sorbent traps or a collection solvent. Solvent traps tend to lose low molecular weight or volatile components. Sorbent traps are difficult to design because the chemical or physical properties of a single stationary phase may not be amenable to a broad class of compounds [122]. In addition, the extraction of polar compounds requires the use of organic modifiers that may elute them from the trap. Stone and Taylor [123] investigated a pressurized collection vial and reported quantitative trapping for compounds as volatile as octane. Miller *et al.* [124] examined the use of solventless collection after rapid depressurization with greater than 90% collection efficiencies.

SFE works on the principle of elevated pressure and temperature to accelerate extraction kinetics. MASE and PFE also work with much the same principles except that an organic solvent is substituted for supercritical CO_2. MASE is very similar to PFE except for the method in which energy is incorporated into the extraction vessel [125]. PFE is much more convenient and represents much of the continued development in this area of extraction methods. One of the chief benefits of PFE is the reduction of extraction time with minimal

solvent usage. Dean [126] investigated PFE to extract PAHs from contaminated soil and was able to achieve quantitative results with a single 5 minute static extraction. Richter *et al.* [127] reported the use of PFE to extract PAHs from various reference materials with results equal to or better than Soxhlet extraction. Their results showed that quantitative extraction was possible with total solvent volumes 1.2 to 1.5 times that of the extraction vessel. Meney and coworkers [128] examined the extraction of low molecular weight PAHs from shale using PFE and discovered that prefilling the extraction vessel before heating increased recovery for these compounds. This leads to an important difference between Soxhlet and PFE extraction methods. Soxhlet extraction requires extended times scale (typically 12-24 hours) to achieve exhaustive extraction. Researchers [129] have shown that recoveries of low molecular weight PAHs such as phenanthrene reach a peak at short extraction times and recoveries diminish if extractions continue for longer intervals. This may result in incomplete extraction of all components of interest. PFE was observed to display slightly better efficiencies for large PAHs such as benzo[*g,h,i*]perylene from complex particulate matter without the loss of low molecular weight components [130]. One role for elevated pressures in PFE is to prevent the volatilization of the solvent held above its normal boiling point. However, studies have indicated a much more important role for pressure. Increased pressures were found to offer improved extraction rates and higher overall recoveries [131]. This was believed to result from the increased ability of the solvent molecules to diffuse into the pores and displace water that may have sealed the pore entrance.

1.11 Analysis of Nitro-PAHs

Nitro-PAHs are generally present at much lower concentrations in air and diesel exhaust particulates compared to their parent PAHs or methoxy substituted PAHs. For this reason the analysis of nitro-PAHs requires either several chromatographic steps to fractionate and enrich the concentration of nitro-PAHs in the particulate extracts or very selective and sensitive detection methods. In some cases a combination of these is required. Typically, either a reversed phase C18 separation or a capillary GC separation is used for analysis after a normal phase fractionation or cleanup of the sample. The amount of sample pretreatment is dependent upon the specificity of the analytical method for the target nitro-PAHs. There have been investigations that involved the analysis directly without sample pretreatment. However, most methods required at least one chromatographic cleanup separation of the extracts before analysis of the nitro-PAHs could be performed. Bezabeth *et al.* [132] used negative ion laser desorption and time of flight mass spectrometry to analyze diesel exhaust particulates directly, without extraction or sample cleanup. The authors conceded that the technique lacked the precision and accuracy for successful quantitation of nitro-PAHs in real samples.

Gas chromatography has been a popular method for the investigation of nitro-PAHs. Vincenti *et al.* [133] were able to use GC-negative ion chemical ionization (NICI) and tandem mass spectrometry without prior sample fractionation to analyze the nitro-PAHs in air particulates and soil extracts. The use of NICI provides additional selectivity compared to chemical ionization (CI) as compounds with electronegative substituents are preferentially ionized. Further selectivity is introduced with tandem mass spectrometry (MS/MS).

However, the authors cited that the presence of oxy-PAHs could cause difficulty with quantification depending on the concentration of such species relative to that of the nitro-PAHs.

The use of GC-MS coupled with NICI (without MS/MS) has also been investigated for the analysis of nitro-PAHs [133-135]. In each of these studies, a cleanup procedure was required to provide accurate quantitative results for the nitro-PAHs in both air and diesel exhaust particulate extracts. Typical detection limits for NICI GC-MS were on the order of 40 pg and a calibration curve of nitro-PAH standards was found be linear over 3 orders of magnitude. Korfmacher *et al.* [136] compared GC-MS negative ion atmospheric pressure chemical ionization (NIAPCI) and positive electron ionization (EI+). The NIAPCI was more selective than EI+ resulting in reduced cleanup requirements. The use of EI+ required two HPLC cleanup separations whereas the use of NIAPCI required only one. The main disadvantage to the use of NIAPCI was a limited linear range observed for 4-nitropyrene. The authors concluded that NIAPCI would be a poor choice for the quantitative analysis of nitro-PAHs. Jinhui *et al.* [137, 138] investigated a derivatization procedure that increased the electronegativity of the nitro-PAHs with heptafluorobutryic anhydride derivative. The authors used NICI-MS and an electron capture detector (ECD) to analyze the derivatized nitro-PAHs. The authors reported better relative precision for the GC-ECD compared to GC-MS (5.2% vs 21.7%) and comparable detection limits (~1 pg) between the two methods. The derivatives were found to have a higher thermal stability compared to the parent nitro-PAH. This is important because nitro-PAHs such as 1-nitropyrene have been shown [139] to degrade in the injection port, column, and heated transfer line associated with GC-MS.

Liquid chromatography is also popular for the analysis of nitro-PAHs in air and diesel exhaust particulate extracts. As with the GC methods, a cleanup separation of the sample is often required before LC analysis. Viegl *et al.* [140] used pyrenebutyric acid coupled to an aminopropyl stationary phase to pre-concentrate the nitro-aromatics. This was coupled to a reversed phase C18 separation and post-column reduction to the corresponding amine for fluorescence detection. A successful quantification of 1-nitropyrene at the picogram level was observed for diesel exhaust particulate extracts. The use of fluorescence detection required the reduction of the nitro group to the amine because nitro-PAHs do not fluorescence well. Several methods for reduction have been investigated [139, 141-144]. Reduction with chemical agents such as sodium borohydride has been shown to be less favorable than catalytic columns involving platinum and rhodium or the use of zinc powder. This is due to both the formation of reaction by-products and a general decrease in reduction efficiency associated with reduction using sodium borohydride. Catalytic columns that contain platinum and rhodium can be used for several months before replacement. Zinc reduction columns require frequent replenishment of the zinc powder. The consumption of the zinc dust can create voids in the column decreasing the chromatographic efficiency associated with on-line analysis. This is particularly the case with post column reduction. Typical detection limits [105, 139, 140] between 1-100 pg have been reported and linear calibration curves over three orders of magnitude.

The use of reversed phase LC coupled with chemiluminescence detection has been reported [141, 145, 146] to deliver better detection limits than fluorescence detection. Detection limits between 0.3-5 femtograms have been reported using commercial fluorescence detectors with the light source turned off. In addition, chemiluminescence tends

to be more selective than fluorescence detection. However, method development using chemiluminescence tends to be more labor intensive due to the increased number of experimental parameters that need to be optimized. Mass spectrometers have also been used with LC separations. Bonfanti *et al.* [147] developed a particle beam interface to analyze PAHs and nitro-PAHs. Good analytical precision was reported for the analysis of 1-nitropyrene but detection limits were only 100 pg. Williams and Perreault [148] exploited the loss of NO to monitor nitro-PAHs using electrospray and mass spectrometry. This technique required isocratic chromatographic conditions. Gradient elution resulted in non-optimized solvent conditions dramatically decreasing sensitivity.

1.12 Research Objectives

This research project had two main objectives. The first objective of this research project was the development of multi-dimensional chromatographic techniques for the identification of compounds in oils and tars. The analysis and characterization of a light gas oil was examined using four separation approaches listed below. A three-dimensional LC approach using either normal phase - reversed phase (monomeric) - reversed phase (polymeric) or normal phase - reversed phase (monomeric) - normal phase (TCP) was described. The power of combining multi-dimensional LC and multi-dimensional detection was also illustrated. Alternatively, two-dimensional methods LC-GC/MS, LC-LC/MS, and LC (DNBS)-SFC (DNBS) were investigated. One-dimensional SFC was used to characterize light gas oils using ultraviolet absorbance and laser excited fluorescence detection through a high-pressure flow cell designed by Dr. L. Ramaley. The second objective was to develop

a cleanup procedure for diesel exhaust particulate extracts that would allow identification and quantification of the priority PAHs and nitro-PAHs. The first step in each method involved the extraction of the particulate samples using pressurized fluid extraction. Subsequently, the extracts were fractionated using a normal phase separation with a DNBS stationary phase. Each of the quantification methods was examined to provide reliable data for the priority PAHs and nitro-PAHs. A SFC separation using an aminopropyl column was investigated to analyze the priority PAHs and nitro-PAHs with prior sample fractionation. The protocol listed below outlines the analytical methods used to accomplish the objectives.

The following four schemes were investigated for the multi-dimensional analysis of light gas oils:

(1) One-dimension

(1.1) SFC

(2) Two-dimensions

(2.1) LC (normal phase/reversed phase) –GC/MS;

(2.2) LC-SFC;

(3) Three-dimensions

(3.1) LC (normal phase) - LC (reversed phase) – LC (reversed phase or normal phase).

Additional dimensions were added through selective detection:

UV absorption and fluorescence for LC and SFC;

MS / APCI for LC;

MS / EI for GC.

Quantification of the priority PAHs was facilitated through the following methods:

(1) LC(DNBS)-LC/laser excited fluorescence

(2) LC(DNBS)-GC/MS

(3) SFC/laser excited fluorescence

Quantification of the nitro-PAHs was facilitated through the following methods:

(1) LC(DNBS)-LC(C18) zinc reduction/fluorescence detection

(2) SFC/laser excited fluorescence detection

Chapters 2 through 5 of this thesis focus primarily on the characterization of chromatographic methods suitable for the analysis of light gas oils provided through a collaboration with Syncrude Canada. Chapters 2 and 3 are principally oriented to one-dimension separations of the oils into classes based on the number of rings in the aromatic compound. Chapter 2 characterizes four stationary phases suitable for the normal phase fractionation of aromatics using liquid chromatography (LC) and diode array detection. Chapter 3 characterizes the same stationary phases for aromatic separations using supercritical fluid chromatography (SFC). This chapter also introduces a laser excited fluorescence instrument with a charge coupled device (CCD) array detector suitable for the acquisition of high-resolution fluorescence spectra. Chapters 4 and 5 introduce the potential of multi-dimensional chromatography. Chapter 4 examines two-dimensional chromatography and Chapter 5 explores three-dimensional methods.

Chapter 2 Single Dimension Normal Phase Chromatography

2.1 Introduction

Most multi-dimensional chromatographic procedures that have been reported to date have used a normal phase separation as the first dimension. The goal of the first separation is to fractionate the sample according to aromatic class as defined by the number of aromatic rings present in the compound. The ability of a single stationary phase to effect a class separation depends on the role that alkyl substitution plays in the retention mechanism. Hydrotreated oil products typically contain very large numbers of highly substituted small aromatics that cause the group separation to fail due to overlap with less substituted higher aromatic classes. The use of electron donor-acceptor interactions have been discussed in the literature as a means to separate large polars from heavy crude extracts [149]. These compounds are insoluble in typical normal phase solvents such as hexane and dichloromethane and require much more powerful eluents such as *o*-xylene. Therefore, strong interactions with the stationary phase are required to produce reasonable separations between components with such high eluent strengths. The DNBS stationary phase is an example of a stationary phase that can act as an electron acceptor. The donor-acceptor relationship between the PAH and the column increases with the number of aromatic rings and should provide better group separation compared to standard stationary phases such as silica or aminopropyl.

2.2 Experimental

2.2.1 Apparatus

A schematic of the multi-dimensional LC experimental system is shown in Figure 2.1. The system consisted of three individual chromatographic modules. Each module could be operated as a stand-alone off-line system or combined and integrated for on-line analysis. System 1, was comprised of an Agilent Model 1100 quaternary HPLC pump, a Rheodyne 7725i injection valve (shown as A), a chromatographic column (silica, aminopropyl, DIOL, or DNBS), an Agilent Model 1100 diode array detector or a laser excited fluorescence array detector, and a Gilson FC-80K fraction collector. System 2 consisted of an Agilent Model 1100 binary gradient pump, either a Rheodyne 7000 switching valve or a Rheodyne 7725I injection valve (shown as B) with one of a 20, 50, or 100 microliter sample loop, a Supelcosil LC18 column (25 cm x 4.6 mm), and either a laser excited fluorescence array detector or a Fisons Quattro mass spectrometer with a Quattro II APCI source.

The laser excited fluorescence array detector consisted of a Kimmon Model IK5451R-E He-Cd laser (325 nm and 442 nm) or a Uniphase Model NV 20001-100 pulsed solid state laser (266 nm), a 7 microliter capillary flow cell fabricated in-house, a bifurcated fiber optic bundle that coupled the flow cell to an Acton Research Model 150 monochromator, and a Princeton Instruments Model TE/CCD-1024-MI CCD camera controlled by a Princeton Instruments ST-1509 controller. Data collection and processing were done using Windows based personal computers with software written in-house.

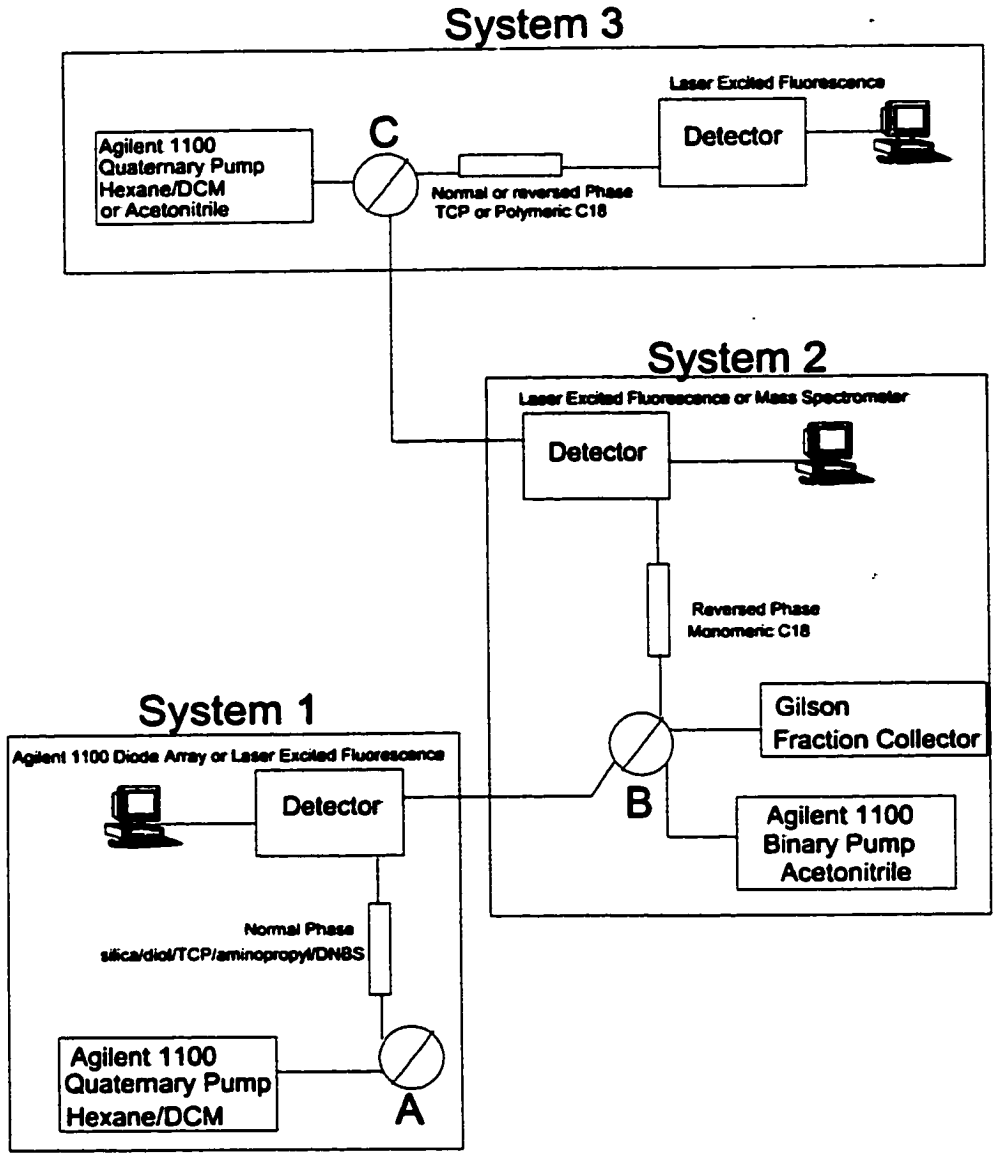

Figure 2.1 Multidimensional Chromatographic Apparatus. Three separate systems are defined in the figure. System 1 was used exclusively for normal phase separations. System 2 was used for reversed phase separations. System 3 was used for either normal phase or reversed phase separations.

System 3 consisted of an Agilent Model 1100 quaternary gradient pump, either a Valco Model EMTCST6UW with electronic actuator and 6 sample loops (50 or 100 microliter) or a Rheodyne 7725i injection valve with a 20 microliter sample loop (shown as C), a Vydac Model 201TP54 column (25 cm x 4.6 mm) immersed in an ice/water bath or a TCP column (25 cm x 2.0 mm) prepared in-house, and a laser excited fluorescence array detector. Although all three chromatographic systems could be integrated for on-line analysis, the majority of the experiments were performed off-line using a fraction collector. The rationale behind this decision is discussed in detail in chapter 5.

2.2.2 Chemicals

Light gas oil samples were provided by Syncrude Canada and used as received. Pesticide grade dichloromethane, Optima grade hexane and acetonitrile were provided through Fisher Scientific. PAH standard solutions were prepared from compounds purchased from Sigma-Aldrich and used without further purification. The compounds hexyl- through ethyl-naphthalene were obtained from Professor J. Stuart Grossert.

2.2.3 Procedures

The first dimension in our chromatographic scheme was a normal phase separation. Five stationary phases were examined in an attempt to ascertain which would be the most useful as the initial separation of the sample. A DIOL column (Supelco, 25 cm x 6.2 mm), an aminopropyl column (Supelco, 25 cm x 4.6 mm), a silica column (Supelco, 25 cm x 10.0

mm), and a dinitrobenzenesulfonyl (DNBS) aminopropylsilica column (25 cm x 4.6 mm) were tested. The DNBS column was prepared in-house using a procedure adapted from the literature [22]. Specifically, a Supelco 25cm x 4.6 mm LC-NH_2 column was derivatized by passing a solution of 100 mM 2,4-dinitrobenzenesulfonylchloride (Aldrich) in acetone/5% sodium bicarbonate through the column (0.2 mL/min) overnight using a Constametric Series III HPLC pump. The column was washed with 50 mL volumes of acetone, water, acetonitrile, dichloromethane, and hexane. The TCP column (25 cm x 2 mm) was prepared according to a synthetic procedure adapted from the literature [75]. Each phase was characterized by measuring retention times for a series of standards and by injecting a light gas oil as a real sample. Chromatographic system 1 was used for all four of the stationary phases examined. The DIOL and aminopropyl stationary phases were used with hexane as the mobile phase. The DNBS column was more retentive than either of these columns so a linear gradient was developed to elute the compounds. The gradient is given in Table 2.1. A step gradient was used with the silica column to obtain better precision between chromatographic runs. The conditions are given in Table 2.2. Each column was then reequilibrated after gradient elution for an additional 5 minutes using hexane.

Table 2.1: Gradient used for elution of oils from DNBS column.

Time (minutes)	Hexane (percent)	Dichloromethane (percent)
0 – 20	100	0
20 – 40 (linear gradient)	0	100

Table 2.2: Gradient used for elution of oils from silica column.

Time (minutes)	Hexane (percent)	Dichloromethane (percent)
0 – 30	100	0
30 (step gradient)	0	100
40	0	100

2.3 Characterization of First Chromatographic Dimension

The four stationary phases studied for the fractionation of the oil by aromatic ring number involved only normal phase separations. In the process of determining which stationary phase would provide the best means to fractionate the oil several criteria will be explored. Principally, the separation must be capable of resolving the oil into distinguishable fractions. The retention characteristics of the column should be reproducible and predictable. The oil contains compounds that do not have standards available for comparison. If the retention profile of the stationary phases is suitably characterized and predictable, then inferences can be made about the structure of an unknown compound present in the sample. Although important, analysis times were not a fundamental consideration in selecting the first dimension separation. The final consideration in the analysis of the first dimension was column capacity. Since each of the columns except for the aminopropyl and DNBS columns used in this study has different column diameters, the capacity of each column will be affected accordingly. Specifically, based on column dimensions alone, the capacity of each column would follow the order silica > DIOL > aminopropyl ≈ DNBS > TCP. It is important to

maintain high sample loading capacity in order to avoid compromising sensitivity in the second and third dimensional separations. Sample loading capacity becomes less important with off-line fraction collection. However, reduced sample loading capacities will increase the number of required replicate collections. This not only increases the labor required but also increases the opportunity for operator error.

A preliminary characterization of each stationary phase was done with standard compounds. This will facilitate the characterization of each stationary phase according their respective ability to fractionate according to aromatic ring number, the time for analysis, and the retention mechanism. The retention times for each compound on each stationary phase are listed in Table 2.3. The k' values listed in this table do not represent true values according to the conventional definition. For the purpose of this discussion, k' was defined as:

$$k' = (t_r - t_b)/ t_b \qquad [2\text{-}1]$$

where t_r, represents the retention time for the compound and t_b represents the retention time for benzene. Benzene was chosen because it was the least retained compound with respect to PAHs and for the fact that it is readily detected with a diode array detector.

The data in Table 2.3 suggest that the strength of the stationary phase increases in the order diol (k' 0.01 to 0.68) < silica (k' 0.28 to 2.47) < aminopropyl (k' 0.17 to 3.44) < DNBS (k' .0.4 to 6.56). The objective of the first dimension in a multidimensional separation is to separate the aromatic compounds by the number of rings or by the number of pi electrons in the molecules. Under ideal circumstances the effect of alkyl substitution should be small and not cause overlap between classes of aromatic compounds. Inspection of the data in Table 2.3 indicates that group separation was possible using the diol, aminopropyl, and DNBS stationary phases but the silica column showed a strong overlap between the phenanthrene

and pyrene series of compounds. The limited separation strength of the diol stationary phase suggests that the phase would be unsuitable for a very complex sample such as a light gas oil. The DNBS stationary phase was prepared by the reaction between dinitrobenzenesulfonyl chloride and the aminopropyl functional group of a commercial column. It is interesting to compare the retention behavior of the two columns. The retention characteristics of the two stationary phases are similar within groups but the effect of alkyl substitution on the retention is stronger for the DNBS column than for the aminopropyl column. This could be expected because the electron donating ability of the alkyl groups into the aromatic rings would have a greater effect for a donor-acceptor mechanism than for a dipole-dipole interaction. The addition of one or two methyl groups to phenanthrene increases the retention for both phases but the increase is much greater for the DNBS phase. For both phases the addition of a methylene group to form the cyclopenta ring decreases the retention such that the compound elutes before the parent compound. This is probably because the hybridization of the methylene group adds strain to the ring system and also introduces a steric hindrance to the overlap of the pi system between the analyte and the DNBS phase. The alkyl substituted pyrene series of compounds also shows an increased retention with the addition of electron donating groups onto the rings. The addition of ethyl groups lowers the retention time such that the elution order becomes the parent compound <ethyl substituted compounds< methyl compounds. The decrease in retention time for the addition of ethyl groups probably results from two effects–the increased solubility of the compound in the mobile phase and a steric hindrance.

A stronger stationary phase was prepared using tetrachlorophthalimide bonded to a silica support using a propyl linkage. The retention times and k' values for a series of

naphthalenes, phenanthrenes, and pyrenes are shown in Table 2.4. The data for the naphthalenes shown in this table used isocratic conditions with pure hexane whereas the phenanthrenes and pyrenes were done using 30% dichloromethane in hexane. First, if the k' data for DNBS are compared with the TCP stationary phase for the naphthalenes we see that the phase is considerably stronger–k' for naphthalene on the TCP column is 3.71 whereas it was only 0.69 on the DNBS. The range for naphthalenes is 0.43 to 1.23 on the DNBS and 2.14 to 17.28 for the TCP. Both phases show a similar behavior with respect to the addition of methylene groups to side chains–the addition of a methylene group decreases the retention time. The data for the phenanthrenes and pyrenes indicates that the TCP phase is very sensitive to both the presence and position of alkyl substituents. The addition of methylene groups decreases the retention times to a very significant degree such that diethylpyrene would elute in the phenanthrene region of a chromatogram. This suggests that the TCP phase would not be suitable for a first dimension separation based on the number of aromatic rings. The next section of this Chapter will look at the actual fractionations possible using a real Light gas oil as as the sample and the four stationary phases aminopropyl, silica, diol and DNBS.

2.4 Normal Phase Separation of Light Gas Oil MB13C (First Dimension)

In order to further characterize the fractionation of oils, each stationary phase was tested using a light gas oil MB13C provided by Syncrude Canada. Nominally, this light gas oil contains compounds with boiling points less than 340 C. This light gas oil has been subjected to upgrading processes. These processes tend to reduce the aromaticity of the oil

Table 2.3: Retention data using standards for normal stationary phase characterization. Retention times are in minutes. Benzene was used to establish relative k' values for each individual column.

Compound	Silica t_r (k')	DIOL t_r (k')	Amino (k')	DNBS t_r (k')
Benzene	7.72 (0)	6.03 (0)	3.86 (0)	3.63 (0)
Biphenyl	14.31 (0.85)	6.69 (0.11)	5.53 (0.43)	6.91 (0.90)
Naphthalene	10.12 (0.31)	6.42 (0.06)	4.62 (0.20)	6.15 (0.69)
2,3,5-trimethylnaphthalene	13.84 (0.79)	6.08 (0.01)	5.14 (0.33)	8.10 (1.23)
1-hexylnaphthalene	9.86 (0.28)	9.86 (0.64)	4.50 (0.17)	5.19 (0.43)
Phenanthrene	15.03 (0.94)	7.67 (0.27)	7.52 (0.95)	13.92 (2.83)
2-methylphenanthrene	17.10 (1.22)	7.42 (0.23)	7.54 (0.95)	14.43 (2.98)
3,6-dimethylphenanthrene	18.92 (1.45)	7.25 (0.20)	7.82 (1.03)	16.11 (3.43)
4H-cyclopenta[*def*]phenanthrene	15.45 (1.00)	7.42 (0.23)	7.33 (0.90)	13.37 (2.68)
Pyrene	14.80 (0.92)	8.25 (0.37)	8.85 (1.29)	18.25 (4.02)
1-methylpyrene	16.52 (1.14)	8.16 (0.35)	9.36 (1.42)	22.23 (5.12)
1-ethylpyrene	15.95 (1.07)	8.00 (0.33)	8.95 (1.32)	18.76 (4.16)
1,8-diethylpyrene	16.83 (1.18)	*ND	8.16 (1.11)	20.96 (4.77)
Chrysene	23.85 (2.09)	9.17 (0.52)	13.86 (2.59)	26.31 (6.25)
Benzo[*a*]pyrene	23.85 (2.09)	10.16 (0.68)	17.14 (3.44)	27.47 (6.56)
7-methylbenzo[*a*]pyrene	26.75 (2.47)	9.75 (0.62)	16.89 (3.38)	27.86 (6.67)

* Not Done

Table 2.4: Retention data for TCP Column.

30/70% Hexane-DCM Eluent		**100% Hexane Eluent**	
Compound	**t_r(k')**	**Compound**	**t_r(k')**
Benzene	1.70 (0)	Hexylnaphthalene	5.33 (2.14)
Fluorene	2.85 (0.62)	Butylnaphthalene	5.75 (2.38)
9-ethylfluorene	2.63 (0.55)	Propylnaphthalene	6.00 (2.53)
Phenanthrene	4.67 (1.75)	Ethylnaphthalene	7.58 (3.46)
9-ethylphenanthrene	4.26 (1.51)	Naphthalene	8.00 (3.71)
2-methylphenanthrene	5.25 (2.09)	1-methylnaphthalene	11.58 (5.81)
4H-cyclopenta[*def*]phenanthrene	6.42 (2.78)	1,2-dimethylnaphthalene	20.00 (10.76)
3,6-dimethylphenanthrene	5.75 (2.38)	1,4-dimethylnaphthalene	15.17 (7.92)
Retene	3.77 (1.22)	1,8-dimethylnaphthalene	19.25 (10.32)
Pyrene	10.50 (5.18)	1,6-dimethylnaphthalene	17.25 (9.15)
1-methylpyrene	14.92 (7.78)	2,3,5-trimethylnaphthalene	31.08 (17.28)
1-ethylpyrene	9.08 (9.08)		
1,8-diethylpyrene	6.42 (2.78)		

by reduction of aromatic bonds. The resulting mixture is generally limited to aromatic species of one to four aromatic rings and the concentration distribution is mono > di- > tri- > tetra-aromatic rings. This increases the difficulty of fractionating the oil cleanly.

Array detectors can be used with single dimension chromatographic separations to provide an additional dimension of information – the UV or fluorescence spectrum of the compound. For the stationary phase characterization two wavelengths were used to display the chromatograms – 254 nm suitable for general aromatics and 336 nm, a wavelength that emphasizes pyrenes and alkylated pyrenes. The chromatogram for the light gas oil on the diol column and associated spectra are shown in Figures 2.2 and 2.3, respectively. Inspection of the chromatograms in Figure 2.2 shows that there is minimal separation of the compound classes, confirming the earlier conclusions that the diol column offers inadequate resolution to effect a reasonable fractionation. In addition, the chromatograms in Figure 2.2 result from a five-microliter injection of light gas oil. This suggests that, even though the diol stationary phase possessed a large column diameter, the column had a low sample loading capacity.

The separations of the MB13C oil and a standard mixture on the silica column are shown in Figure 2.4 and the accompanying spectra are shown in Figure 2.5. The trace at 336 nm tends to emphasize pyrene and alkylated pyrene components whereas the chromatogram at 254 nm is representative of a broader range of compounds. The spectrum associated with the peak at 11.5 minutes is superimposed with that of pyrene. The poor agreement between these spectra suggests that several aromatic classes were co-eluting with pyrene. This confirms that a class fractionation may not be viable. Furthermore, the chromatogram at 254 nm extends to longer retention times than that of the chromatogram resulting from 336 nm. This suggests that compounds with a lower aromatic group number

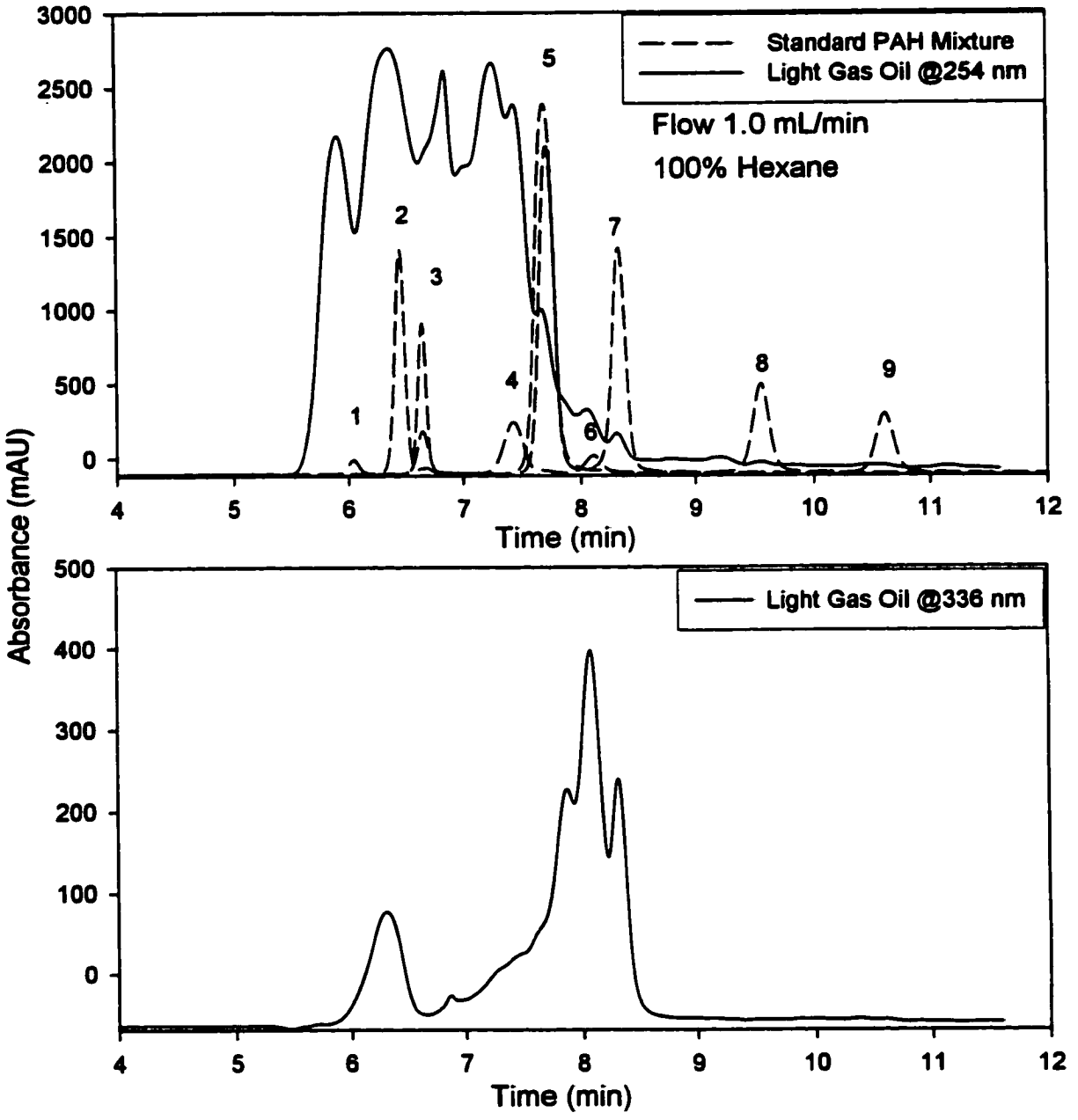

Figure 2.2: LC Chromatogram of a Light Gas Oil (MB13C) separated on the diol column using UV detection at 254nm and 336 nm. A standard PAH mixture was superimposed to characterize the separation. Experimental conditions are given in the figure.

Peak Identification: 1 benzene, 2 naphthalene, 3 biphenyl,
4 cyclopenta[*d,e,f*]phenanthrene, 5 phenanthrene, 6 1-methylpyrene, 7 pyrene,
8 chrysene, 9 benzo[*a*]pyrene

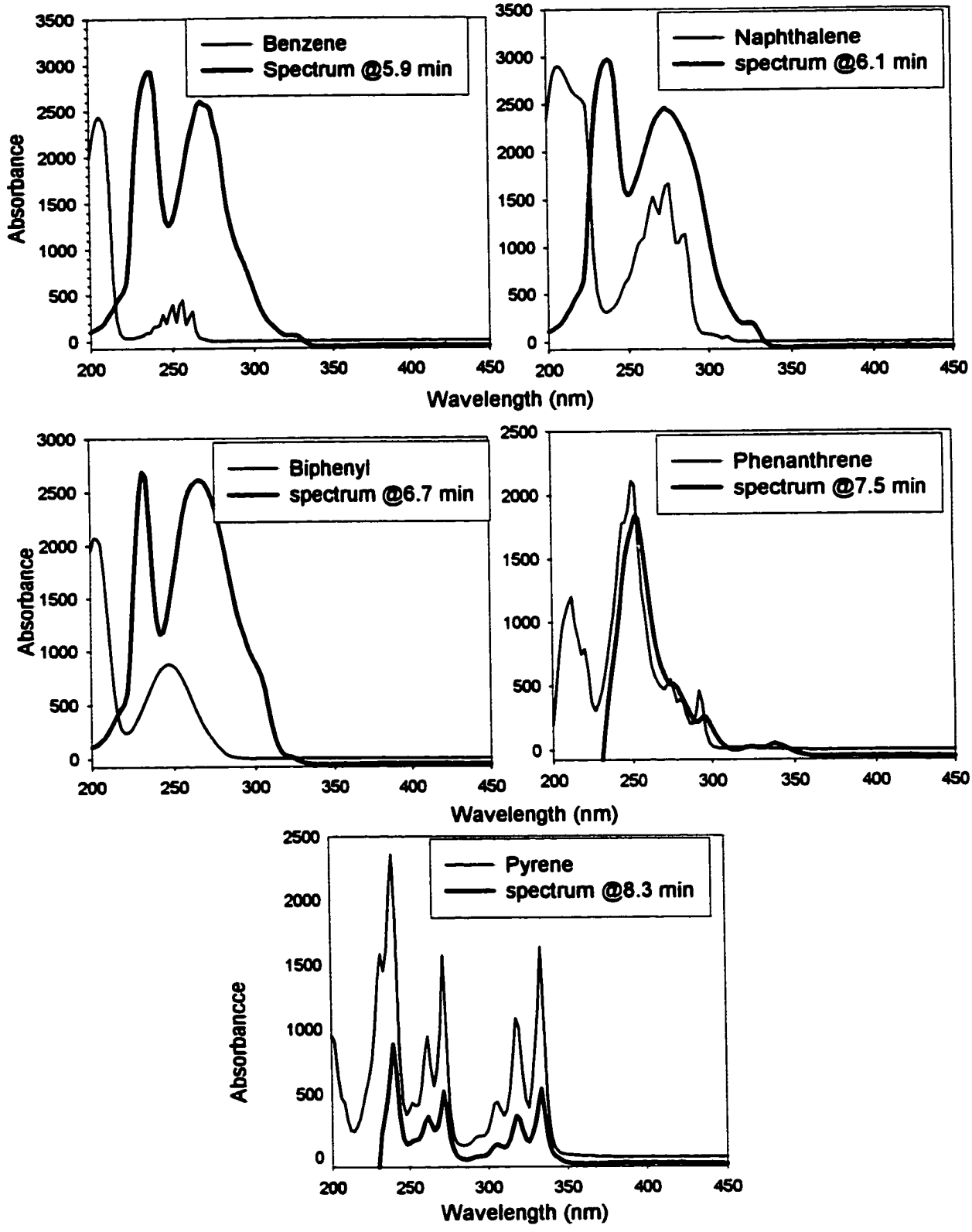

Figure 2.3: Ultraviolet spectra from diol LC separation superimposed with standard spectra. The units of the ordinate scale are mAU.

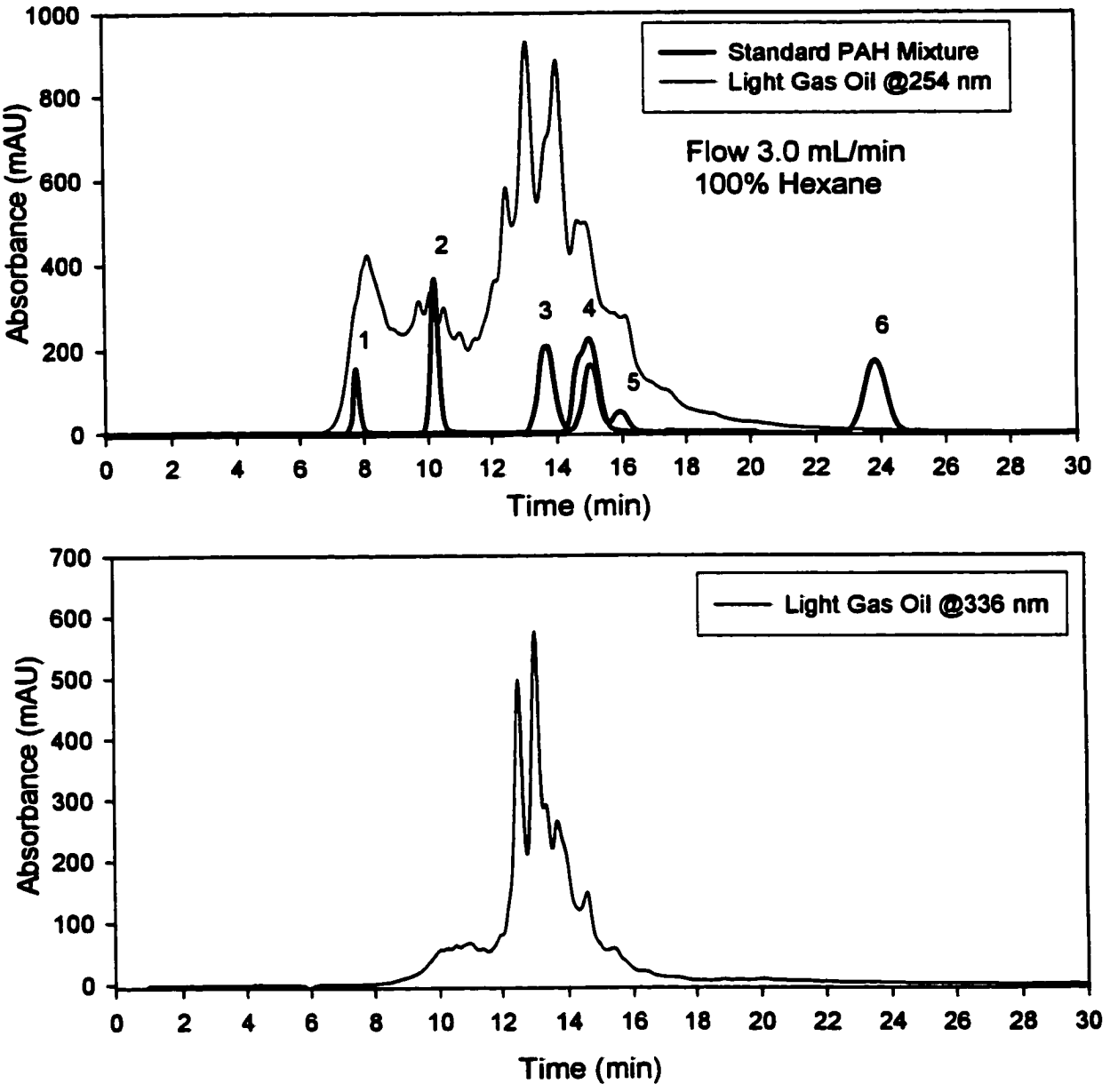

Figure 2.4: LC Chromatogram of a Light Gas Oil (MB13C) separated on silica column using UV detection at 254nm and 336 nm. A standard PAH mixture was superimposed to characterize the separation. Experimental conditions are given in the figure.

Peak Identification: 1 benzene, 2 naphthalene, 3 biphenyl, 4 phenanthrene, cyclopenta[*d,e,f*]phenanthrene, pyrene, 5 1-methylpyrene, 6 chrysene, benzo[*a*]pyrene

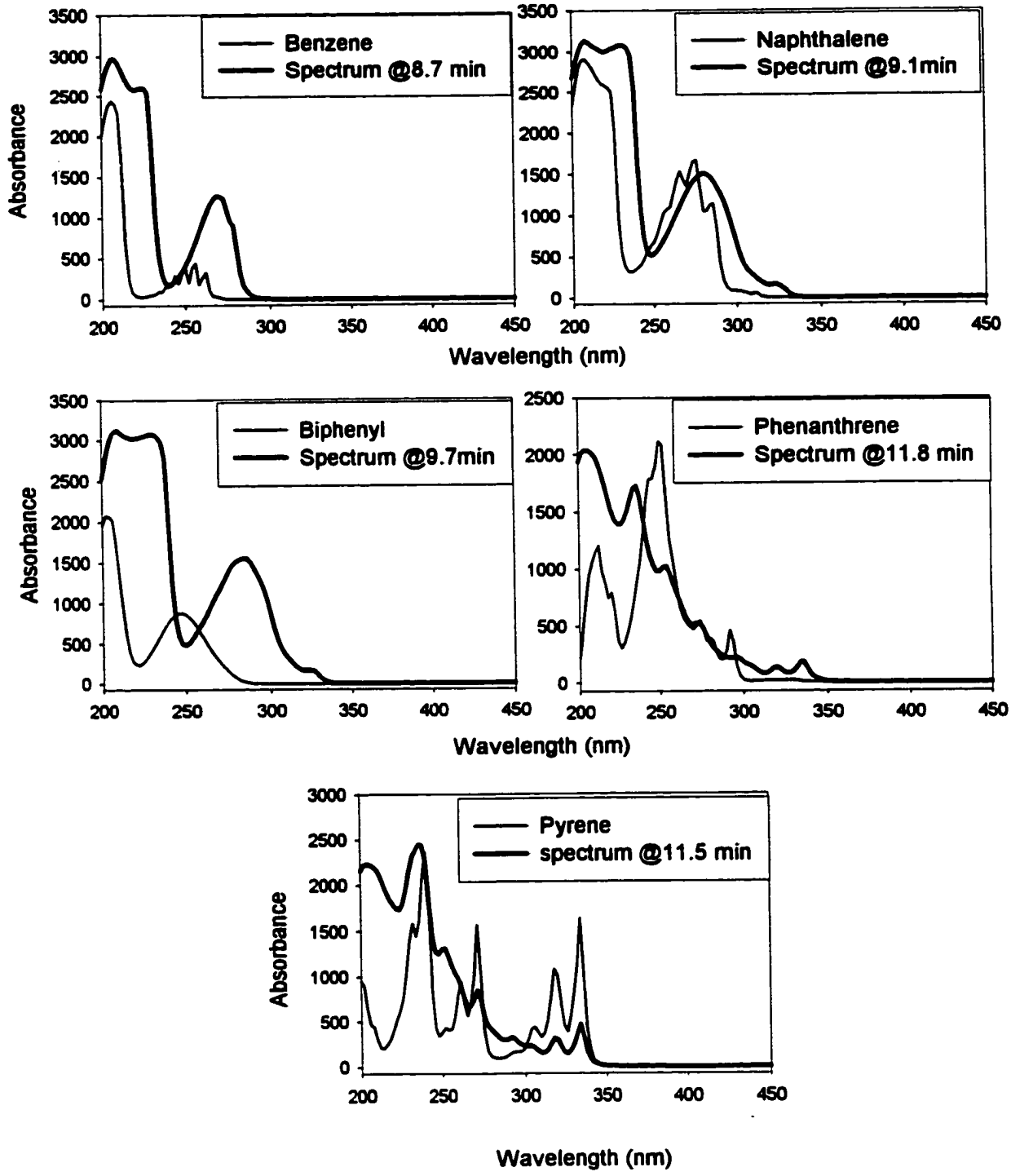

Figure 2.5: Ultraviolet spectra from silica LC separation superimposed with standard spectra. The units of the ordinate scale are mAU.

elute after pyrene and alkylated pyrenes. This observation is a result of the strong dependence of the silica retention mechanism to alkyl substitution and the large number of aliphatic substituents associated with processed oil. A comparison of the standard chromatogram and the chromatogram at 336 nm for the oil suggest a discrepancy with respect to the retention times between like compounds. For example, the retention time for pyrene appeared to differ by almost two minutes for the standard and pyrene in the light gas oil. In the oil pyrene eluted earlier than in the standard. This arises due to the complexity of the oil sample relative to the standard mixture. The use of a dichloromethane gradient provided reproducible retentions for either the standards or the oil, but a shift between sample and the standard was still observed. This is may be partially due to column overloading in the oil sample and also may result from the large numbers of aliphatic compounds in the oil adsorbing onto active silanol sites thereby decreasing the retention of the PAHs.

Similar separations of the light gas oil superimposed with standards are shown in Figure 2.6 and Figure 2.8 for the aminopropyl and DNBS columns, respectively. The corresponding spectra from each separation are shown in Figure 2.7 and Figure 2.9. Each of these columns separates the oil into fractions better than either the silica or diol columns. The greatest resolution between aromatic classes was observed for the DNBS stationary phase. As well, the 336 nm chromatograms in each figure suggest that the different pyrene species are much more resolved on the DNBS separation compared to the aminopropyl. This will allow the collection of multiple fractions within an aromatic class. This should result in better resolution with the second dimension chromatographic methods. The spectra for each region appear to follow characteristics associated with that particular aromatic class. This suggests that there is less overlap between aromatic classes for the aminopropyl and DNBS

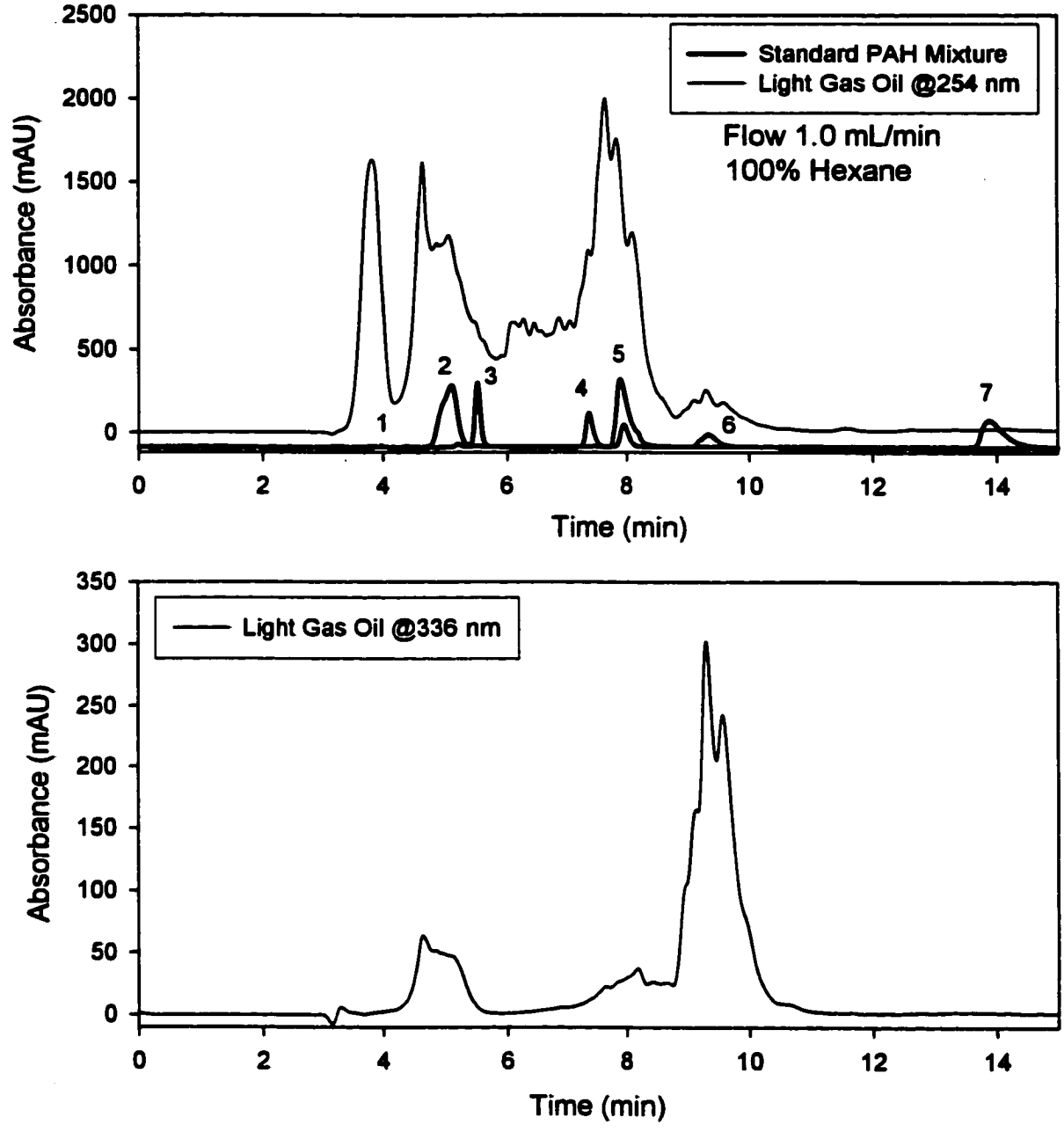

Figure 2.6: LC Chromatogram of a Light Gas Oil (MB13C) separated using the aminopropyl column with UV detection at 254nm and 336 nm. A standard PAH mixture was superimposed to characterize the separation. Experimental conditions are given in the figure.

Peak Identification: 1 benzene, 2 naphthalene, 3 biphenyl,
4 cyclopenta[*d,e,f*]phenanthrene, 5 phenanthrene, 6 pyrene, 7 chrysene

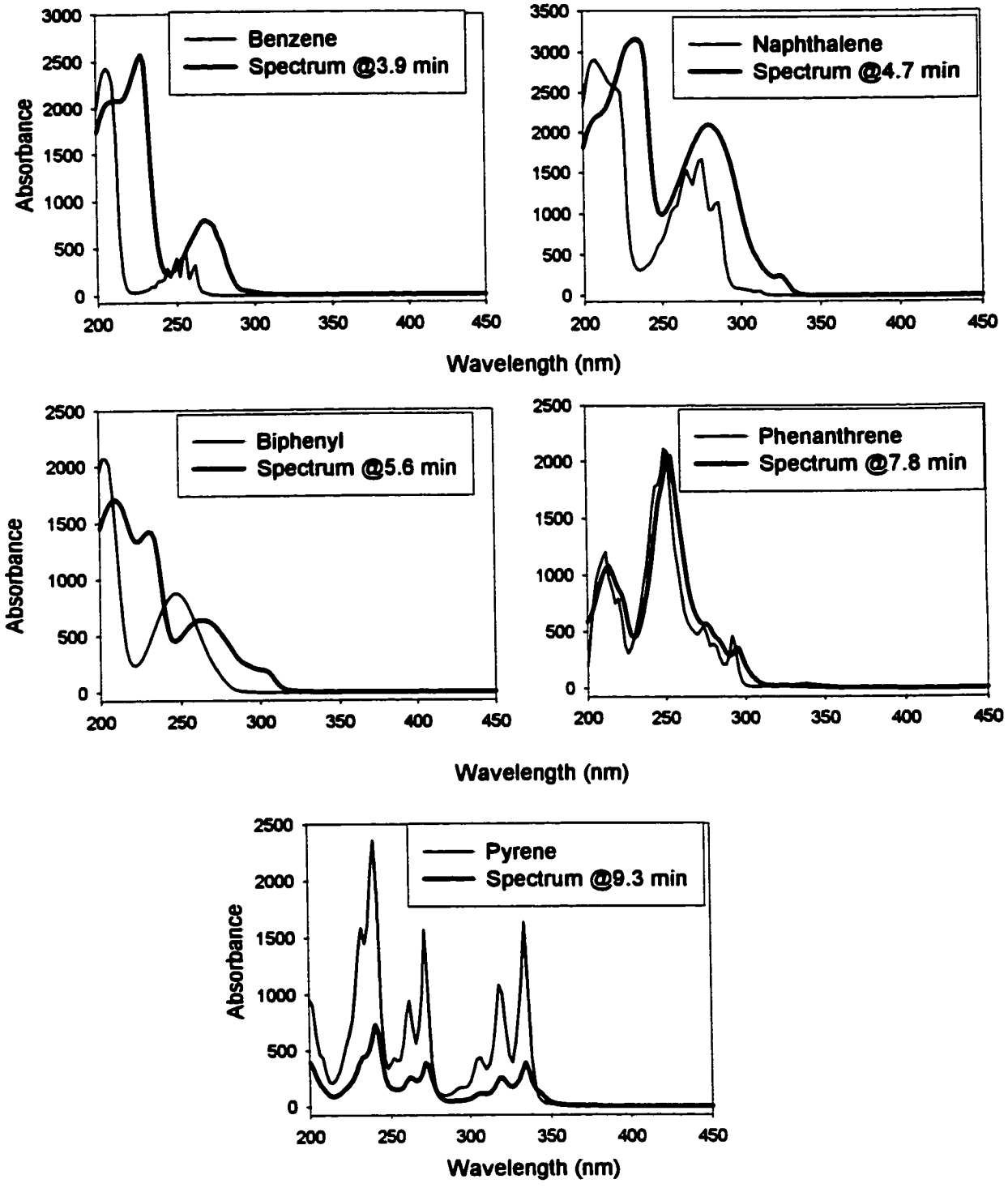

Figure 2.7: Ultraviolet spectra from LC aminopropyl separation superimposed with standard spectra. Units of the ordinate axis are mAU.

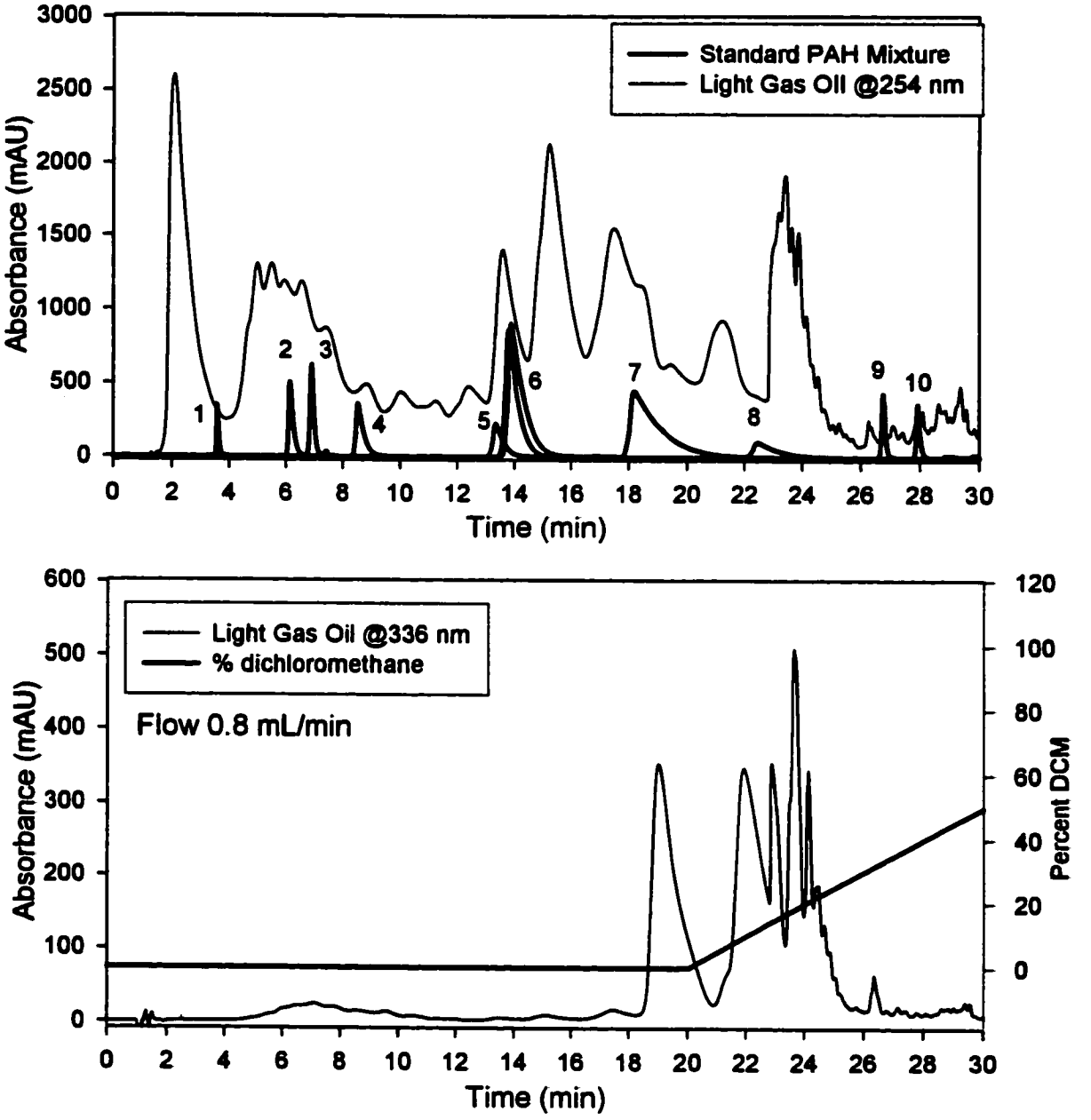

Figure 2.8: LC Chromatogram of a Light Gas Oil (MB13C) separated on DNBS column using UV detection at 254nm and 336 nm. A standard PAH mixture was superimposed to characterize the separation.

Peak Identification: 1 benzene, 2 naphthalene, 3 biphenyl, 4 2,3,5-trimethylnaphthalene, 5 cyclopenta[*d,e,f*]phenanthrene, 6 phenanthrene, 7 pyrene, 8 1-methylpyrene, 9 chrysene, 10 benzo[*a*]pyrene

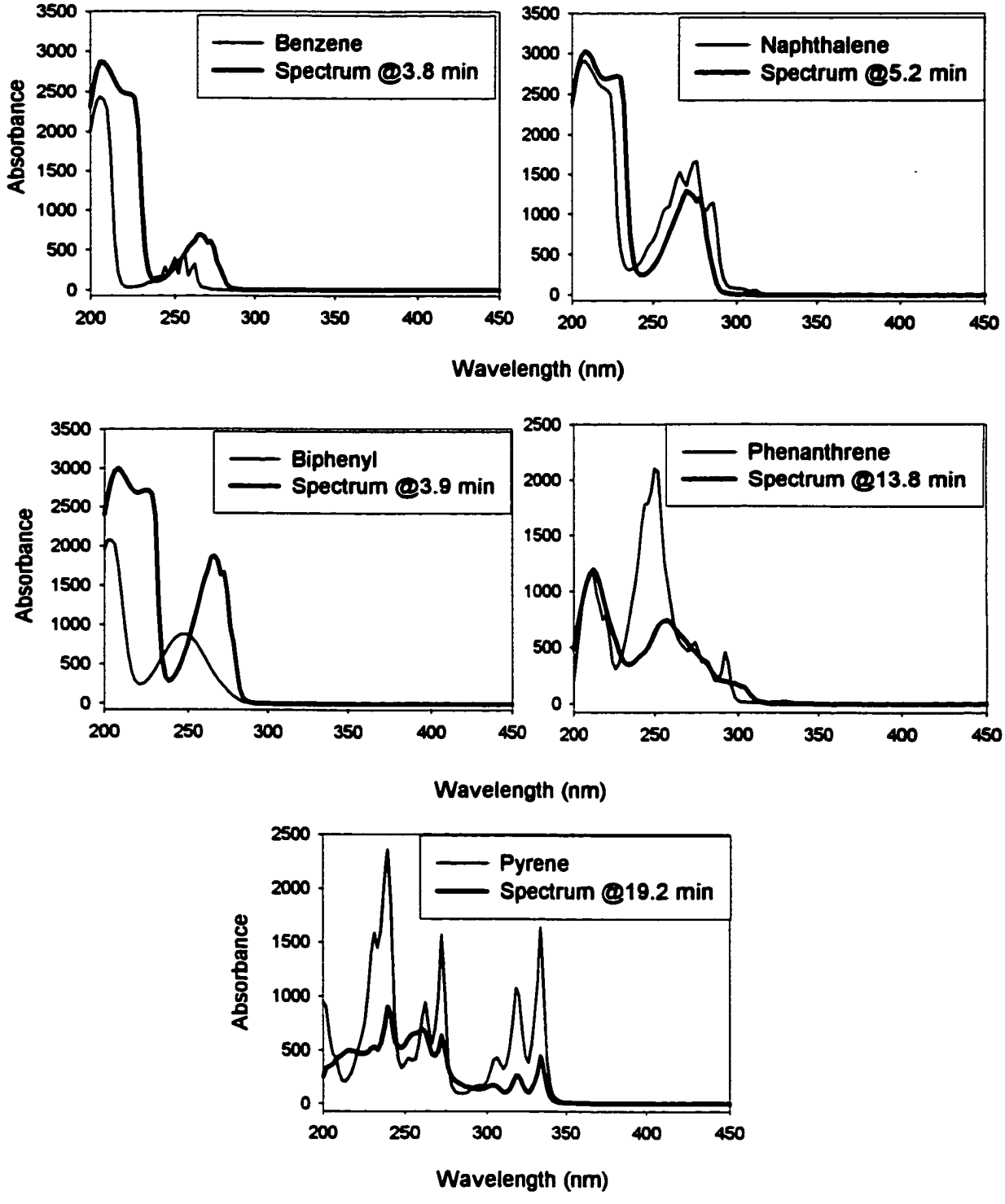

Figure 2.9: Ultraviolet spectra from LC-DNBS separation with standards spectra. The units of the ordinate scale are mAU.

columns compared to the silica and diol separations. As with the silica column, there appears to be some slight discrepancy with respect to retention between like compounds in the oils and standards. The effect was slightly more pronounced for the DNBS column than for the aminopropyl separation. In either case, the effect was much less than that observed for the silica separation.

The final factor to be examined for each stationary phase was column capacity. Figure 2.10 displays the light gas oil MB13C separated on the silica column using injection volumes of 5, 20, 50, and 100 microliters. These chromatograms suggest a loss of resolution and decreasing retention times with increasing injection volume. At 100 microliter injection volumes the detector begins to overload giving an exaggerated effect of resolution loss. It would appear that the maximum capacity for this column would be between 50 and 100 microliters. Figure 2.11 shows the chromatograms that result from 5, 20, 50, and 100 microliter injections of the light gas oil MB13C on the DNBS column. The column appears to exhibit signs of overloading with the 50 microliter injection volume. There appears to be some small loss of resolution as the injection volume was increased from 5 to 20 microliters. For the purposes of collecting fractions, 20 microliter injections were considered the maximum capacity for this column. In a similar manner 5 and 20 microliter injections of MB13C were separated with the aminopropyl column. Figure 2.12 displays chromatograms that result. From these chromatograms it is obvious that 5 microliters is the maximum injection volume. This is interesting as the aminopropyl and the DNBS have the same column dimensions. The more retentive nature of the DNBS improves the column loading capacity compared to the aminopropyl stationary phase from which it is derived.

The DNBS column offers better resolution and selectivity than the silica, diol,

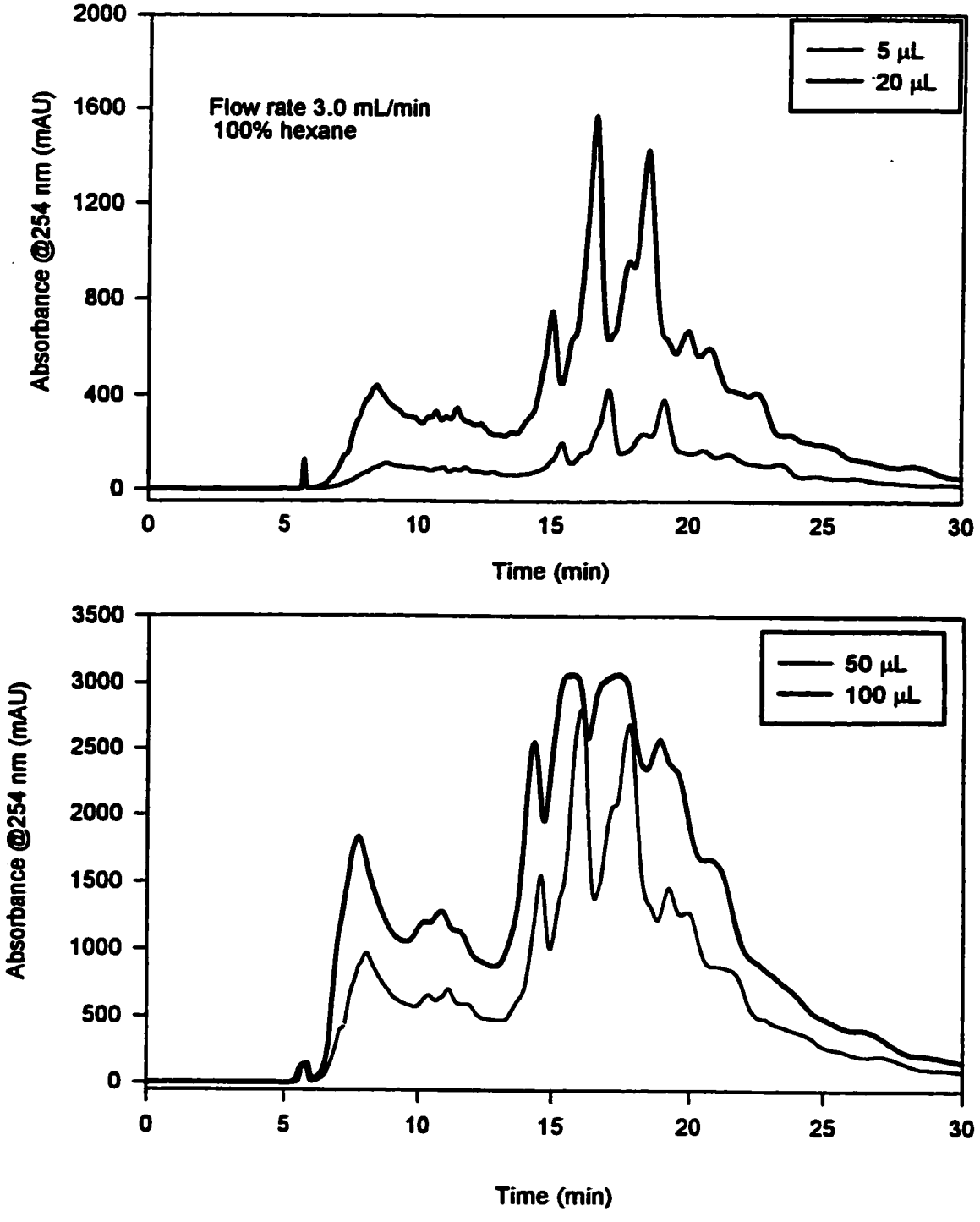

Figure 2.10: LC chromatograms at various injection volumes separated using the silica column.

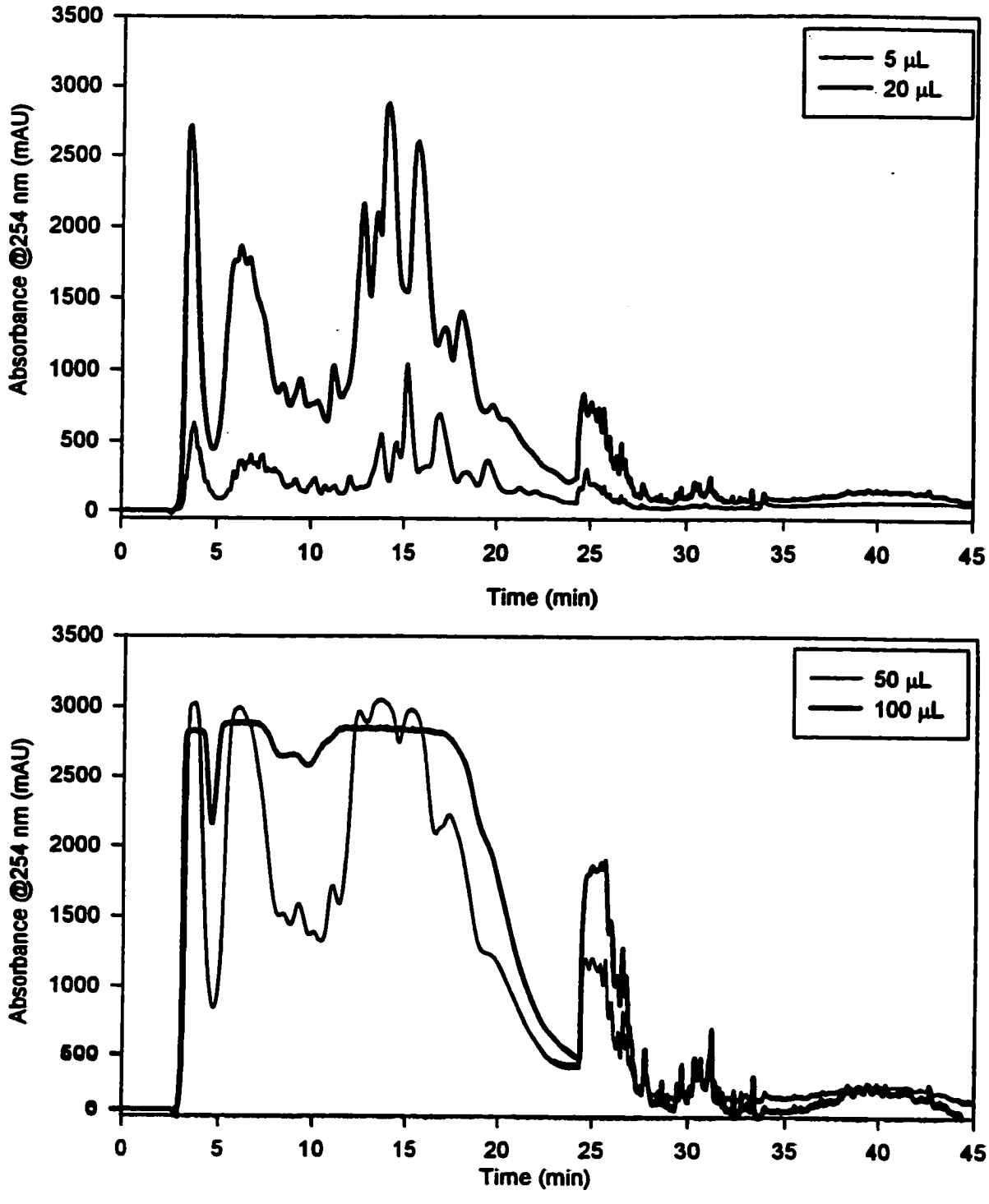

Figure 2.11: LC chromatograms of the light gas oil MB13C on DNBS column using 5, 20, 50, and 100 microlitre injection volumes. Flow rate was 1.2 mL/min. Solvent gradient was shown in Figure 2.8.

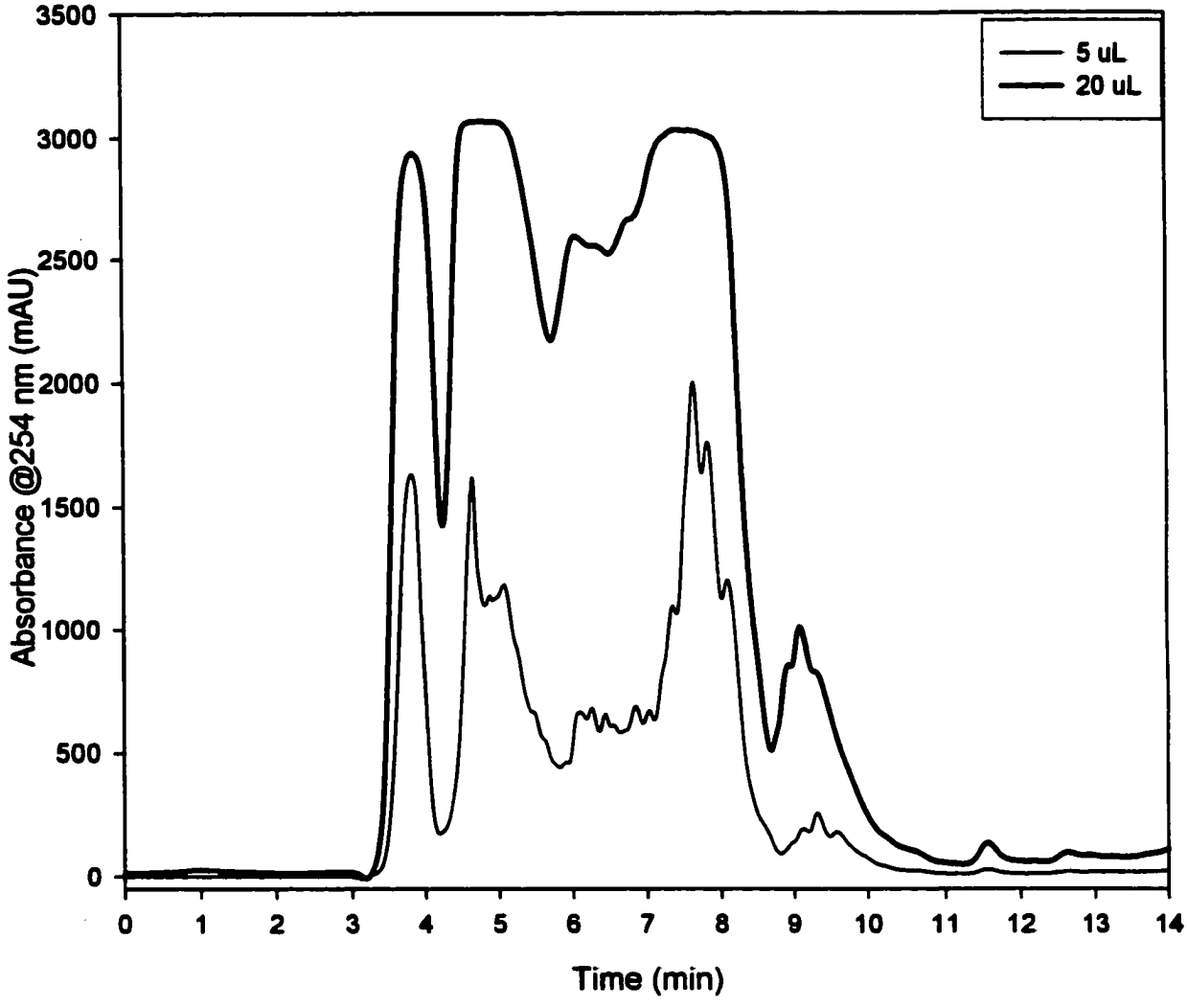

Figure 2.12: LC chromatograms of the light gas oil MB13C on the aminopropyl column. Injections at 5 and 20 microliters demonstrate capacity of column. The flow rate was 1.0 mL/min. The eluent was 100% hexane.

or aminopropyl stationary phases with respect to aromatic class. As well, the DNBS column was second only to the silica column for capacity but this was a function of column size. A DNBS column with the same dimensions as the silica column would have a larger capacity. The longer analysis times associated with the DNBS were not a fundamental concern with regard to the objectives of this study. Furthermore, the DNBS stationary phase provided the best between class resolution for the PAH components. This may allow each aromatic class to be further fractionated to provide a less complicated fraction for the second chromatographic dimension.

A light gas oil sample was fractionated using the DNBS column. The fractions collected are shown in Figure 2.13. The separation was repeated 5 times to give a total oil injection of 100 microliters. The collected samples were evaporated to 1.0 mL using a Kuderna-Danish apparatus. The fractions therefore, were in a mixed hexane/dichloromethane solvent. The fractions were used for multi-dimensional separations described in Chapters 4 and 5.

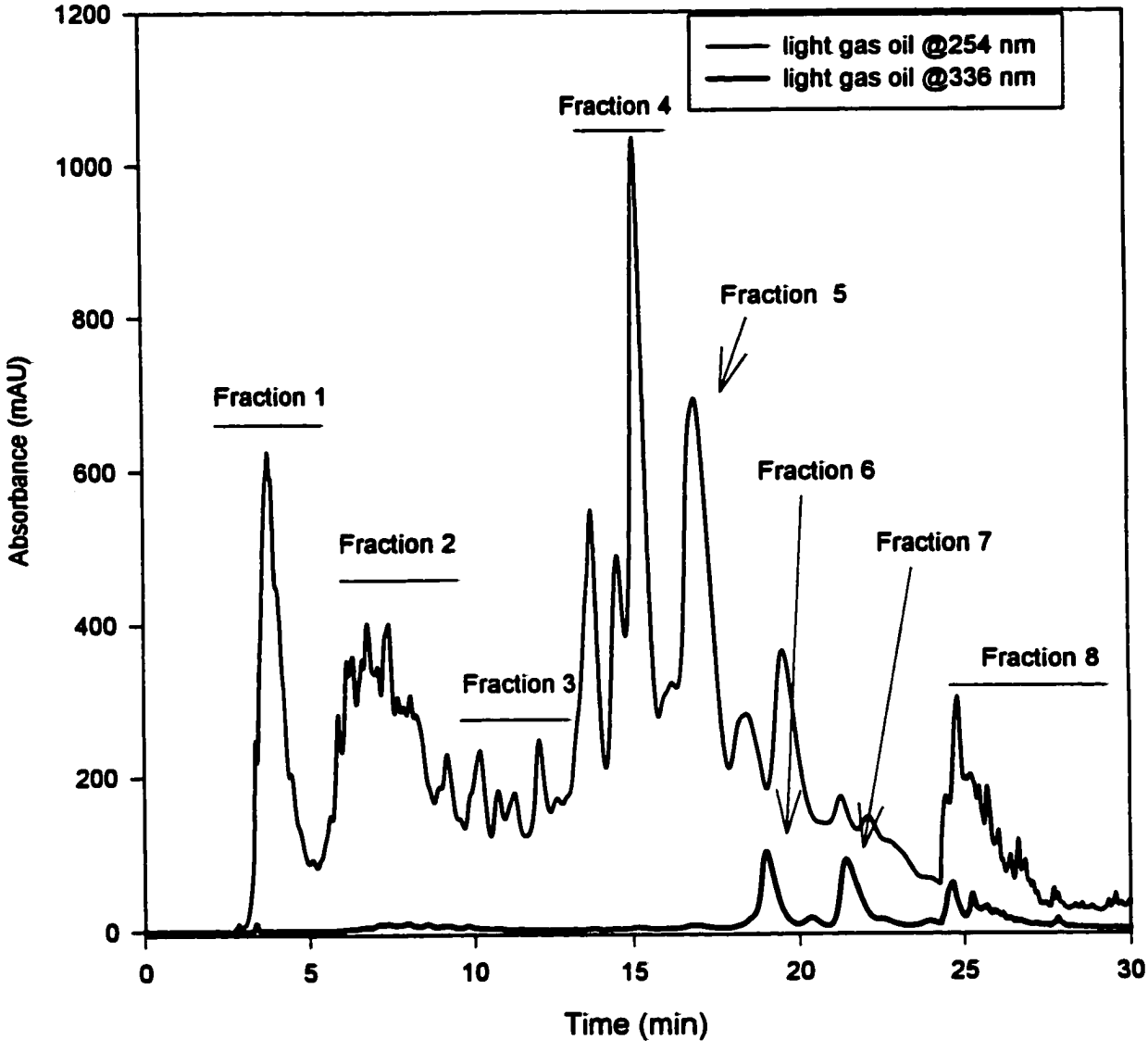

Figure 2.13: LC Chromatogram of the light gas oil (MB13C) separated on DNBS column using UV detection at 254nm and 336 nm. The flow rate was 1.2 mL/min. Gradient conditions were as in Figure 2.8. Each region corresponds to a collected fraction for analysis with two-dimensional and three-dimensional chromatography.

Chapter 3 SFC Chromatography

3.1 Introduction

Supercritical fluid chromatography has seen a dramatic increase in utility in recent times. This is due to advances in instrumentation and increasing pressure on the analyst to provide faster and more efficient analysis. SFC fulfills this role as an intermediate between gas and liquid chromatography. Specifically, SFC operates in much the same way as a typical LC normal phase separation but often with much faster analysis times compared to similar LC separations. As a rule, however, capillary GC still offers the greatest resolution and fastest analysis times but suffers from limited sample ranges due to limitations imposed through volatility or thermal instability of the analyte. Certain SFC applications approach and even surpass the analysis speed for GC [47].

Separations of polar compounds often require high organic modifier concentrations to be added to the supercritical mobile phase. This can lead to separations with a subcritical mobile phase. CO_2 has a very low viscosity allowing higher flow rates and a greater number of analyses can be performed within a given time frame. SFC is often used within the petroleum industry for hydrocarbon analysis, but generally a silica stationary phase has been used [150]. Although better resolution is often observed with SFC, when compared to equivalent separation using LC, the silica stationary phase still has a limited class fractionation. An investigation of more powerful stationary phases may lead to better resolution through a single dimension of chromatography. Specifically, since the DNBS

column provided an optimal separation of a light gas oil using LC conditions, the use of this column under SFC conditions may provide additional resolution. This may allow sufficient resolution using SFC conditions to provide fast and efficient methods for process monitoring.

Typical detection methods such as flame ionization are sensitive and "universal" but do not provide information about chemical structure. Furthermore, the use of FI detectors is limited to weak stationary phases. A strong stationary phase requires a more powerful eluent. The eluotropic strength of carbon dioxide increases with increasing density but, even at high densities, carbon dioxide still may be unable to elute the larger PAHs. The addition of an organic modifier to the carbon dioxide facilitates the elution of polar components from strong stationary phases. These modifiers have the effect of overloading the FI detector and must be used with a spectrometric detector. The use of a fluorescence detector in series with a diode array detector allows identification of compounds by their spectra. A wealth of information can be obtained quickly and efficiently.

Process monitoring requires a slightly different priority to be assigned to each of the factors considered important in judging the effectiveness of the separation. For example, the analysis time for the fractionation of a light gas oil was considered of minimal importance in the previous chapter. A fast analysis may be preferential if a process is to be monitored that is subject to rapid fluctuations. On the other hand, factors such as capacity could conceivably play a much less important role. It stands without question that the methods must provide regions that are resolved either chromatographically or by spectral fingerprints.

In addition to using the SFC for the analysis of PAHs in light gas oils, it is possible that SFC may provide a rapid separation of the PAHs in complex environmental samples such

as air or diesel exhaust particulates. Four stationary phases (silica, TCP, aminopropyl, and DNBS) were investigated as possibilities for such a task. The effect of density programming through temperature and pressure control was examined for the silica column as a means to characterize the effect of these parameters upon SFC separations. As well, the effect of modifier was examined for the DNBS column.

3.2 Experimental

3.2.1 Apparatus

The one-dimensional SFC apparatus consisted of a Berger model SFC system FCM 1200, Alcott model 718 autosampler with either a 0.5 microliter internal or a 5 microliter external sample loop, a chromatographic column (silica or aminopropyl or DNBS or TCP) and an Agilent model 1100 diode array detector. A high-pressure flow cell was designed by Professor L. Ramaley, Department of Chemistry, Dalhousie University for use with a laser excited fluorescence detector. A schematic of the high-pressure flow cell is shown in Figure 3.1. The operation of the laser excited fluorescence system and autoranger was described in a recent publication [151]. The data files saved by the CCD/array acquisition program (FLUOROCHROME, written in Windows C++ by Louis Ramaley) was written in a format compatible with the Winspec version 1.4.3 (Princeton Instruments, Inc. (now Roper Scientific)) data acquisition program. The header was augmented to include an experimental description, the laser intensity, the maximum shutter time, and the number of pixels per scan.

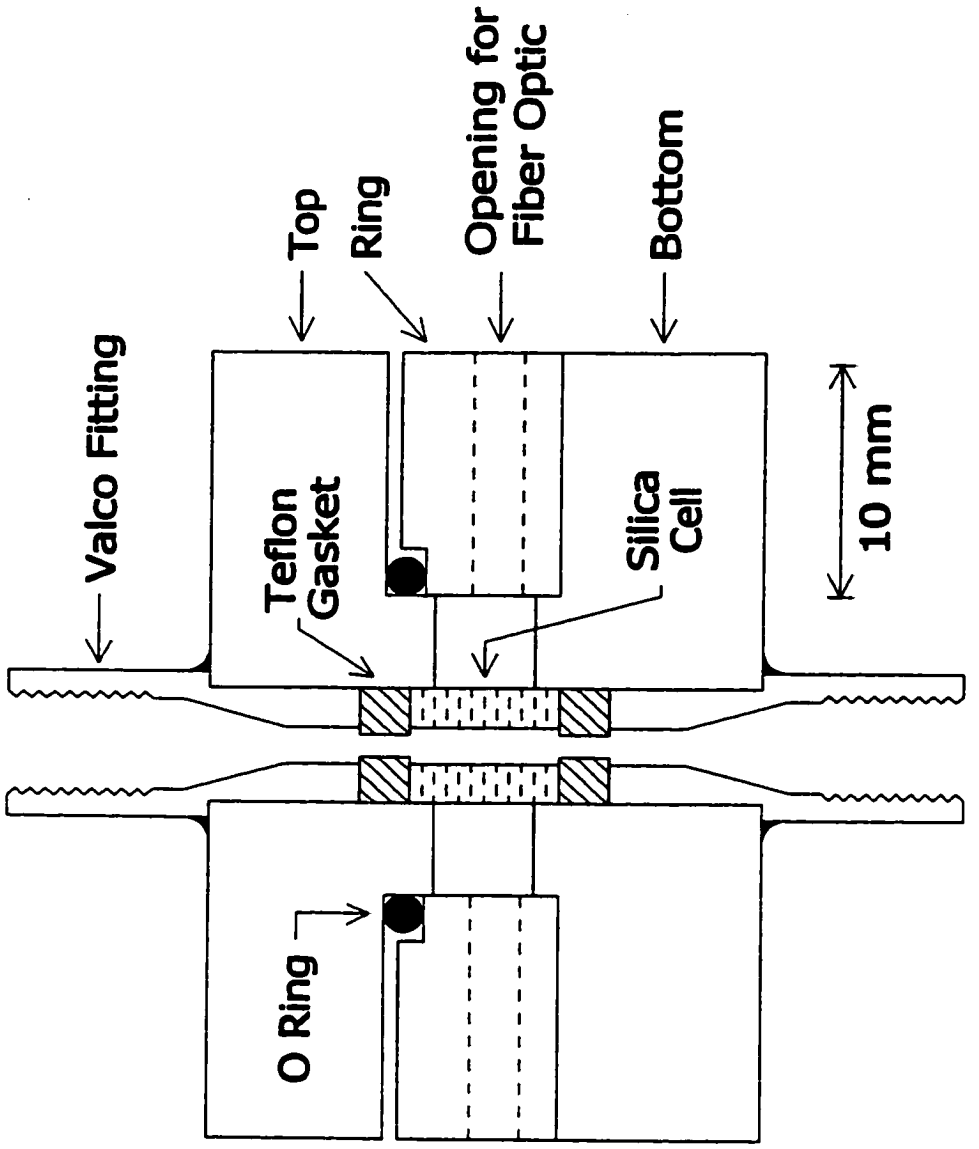

Figure 3.1: Side view schematic of high-pressure fluorescence flow cell used in SFC experiments.

Typically, in the data collection using the 1024 x 256 pixel array, four columns of pixels were binned along the wavelength axis. This increased the sensitivity of the detector and reduced file size by a factor of 4 with no significant effect on spectral resolution (ie. 256 data points for a wavelength range of 250 nm). The FLUOROCHROME program stored the binned data that has been corrected for a background spectrum at the start of the chromatogram. The FLUOR1 program (versions 1 through 4, written in Visual Basic by Robert Guy) read the header, calculated the wavelength associated with each pixel using the calibration data stored in the header, and stored the spectra in a data array. The program generated a chromatogram by finding maximum fluorescence intensity in each spectrum and plotting this versus time. Unless otherwise specified, the maximum fluorescence response was labeled as "TOTAL FLUORESCENCE" to differentiate this from a chromatogram created by plotting the fluorescence at a certain wavelength versus time. The FLUOR1 program was written to display data for the qualitative comparisions of the chromatograms obtained for the light gas oils and allow either chromatograms or spectra to be copied and transferred to the commercial programs EXCEL (Microsoft) and SIGMAPLOT (SPSS, Inc.) for printing purposes. Chromatographic peak areas could not be determined using the versions of the FLUOR1 program available during the period of this research. Quantitative data was obtained using a module that allows one to select the spectrum at the peak maximum, a spectrum at the start or end of the peak, and subtract the two spectra. The residual spectrum was corrected for the laser intensity and transferred to an EXCEL spreadsheet. A similar procedure was used for a standard chromatogram and the spectra were used for the determination of the concentration of the compound.

3.2.2 Chemicals

The light gas oils were provided by Syncrude Canada. Chromatographic grade liquid carbon dioxide was supplied by Praxair. Optima grade acetonitrile for use as the organic modifier was supplied by Fisher Scientific. To avoid leaks in SFC the columns must use compression type fittings with no Teflon® or polymeric components. Two silica columns were used in the experiments–the silica column (Supelcosil, 25 cm x 10 mm, 5 micron particle size) used in Chapter 2 and a Keystone Betasil silica (15 cm x 4.6 mm, 5 micron particle size) supplied by Berger for use in oil analysis. The aminopropyl column was a Keystone "carbohydrate" phase (25 cm x 4.6 mm, 5 micron particle size). A second Keystone carbohydrate column was derivatized using the procedure described in Chapter 2 to prepare a DNBS stationary phase. The TCP column used in this work was the same column as used in the LC work described in Chapter 2.

3.2.3 Procedures

The stationary phases were characterized using three types of samples. The first sample mixture was prepared as a 25-fold dilution of a NIST 1647d reference standard. This standard sample was used to illustrate the ability of the stationary phases to separate the priority PAHs. A second sample mixture consisted of a mixture of aromatic compounds (about 0.020 M each of benzene, toluene, xylene, mesitylene, 4-ethyltoluene, tetramethyl benzene, tetralin, pentamethylbenzene, naphthalene, biphenyl, bibenzyl, fluorene, phenanthrene, o-terphenyl, fluoranthene, and pyrene). This mixture was used to test the ability of the phases to separate aromatic compounds found in light gas oils. The final test

samples were the Syncrude light gas oils described in Chapter 2.

All chromatograms were run using an oven temperature of 50 C except where specified on individual chromatograms. Typical operating conditions for the NIST standard sample are shown in Table 3.1. These conditions were modified slightly for the analysis of the light gas oils and the chromatographic conditions will be shown on the relevant chromatograms shown in the Results and Discussion section.

Four different light gas oils were chosen for SFC analysis. Each of the oils represented a set of processing conditions in which all experimental parameters were kept constant (i.e. catalyst, H_2 pressure, flow etc.) except for temperature. Five microliter injections were introduced onto the DNBS column and eluted according to the appropriate conditions for each separation. The diode array and fluorescence detectors were placed in series. The diode array was monitored at the following wavelengths: 220, 254, 280, and 336 nm.

3.3 Characterization of the stationary phases using SFC conditions

Supercritical fluid chromatography allows the setting of three variables – temperature, pressure, and modifier concentration. The combination of temperature and pressure defines the density of the mobile phase. At constant temperature, an increase in pressure increases the density of the supercritical fluid and increases the solvating power of the mobile phase. An increase in the temperature at constant pressure lowers the density and makes the mobile phase weaker but may improve transfer kinetics between the mobile and stationary phases.

Table 3.1: Experimental conditions used for the separation of the NIST standard for each stationary phase.

Stationary phase	Flow rate ml/min	Pressure gradient	Modifier (CH_3CN)
Silica	1.5	0-8 min 150 bar then 10 bar/min to 200 bar	None
aminopropyl	2.0	0-1 min 150 bar then 5 bar/min to 250 bar	5%
DNBS	2.0	250 bar	1 to 10% at 0.5%/min
TCP	2.0	150 to 300 bar at 10 bar/min	1 to 10% at 0.5%/min

The role of a modifier in supercritical fluid chromatography is to increase the polarity of the mobile phase. Supercritical carbon dioxide has a polarity similar to weak organic solvents such as hexane and pentane. A modifier, such as methanol or acetonitrile, dissolves in the supercritical carbon dioxide and interacts with the active sites on the stationary phase (which are usually polar sites) so the modifier competes with the analyte for the sites. At high modifier concentrations the increased competition for sites decreases the retention of the analytes. The addition of high concentrations of a modifier to the carbon dioxide may result in subcritical fluids. In general, the separations described in this chapter used either pressure gradients at constant temperature or constant pressure and temperature with a modifier

gradient. Chromatograms that use laser excited fluorescence detection were displayed with the signal intensity as a function of "TOTAL FLUORESCENCE".

3.3.1. Characterization of the phases using the PAH standard mix

The NIST 1647d standard contains the 16 priority PAHs at concentrations that reflect the distribution of compounds in environmental samples. The standard was diluted 1/25 for the purposes of characterization of the stationary phases using the laser excited fluorescence CCD array detector. Figure 3.2 (a-c) shows the chromatograms for this standard on the 15 cm Keystone silica column. A comparison of the two isobaric chromatograms at 35 and 50 C showed the effect of temperature -as the temperature was raised the density decreased and the retention times for the later eluting compounds increases. A comparison of Figures 3.2a and 3.2c shows that, for the silica column and the simple PAH mixture, a density gradient did not improve the separation. The chromatograms also illustrate the poor sensitivity of the laser system for the low molecular weight PAHs and anthracene was not detected at all using the 266 nm laser. The silica column did not provide adequate resolution for the determination of the priority PAHs using supercritical fluid chromatography. The separation did not resolve the compound pairs fluoranthene and pyrene or benzo[*b*]-and benzo[*k*]fluoranthene.

The separation of the PAH standard on the Keystone aminopropyl column is shown in Figure 3.3. This chromatogram was obtained using a constant modifier concentration (5% acetonitrile) and a pressure gradient. This column was found to be more retentive than the silica column but the gradient conditions permitted a relatively rapid separation of the PAHs

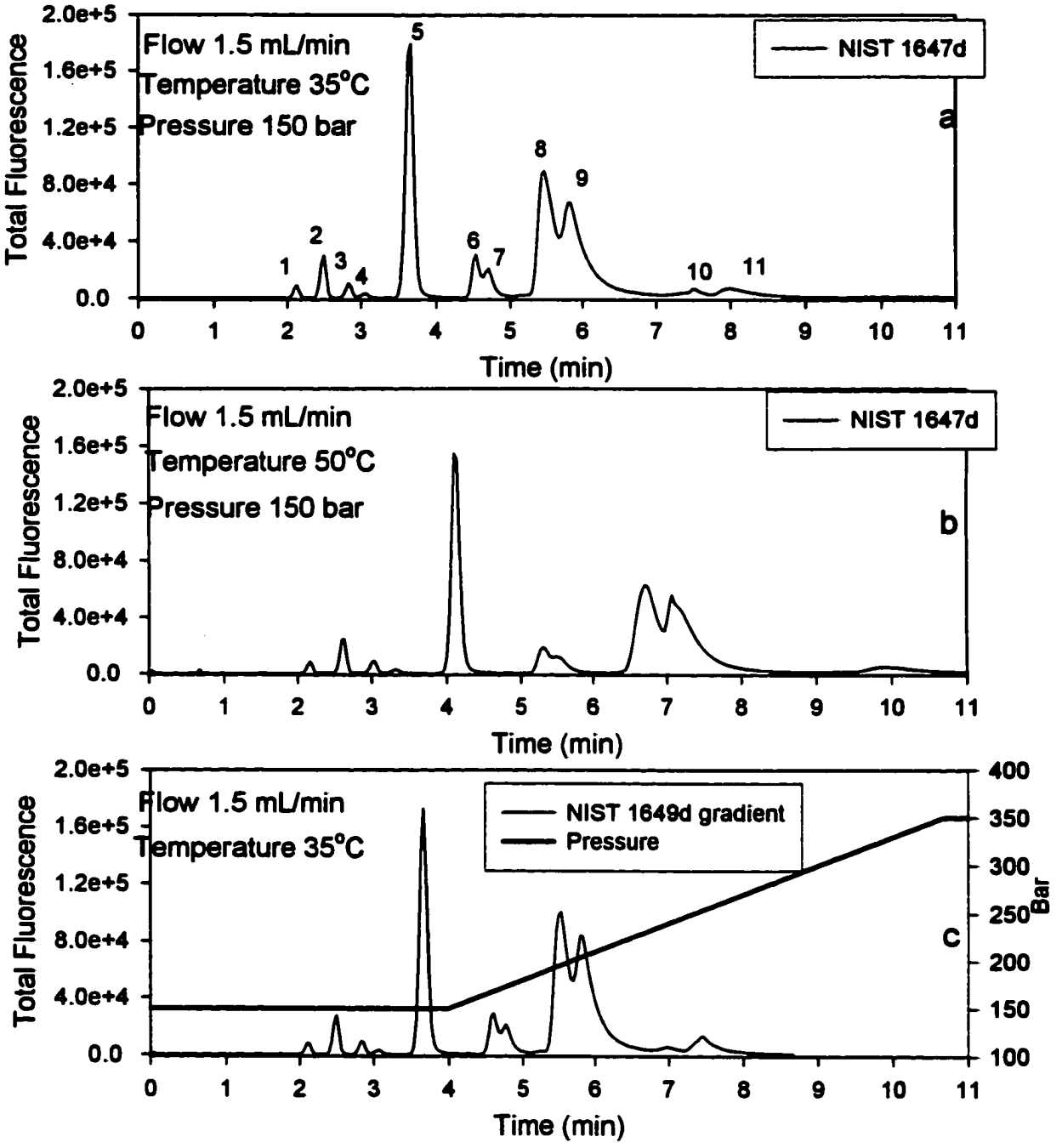

Figure 3.2(a-c): SFC separation of NIST 1647d priority PAH standard using the silica Keystone Betasil coumn. Top two graphs (a & b) developed using isobaric conditions at selected temperatures. Lower chromatogram (c) uses a pressure gradient.

Peak Identification: 1 acenaphthylene, 2 acenaphthene, 3 fluorene, 4 phenanthrene, 5 fluoranthene, pyrene 6 benz[*a*]anthracene, 7 chrysene, 8 benzo[*b*]fluoranthene, benzo[*k*]fluoranthene, 9 benzo[*a*]pyrene, 10 dibenz[*a,h*]anthracene, indeno[*1,2,3-c,d*]pyrene, 11 benzo[*g,h,i*]perylene

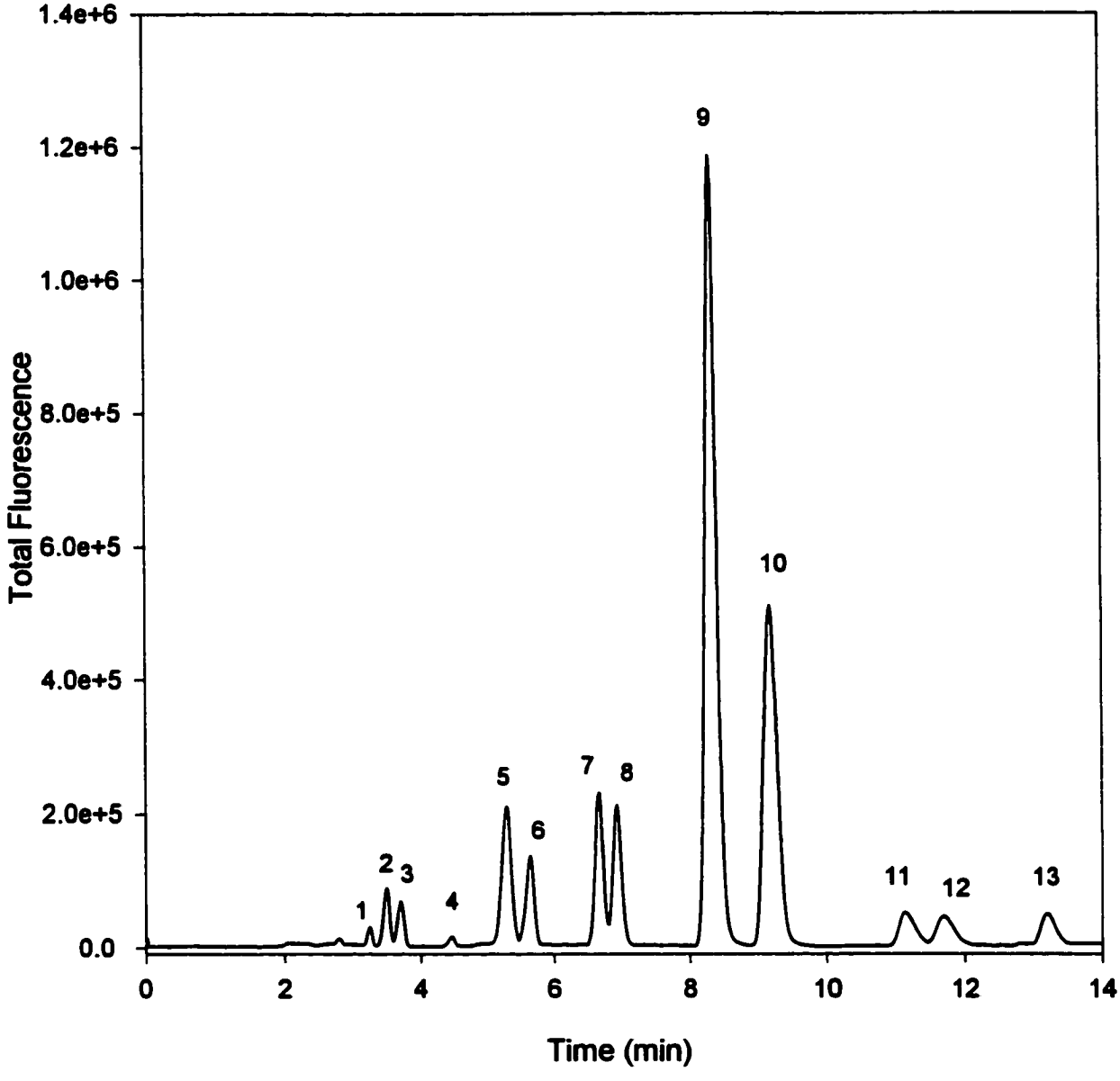

Figure 3.3: SFC chromatograms of PAH standards separated using the Keystone aminopropyl column. Experimental conditions given in Table 3.1. Fluorescence results from 266 nm laser excitation.

Peak identification: 1 acenaphthene, 2 acenaphthylene, 3 fluorene, 4 phenanthrene, 5 fluoranthene, 6 pyrene, 7 benz[*a*]anthracene, 8 chrysene, 9 Benzo[*b*]fluoranthene, benzo[*k*]fluoranthene, 10 benzo[*a*]pyrene, 11 dibenz[*a,h*]anthracene 12 indeno(*1,2,3-c,d*)pyrene 13 benzo(*g,h,i*)perylene

with only the benzo[*b*]- and benzo[*k*]-fluoranthene pair not being resolved. Figure 3.4 shows the same chromatogram monitored at two different wavelengths, 405 and 525 nm, suggesting the pair can be resolved spectroscopically. The rationale for the choice of the selected wavelength pair for benzo[*b*]- and benzo[*k*]fluoranthene is shown by the fluorescence spectra for each in Figure 3.5. Figure 3.6 shows the chromatogram of the PAH mixture on the aminopropyl column that has been derivatized with dinitrobenzenesulphonyl chloride. The separation conditions are harsher than the aminopropyl phase because both the pressure and the modifier concentration are higher. The increased strength of the phase does show a slight resolution of the benzo[*b*]- and benzo[*k*]fluoranthene pair.

The strongest stationary phase used for SFC was the tetrachlorophthalimidopropyl phase. The separation of the PAH on this phase is shown in Figure 3.7. The run-time for this phase was very long (50 min) and the pressure/modifier gradient failed to elute indeno[*1,2,3-cd*]pyrene and benzo[*g,h,i*]perylene. The resolution between the pyrene, benz[*a*]anthracene, and chrysene was poorer than the DNBS phase but the resolution between the benzo[*b*]- and benzo[*k*]fluoranthene pair improved. Of the four stationary phases, the aminopropyl and DNBS stationary phases are the most promising for the separation of the priority PAHs. The pressure/modifier conditions for the aminopropyl phase were easier on the pump and restrictor of the chromatograph so this was the phase selected for further studies on the separation of PAHs in environmental samples.

The primary goal for the aminopropyl SFC separation would involve both qualitative identification and quantitation of the priority PAHs in complex environmental samples. Two important figures of merit consistent with any separation and method of detection are the

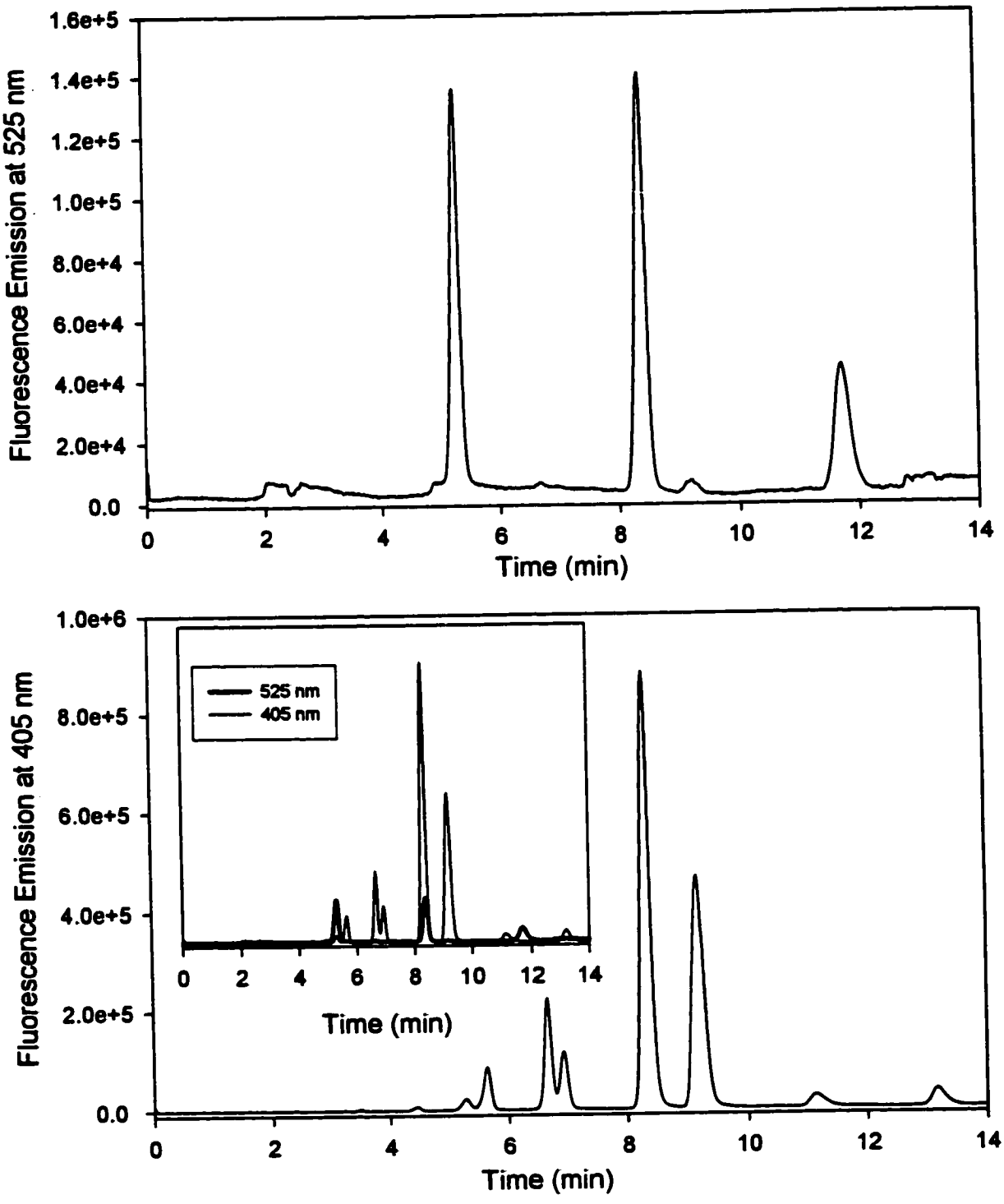

Figure 3.4: SFC chromatograms of NIST PAH standard mixture on Keystone aminopropyl column. Upper chromatogram results from fluorescence emission at 525 nm while lower chromatogram results from fluorescence emission at 405 nm. Inset in lower figure superimposes two chromatograms demonstrating spectral resolution.

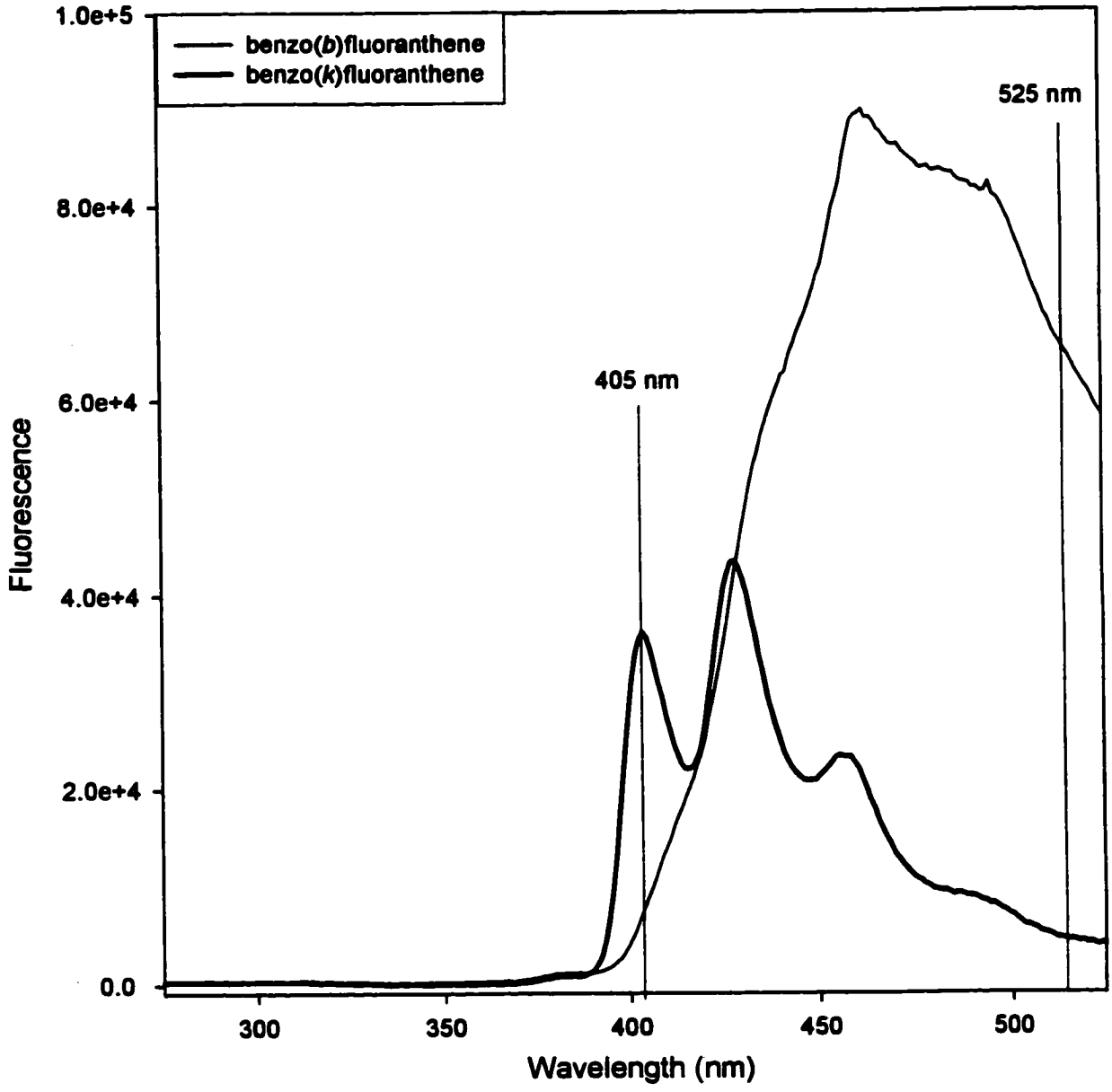

Figure 3.5: Fluorescence spectra of benzo[*b*]fluoranthene and benzo[*k*]fluoranthene. Spectra result from excition with the 266 nm laser.

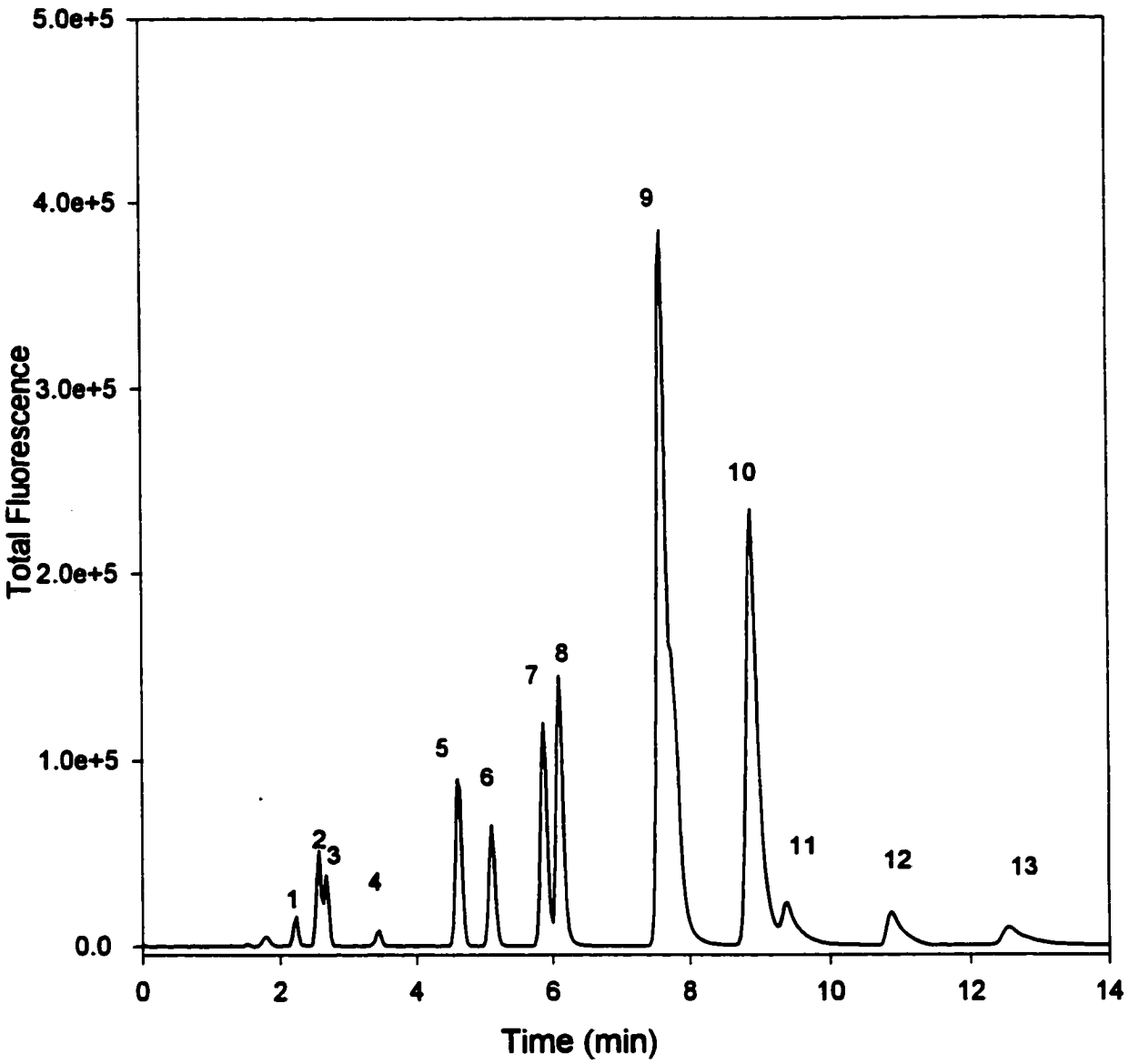

Figure 3.6: A chromatogram of PAH standards separated using the derivatized Keystone aminopropyl column under SFC conditions. The derivatizing agent was 3,5-dinitrobenzenesulphonylchloride (DNBS). Chromatographic conditions given in Table 3.1. Fluorescence results from 266 nm laser excitation.

Peak identification: 1 acenaphthene, 2 acenaphthylene, 3 fluorene, 4 phenanthrene, 5 fluoranthene, 6 pyrene, 7 benz[*a*]anthracene, 8 chrysene, 9 Benzo[*b*]fluoranthene, benzo[*k*]fluoranthene, 10 benzo[*a*]pyrene, 11 dibenz[*a,h*]anthracene 12 indeno[*1,2,3-c,d*]pyrene 13 benzo[*g,h,i*]perylene

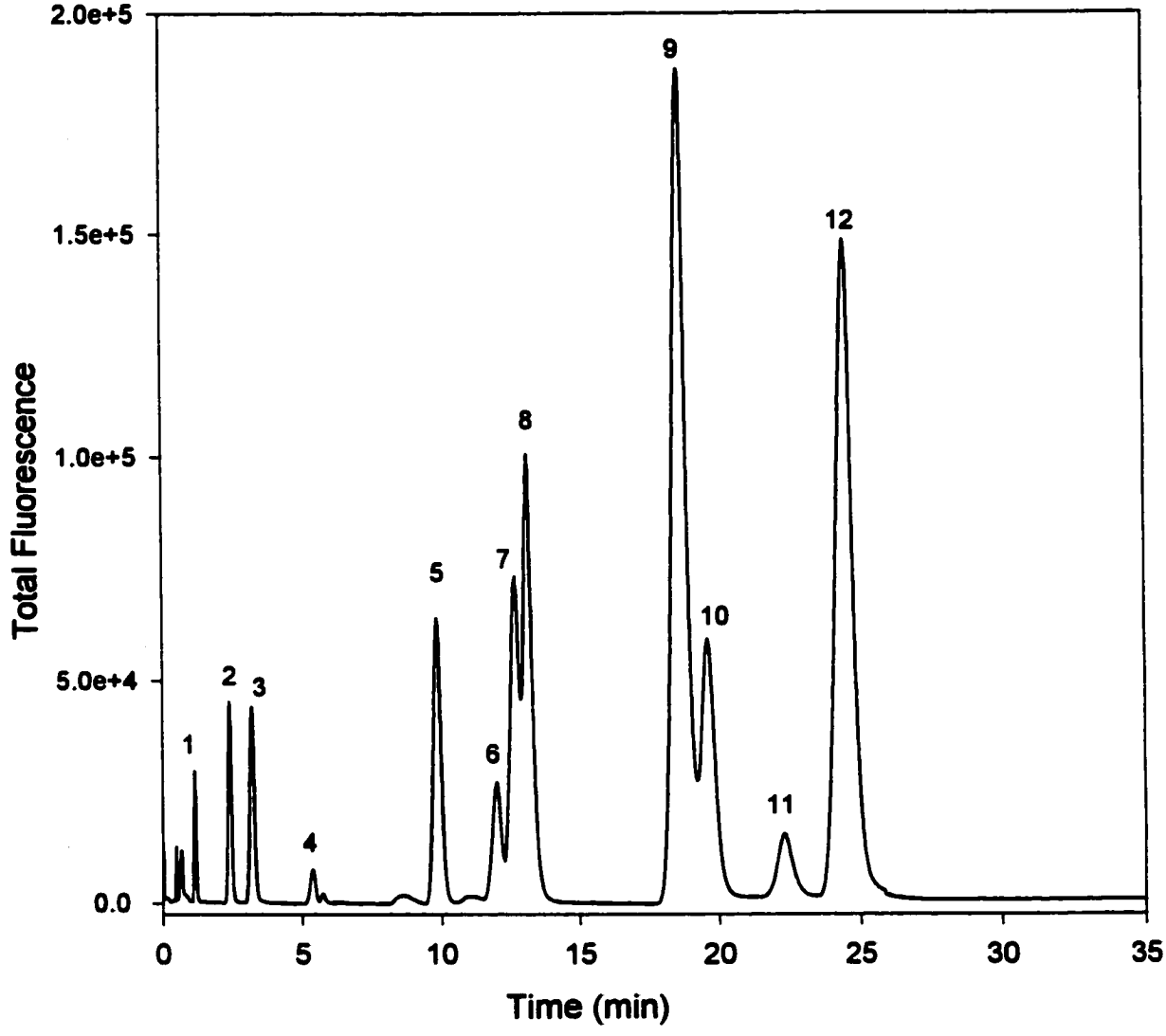

Figure 3.7: A chromatogram of NIST PAH standard separated on the TCP column using SFC conditions. Experimental conditions are given in Table 3.1.

Peak identification: 1 acenaphthene, 2 acenaphthylene, 3 fluorene, 4 phenanthrene, 5 fluoranthene, 6 pyrene, 7 benz[*a*]anthracene, 8 chrysene, 9 benzo[*b*]fluoranthene, 10 benzo[*k*]fluoranthene, 11 dibenz[*a,h*]anthracene, 12 benzo[*a*]pyrene

detection limits and the linear range of the calibration curve. The detection limits for several of the priority PAHs separated using the aminopropyl column under SFC conditions are shown in Table 3.2. The detection limits were estimated from the calibration curve using a signal that was approximately three times the standard deviation of the background. In addition, the typical detection limits are shown for a liquid chromatographic reversed phase separation coupled to an Agilent 1100 fluorescence detector. Although the Agilent detector was more sensitive, it suffered from very poor spectral resolution due to a large bandpass. Many of the detection limits for the priority PAHs were comparable for both detection methods with the exception of anthracene. The laser excited fluorescence detectors fails with this compound because anthracene does not absorb well at 266 nm. For this compound the 325 nm laser would be a better choice. The linearity of the fluorescence response can be compromised if high analyte concentrations are present in the sample matrix. Figure 3.8 shows the calibration data for benz[a]anthracene using the 43 mW, 266 nm laser for molecular excitation. This data suggests that the fluorescence response for this system was linear from the detection limit of 0.57 ng/mL to 0.24ug/mL. The upper limit for this range is well above that expected for typical PAH concentration in environmental samples.

These figures of merit represent a significant engineering accomplishment. The walls of the high-pressure fluorescence flow cell were enlarged in order to withstand the significant pressures associated with typical SFC operating conditions. In general increasing the thickness of the flow cell decreases sensitivity and increases laser light scatter. In SFC mode the laser high pressure cell showed very noisy baselines that varied considerably as the

Table 3.2 Detection limits for SFC Separations of Priority PAHs as well as detection limits for priority PAHs using an Agilent 1100 fluorescence detector and a reversed phase LC separation.

Compound	Detection Limit Agilent 1100 ng/mL	Detection Limit Laser System ng/mL
Naphthalene	0.7	6.7
Acenaphthene	Not done	3.7
Acenaphthylene	Not done	3.9
Fluorene	0.1	0.6
Phenanthrene	0.4	2.0
Anthracene	0.01	>32
Fluoranthene	0.6	1.1
Pyrene	0.5	0.8
Benz[*a*]anthracene	0.1	0.6
Chrysene	0.1	0.2
Benzo[*b*]fluoranthene	0.1	0.8
Benzo[*k*]fluoranthene	0.1	0.8
Benzo[*a*]pyrene	0.2	0.6
Dibenz[*a,h*]anthracene	0.2	0.9
Benzo[*g,h,i*]perylene	0.1	0.2
Indeno[*1,2,3-c,d*]pyrene	0.2	1.1

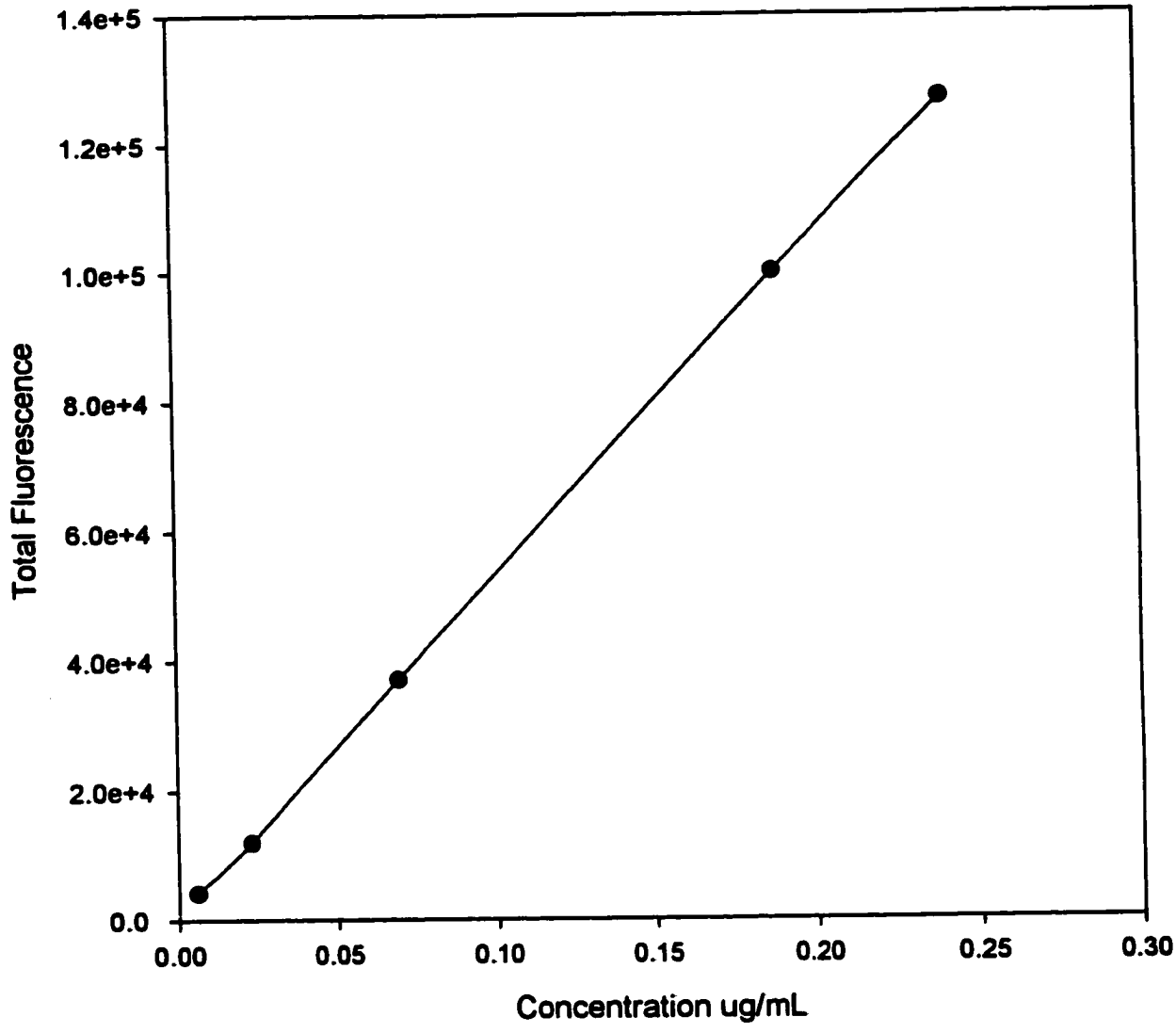

Figure 3.8: Calibration curve for benz[*a*]anthracene using laser excited fluorescence detection. Molecular excitation provided with 266 nm laser. The Keystone aminopropyl column was operated using the SFC conditions given in Table 3.1. Twenty-five microliter injections were performed in each case.

pressure or modifier gradients were changed. These difficulties can be improved upon with the use of a 290 nm cutoff filter (wavelengths below 290 nm are removed) placed in the light path between the fiber optics and the CCD array. Figure 3.9 shows two typical background spectra from the flow cell. The upper spectrum uses no correction while the lower spectrum was taken with a 290 nm cutoff filter installed. The filter provided a significant reduction in background noise. The detection limits in Table 3.2 were obtained using the 290 nm cut-off filter.

3.3.2 Characterization of the silica and DNBS columns for aromatics in a light gas oil

Both the silica and DNBS stationary phases were characterized under LC conditions as a means to fractionate a light gas oil. Using LC conditions the silica column was less successful than the DNBS column for this task. However, since the silica column is commonly used within the oil industry to separate light gas oils a comparison of the silica behavior to the DNBS behavior was undertaken. It was previously shown that a separation of the priority PAHs using typical SFC conditions was not effective with a silica column. Particularly, resolution and peak shape suffered for high molecular weight PAHs. Since the upgrading process for a light gas oil tends to eliminate PAHs larger than pyrene it was postulated that a rapid separation optimized for small molecular weight PAHs may be feasible for the silica column. Figure 3.10 shows the light gas oil MB13C with a simple PAH standard mixture separated on the silica column. This chromatogram suggests that a very rapid separation may be possible as pyrene was eluted in less than 4 minutes. Furthermore, baseline

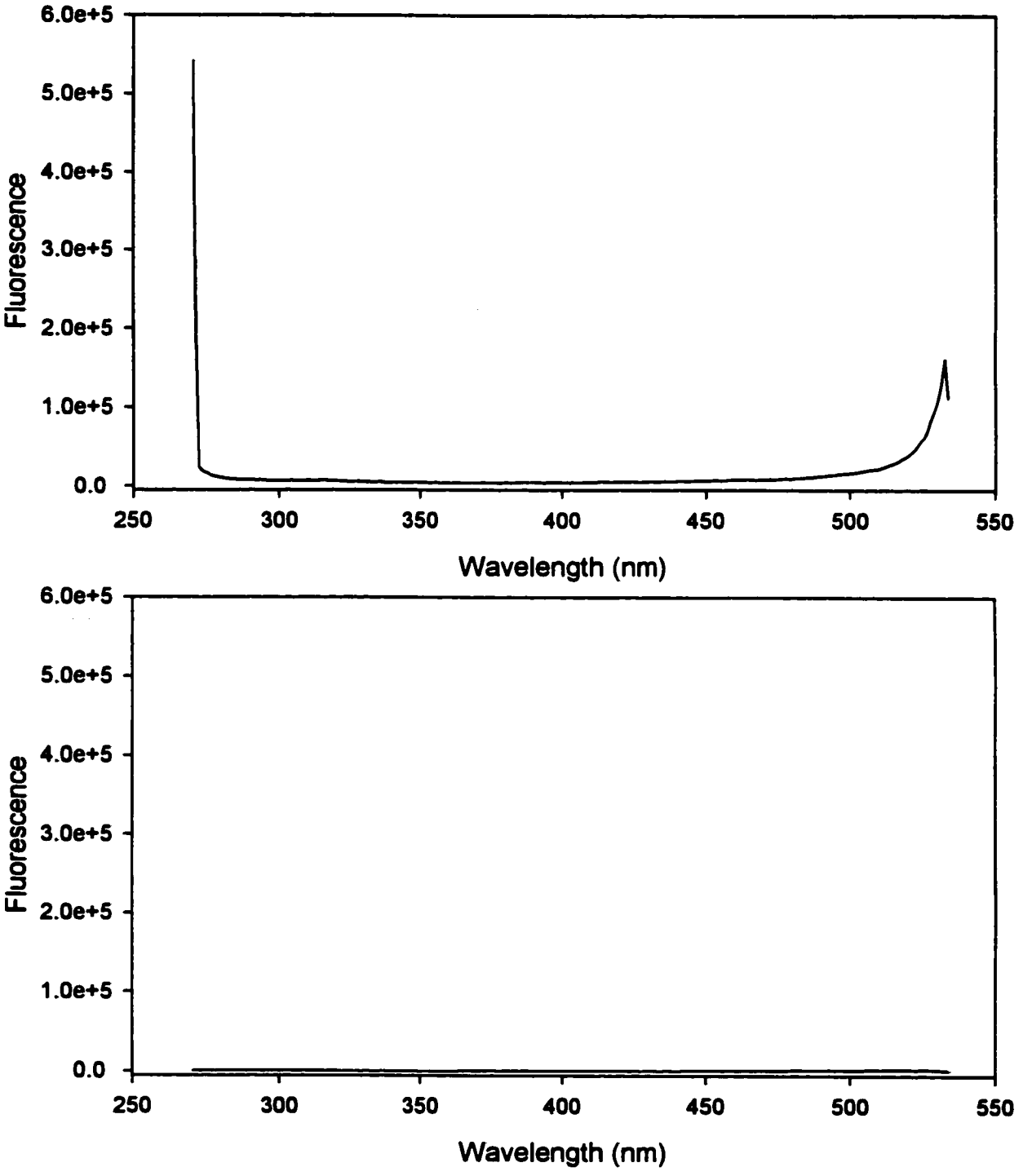

Figure 3.9: Upper figure represents background spectrum of high pressure fluorescence cell using the 266 nm laser without 290 nm cutoff filter. The lower figure is the background spectrum with the filter installed.

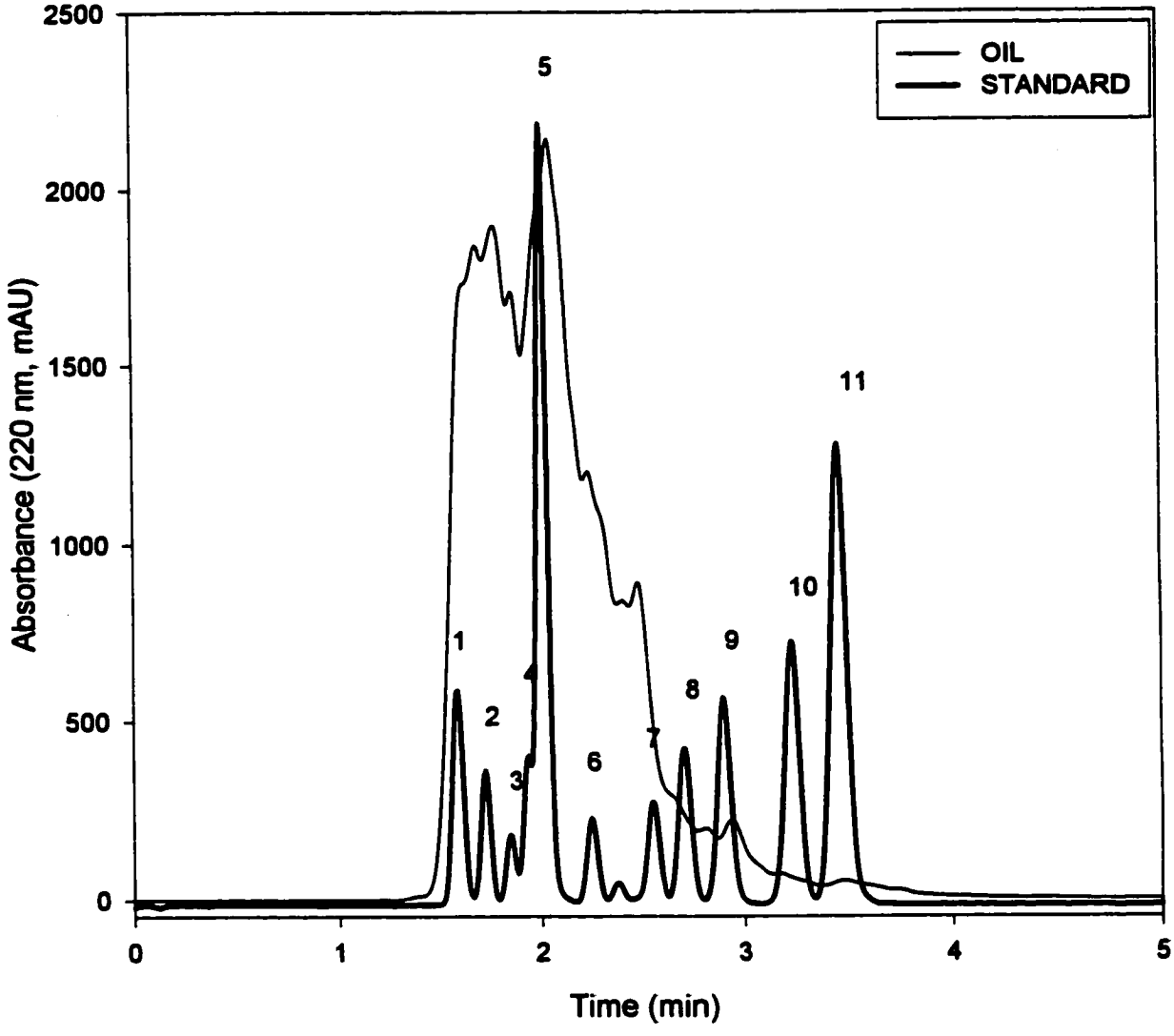

Figure 3.10: SFC chromatograms of a light gas oil and aromatic PAH mixture. The chromatograms were obtained on a Keystone Betasil silica 150 x 4.6 mm column. The chromatographic conditions were 35°C and 150 bar pressure at a flow rate of 1.5 mL/min.

Peak Identification: 1 benzene, toluene, xylene, mesitylene, 4-ethyltoluene, 2 tetramethylbenzene, 3 tetralin, 4 pentamethylbenzene, 5 naphthalene, 6 biphenyl, 7 bibenzyl, 8 fluorene, 9 phenanthrene, 10 o-terphenyl, 11 fluoranthene, pyrene

resolution exists for many of the components in this chromatogram. However, the standard chromatogram results from a relatively simple mixture. The chromatogram that results from the light gas oil presented a much more complex mixture. This chromatogram used absorbance at 220 nm and was intended to emphasize the mono- and di-aromatic species. It was determined that additional resolution would be required to enable peak identification in this region of the chromatogram.

The silica column was operated without organic modifier. Optimization of the resolution on this column would have to be facilitated through changes in temperature or pressure associated with the mobile phase. The effect of changes in temperature and hence, density of the mobile phase, was partially addressed earlier in this chapter. Decreasing the density of the mobile phase has the effect of reducing the eluotropic strength and increasing the retention times of PAHs on the column. Another way to accomplish this is to reduce the pressure of the mobile phase. Figure 3.11 shows two chromatograms of the simple PAH mixture separated on the silica column at 125 and 250 bar. In each case the temperature remained constant at 40 C. Decreasing the pressure by a factor of 2 has the effect of doubling the retention times for the PAHs. More importantly, the separation between components has increased dramatically at the lower pressure. Furthermore, additional peaks have been resolved at the lower pressure. Unfortunately, the peaks at longer retention times have been significantly broadened. This would compromise sensitively as well as resolution of the larger PAHs such as phenanthrene and pyrene. A chromatogram of the light gas oil MB13C is shown in Figure 3.12 separated using the lower pressure conditions given in Figure 3.11. Although there does appear to be an improvement in the peak resolving capacity of the silica

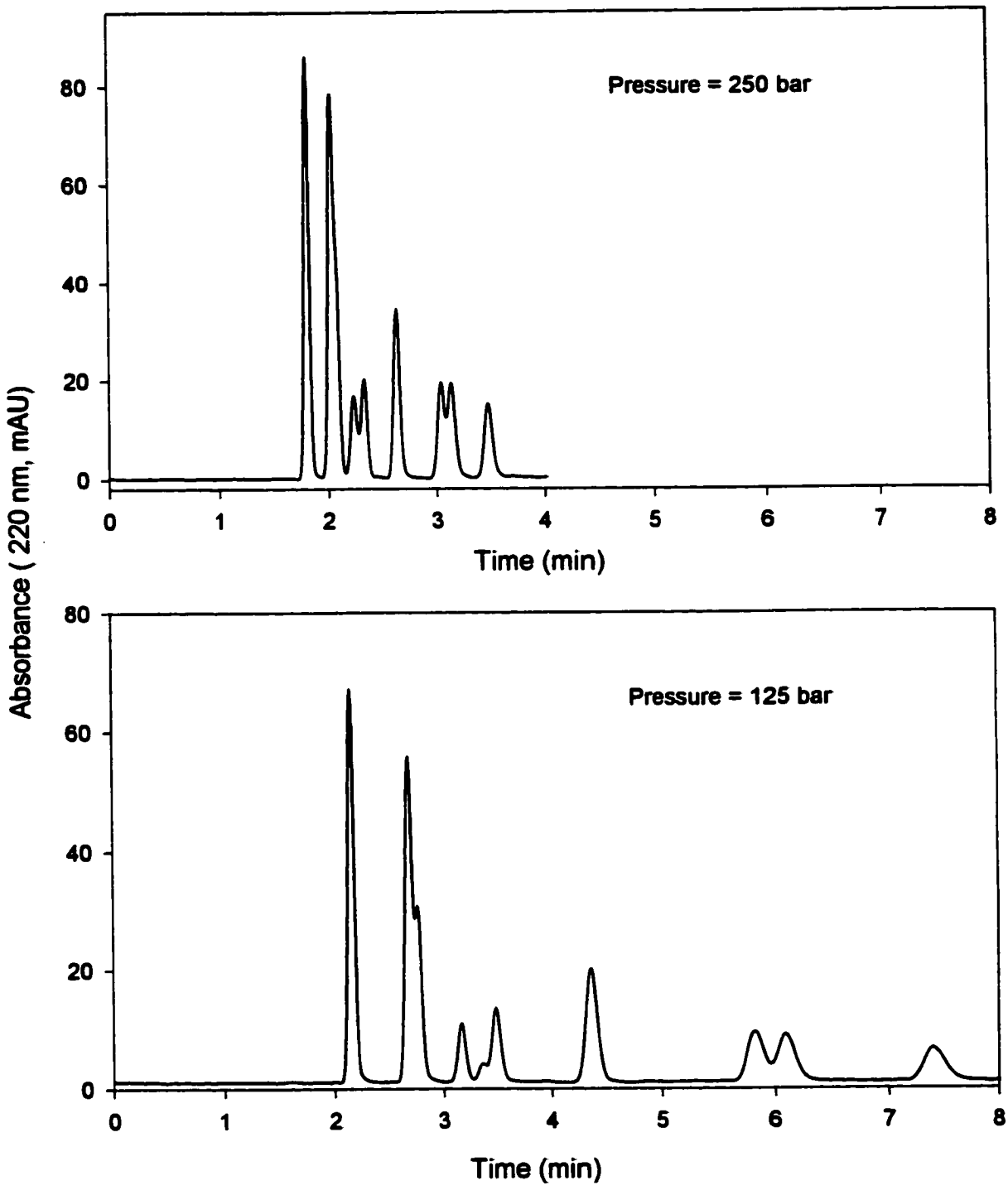

Figure 3.11: SFC separations of a simple PAH mixture on Keystone silica column. The flow rate was 1.5 mL/min supercritical CO_2. The temperature was 40 C for each separation.

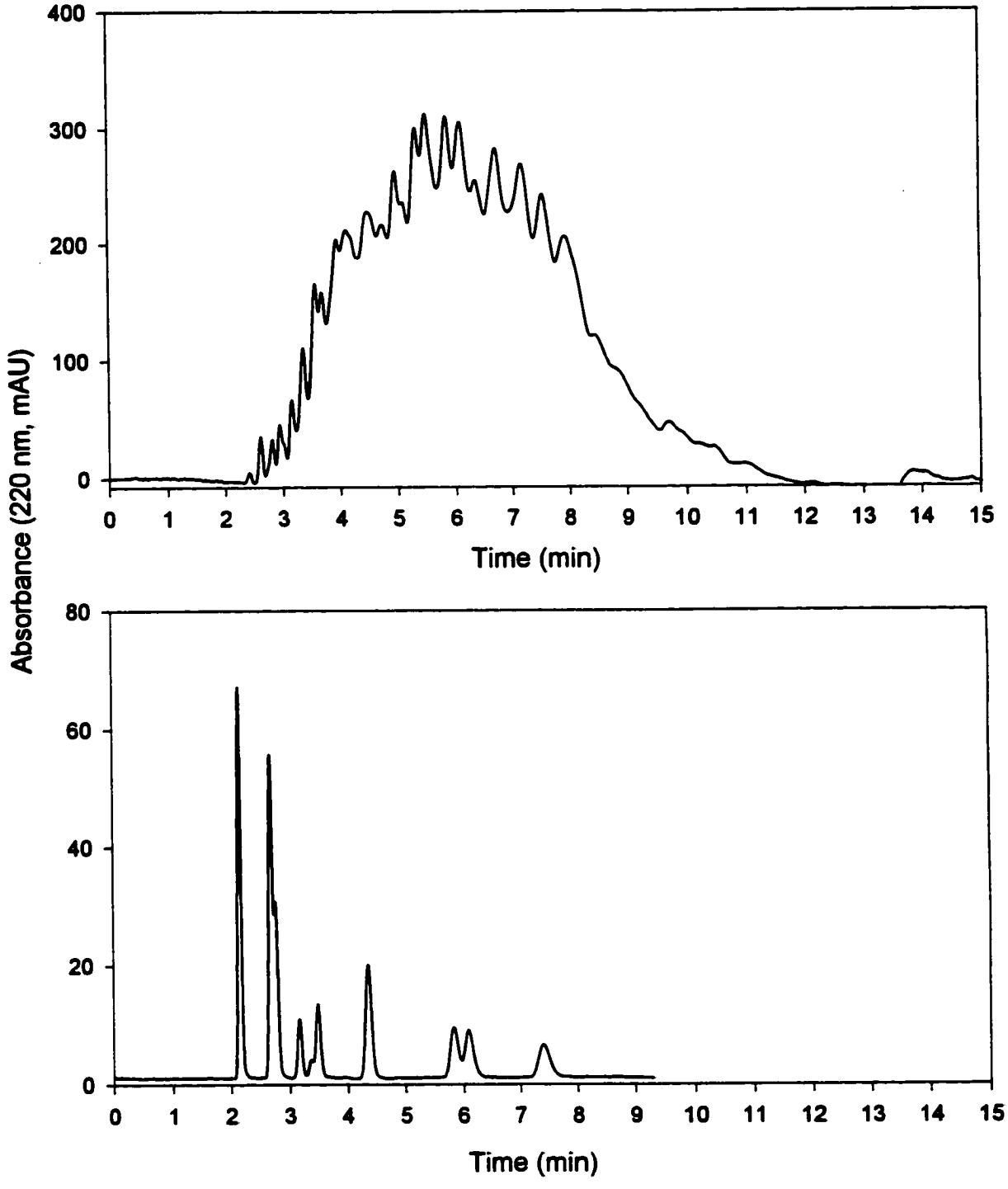

Figure 3.12: SFC separation of a simple PAH mixture on Keystone silica column. The flow rate was 1.5 mL/min. supercritical CO_2. The temperature was 40°C for each separation. Top chromatogram resulted from light gs oil MB13C. Each chromatogram used a pressure of 125 bar.

column under these conditions, the complex nature of the oil sample still presents difficulties for peak identification.

The DNBS column was a more powerful stationary phase and was believed to offer an alternative to the silica separation. The use of more powerful stationary phases required the use of organic modifiers to be added to the mobile phase. This increased the flexibility allowing additional chromatographic parameters to be adjusted in order to optimize the separation. Figure 3.13 shows the separation of the light gas oil MB13C on the DNBS column using a pressure gradient without organic modifier. The more powerful stationary phase required longer analysis times as well as higher pressures to elute the standard PAH mixture. The DNBS column operated under these conditions would require in excess of 30 minutes to elute all of the components in the oil sample. However, resolution vastly improved compared to the silica column. Poorly defined humps with the silica separation of the oil were replaced with sharp partially resolved peaks with the DNBS separation.

At first glance, it would appear from the chromatogram of the oil in Figure 3.13 that phenanthrene and pyrene were absent from this sample. This was not the case. The chromatogram in this figure shows the absorbance at 220 nm. This tends to emphasize the most complex region of the oils represented by mono- and di-aromatics. Figure 3.14 shows the same separation on the DNBS using absorbances at 254, 280, and 336 nm. Each of these wavelengths favors a particular class of compounds. Specifically, 336 nm emphasizes pyrene and alkylated pyrenes while 254 nm favors the phenanthrenes. Naphthalenes, fluorenes, and biphenyls are highlighted using absorbance at 280 nm. The use of selective wavelength

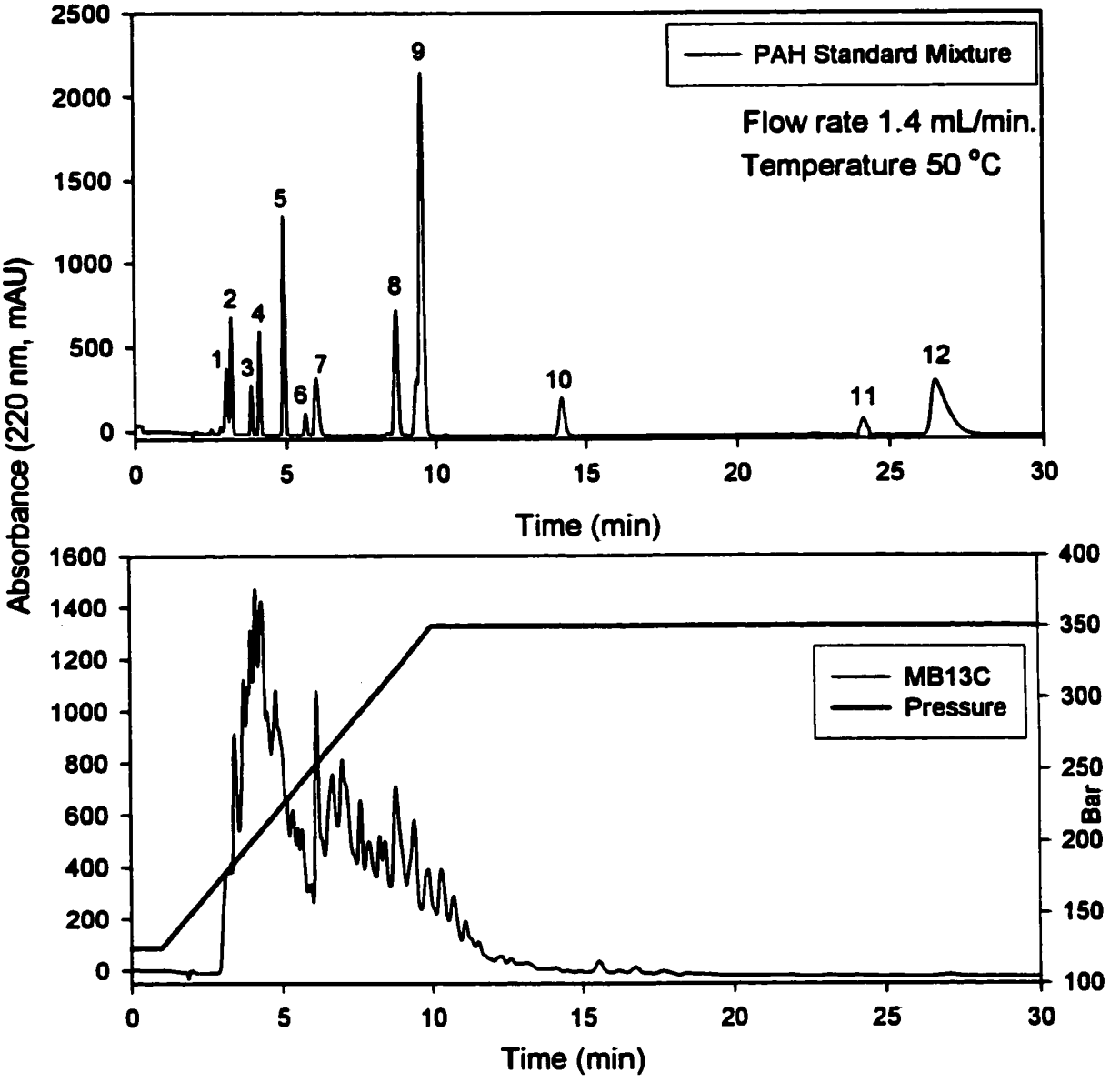

Figure 3.13: SFC chromatograms of a PAH standard mixture superimposed with the light gas oil MB13C separated using the DNBS column. The separation was performed without modifier using a pressure gradient.

Peak Identification: 1 benzene, toluene, ethyltoluene 2 xylene, mesitylene, 3 tetramethylbenzene, 4 tetralin, 5 pentamethylbenzene, 6 naphthalene, 7 biphenyl, 8 o-terphenyl, 9 fluorene, 10 phenanthrene, 11 fluoranthene, 12 pyrene.

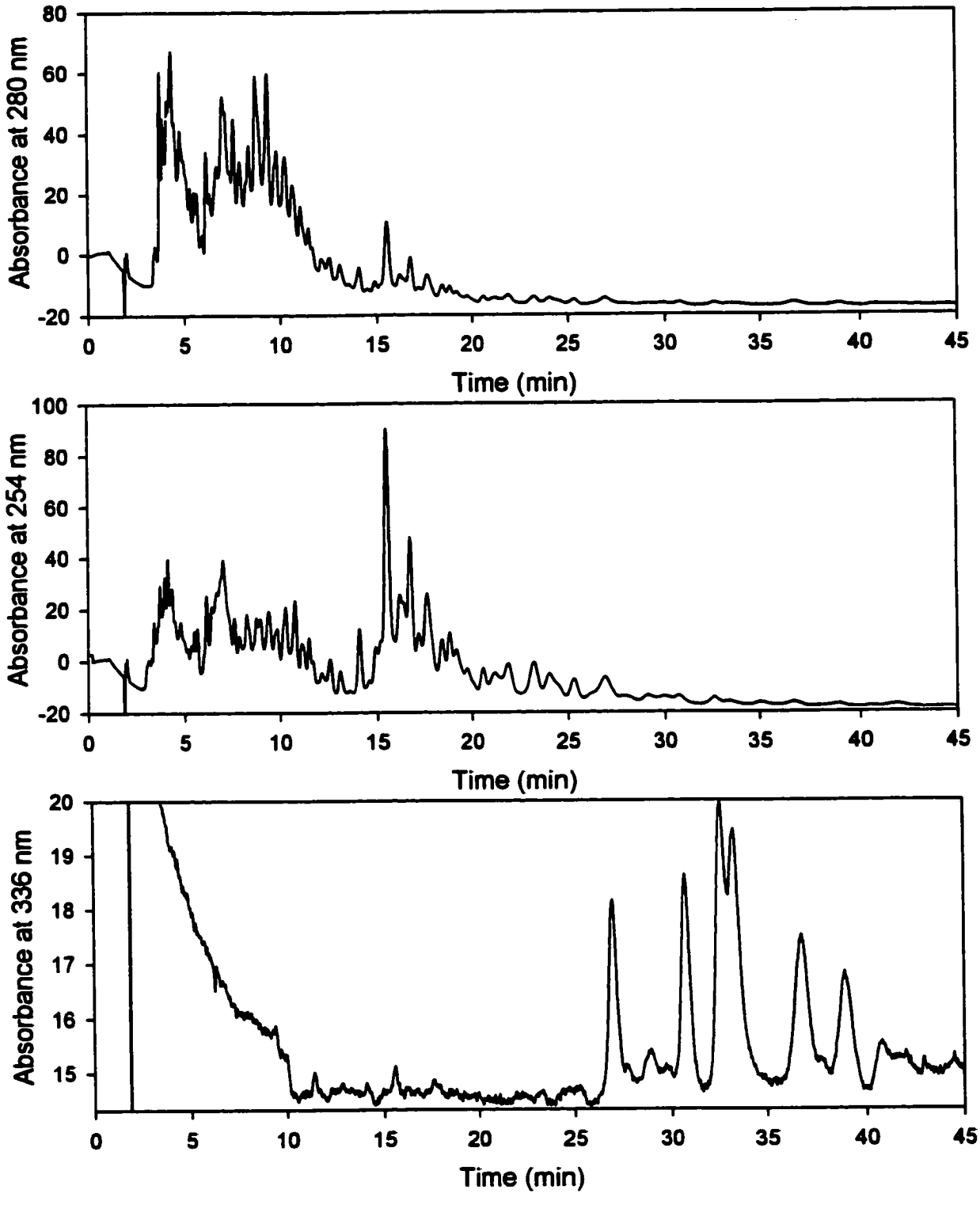

Figure 3.14: SFC chromatogram of light gas oil MB13C separated on DNBS column. Experimental conditions were shown in Figure 3.13. The baseline drift observed in the early portion of the chromatogram results from the use of the gradient. The units of the ordinate scale were mAU.

detection may provide additional compound information if complete chromatographic resolution is not obtained.

The longer analysis times using the DNBS column does not present a problem for a limited number of samples. Problems arise if multiple samples require analysis within short periods of time. This may be the case if the DNBS separation was used to monitor the processing of the gas oils on-site. In this case it would be advantageous to reduce the separation time. As mentioned at the beginning of this chapter, the addition of an organic modifier to the mobile phase will reduce retention times. Figure 3.15 shows the effect of combining an acetonitrile modifier gradient with a pressure gradient. The analysis time was cut in half from 30 minutes to 15 minutes. Under these conditions there is some loss of resolution in the mono- and di-aromatics regions mainly due to the gradient profile. The pyrene and phenanthrene regions exhibit a larger loss of separation. However, the use of selective wavelengths allowed aromatic class information to be obtained even though individual peak speciation was compromised.

3.4 Light gas oil temperature series separated on DNBS column

The previous section mentioned the possibility of using the DNBS separation for process-monitoring of the light gas oils. Figure 3.16 shows two Syncrude light gas oils processed using two different temperatures. Each of the oils was processed with all of the other experimental variables such as catalyst and hydrogen pressure held constant. The resulting samples therefore, display the effect of temperature on the levels of aromatics

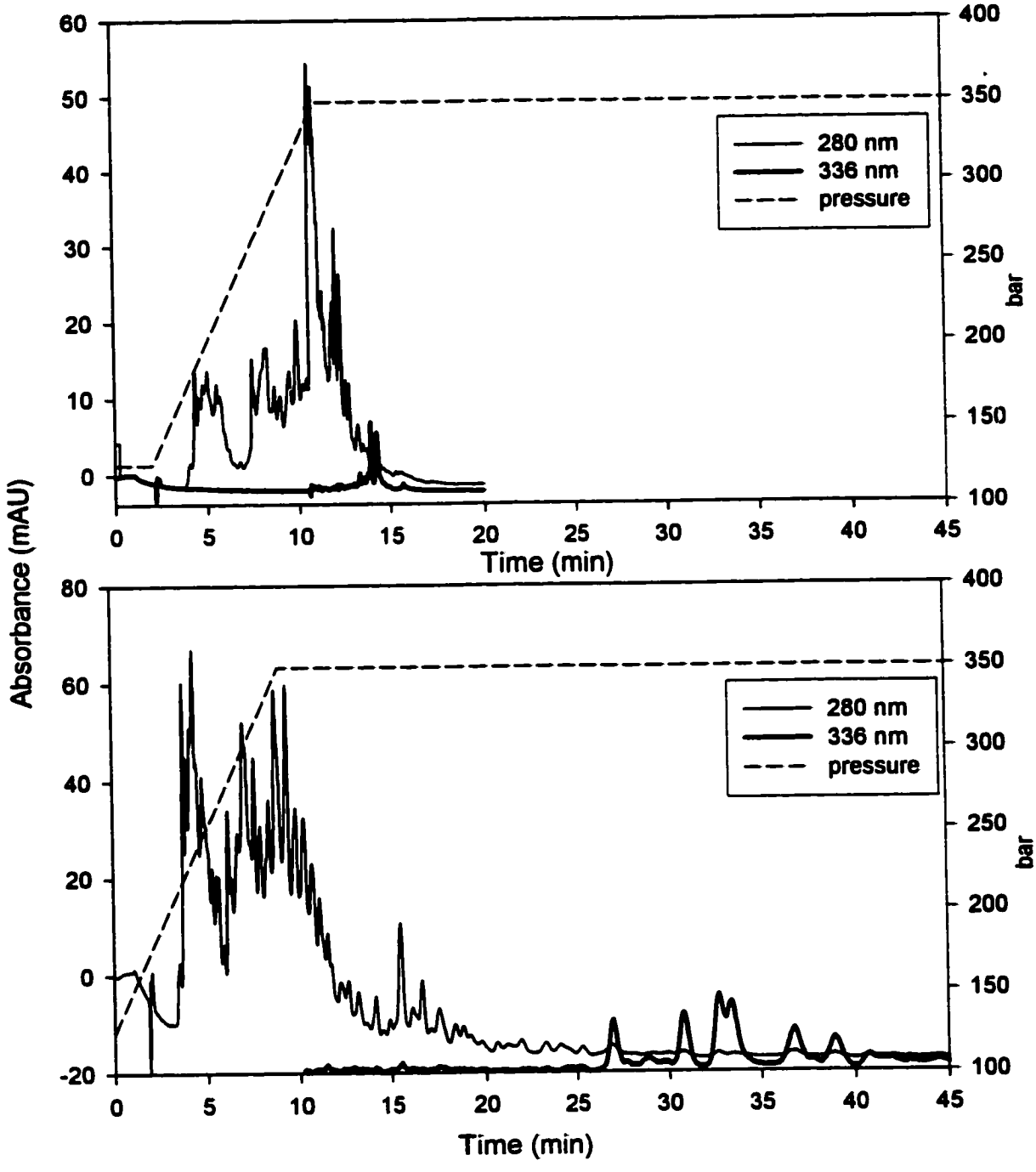

Figure 3.15: SFC chromatograms of the light gas oil MB13C on the DNBS column. Top chromatogram used acetonitrile as an organic modifier. Modifier gradient was as follows, 0-6 min @1%, then linearly to 20% over 7.5 min. The lower chromatogram did not use a modifier. The pressure gradient for each separation is superimposed on each chromatogram. The column temperature was 50 C. The flow rate was 1.4 mL/min.

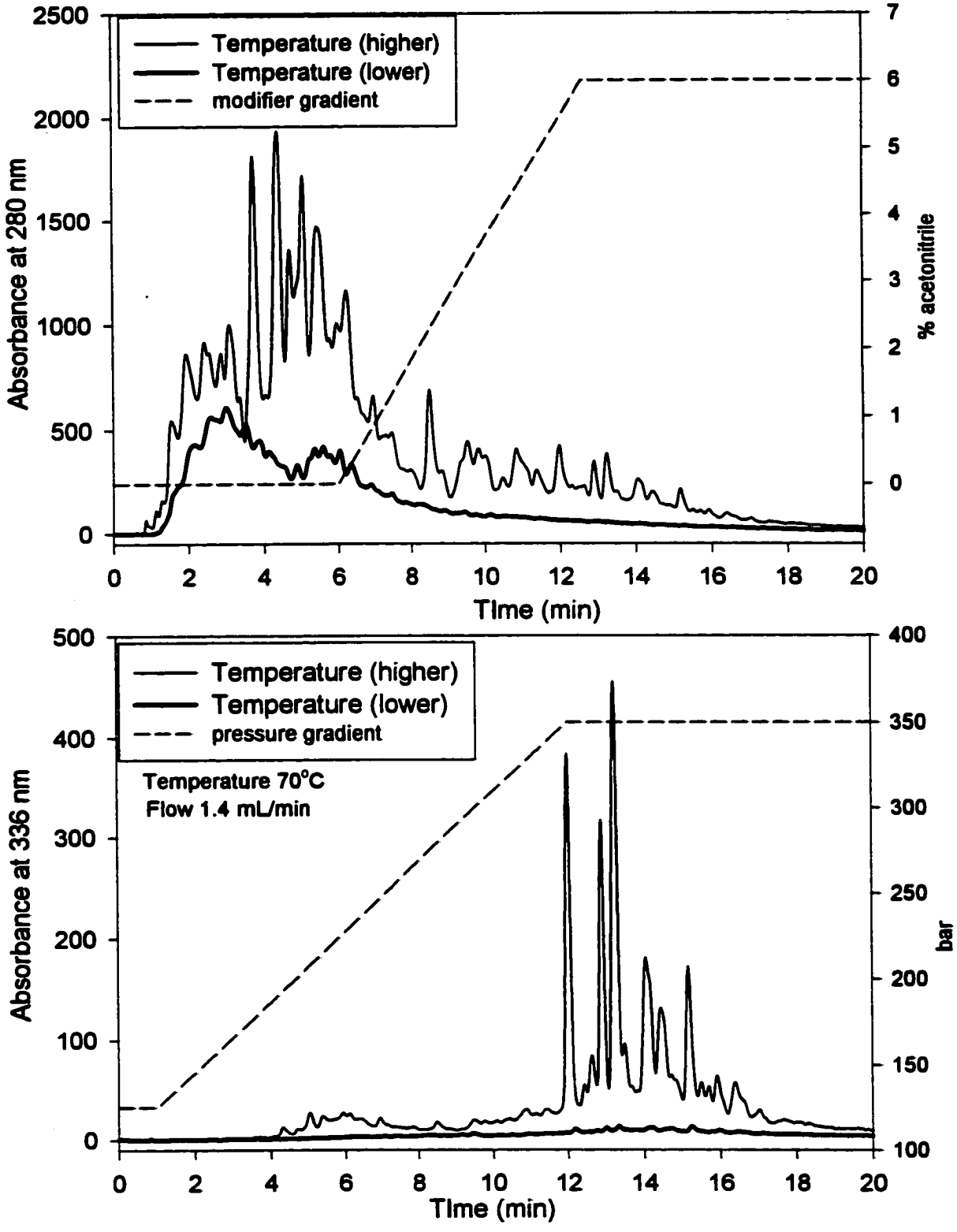

Figure 3.16: Two light gas oils hydrotreated at a higher and lower temperature separated on the DNBS column using SFC conditions. The upper chromatogram results from absorbance at 280 nm whereas the lower figure results from absorbance at 336 nm. The experimental conditions are given in the figure.

present after upgrading of the light gas oil. The upper chromatogram in Figure 3.16 shows the results for an oil monitored at 280 nm. This suggests that a significant increase in the levels of mono- and di- aromatic species is achieved when the oils were subjected to higher processing temperatures. Perhaps more striking are the chromatograms in Figure 3.16 using the detector set at 336 nm. The chromatogram corresponding to the higher processing temperature suggests a marked increase in the level of pyrene species present in this sample. Since the goal for the upgrading process is to reduce aromatic species, this observation has implications for optimizing the processing conditions. Specifically, elevated temperatures resulted in either inefficient reduction of the PAHs or in fact may have contributed to formation of larger aromatic species such as pyrene.

Additional sensitivity with laser excited fluorescence detection (compared to UV absorbance) was derived from design and implementation of a high-pressure quartz flow cell. This allowed several SFC separations to be characterized and examined as possible candidates for the determination of the priority PAHs in atmospheric particulates. However, reversed phase LC was able to provide better resolution for the priority PAHs compared to the SFC separations. Conversely, the use of a DNBS column was able to provide a rapid class separation of a light gas oil based on the number of aromatic rings. However, additional information such as the number of isomers or the amount of alkylation will require multi-dimensional chromatography.

Chapter 4 Two-Dimensional Chromatographic Analysis of MB13B

4.1 Introduction

Chapter 2 discussed the separation of a light gas oil using several typical normal phases. None of these separations were able to provide resolution sufficient to prevent co-elution of multiple components. Two-dimensional chromatography was investigated next to provide additional peak capacity. In two-dimensional chromatography, the phases are chosen to provide maximum orthogonality between dimensions. Orthogonality between chromatographic dimensions can often be achieved by exploiting the different retention mechanisms in the different forms of chromatography. For example, retention with the DNBS phase is based primarily on the strength of the donor-acceptor complex. Alkyl substitution increases the donating properties of the parent PAH and therefore, increases the retention time on the DNBS column. However, substitution has a lower effect than increasing the number pi electrons so the general result is a separation according to aromatic class. By contrast, a capillary GC separation (using a non-polar stationary phase) is more sensitive to alkyl substitution because of the increase in boiling points as molecular weight increases. This would provide a good second dimension to the DNBS separation.

Off-line two-dimensional chromatography was investigated using the light gas oil MB13B. Several modes were investigated in this work:

i. Supercritical fluid chromatography with the DNBS column using fluorescence and UV detection. The DNBS column was used for both separations so this was not

explored as an orthogonal two-dimensional procedure. This mode was investigated primarily to characterize the differences between liquid chromatography and supercritical fluid chromatography. Spectroscopic detection permits a tentative identification of the aromatic classes present in the different peaks;

ii. Capillary gas chromatography and mass spectrometric detection. This mode provides a high resolution separation and a tentative compound identification based on the mass to charge ratio. The mass to charge ratio was used to estimate the molecular weight of the compound, and assuming that the compound contains only carbon and hydrogen, a tentative molecular formula. The molecular formula can be used to estimate the number of double bond equivalents (DBE) in the compound.

iii. Normal phase chromatography as a first dimension and reversed phase chromatography as a second dimension. This will be discussed in Chapter 5.

4.2 Experimental

4.2.1 Apparatus

The LC apparatus consisted of system 1 used for the normal phase DNBS separation described in chapter 2. The GC apparatus consisted of Agilent 6890 gas chromatograph, an HP5-MS (30 m x .25 mm -0.25 μ film thickness) capillary GC column, a split/spiltless injection port, and a Micromass Fisons Quattro mass spectrometer. The SFC apparatus used was described in Chapter 3.

4.2.2 Chemicals

All LC chemicals and samples used were previously described in Chapters 2 and 3. Helium was used as carrier gas for the GC and was provided by Praxair.

4.2.3 Procedures

The experimental conditions for the first dimension normal phase LC separations using the DNBS stationary phases were described in chapter 2. A twenty microliter sample of the light gas oil MB13B was injected onto the DNBS column. A total of 100 microliters of oil was fractionated. The absorbance of the eluent was monitored at 336 nm and 254 nm using the diode array detector. Off-line fractions were collected as outlined in chapter 2. Two microliter injections (splitless) of these fractions were then introduced into the GC-MS and eluted using the chromatographic conditions shown in Table 4.1. The injection port was held at 325 °C. The mass spectrometer was operated in

Table 4.1: Chromatographic conditions used for the GC separation.

Time (min)	Temperature (C)	Flow Rate (mL/min)
0	50	2.0
2	50	2.0
47	320	2.0
57	320	2.0

EI positive mode at 70 eV with a source temperature of 325 °C, a GC transfer line temperature of 325 °C, and probe temperature of 325 °C. Mass spectra were collected with the mass spectrometer in scan mode over the range of 100-400 mass units using 0.5 second scan times. At times the scan range was changed to enhance sensitivity. Specifically, once the mass range of each of the fractions had been determined using a scan range of 100-400, the scan range was reduced to 120 –260 to enhance sensitivity. Mass spectral data were analyzed using Masslynx version 3.4.

Twenty-five microliter injections of each fraction were introduced into the SFC and eluted using a density program without the aid of organic modifier. The chromatographic conditions are shown in Table 4.2. The eluent was monitored using fluorescence detection excited with a 266 nm laser. Column temperature was maintained at 50 C.

Table 4.2: SFC chromatographic conditions.

Time (min)	Pressure (bar)	Flow Rate (mL/min)
0	125	1.5
10	350	1.5
50	350	1.5

4.3 Results and Discussion

4.3.1 Two-dimensional LC-SFC (DNBS) Analysis of MB13B

The DNBS column was used for both the first and second dimensions of chromatography. Under normal circumstances this would not be a good choice to obtain maximum peak capacity. The priority of this experiment was to examine the differences in behavior between LC and SFC modes of operation. Figures 4.1-4.7 display the chromatograms that result from each fraction collected on the LC-DNBS separation injected onto the SFC. Fractions 2 and 3 showed little improvement in chromatographic resolution. The spectra observed at different times in each fraction were quite similar suggesting that each belonged to a single class. Fraction 2 was believed to contain naphthalenes and fraction 3, biphenyls. The remainder of the fractions were much more interesting.

The SFC chromatogram of fraction 4 produced about 18 peaks compared to 3 peaks in LC. Furthermore, these peaks were separated into two distinct classes according to their spectra. The fluorescence spectra were indicative of phenanthrenes (class 3) and either fluorenes or biphenyls (class 2). The fluorescence spectrum of fluorene was similar to biphenyl so that distinguishing between the two compound classes was not possible. Figure 4.8 shows the typical UV spectrum for this unknown class of compounds compared to the spectra of biphenyl and fluorene. These spectra suggest that this series of compounds may be alkylated fluorenes. The spectra are not identical but the positions of the three absorption bands for the unknown have better agreement with

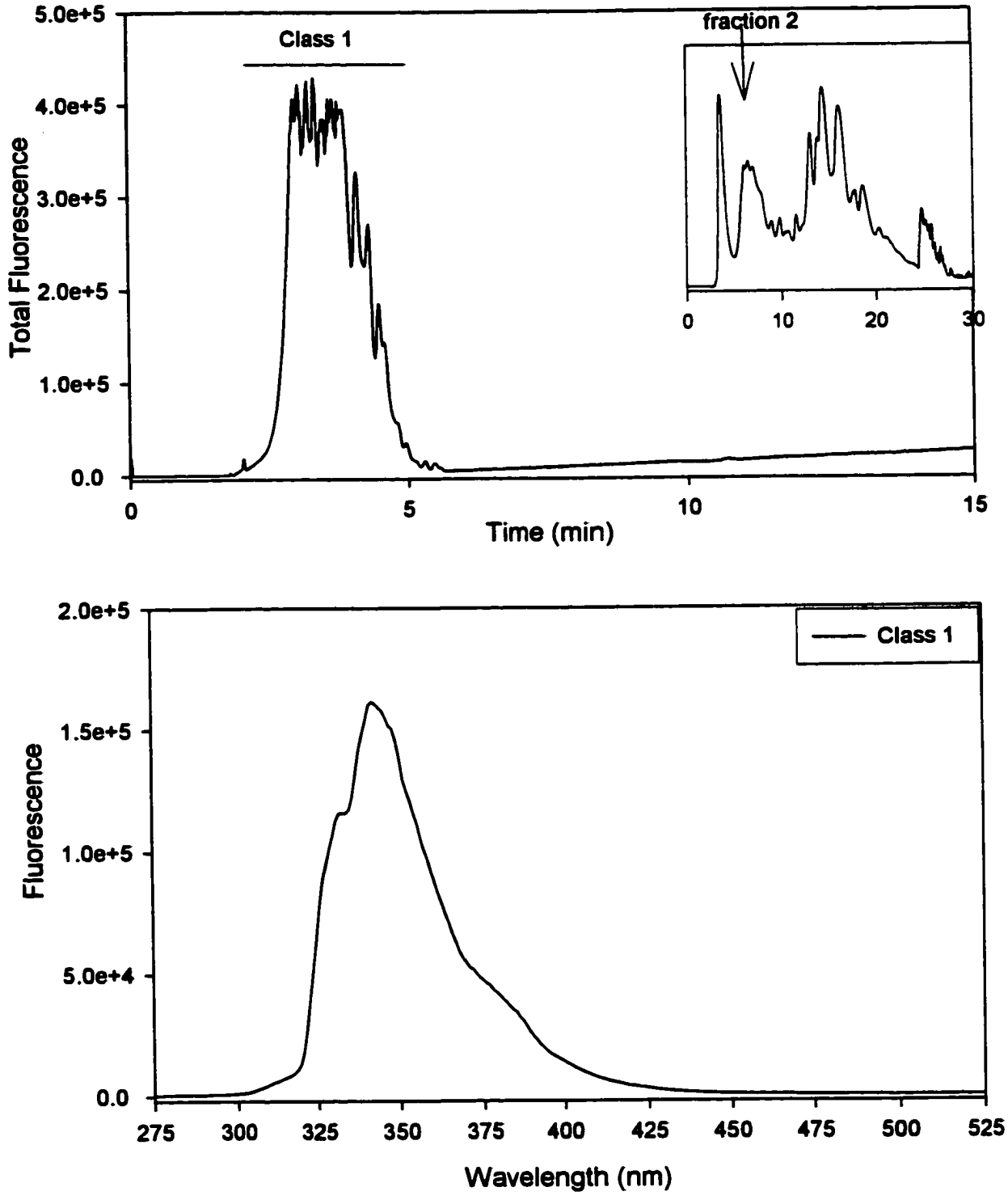

Figure 4.1: SFC Chromatograms of LC-DNBS fraction 2. Inset of each chromatogram shows separation of oil using LC conditions. Fractions marked within each inset chromatogram. SFC chromatograms of fraction use laser excited fluorescence at 266 nm. The spectrum in the lower figure was representative of each of the peaks.

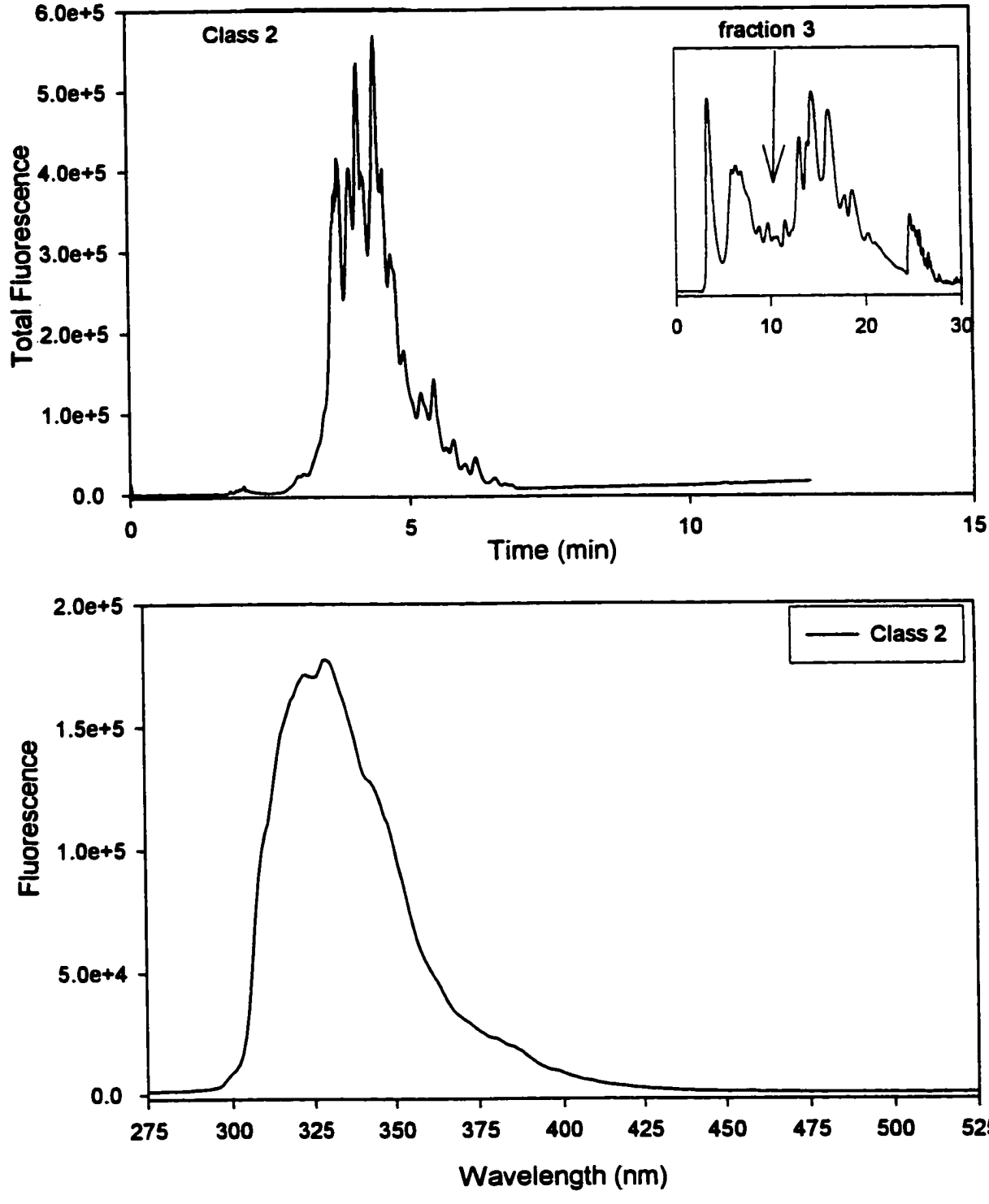

Figure 4.2: SFC Chromatograms of LC-DNBS fraction 3. Inset of each chromatogram shows separation of oil using LC conditions. Fractions marked within each inset chromatogram. SFC chromatograms of fraction use laser excited fluorescence at 266 nm. The spectrum in the lower figure was representative of each of the peaks.

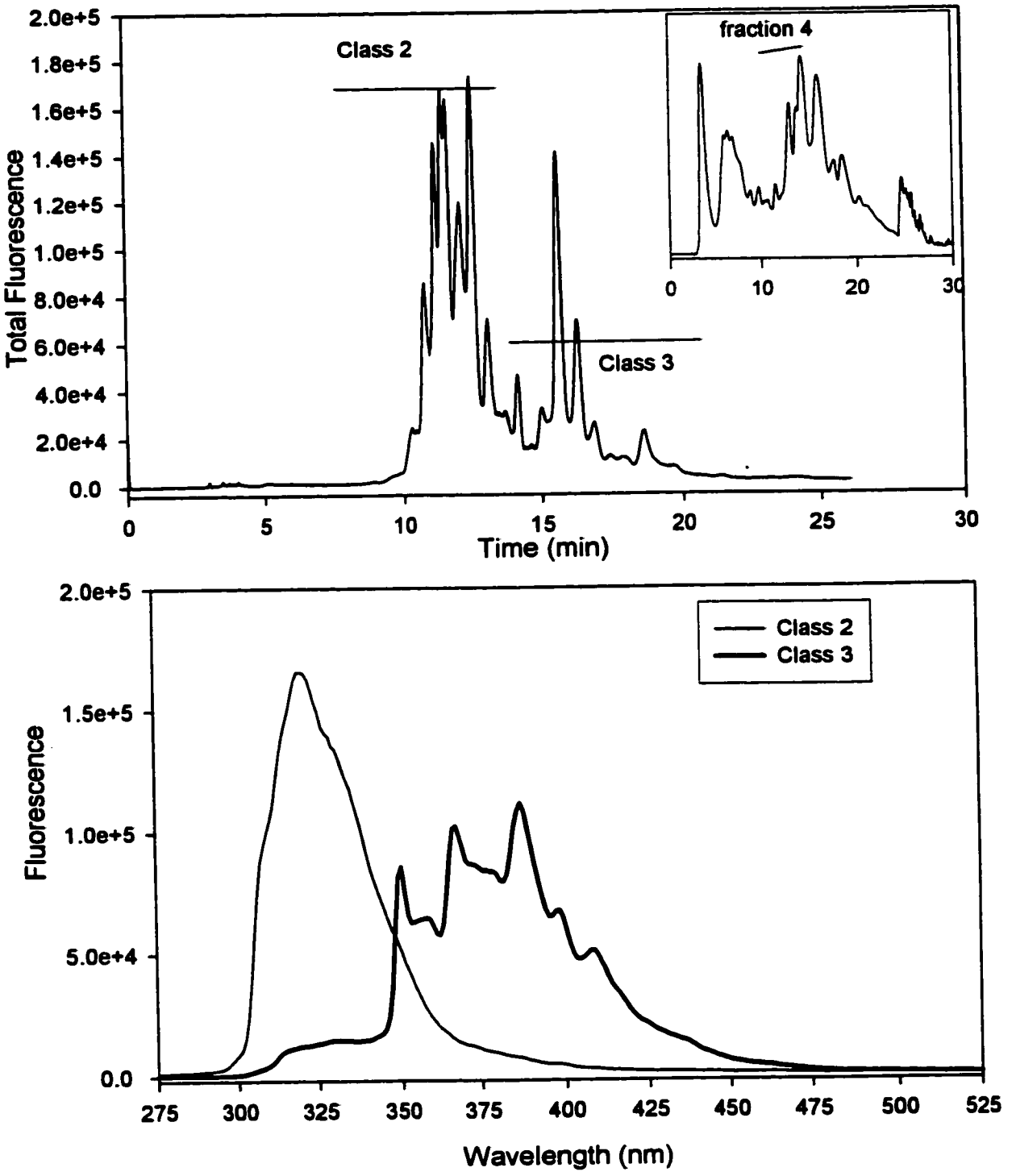

Figure 4.3: SFC Chromatograms of LC-DNBS fraction 4. Inset of each chromatogram shows separation of oil using LC conditions. Fractions marked within each inset chromatogram. SFC chromatograms of fraction use laser excited fluorescence at 266 nm. Spectra in the lower figure were representative of each class of compounds.

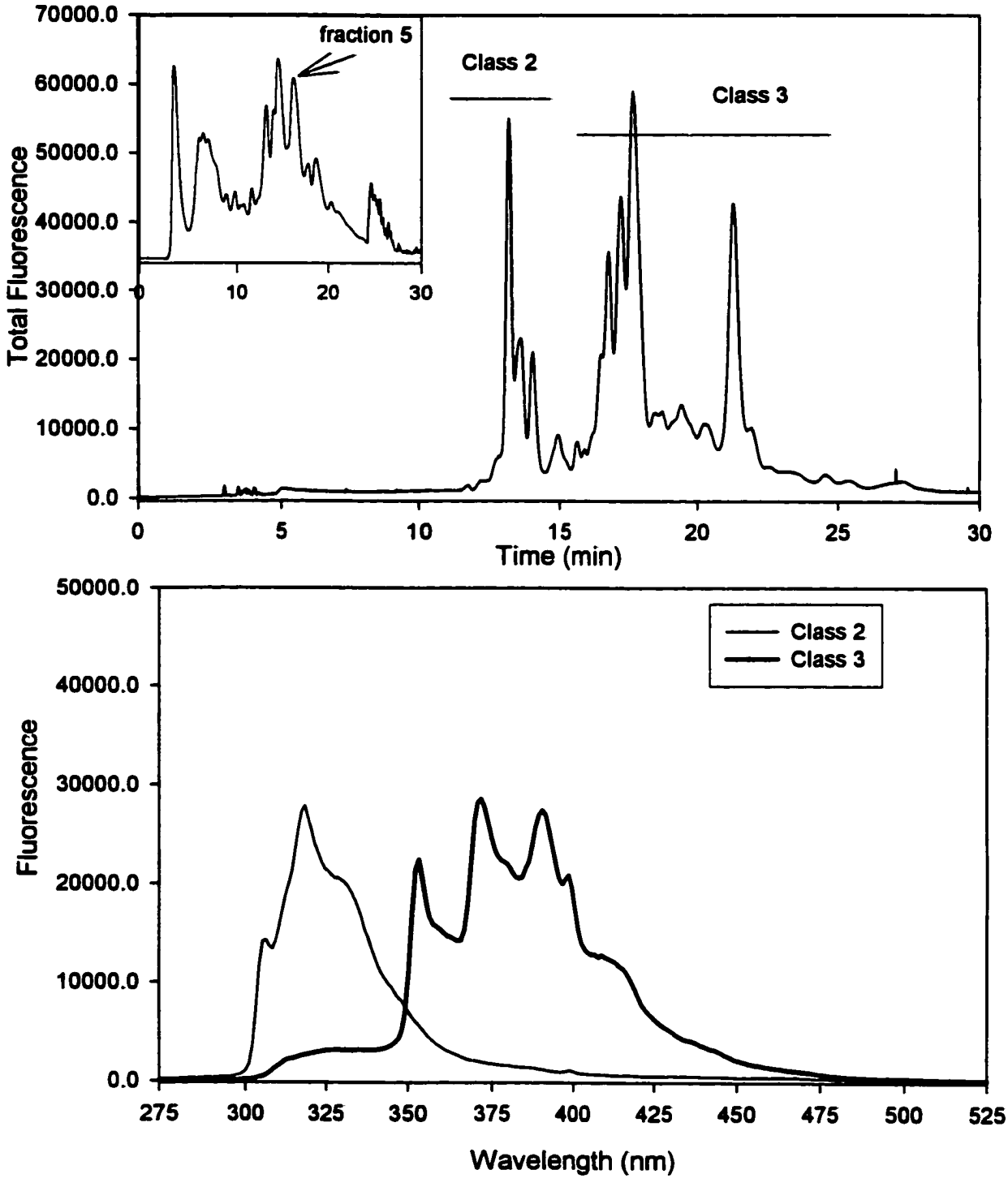

Figure 4.4: SFC Chromatograms of LC-DNBS fraction 5. Inset of each chromatogram shows separation of oil using LC conditions. Fractions marked within each inset chromatogram. SFC chromatograms of fraction use laser excited fluorescence at 266 nm. The spectra in lower the figure were representative of each class of compounds.

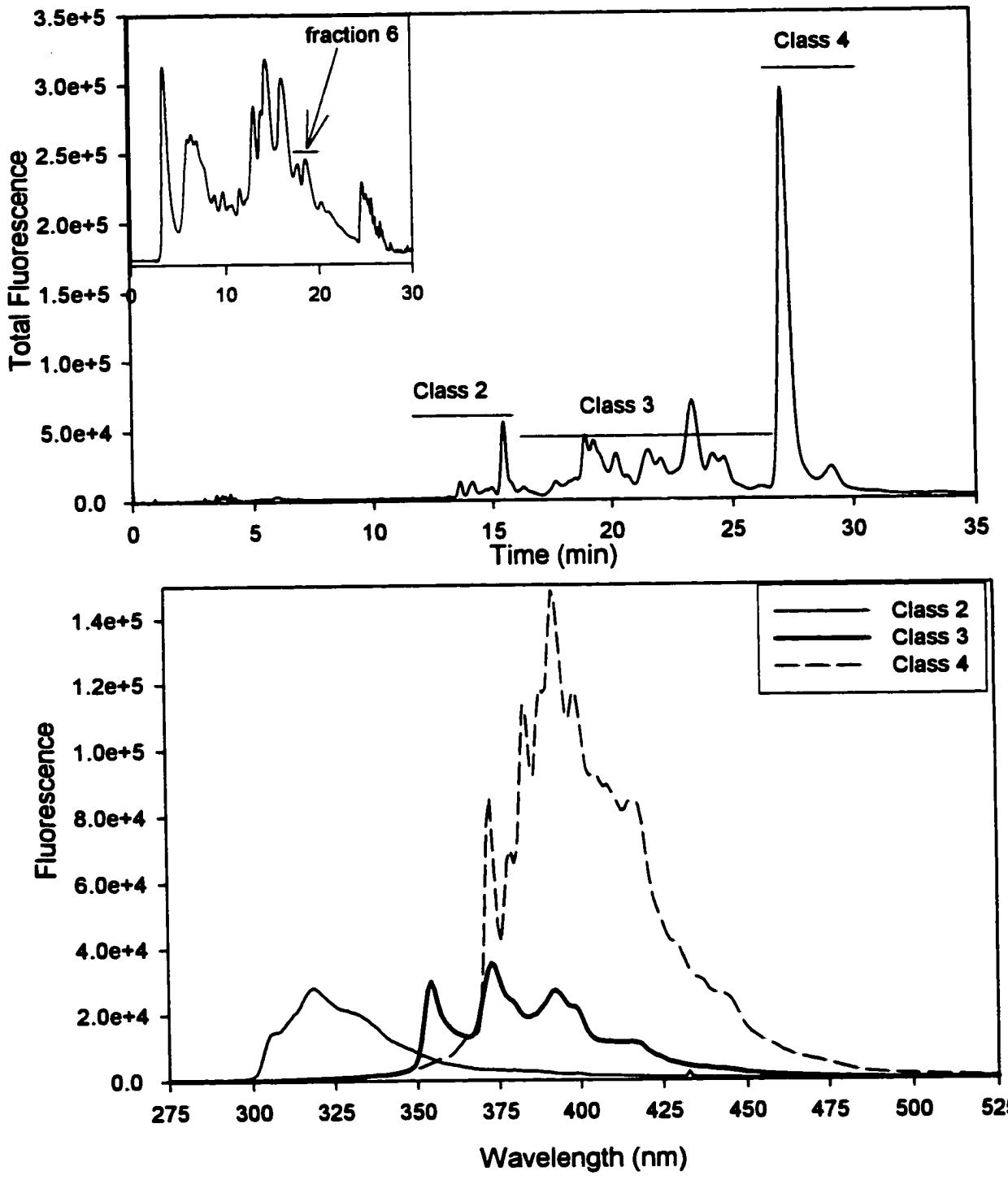

Figure 4.5: SFC Chromatograms of LC-DNBS fraction 6. Inset of each chromatogram shows separation of oil using LC conditions. Fractions marked within each inset chromatogram. SFC chromatograms of fraction use laser excited fluorescence at 266 nm. The spectra in the lower figure were representative of each class of compounds.

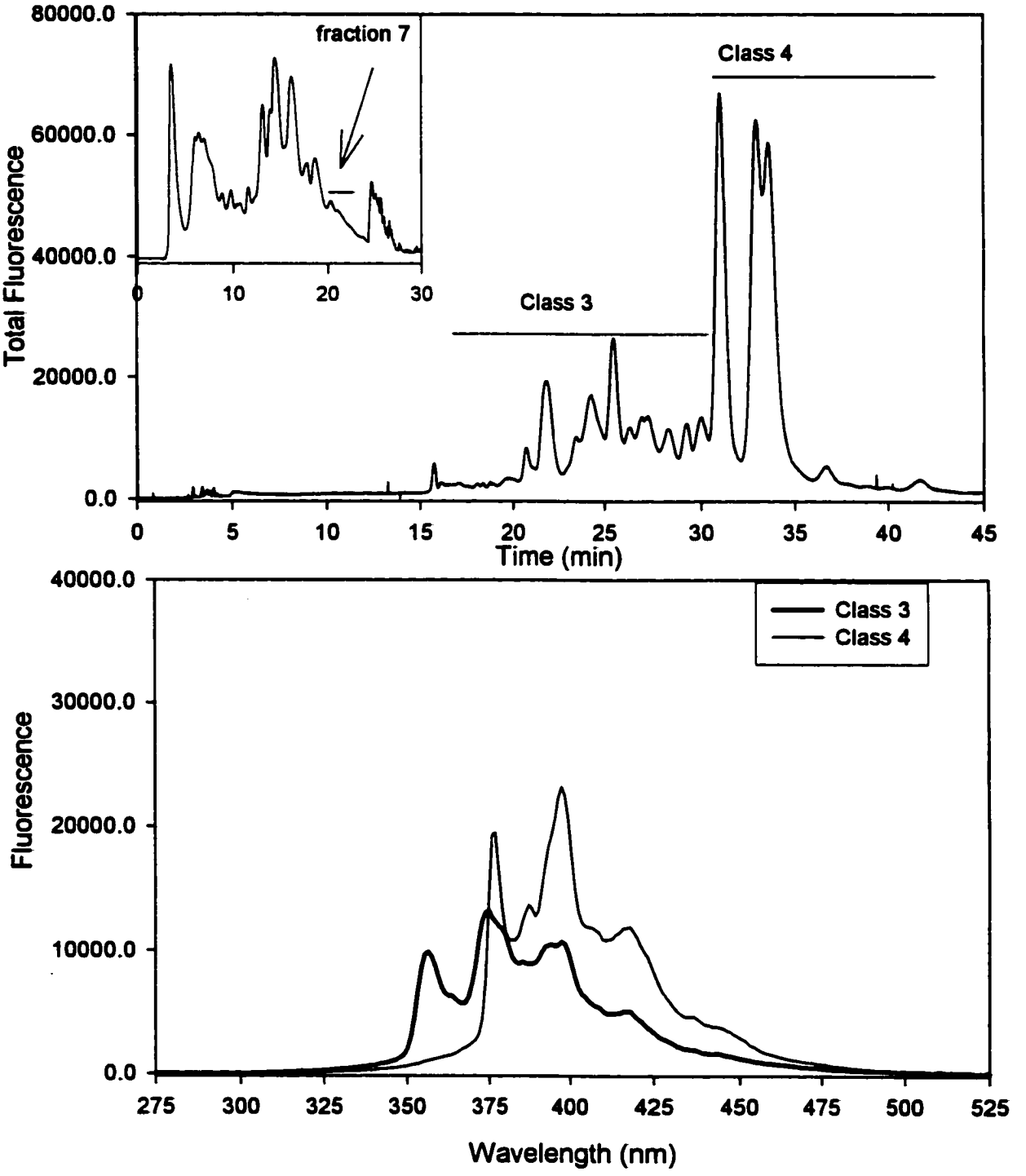

Figure 4.6: SFC Chromatograms of LC-DNBS fraction 7. Inset of each chromatogram shows separation of oil using LC conditions. Fractions marked within each inset chromatogram. SFC chromatograms of fraction use laser excited fluorescence at 266 nm. The spectra in the lower figure were representative of each class of compounds.

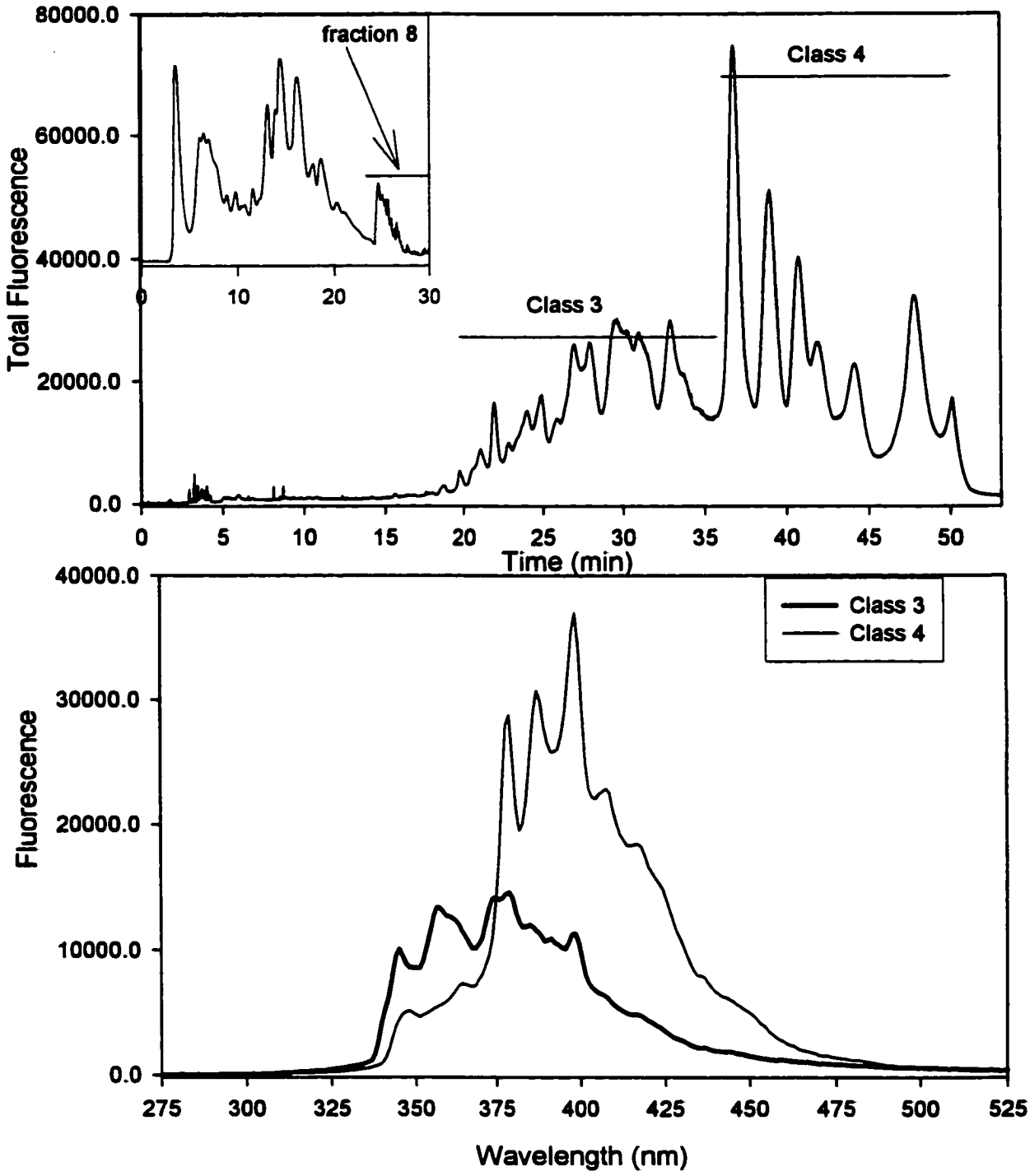

Figure 4.7: SFC Chromatograms of LC-DNBS fraction 8. Inset of each chromatogram shows separation of oil using LC conditions. Fractions marked within each inset chromatogram. SFC chromatograms of fraction use laser excited fluorescence at 266 nm. Spectra in the lower figure were representative of each class of compounds.

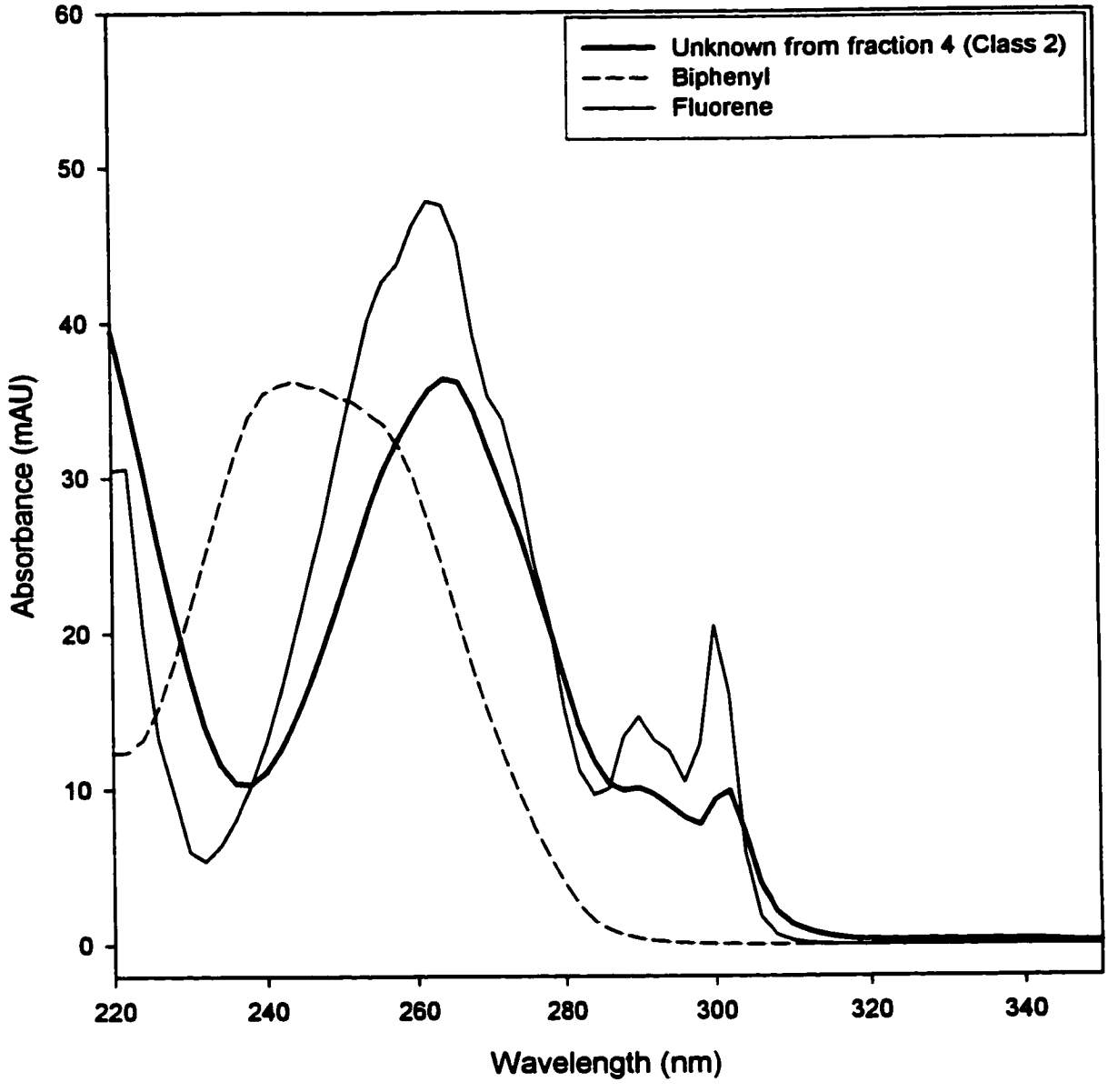

Figure 4.8: UV spectrum of a compound in Class 2 region of SFC separation of fraction 4. Standard UV spectra of fluorene and biphenyl superimposed.

fluorene than for biphenyl. Conclusive assignment was difficult due to the limited availability of standards. Similar class separations were observed with the remaining fractions. In fact, fraction 6 showed evidence for three different aromatic classes according to their spectra, fluorenes, phenanthrenes, and pyrenes. This two-dimensional study was able to provide information about the aromatic class of each peak from the fractions. The aromatic classes were characterized with UV and fluorescence detection and summarized in Table 4.3.

Table 4.3: Aromatic Classes observed in each of the DNBS fractions.

LC-DNBS Fraction	**Aromatic Classes Observed**
Fraction 2	Naphthalenes
Fraction 3	Biphenyls
Fraction 4	Fluorenes, Phenanthrenes
Fraction 5	Fluorenes, Phenanthrenes
Fraction 6	Fluorenes, Phenanthrenes, Pyrenes
Fraction 7	Phenanthrenes, Pyrenes
Fraction 8	Phenanthrenes, Pyrenes

Spectroscopic detection permits the tentative assignment of aromatic class but did not provide reliable information about other parameters such as the level of alkylation or the number of isomers with similar alkylation patterns. This was a function of a lack of

standards, overall column peak capacity and the detection methods that were used. Capillary GC separations offer more peak capacity and mass spectrometry provides molecular weights that may be better suited to these tasks.

It was evident that the DNBS column showed better resolution under SFC conditions when compared to the original LC conditions. This is not totally unexpected as one benefit associated with SFC is an increase in separation efficiency. Generally, SFC is considered an intermediate between LC and GC in terms of efficiency and analysis speed. The apparent enhancement of class separation with SFC conditions was most likely a direct result of the observed increase in column efficiency or differences in mobile phase chacteristics between hexane and CO_2.

The enhanced efficiency with SFC makes it a more attractive alternative to standard LC fractionations. However, the high pressures associated with SFC separations provide difficulties when interfacing between chromatographic dimensions and collecting fractions. However, in light of the efficiency gains with the DNBS column under SFC conditions a high temperature transfer line was developed to interface into a cryo inlet for GC-MS as an MSc. project [154]. This interface was successful and allowed a more controlled transfer of compounds between dimensions, particularly with the smaller aromatic classes. The work reported in the MSc. thesis complements the work described in the next section.

4.3.2 Characterization of the GC Separation

This section outlines a general characterization of the 95%-methyl/5%-phenyl

siloxane stationary phase used with the capillary GC separation. This type of column is often referred to as a "boiling point column" because it has a non-polar stationary phase. This phase is expected to have limited interactions with the analytes. Therefore, the primary mechanism for separation is based on the vapor pressure differences of the compounds at any given column temperature. Table 4.4 provides a list of the retention times for several hydrocarbon and PAH standards separated on the methyl/phenyl stationary phase. As expected, retention times increase as the number of carbon atoms increase because the boiling point tends to increase with molecular weight. To generalize, the addition of a methylene group to a saturate or a methyl group to an aromatic ring tends to raise the boiling point by 18-20 C and increase retention time by about 2.4 minutes (for the chromatographic conditions used in this work). Figure 4.9 shows a graph of the retention times versus boiling points for the aromatic and aliphatic compounds separated using our GC conditions. The data is typical of the behavior expected for a hydrocarbon series separated using temperature programming. The aliphatic and aromatic compounds represented two lines that have different slopes on the graph. This suggests that an aromatic and an aliphatic compound with similar boiling points should be resolved. Furthermore, according to the data in Table 4.4 the difference in retention times increases as the number of carbons in each series progresses. Boiling points can be used to estimate relative retention times within a hydrocarbon series but boiling points may not always provide good relative retention times for compounds in different series. For example, consider the vapor pressure curves for naphthalene and dodecane shown in Figure 4.10. Naphthalene would be expected to elute after dodecane

Table 4.4: Retention times for selected standards using capillary GC separation.

Compound	Retention Time (min)	Boiling Point (C)
Decane $C_{10}H_{22}$	6.42	174
Undecane $C_{11}H_{24}$	8.80	196
Naphthalene $C_{10}H_{10}$	10.71	218
Dodecane $C_{12}H_{26}$	11.18	216
1-methylnaphthalene $C_{11}H_{12}$	13.27	240-243
Tridecane $C_{13}H_{28}$	13.45	234
Tetradecane $C_{14}H_{30}$	15.61	252-254
Hexadecane $C_{16}H_{34}$	19.60	280
Phenanthrene $C_{14}H_{10}$	22.73	340
Octadecane $C_{18}H_{38}$	23.20	308
2-methylphenathrene $C_{15}H_{12}$	24.96	359
9-methylphenathrene $C_{15}H_{12}$	25.06	355
2-methylanthracene $C_{15}H_{12}$	25.14	359
Eicosane $C_{20}H_{42}$	26.49	343
Pyrene $C_{16}H_{10}$	28.04	393
9,10-dimethylanthracene $C_{16}H_{14}$	28.42	
Docosane $C_{22}H_{46}$	29.48	369
Retene $C_{18}H_{18}$	29.65	390
1-methylpyrene $C_{17}H_{12}$	30.32	
Tetracosane $C_{24}H_{50}$	31.25	391
Benz(*a*)anthracene $C_{18}H_{12}$	32.76	438
Hexacosane $C_{26}H_{54}$	34.85	412
Octacosane $C_{28}H_{58}$	37.20	432
Tricontane $C_{30}H_{62}$	39.42	445
Dotricontane $C_{32}H_{66}$	41.50	467
Hexatricontane $C_{36}H_{74}$	45.25	

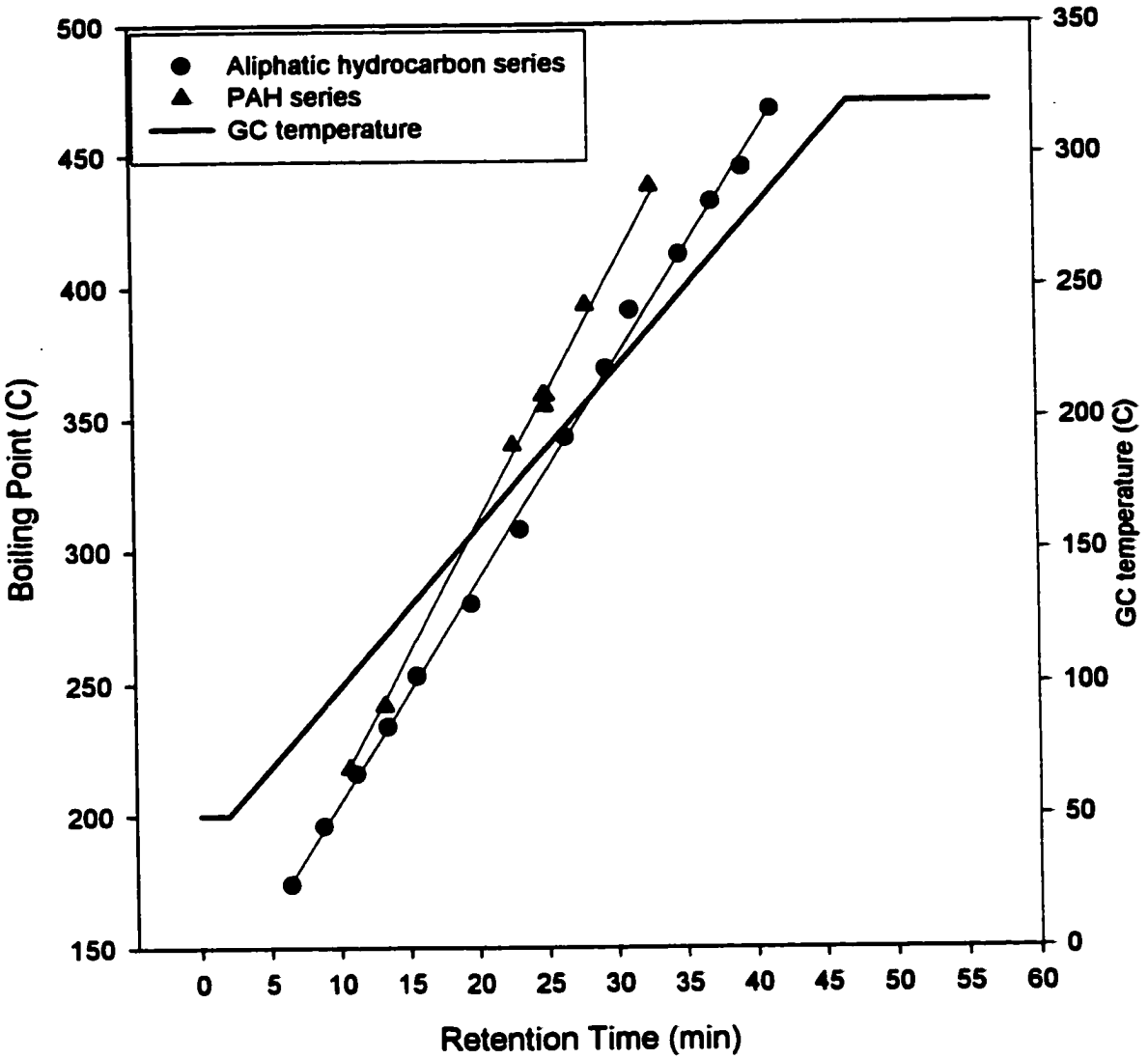

Figure 4.9: Graph of retention times and boiling points for a normal straight chain hydrocarbon series and a PAH series.

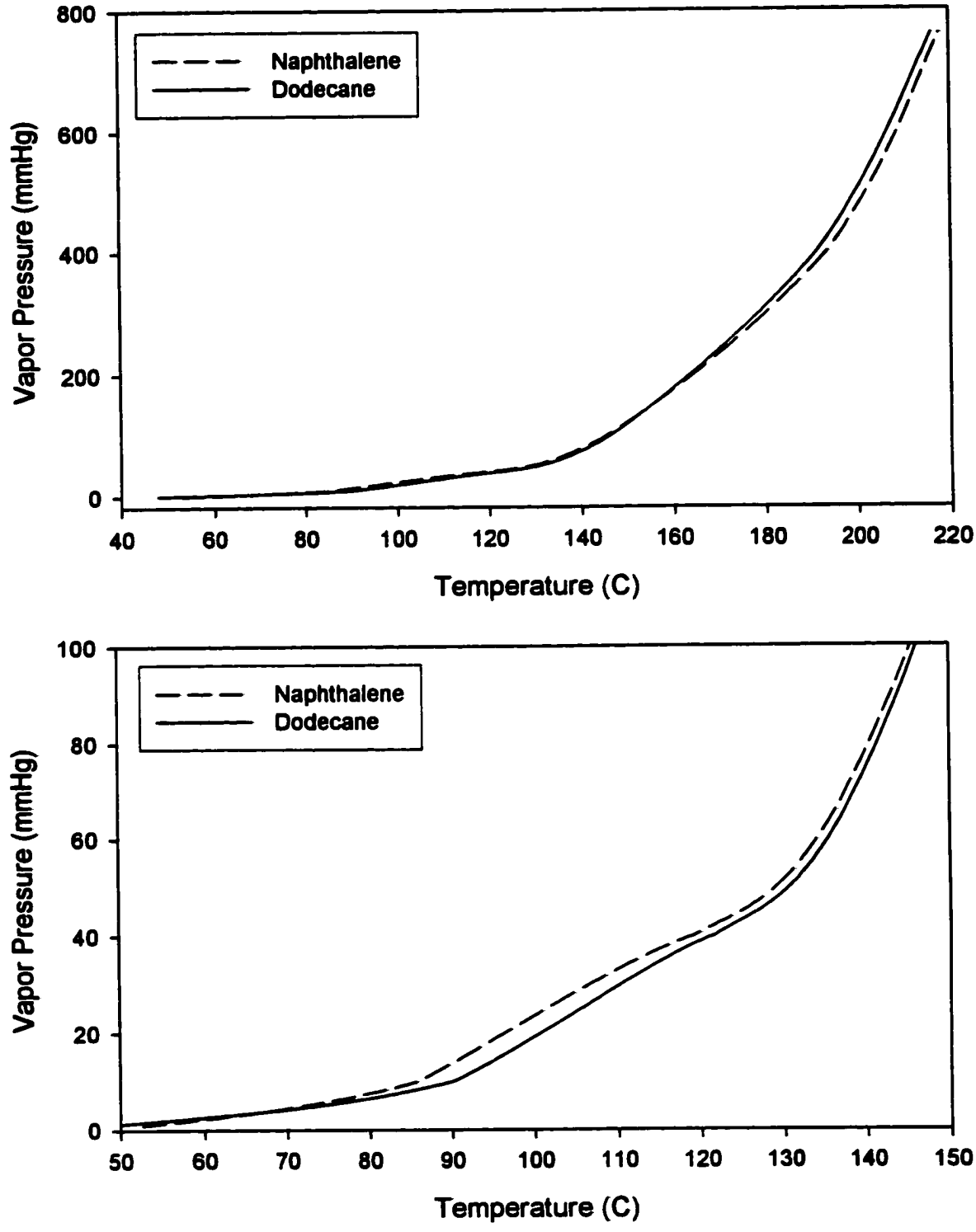

Figure 4.10: A temperature versus vapor pressure curve for Naphthalene and Dodecane. The lower figure is a scaled version of the upper figure to emphasize the region below 150 C.

based upon their respective boiling points. A closer look at the vapor pressures for naphthalene and dodecane between 75 and 150 C suggests that naphthalene has a higher vapor pressure in this temperature range. This causes naphthalene to elute before dodecane regardless of the boiling points of the two compounds.

4.3.3 Two-dimensional LC(DNBS)-GC/MS

Molecular weight information was gathered for each of the peaks using a high resolution GC separation. The molecular weight allowed a tentative assignment of the molecular formula and an estimation of the number of double bond equivalents (DBE), assuming that the compounds were formed purely from carbon and hydrogen. For example, the mass 206 has three possible formulae: $C_{17}H_2$, $C_{16}H_{14}$, $C_{15}H_{26}$ which give 17, 10, and 3 double bond equivalents, respectively. Of these three possibilities the most likely aromatic compound in the light gas oil would be 10 double bond equivalents. There are several 10 double bonds equivalent compounds that could be proposed:

phenanthrene (10 DBE). A mass of 206 would result from the parent compound (178 m/z) plus either one ethyl or two methyl substituents. The mass spectrometer would not necessarily be able to differentiate between these isomers;

biphenyl (8 DBE) with two reduced rings attached (2 DBE). A compound that could be formed by the addition of hydrogen to two of the aromatic rings on pyrene which would give an ion at 206 *m/z*;

fluorene (9 DBE) with a reduced ring attached (1 DBE) could be formed by the reduction of one of the rings of fluoranthene which would also result in a mass of 206.

The partial reduction of benzofluorene would not result in a mass of 206 so this would not be a possibility but fluorene with a 5 membered ring would also give a mass of 206.

Fractions 2 and 3 were very complex but the mass information was obtained for the major peaks. The GC-MS chromatogram of fraction 4 shown in Figure 4.11 was typical of the fractions 4-8. In general, the amount of material decreased as the fraction number increased. The complexity of the GC chromatogram for fraction 4 suggests that many compounds were present with several of the peaks displaying only partial resolution. Figure 4.12 shows the mass spectra for the peaks at 23.59 and 24.76 minutes. The spectrum shown for the peak at 24.76 minutes was relatively easy to interpret based upon the assumption that compounds contain only carbon and hydrogen and the NIST library spectra shown in Figure 4.13e. The unknown spectrum corresponds to a methyl substituted phenanthrene (10 DBE). This agreed with the data presented from the two-dimensional LC-SFC discussed earlier in this chapter. Specifically, fluorescence spectra were observed that corresponded to phenanthrenes.

The spectrum for the peak at 23.59 minutes has a fragmentation pattern that suggests that a loss of 14 might occur (208-194). This usually corresponds to a CH_2 group for a compound containing only carbon and hydrogen. This fragmentation would be unlikely which suggests that the spectrum results from a mixture of two compounds with masses of 194 and 208 *m/z*. A comparison of this spectrum with that of 2,3-dimethylfluorene (Figure 4.13f) from the NIST library supports this interpretation. Exact identification is not possible, however, without standards (to give retention times) since the mass spectrometer cannot distinguish between the dimethyl or ethyl isomers of

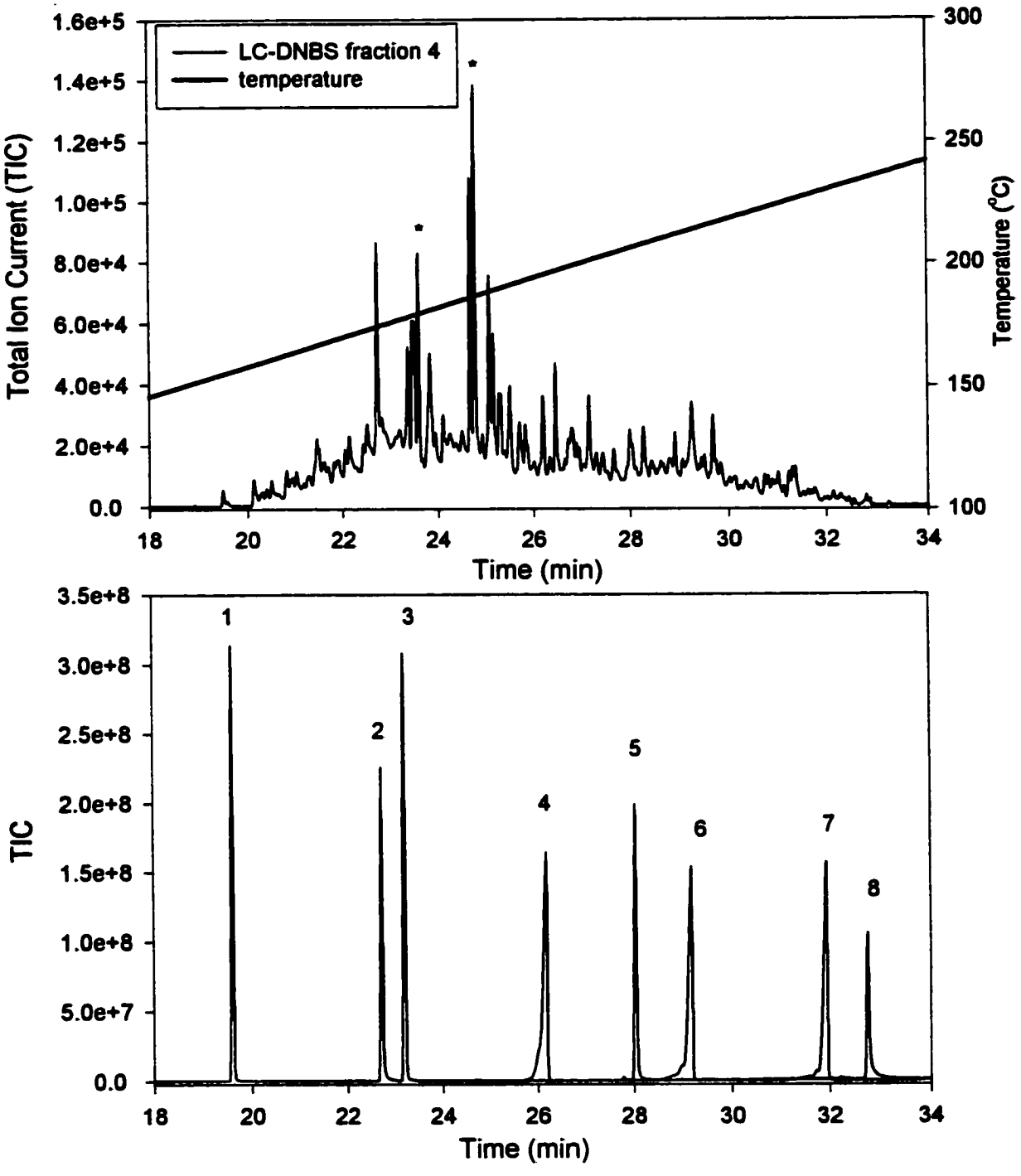

Figure 4.11: GC separation of LC-DNBS 4 using mass spectrometric detection. Two peaks marked in the upper chromatogram correspond to the spectra shown in Figure 4.12. The lower chromatogram corresponds to a series of PAH and saturated standards.

Peak indentification: 1 hexadecane, 2 phenanthrene, 3 octadecane, 4 eicosane, 5 pyrene, 6 docosane, 7 tetracosane, 8 chrysene

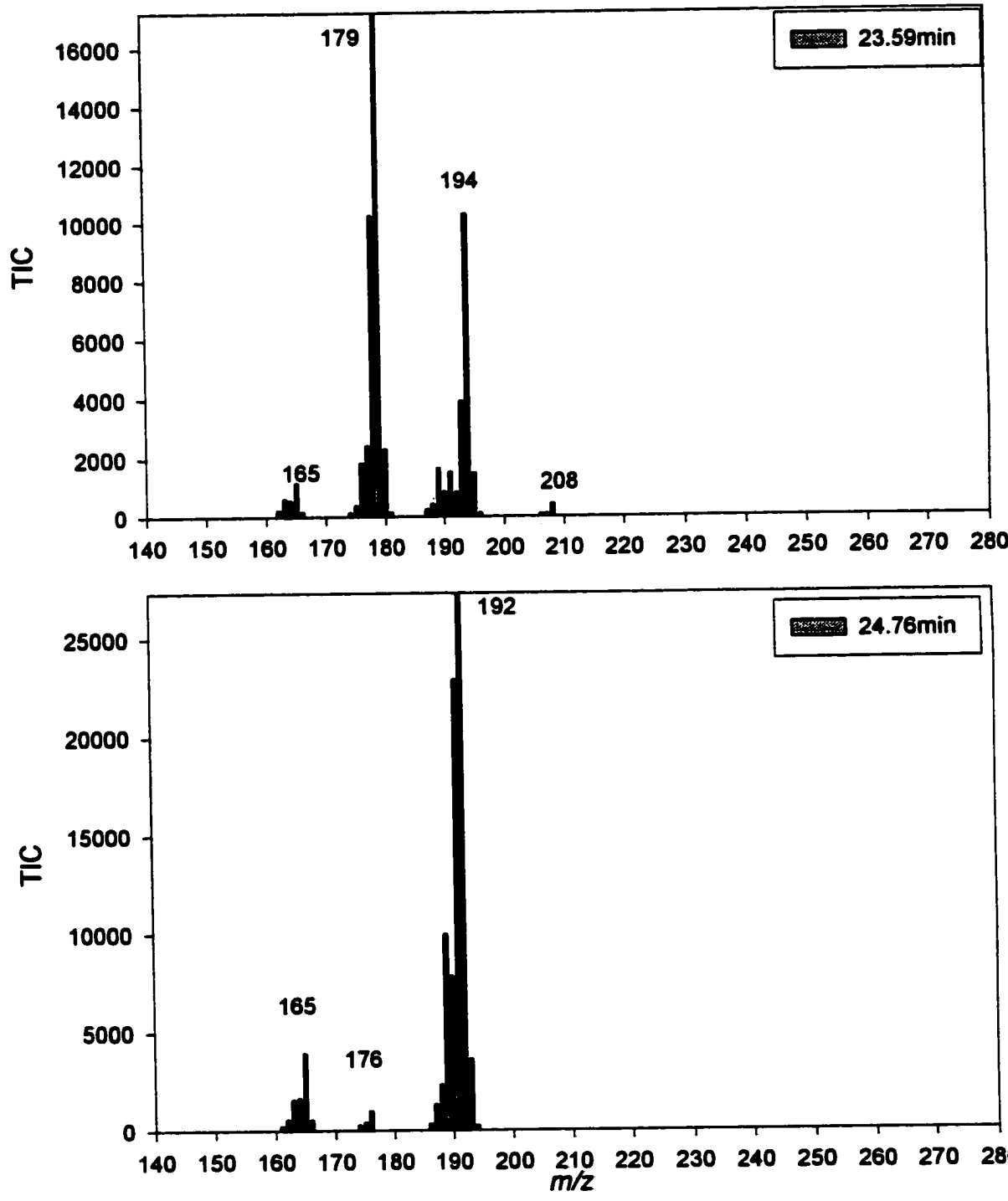

Figure 4.12: Spectra of selected peaks from GC-MS separation of LC-DNBS fraction 4 shown in Figure 4.11.

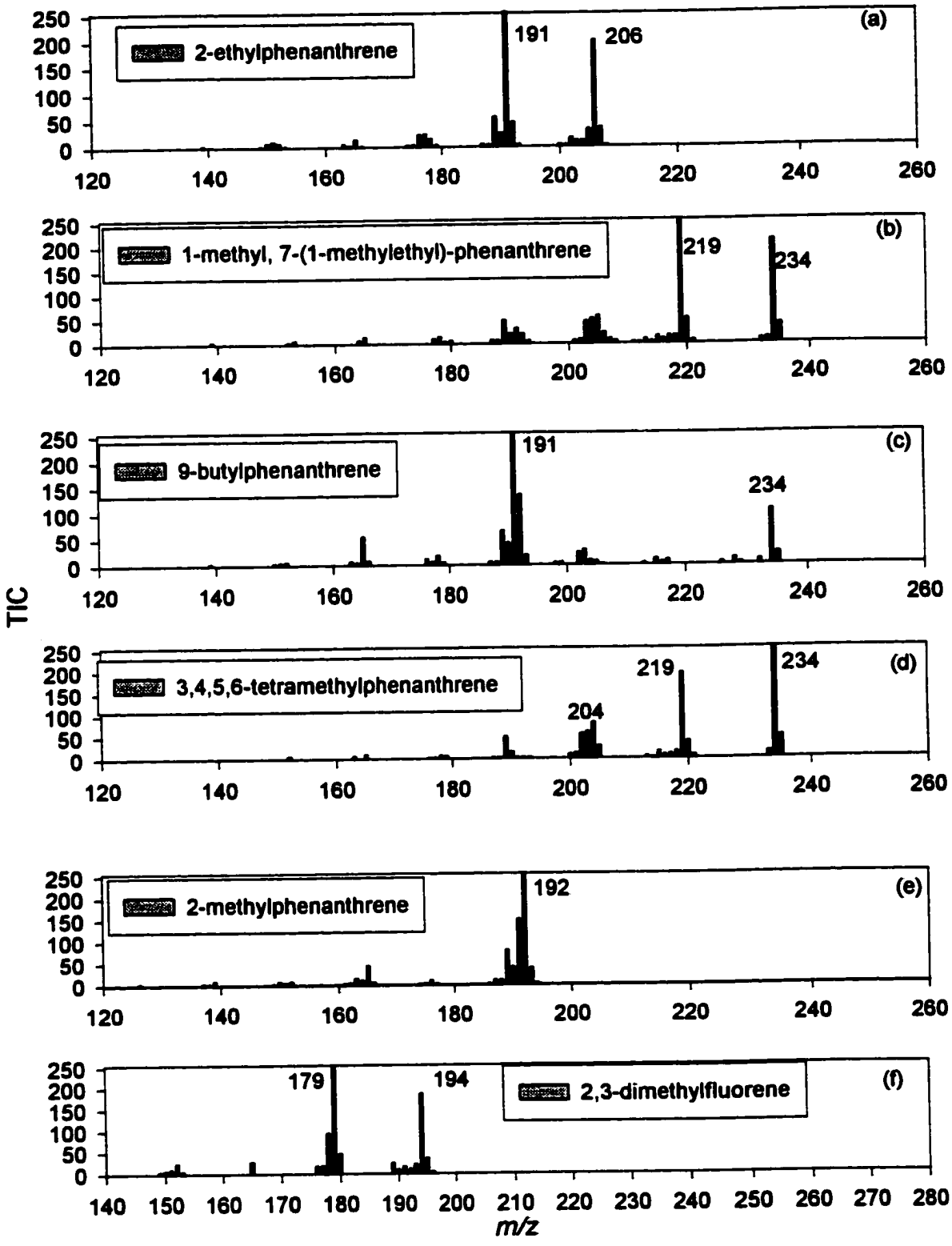

Figure 4.13: Mass spectra adapted from the of NIST library of compounds using EI+ ionization.

fluorene. However, this observation further supports the assignment of class made earlier with the UV spectrum. It is interesting to note that the NIST library spectra indicate that the base peak is the molecular ion for 3,4,5,6-tetramethylphenanthrene but not for 2,3-dimethylfluorene. This variable behavior makes identification of compounds difficult and underscores the need for additional standards to properly characterize these mixtures.

The spectrum for each peak in each fraction was analyzed and the data are summarized in Tables 4.5-4.11. A single asterisk (*) was used to denote the most intense ion in the mass spectrum (base peak) for each entry. For example, the first entry in Table 4.7 was a dimethylfluorene (194 *m/z*). The most intense ion in the mass spectrum for this compound was observed at 179 *m/z* which represents a loss of 15 *m/z* from 194 *m/z*. Hence, 15* was used to denote the most intense ion in the mass spectrum or the base peak. A double asterisk (**) was used to indicate the presence of at least two compounds in the mass spectra. The complexity of the data for fractions 2 and 3 added a certain level of ambiguity to the interpretation. The data for these fractions have been reported only in terms of double bond equivalents. This was done to prevent false peak assignment. Consider, for example, the ion at *m/z* 142. This might correspond to a methyl substituted naphthalene for which there are only two isomers but 14 "peaks" were observed in fraction 2. Most of these peaks must correspond to other species with 7 double bond equivalents or fragments. A more detailed analysis was not possible at this time.

Fraction 4 contained species with 9, 10, and 11 double bond equivalents. Several possible species were suggested for 10 double bond equivalents. The major species (10 DBE) showed 4 peaks at mass 192 corresponding to methyl phenanthrenes. The spectra

Table 4.5: Masses identified with GC-MS separation of fraction 2.

Mass	DBE	Mass	DBE
134	4	128	7
148	4	142	7
162	4	156	7
176	4	170	7
160	5	184	7
174	5	198	7
188	5	212	7
202	5	226	7
172	6	240	7
186	6	254	7
200	6	268	7
214	6	168	8
228	6	182	8
		196	8
		210	8
		224	8
		238	8
		252	8

Table 4.6 Masses identified with GC-MS separation of fraction 3.

Mass	DBE	Mass	DBE
184	7	166	9
198	7	180	9
168	7	194	9
182	8	208	9
196	8	222	9
210	8	236	9
224	8	250	9
238	8	264	9
252	8	278	9
266	8		
280	8		

Table 4.7: Masses identified with GC-MS separation of fraction 4.

Mass	DBE	Time	Assignment	Mass	DBE	Time	Assignment
194	9	23.36	15*, 29	178*	10	22.78	1,2,13
194	9	23.45	15*, 29	192*	10	24.67	1,2,3,27
194	9	23.50	15*, 29	192*	10	24.76	1,2,3,27
194	9	23.59	15*, 29	192*	10	25.07	1,2,3,27
194	9	23.82	1,2,3,15*,29	192*	10	25.15	1,2,3,27
194	9	24.10	1,2 3,15*,29	206	10	26.19	15*
208**	9	24.92	15*, 29, 43	206	10	26.45	15*
208	9	25.08	15*, 29, 43	220	10	27.43	15*,29
208	9	25.20	15*, 29, 43	220**	10	27.65	
208**	9	25.24	15*, 30, 43	220	10	27.99	15,29*
208	9	25.31	15*, 30, 43	220	10	28.05	15*,29
208	9	25.49	15*, 30, 43	220	10	28.28	15*,29
208	9	25.70	15*, 30, 43	220	10	28.42	15*,29
208	9	25.82	15*, 30, 43	220	10	28.63	15,29*
222	9	25.53	15,29*,49,57	220**	10	28.68	
222	9	25.69	15,29*,49,57	234	10	28.85	15,29*,43
222	9	25.87	15,29*,49,57	234	10	29.07	15,29*,43
222	9	26.03	15*, 29, 49, 57	234	10	29.14	15,29*,43
222	9	26.13	15*,29,49,57	234	10	29.25	15,29*,43
222**	9	26.44	15, 29*	234	10	29.35	29*,43
222	9	26.72	15,29*,44,57	234	10	29.45	29*,43
222	9	26.80	15, 29*, 44, 57	234	10	29.60	29*,43
222	9	26.87	15,29*,44,57	234	10	29.68	
222	9	26.94	15,29*,44,57	234	10	29.81	29*,43
222	9	27.11	15,29*,44,57	234**	10	30.01	
222**	9	27.17	15,29*,44,57	234**	10	30.13	
222**	9	27.31	15,29*,44,57	248	10	30.73	15,29,43*,57
222**	9	27.40	15,29*,44,57	248	10	30.79	15,29,43,57*
236**	9	27.94		248	10	30.90	15,29,43*,57
236**	9	28.02		248	10	31.01	15,29,43*,57
236**	9	28.11		248	10	31.23	15,29,43,57*
236**	9	28.45		248	10	31.30	15,29,43*,57
236	9	31.12	15, 29*	248	10	31.36	15,29,43*,57
236**	9	31.31					
236**	9	31.40		204	11	27.15	1*,2,3,4
250**	9	29.64		218**	11	28.91	
250**	9	29.84		232**	11	30.35	
250**	9	31.68					

*base peak
**mixture of compounds

Table 4.8: Masses identified with GC-MS separation of fraction 5.

Mass	DBE	Time	Assignment	Mass	DBE	Time	Assignment
208	9	25.42	1,2,15*,30	218**	11	27.69	
208**	9	25.83		218**	11	27.88	
208**	9	25.93		232	11	30.49	15*,17,30
208**	9	26.01		232**	11	30.58	
208**	9	26.35		232	11	30.65	15*,17,30
222**	9	27.13		232	11	30.79	15*,17,30
222	9	27.22	15*,29	232**	11	30.93	
222**	9	27.36		246	11	32.44	27,29*,31,44
222**	9	27.52					
222**	9	27.61					
236**	9	28.38					
236	9	28.51	15,29*				
206*	10	26.49	1,15,17				
206*	10	26.61	1,15,17				
206*	10	26.68	1,15,17				
206*	10	26.89	1,15,17				
206*	10	26.99	1,15,17				
206*	10	27.08	1,15,17				
206**	10	27.25					
206**	10	27.46					
220	10	27.88	15*,31				
220	10	28.07	15*,31				
220	10	28.23	15*,31				
220	10	28.28	15*,31				
220	10	28.58	15*,31				
220	10	28.69	15*,31				
220**	10	29.22					
234	10	29.37	15*,17,32				
234**	10	29.88					
234**	10	30.01					
234**	10	30.67					
234**	10	30.95					
234**	10	31.13					
248	10	31.01	15,29*				
248	10	31.30	15,29*				
248	10	31.60	15,29*				

*base peak
**mixture of compounds

Table 4.9: Masses identified with GC-MS separation of fraction 6.

Mass	DBE	Time	Assignment	Mass	DBE	Time	Assignment
208	9	26.10	1,15*17,30	218*	11	29.97	1,2,3,15
222**	9	27.12	2,15*	218	11	30.15	1*,2,3,15
222**	9	27.35	15*	232	11	30.49	15*,17,30
222**	9	27.50		232**	11	30.58	
222**	9	27.61		232	11	30.65	15*,17,30
222**	9	27.81		232	11	30.79	15*,17,30
222**	9	28.21		232**	11	30.93	
206**	10	26.49		232**	11	31.59	
206*	10	26.61	15	232**	11	31.78	
206*	10	26.81	15	232**	11	31.86	
206*	10	26.99	15	246	11	31.95	15,31*,44
206*	10	27.17	15	246	11	32.05	15,31*,44
206**	10	27.69		246	11	32.17	15,31*,44
220*	10	28.56	15*,41	246	11	32.25	15,31,44
220*	10	28.60	15*,41	246	11	32.38	15,31,44
220*	10	28.70	15*,41	246	11	32.44	15,31,44
220*	10	28.94	15*,41	246	11	32.67	15,31*,44
				246	11	32.83	15,31*,44
234	10	29.88	15*,17,32	246	11	32.88	15,31*,44
234	10	29.98	15*,17,32	246*	11	33.12	15,31,44
234	10	30.04	15*,17,32	246	11	33.31	15,31*,44
234	10	30.21	15*,17,32	202*	12	28.03	1,2,3
234	10	30.28	15*,17,32				
234	10	30.50	15*,17,32				
234	10	30.92	15*,17,32				
234	10	31.00	15*,17,32				
248**	10	30.77					
248**	10	30.85					
248**	10	30.96					
248**	10	31.45					
248**	10	31.59					
248**	10	31.72					
248**	10	31.88					

*base peak
**mixture of compounds

Table 4.10: Masses identified with GC-MS separation of fraction 7.

Mass	DBE	Time	Assignment	Mass	DBE	Time	Assignment
220*	10	28.82	1,4,5,15,31	216*	12	29.77	1,2,3,27
220*	10	28.93	1,4,5,15,31	216*	12	30.10	1,2,3,27
220*	10	29.09	4*	216*	12	30.20	1*,3,27
220*	10	29.21	1,4*,5,15,31	244	12	32.84	15*,29,42
220*	10	29.31	1,4*,5,15,31	244	12	32.93	15*,29,42
220*	10	29.42	1,4*,5,15,31	244	12	33.16	15*,29,42
234**	10	30.11		244*	12	33.28	15,29
234	10	30.40	15*,17,31,45				
234**	10	30.46					
234**	10	30.55					
234**	10	30.95					
218**	11	29.79					
218*	11	29.91	15				
218*	11	30.03	15				
232*	11	31.43	15,17,30				
232*	11	31.54	15,17,30				
232*	11	31.65	15,17,30				
232**	11	31.79					
232*	11	31.89	15,17,30				
232**	11	31.96					
232	11	32.04	15,17*,30				
232**	11	32.14					
246**	11	30.87					
246**	11	31.17					
246	11	31.98	15*,31,39,44				
246	11	32.27	31*				
246	11	32.37	39*				
246*	11	32.96	39				
246**	11	33.24					
246**	11	33.66					
246	11	33.77	39				
246*	11	34.06	1,39				

*base peak
**mixture of compounds

Table 4.11: Masses identified with GC-MS separation of fraction 8.

Mass	DBE	Time	Assignment	Mass	DBE	Time	Assignment
234*	10	30.77	15,27	230	12	31.33	1,15*
234*	10	30.90	15	230*	12	31.56	1,15
234	10	31.18	15*	230*	12	31.81	1,15
234**	10	31.28		230*	12	31.90	1,15
234	10	31.44	15*	230*	12	32.00	1,15
234	10	31.74	15*	230*	12	32.23	1,15
248**	10	31.85		230*	12	32.32	1,15
248**	10	31.99		244**	12	32.89	
248**	10	32.10		244**	12	33.01	
248**	10	32.33		244**	12	33.12	
248**	10	32.44		244**	12	33.29	
248	10	32.57	15,29*,41	244	12	33.40	15,29
248**	10	32.77		244**	12	33.72	
248**	10	32.94		258**	12	34.29	
248	10	33.02	15*,29	258**	12	34.56	
248	10	33.11	15*,29	258	12	34.69	15*,29
248	10	33.24	15*,29	258**	12	34.86	
248	10	33.33	15*,29	258**	12	35.17	
232**	11	31.49		258**	12	36.08	
232**	11	31.63		258**	12	36.17	
232	11	31.75	15	258**	12	36.46	
232**	11	31.83		258**	12	36.52	
232**	11	32.01		258**	12	36.58	
232*	11	32.16	15,17	272	12	36.78	15,29*
232**	11	32.24		272	12	36.86	53,65*
232**	11	32.45		272	12	38.37	53,65*
246**	11	33.07		228*	13	32.93	2
246*	11	33.21	15	228*	13	33.18	2
246*	11	33.43	15	242*	13	34.45	1,2,3
246*	11	33.55	15,29	242*	13	34.57	1,2,3
246*	11	33.68	15,29	242*	13	34.82	1,2,3
246**	11	33.76		242**	13	34.90	
246**	11	33.84		242**	13	35.01	
246**	11	34.01		256**	13	35.23	
260**	11	33.86		256**	13	35.4	
260**	11	33.97		256*	13	35.91	1
260**	11	34.06		256*	13	36.04	1
260	11	34.26	15,31,41,53*	256*	13	36.15	1
260**	11	34.43		256*	13	36.35	1
260**	11	34.78		256*	13	36.66	1
260**	11	35.17		256**	13	36.78	
260**	11	35.38		270**	13	36.72	
260	11	35.59	41*,53	270*	13	37.02	15,29,51,63
260	11	35.76	41*,53	270*	13	37.24	15,29,51,63
260**	11	35.84		270**	13	37.55	
260**	11	35.93		270**	13	37.71	
274**	11	35.13		270**	13	37.12	
274**	11	35.54					
274**	11	36.01					
274**	11	36.21					

of these peaks were in good agreement with the spectra in the NIST library. In addition, a progressive series was present in 14 mass increments (206, 220, 234, 248) that could correspond to additional phenanthrenes with the increased alkylation. Fragmentation patterns of the larger masses suggested that butyl and propyl substituents were attached to the aromatic ring. However, these species were present at low concentration and often in poorly resolved chromatographic peaks making unambiguous identification difficult. Some of these components may not be phenanthrenes but belong to other aromatic classes with 10 double bond equivalents. A small number of compounds were identified as having 11 double bond equivalents. These were believed to result from a phenanthrene with a reduced ring attached. Several possibilities are shown in Figure 4.14. The compounds with 9 double bond equivalents were believed to be substituted fluorenes. Many of the compounds with larger masses were present at low concentration. Highly substituted compounds could fragment to such an extent that the molecular ion is not observed making it difficult to estimate the correct molecular weight. In fractions 4 to 8 several aromatic series were identified:

fluorenes (9 DBE). A series of alkylated fluorenes with 9 DBE contained in fractions 4 to 6 with the masses 194 to 250;

phenanthrenes. Phenanthrene and substituted phenanthrenes were separated over fractions 4 to 8. Two distinct series were observed. The first series (10 DBE) corresponded to the masses 178, 192, 206, 220, 234, 248 suggesting increasing levels of alkylation. A second series (11 DBE), was observed with the masses 218, 232, 246, and 260 corresponding to substitution with an aliphatic ring structure and additional alkylation;

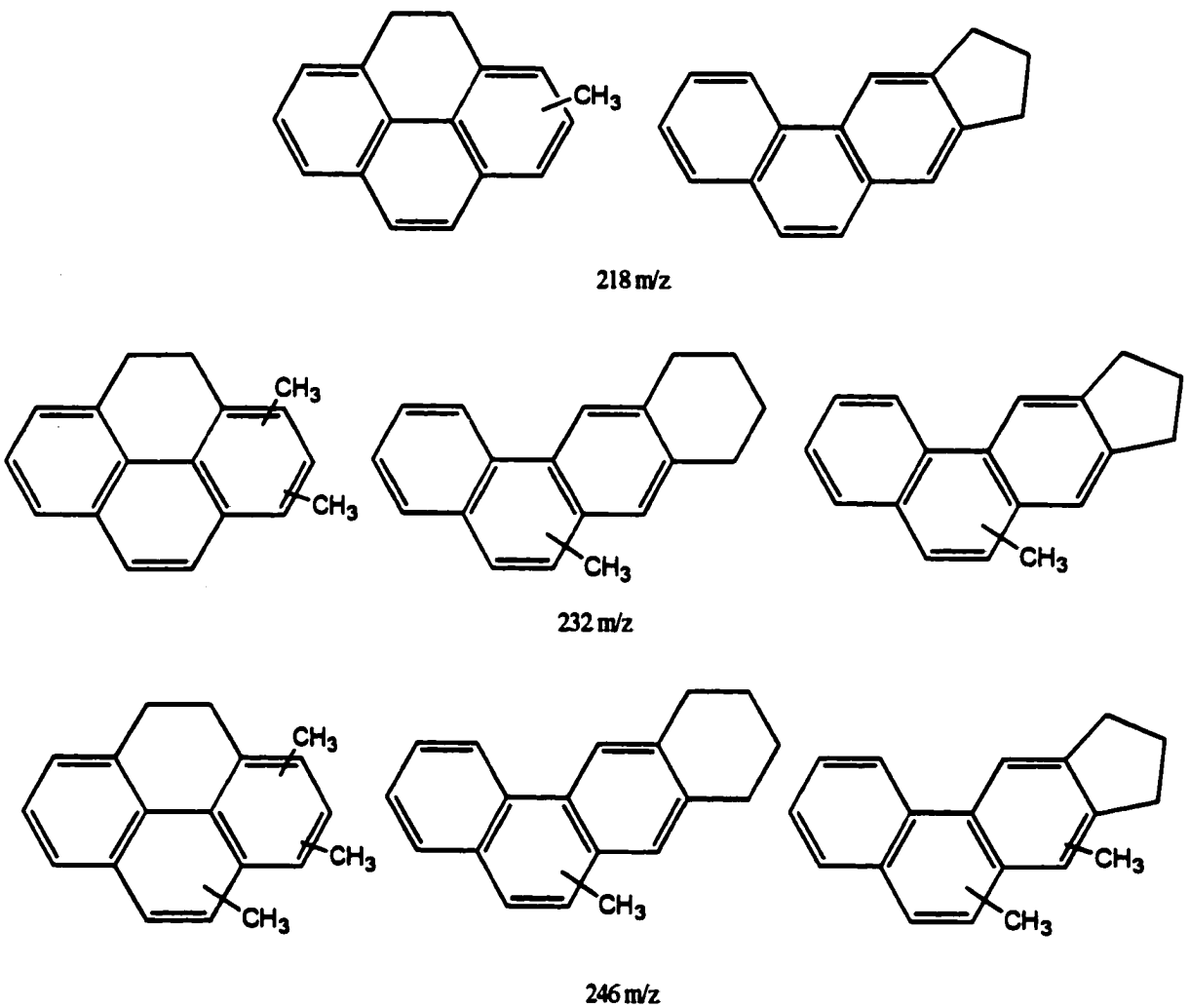

Figure 4.14: Several possible structures to account for the observed masses at 218, 232, and 246 m/z. Each of these structures contains an aromatic backbone consistent with phenanthrene.

pyrenes. Pyrene and substituted pyrenes were separated over fractions 6 to 8. Two series were observed (12 and 13DBE) similar to the phenanthrenes. The first series (12 DBE) had masses present at 202, 216, 230, and 244. The second series (13 DBE) was observed with masses at 228, 242, 256, and 270.

Other aromatic classes were observed but assignment was based on double bond equivalents rather than the actual parent compounds. This was done because spectroscopic and mass spectrometric detection were not able to unambiguously identify compounds in fractions 1, 2, and 3. This was mainly due to the complexity of these fractions and the ability to resolve the components chromatographically. In addition, the possible of combinations of compounds present in the one and two ring classes would be large due to the reduction of larger aromatic classes during hydrotreating. However, a general determination of aromatic class was possible for these fractions based upon spectroscopic information and molecular weights. Specifically, naphthalenes and biphenyls were observed in fractions 2 and 3.

Two-dimensional LC(DNBS)-GC/MS was unable to resolve all of the components that were observed in the light gas oil MB13B. However, several aromatic classes were identified in the oil using spectroscopic detection with the first dimension. This class information was then expanded using a second separation (GC-MS) to determine the level aliphatic substitution present on each compound. Although, reversed phase LC (APCI-MS) was examined as an alternative to GC/MS as a second dimension the reversed phase LC lacked the resolution of the capillary GC leading to an increase in the number of unresolved components. As a result, the data for the LC results were incorporated into the three dimensional studies presented in the next chapter.

Chapter 5 Three-dimensional Chromatographic Analysis of LC_DNBS Fraction 6

5.1 Introduction

This chapter explores three-dimensional LC as an alternative to the two-dimensional studies discussed in Chapter 4. The same LC-DNBS fractionation described in Chapter 2 will be used as the first dimension. A reversed phase monomeric C18 separation was used as the second dimension with APCI-MS and fluorescence detection. The third dimension was either a polymeric C18 or a TCP separation. Each of these separations was much less efficient than the capillary GC separation studied previously. However, additional information may be obtained through the use of multiple detectors and the characteristics of the stationary phases. Furthermore, the combined resolution of multiple LC separations may provide more resolution than the GC separation. Tracking components through multiple separations may provide additional structural information allowing better compound characterization in the absence of adequate standards.

The TCP column and the polymeric reversed phase column offer unique selectivities based on the geometric structure of the molecule. The retention behavior for the TCP column was discussed in Chapter 2: however, additional aspects of this behavior will be addressed in this chapter. Fraction 6 from the DNBS column was examined as a real case using three-dimensional LC analysis. The complex nature of this fraction presented a significant challenge and illustrates the power of three-dimensional chromatography. Specifically, several compound classes were observed in this fraction by previous analysis. However, some doubt exists as to the nature of aliphatic substitution and the length of the alkyl side-chains. The

TCP and Vydac (25 cm x 4.6 mm #201TP54) separations will help characterize the nature of aliphatic substitution.

Ideally, three-dimensional LC is readily amenable to in-line analysis. A single peak can be selected from the first dimension and then sequentially cut onto additional dimensions. However, moving between unlike chromatographic separations can cause difficulty with incompatible solvents such as hexane and acetonitrile, thereby limiting the maximum practical cutting loop size. This may have strong implications on the sensitivity of the subsequent separations. Fluorescence provides an ideal detection method under these circumstances as it is sensitive and allows spectral identification of each component by aromatic class.

5.2 Experimental

5.2.1 Apparatus

The three-dimensional LC-LC-LC apparatus consisted of all three systems shown in Figure 2.1. Each of these systems was described in detail in chapter 2. Specifically, system 1 used the DNBS separation and system 2 used a monomeric C18 separation. The third chromatographic LC dimension used either a polymeric reversed phase separation or a TCP normal phase separation.

5.2.2 Chemicals

Chemical were used as described in chapters 2, 3, and 4.

5.2.3 Procedures

The in-line chromatography using three dimensions was done as follows. A twenty-microliter sample of the light gas oil MB13C or heavy gas oil was injected onto the DNBS column using the experimental conditions described in Chapter 2. The absorbance of the eluent was monitored using the UV detector set to 336 nm and a 50-microlitrer cut of a peak was transferred to the cold C18 monomeric column by switching valve C (Figure 2.1). The second dimension chromatogram was developed using the monomeric C18 column, operated at 0 C using an ice/water bath with pure acetonitrile as the eluent. The chromatogram was monitored using the laser induced fluorescence detector and a cut of a desired peak was transferred to the third dimension by switching a Rheodyne 7000 valve (shown as D). The third dimension was either an additional reversed phase separation using the Vydac polymeric column or a normal phase separation using the TCP column. The Vydac separation was developed at 0 C using acetonitrile as the eluent and was monitored using the laser fluorescence detector. Six cuts of the second dimension were done using the 6 loop Valco valve and Rheodyne 7000 valve coupled together. The Rheodyne 7000 valve was used to transfer the first cut directly to the third dimension and the Valco valve was used to trap 5 additional cuts. After completion of the first chromatogram in the third dimension, the HPLC pump was connected to the Valco valve and the remaining cuts were transferred for analysis. The same procedure was used to characterize the third dimension separation using the TCP column. The eluent was hexane with 30 percent dichloromethane. The TCP column was operated at 30 C using the Agilent Model 1100 oven. All runs were isocratic.

Off-line characterization of the sample was done by collecting fractions from 5

injections of light gas oil onto the DNBS column, combining fractions for the peaks of interest, removing the solvent under nitrogen, and dissolving the samples in acetonitrile. These concentrates were used for additional characterization of the second and third chromatographic dimensions.

5.3 Results and Discussion

5.3.1 Difficulties Associated with On-line LC-Analysis Vs Off-line LC Analysis

Problems are observed in multi-dimensional separations if solvents with different eluotropic strength are used. This can lead to degradation in chromatographic performance. In extreme circumstances the injected solvent plug may be immiscible with the eluent causing the entire separation to fail. In this study, the first dimension used hexane or hexane/dichloromethane as the primary eluent. The second dimension was a reversed phase separation that used acetonitrile as the eluent. Since hexane has limited solubility in acetonitrile, the effect of composition of the solvent plug was examined on the monomeric octadecylsilane (ODS) stationary phase that was to be used as the second dimension. Figure 5.1 shows the results of two chromatograms developed on the monomeric C18 column using a mixture of alkylated pyrenes in hexane and then solvent exchanged to acetonitrile. A dramatic loss in overall retention of the sample was observed for the hexane case along with noticeable degradation of resolution. The solute is not introduced directly onto the stationary phase that is wetted by the immiscible eluent. The solute tends to travel down the column as a plug exhibiting retention only after being extracted into the eluent. This is the type of

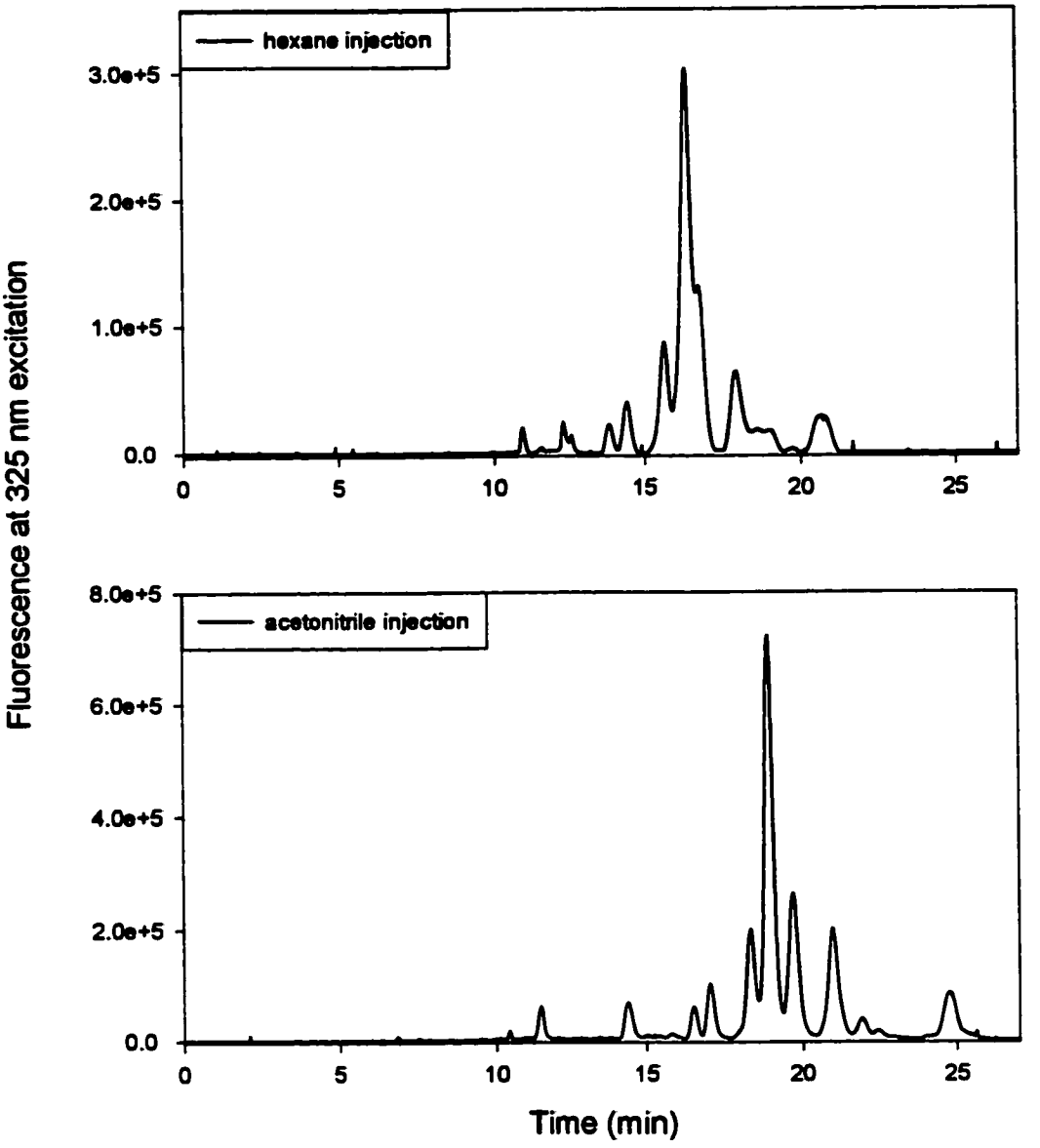

Figure 5.1: Chromatograms developed on the monomeric C18 columns. Top figure shows a mixture of alkylated pyrenes injected in hexane. Lower figure shows the same mixture injected in acetonitrile. Each injection was 20 uL.

behavior expected with in-line analysis of the cuts between dimensions. Retention data for standard compounds were all obtained using acetonitrile as the injection solvent. Characterization of the cuts was not possible due to this discrepancy in k' values obtained from standards and cuts from a normal phase separation. This was overcome with off-line analysis using collected fractions from the normal phase separation. The fractions were evaporated to near dryness and then reconstituted with acetonitrile for direct injection onto the monomeric C18 column.

Resolution decreases as the injection volume increases unless the injection solvent is weaker than the eluent. This is common to HPLC regardless of whether using normal or reversed phase chromatography. It stands to reason, therefore, that the size of the loop used in the cuts would have some effect on the chromatography in the second dimension especially considering the previous discussion concerning unlike solvents. Various loop sizes were tested using cuts from a normal phase column to the monomeric C18 column. In order to maximize sensitivity, it would be preferred to utilize as large a cut loop as possible without sacrificing chromatographic efficiency. Figure 5.2 shows the effect of changing the cut loop volume on retention and resolution on the monomeric ODS. It is obvious that a cut volume of fifty microliters could limit the chromatographic ability of the reversed phase separation. Retention of the compounds on the reversed phase increases as cut volume decreases. Resolution follows a similar relationship.

A twenty microliter cut loop volume displayed good resolution with only a minor decrease in relative k' values for the compounds cut onto the monomeric ODS columns. An apparent loss in fluorescence response (peak height) by a factor of 10 was observed in going from a fifty microliter loop to the twenty microliter loop. A similar loss of a factor of 3 was

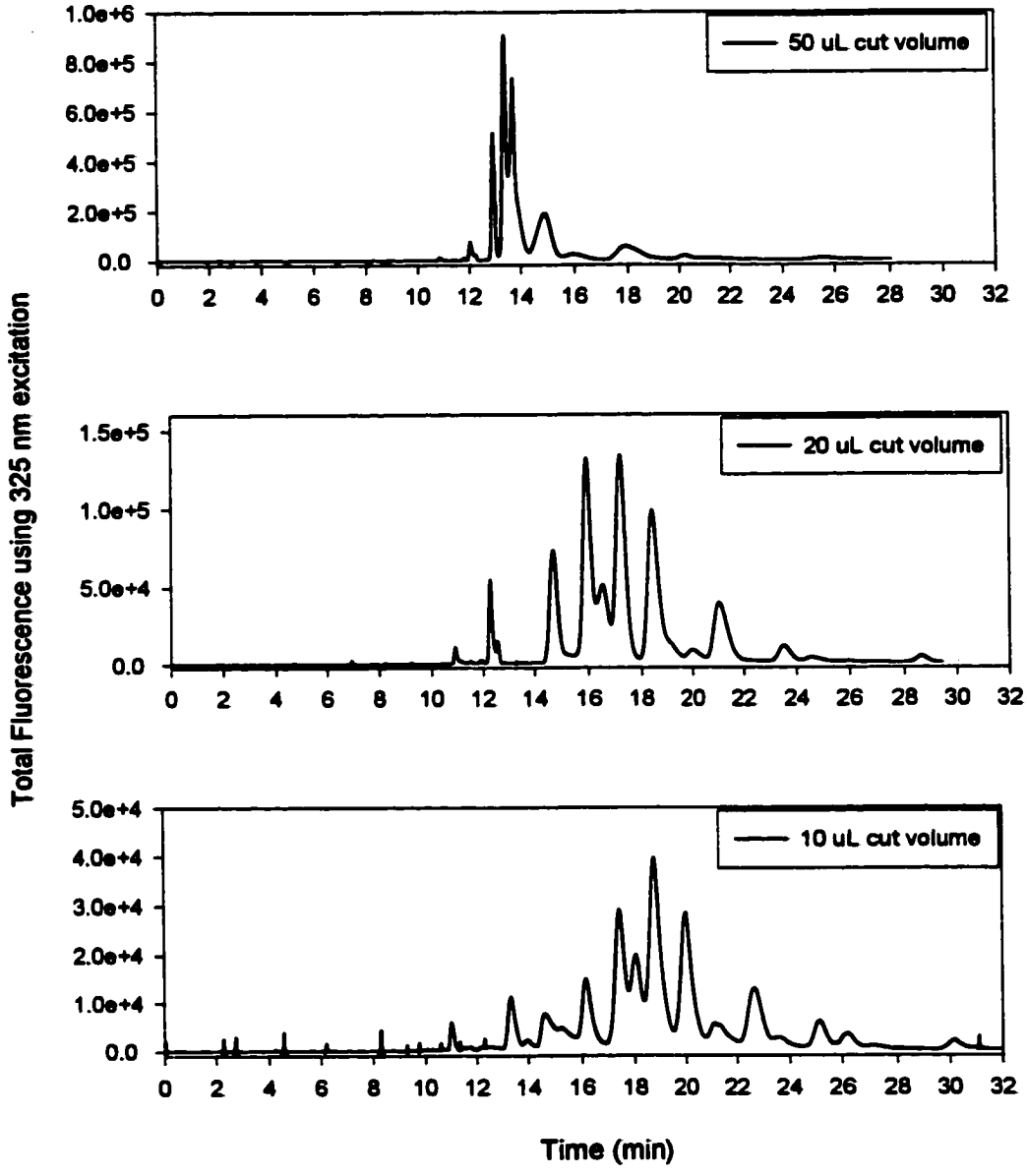

Figure 5.2: Chromatograms of cuts from normal phase separation to monomeric C18 columns in order to probe the effect of cutting loop volume on chromatographic performance. Cutting loop volumes are listed with corresponding chromatograms in figures.

observed in going from the twenty microliter loop to the ten microliter loop. The losses are a result of both the amount transferred from one column to the next, the fraction of peak cut by the loop, and the effect of solvent strength on the chromatography of the second column. For this reason, in-line experiments should proceed with twenty microliter cuts from the first to the second dimension. Increased sensitivity through larger sample volumes will need to be performed using collected fractions so as to maintain reasonable chromatographic performance. The fractionation experiments with the DNBS column were performed using off-line fraction collection.

5.3.2 Characterization of the LC Chromatographic Dimensions

Two columns were chosen in this study to represent the third dimension of liquid chromatography. The first was a Vydac polymeric ODS reversed phase column, operated isocratically with acetonitrile submersed in an ice\water bath. The second separation to be examined used a TCP column as a normal phase separation. Each column is characterized with a series of standards; the retention times for these standards on the monomeric C18 and Vydac polymeric C18 are shown in Table 5.1. The retention times for the standards on the TCP column were outlined in Chapter 2. The differences in selectivity for each column were exploited to develop a method capable of resolving the complex oil mixtures into single compounds and elucidating structural information with respect to the type of aliphatic substitution.

Table 5.1: Retention times and k' values for the Vydac and monomeric C18 columns. Retention times are in minutes. The calculation of k' values were done using the retention time for benzene as t_o.

Compound	Monomeric C18 (k')	Vydac (k')
Naphthalene	3.63 (0.21)	3.33 (0.11)
2,6-dimethylnaphthalene	4.67 (0.56)	4.33 (0.44)
1,8-dimethylnaphthalene	2.93 (0.43)	3.92 (0.31)
2,3,5-trimethylnaphthalene	5.00 (0.67)	4.33 (0.44)
Phenanthrene	4.54 (0.51)	4.17 (0.39)
2-methylphenanthrene	5.29 (0.76)	5.25 (0.75)
9-methylphenanthrene	5.29 (0.76)	5.00 (0.67)
3,6-dimethylphenanthene	5.59 (0.86)	4.83 (0.61)
4H-cyclopenta[*def*]phenanthrene	5.00 (0.67)	4.50 (0.50)
Anthracene	4.75 (0.58)	4.58 (0.53)
2-methylanthracene	5.79 (0.93)	6.83 (1.28)
2-ethylanthracene	6.29 (1.10)	6.25 (1.08)
Pyrene	5.79 (0.93)	5.83 (0.94)
4-methylpyrene	7.25 (1.43)	8.00 (1.67)
1-ethylpyrene	7.92 (1.64)	8.25 (1.75)
1,6-diethylpyrene	11.34 (2.78)	13.67 (3.56)

Typically a gradient is used with a polymeric column. Initial gradient studies with the Vydac required long analysis times due to the retention of PAHs and the need to reequilibrate the column after each gradient separation. Chromatographic operations at subambient temperatures reduced the strength of the eluent which enabled the Vydac separation to be done isocratically. This increased sample throughput during the cutting experiments and reduced solvent mixing difficulties. Retention on the Vydac column is based on the number of aromatic rings, the number of alkyl substituents and the length to breadth ratio of the compound.

The monomeric C18 column (second dimension) separates in a similar fashion as the Vydac polymeric phase. The main difference between the two columns is the degree of geometric recognition. Temperature plays a significant role in the ordering of the stationary phase. A monomeric ODS phase has been shown to exhibit retention behavior comparable to that of a polymeric column at temperatures of -15 C [77]. However, if there is little difference in the retention between theses two columns, they are not useful in multi-dimensional separations under these circumstances. At 0 C the monomeric ODS phase has been shown to display properties intermediate between that of a polymeric phase and a monomeric phase [77]. An examination of k' values shown in Table 5.1 for phenanthrene and anthracene suggests differences in selectivity for the two stationary phases. The similarity of the k' values for anthracene and phenanthrene on the monomeric phase suggests a lack of geometric recognition (0.58 and 0.51 respectively). The k' values for phenanthrene and anthracene on the polymeric phase (0.39 and 0.53 respectively) show more resolution between these two compounds. Phenanthrene has a decreased k' value on the polymeric phase due to a smaller length to breadth ratio compared to anthracene.

The second separation examined was a normal phase TCP separation. The TCP separation offers more selectivity than the Vydac polymeric stationary phase due to the nature of the interactions between the solute and the stationary phase. The TCP phase is electron deficient and therefore acts as an electron acceptor. For maximum interaction the PAH should align parallel to the TCP group. Non-planarity of the parent PAH or sterically hindering substituents will force the PAH to have larger distances between the stationary phase and the pi cloud of the PAH. This may result in lower energies of formation for the electron donor-acceptor complexes, hence retention will be reduced. The addition of small substituents which are not able to rotate out of the plane which contains the PAH's aromatic carbons will tend to increase the k' value of the parent compound. The addition of a methyl group to a parent PAH donates electrons to the PAH, which increases the electron density within the aromatic pi cloud. A comparison of the k' values for the series of anthracene (1.94) standards illustrates this observation. The k' for 2-methylanthracene (2.34) is greater than that of anthracene. However, the value of 2-ethylanthracene (1.50) is less than that of anthracene. In general, the elution of PAHs within an aromatic class will follow this order: ethyl; parent PAH, methyl; dimethyl. 2,3,5-trimethylnaphthlene with a k' value of 1.54 is more retained than naphthalene (k' 0.37) but is less retained than either 1,8-dimethylnaphthalene (k' 2.09) or 2,6-dimethylnaphthalene (k' 1.84). This suggests that several methyl groups surrounding a considerable portion of the perimeter of the parent PAH could cause steric interactions that would decrease the retention of the solute.

5.3.3 Analysis of LC DNBS Fraction 6 using Three-Dimensional LC

Three-dimensional LC allows mixtures to be further separated if resolution is not obtained after two dimensions of chromatography. First, multiple separations may allow a greater number of isomer to be identified. Second, the utilization of analyte retention behavior on each dimension may enable the elucidation of structural information. Fraction 6 from the DNBS normal phase separation of the light gas oil separated on the cold monomeric ODS column is shown in Figure 5.3 with 6 peaks identified. The six peaks identified were examined using both the Vydac polymeric reversed phase separation and a normal phase TCP separation. Also present in this figure are mass chromatograms that result from APCI-MS. The masses were monitored using single ion recording. The mass spectrometer was unable to collect data in scan mode due to limited sensitivity. The masses were selected from the GC-MS data for this fraction in Chapter 4.

These six peaks were chosen to represent a significant cross section of the major components present in this fraction. Many of the fluorescence spectra observed in this chromatogram were closely related except for the peak at 7.80 minutes, which was identified as pyrene. Three aromatic classes of compounds were observed in this fraction, fluorene, phenanthrene, and pyrene. The fluorescence spectrum of peak 4 from the monomeric C18 separation of DNBS fraction 6 is shown in Figure 5.4. Examination of this fluorescence spectrum suggests that there is indeed a possibility that two compounds were present under this peak. In addition, three ions (*m/z* 218, 220, 222) were observed for this peak according to the APCI-MS data. The fluorescence spectra suggest the presence of a fluorene and phenanthrene species. The APCI-MS data allows a tentative assessment as to the amount

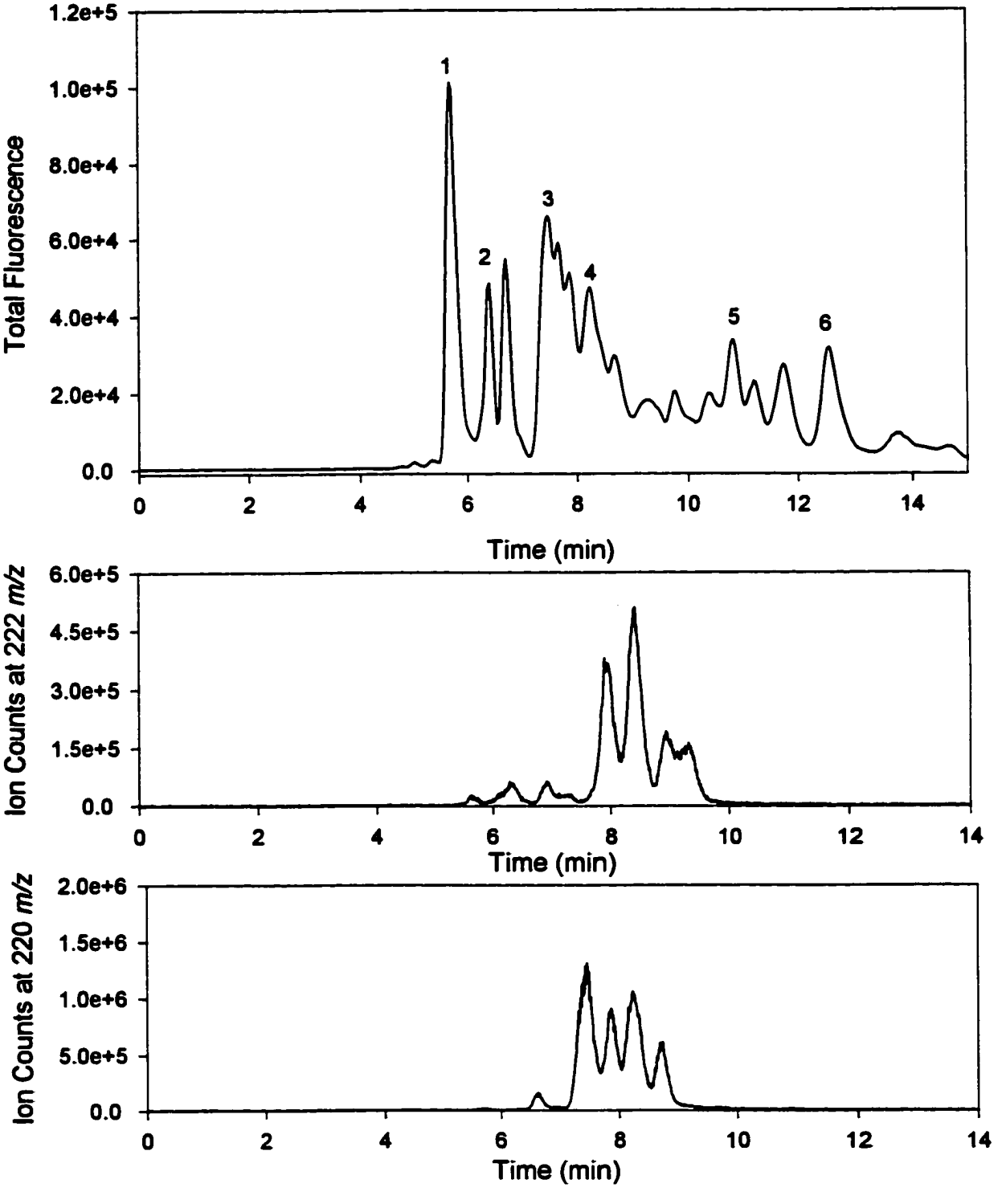

Figure 5.3: LC fraction 6 from the DNBS separation on the monomeric C18 column. Each chromatogram was developed with 100% acetonitrile at a flow rate of 1.0 mL/min. Temperature was maintained at 0 C. Heartcuts onto the third dimension were done for the six peaks labeled in the figure. APCI-MS mass chromatograms shown in lower figures used single ion recording.

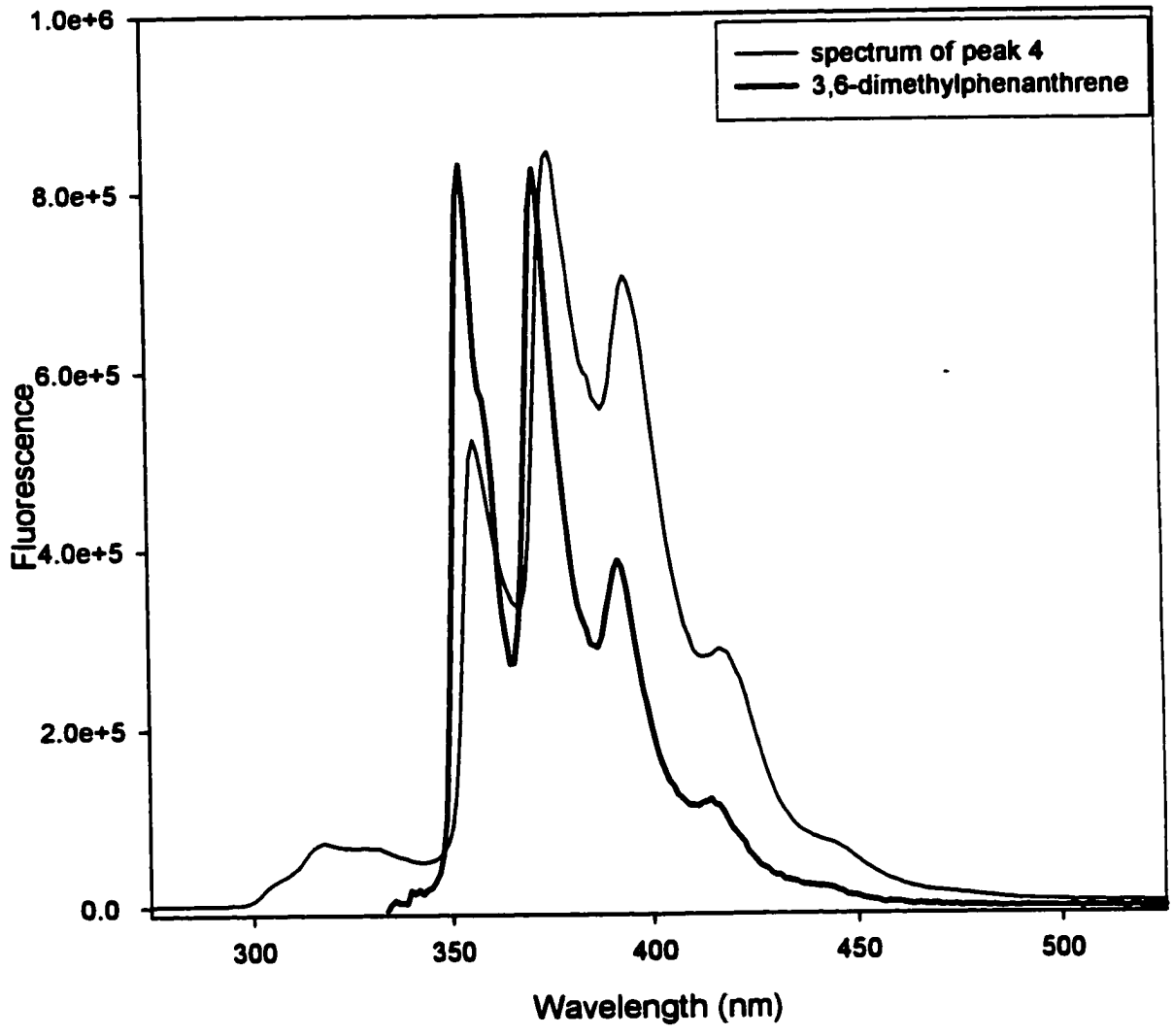

Figure 5.4: Fluorescence spectrum of peak 4 from the chromatogram shown in Figure 5.3 The spectrum resulted from excitation with the 266 nm laser.

of aliphatic substitution. It is believed that these compounds in peak 4 were a phenanthrene with a reduced ring attached (218 m/z), a phenanthrene with 3 aliphatic carbons (220 m/z), and a fluorene with 4 aliphatic carbons (222 m/z). This assignment was supported by the GC-MS data.

The chromatograms that result from a cut of peak 4 onto the Vydac and TCP columns are shown in Figure 5.5. The single peak from the monomeric C18 separation was further separated into 7 additional peaks on the polymeric C18 column and 7 peaks with the TCP column. The spectra associated with each of the peaks observed in the Vydac chromatogram of the cut are shown in Figure 5.6 and the spectra for the TCP separation are shown in Figure 5.7. The spectra of the peaks labeled "d" and "e" from the RP chromatogram show the presence of two species. Therefore, 8 compounds were observed in total in this separation. Each of these peaks in the third dimension was believed to result from a single peak in the second dimension. The cuts were performed using a twenty microliter loop. A cut of this volume corresponds to a time of 1.2 seconds in the chromatogram at a flow rate of 1.0 mL/minute. This time is short relative to peak separation time of 48 seconds. Under these circumstances very little overlap was expected between adjacent peaks for each of the six cuts from the monomeric C18 column. Many of these spectra are quite similar to each other. The determination of the exact number of individual compounds co-eluting can be difficult if they all have similar spectra. However, there were subtle differences between the spectra that were used to follow the elution of compounds on the Vydac and TCP separations.

The use of three dimensions of chromatography was able to increase the number of compounds observed in LC-DNBS fraction 6. Still, without a complete complement of

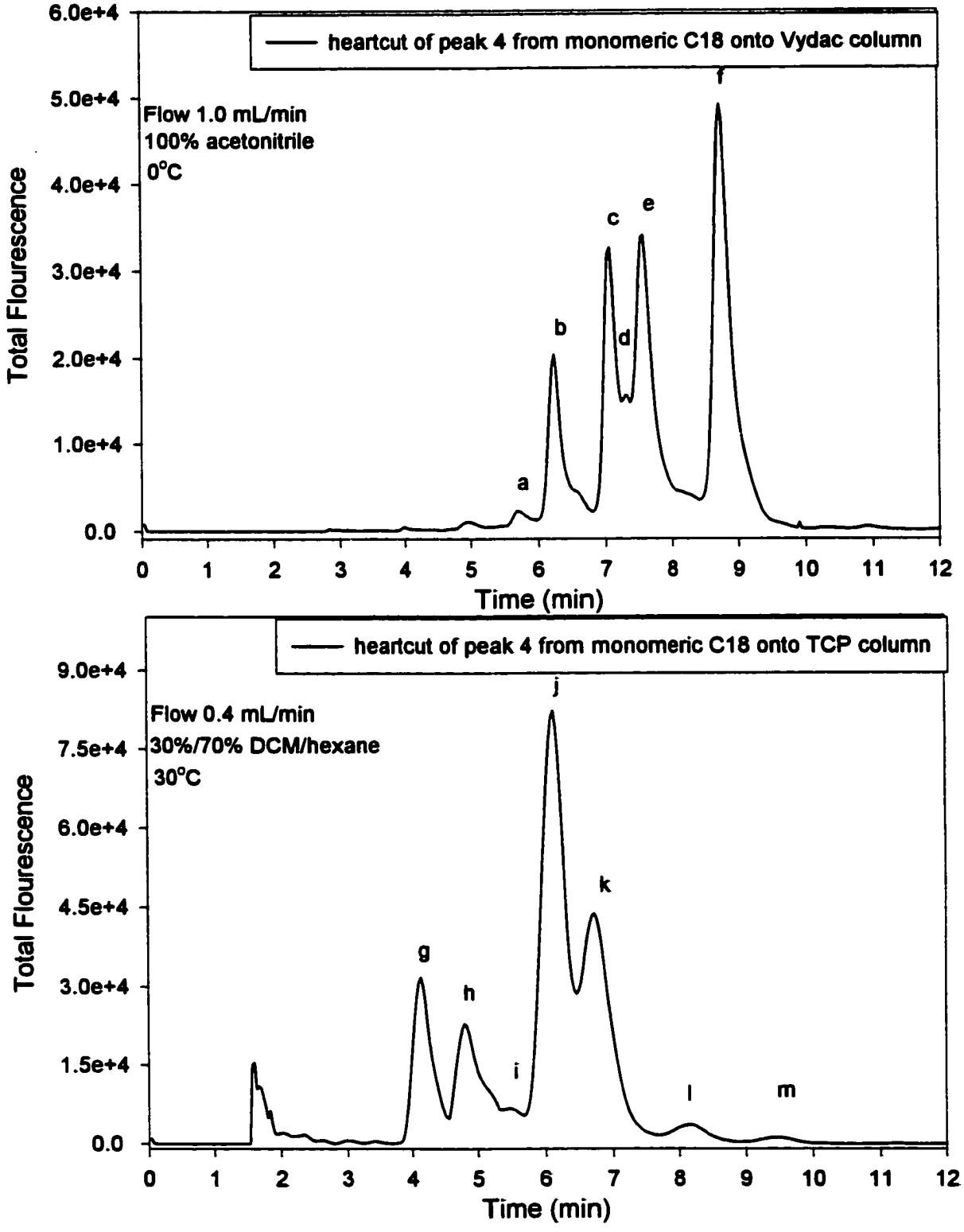

Figure 5.5: Top chromatogram represents a heartcut of peak 4 from the monomeric C18 separation shown in Figure 5.3. Similarly, the lower chromatogram results from a cut of the same peak onto the TCP column. Each separation was performed isocratically according to the conditions provided with each chromatogram.

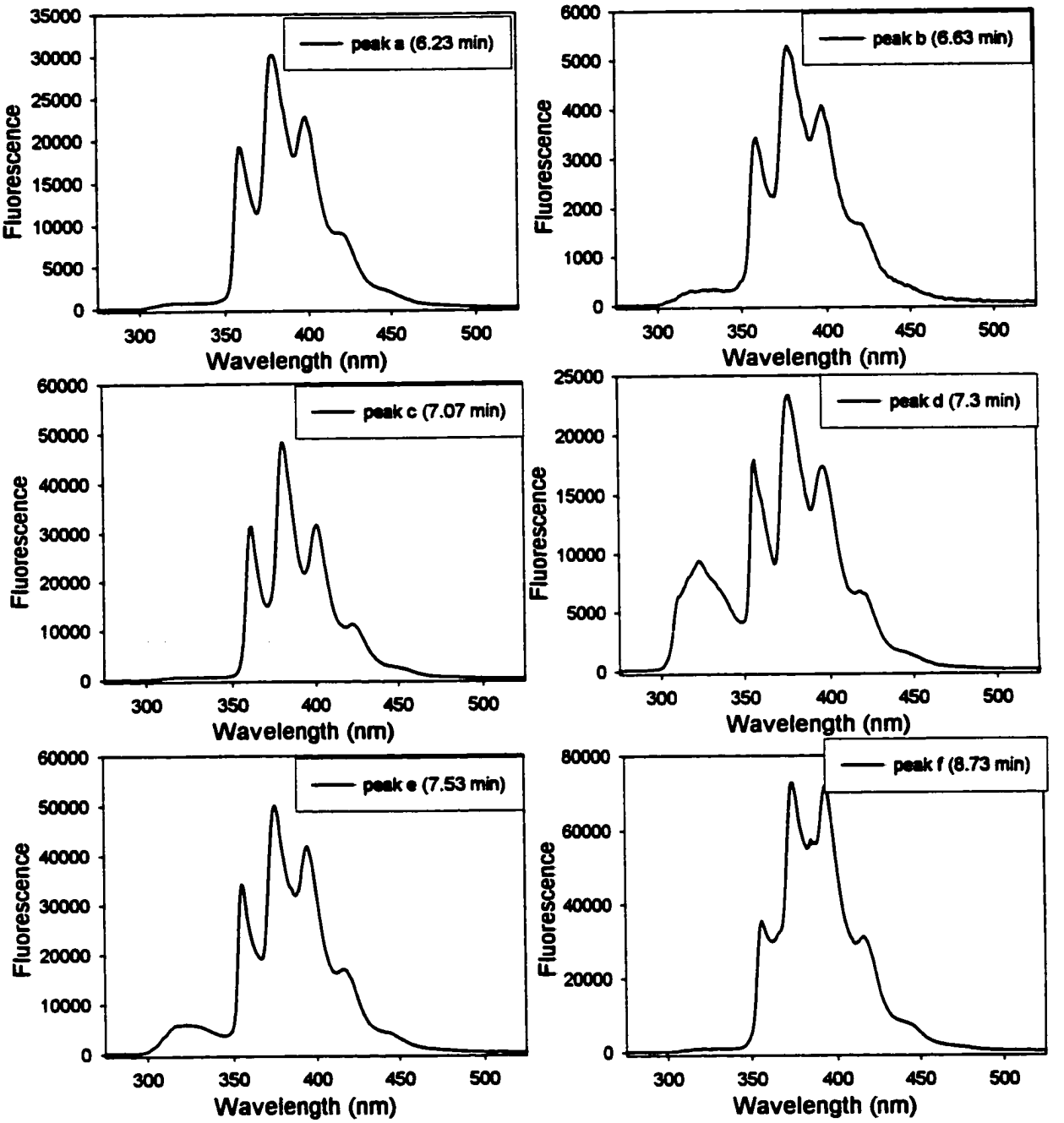

Figure 5.6: Fluorescence spectra of the peaks labeled in the chromatogram shown of the cut onto Vydac column in Figure 5.3. Fluorescence spectra used the 266 nm laser for excitation.

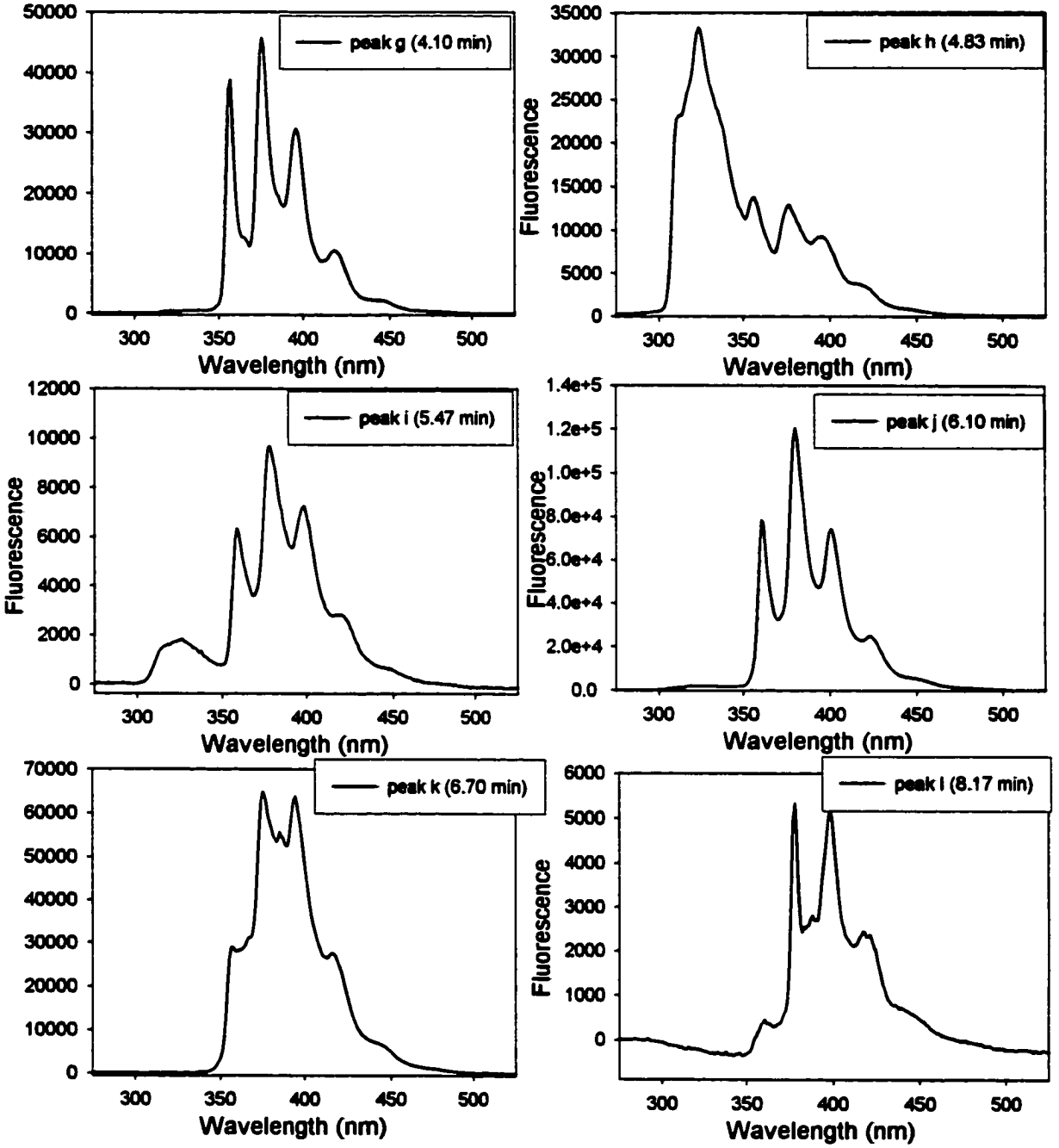

Figure 5.7: Fluorescence spectra of the peaks labeled in the chromatogram shown of the cut onto TCP column in Figure 5.3. Fluorescence spectra used the 266 nm laser for excitation.

standards, identification of the additional peaks can be difficult. The geometric selectivity of both the Vydac column and the TCP column may help to infer additional information with regards to aliphatic substitution patterns. Consider the fluorene species observed. The LC-MS data suggest that fluorene was substituted with 4 aliphatic carbons (222 *m/z*). Two compounds were observed on the RP Vydac separation (retention times 7.30 and 7.53 minutes) and two were observed for the TCP separation (4.83 and 5.50 minutes). The retention times for these two compounds on the TCP column were greater than that of fluorene (2.85 minutes). This suggests that both compounds were tetramethyl substituted fluorenes because they were strongly retained compared to fluorene. These fluorenes were also well retained by the Vydac column. This suggests that the majority of the methyl substitution may predominate at the 2, 3, 7, and 8 positions. Substitution at these positions will produce larger length to breadth ratios for a tetramethyl fluorene resulting in longer relative retention times on the Vydac column.

Seven peaks with fluorescence spectra indicative of phenanthrene species were observed from the Vydac separation. These peaks ranged in retention times from 6.20 to 8.73 minutes. Earlier it was discussed that most of these compounds were phenanthrenes with three aliphatic carbons (220 *m/z*) and at least one phenanthrene with an aliphatic ring attached (218 *m/z*). The broad range of retention times suggests that different alkyl substitution patterns were present. Similarly, these peaks produced a wide range of retention times on the TCP column. The peak at 4.10 minutes on the TCP column was of particular interest since it eluted before phenanthrene (4.67 minutes) suggesting the presence of ethyl or branched alkyl substitution. The later eluting peaks most likely correspond to methylated materials or possibly compounds substituted with an aliphatic ring (218 *m/z*).

The analysis of peak 4 was extended for the remaining five heartcuts from the monomeric C18 to the Vydac and TCP columns. Table 5.2 contains a summary of the cuts for each peak. A survey of the information presented displays the apparent mixture of compounds that were separated on the monomeric stationary phase. Specifically, 6 peaks on adjacent peaks for the monomeric C18 separation. Several exceptions were observed for the cuts of peaks 2, 3, and 4 from the monomeric C18 separation. However, as mentioned earlier overlap was not expected for cuts between adjacent peaks. Therefore what may appear as overlap between cuts, most likely represents different compounds that share the same retention time on the Vydac column.

The analysis of LC-DNBS fraction 6 using multiple chromatographic dimensions further supports and confirms the finding from earlier GC analysis. However, adequate structural determination was not always viable through with GC analysis, particularly when multiple components elute at low concentrations. The added geometric recognition capability of the Vydac and TCP columns provided additional information about structure and class. Furthermore, three-dimensional LC was capable of resolving approximately 40 unique peaks compared to roughly 70 peaks observed using LC-GC. However, not all peaks were cut from the second dimension monomeric separation onto the third dimension LC. If all of the peaks were cut from the second dimension monomeric column onto the third chromatographic dimension then three-dimensional LC might be able to surpass LC-GC in overall peak speciation. This coupled with the additional information provided through array detection creates a powerful tool for the elucidation of components in complex mixtures.

Table 5.2: Summary of the 6 cuts from monomeric ODS onto Vydac and TCP columns.

Peak Number	Mass	Monomeric C18 t_r(min)	Polymeric C18 t_r(min)	TCP t_r(min)
1	202, 206	5.76	4.70 *	2.73 *
			5.20 *	6.20 *
			5.43 ***	9.90 *
				10.83 ***
2	206, 208	6.18	5.63 *	4.73 *
			6.00 **	5.27 **
			6.67 *	7.10 *
				8.10 *
				9.90 *
				11.07 *
3	206, 218	7.34	5.7*	4.57 *
			6.00 *	5.30 *
			6.23 *	7.03 *
			7.93 *	
			8.10 *	
4	218,220, 222	8.11	6.20 *	4.10 *
			5.80 *	4.83 * **
			6.57 *	5.50 * **
			7.07 *	6.10 *
			7.27 * **	6.73 *
			7.53 * **	8.13 *
			8.73 *	
5	232, 246, 248	10.88	9.86 *	4.90 *
			12.13 *	5.77 *
			12.73 *	6.93 *
			13.20 *	
			15.47 *	
			17.90 *	
6	246, 248	12.42	16.0 *	3.36 *
			16.40 *	4.97 *
			17.37 *	4.60 *
			20.38 *	5.27 *
				7.10 *

* fluorescence spectrum of substituted phenanthrene
** fluorescence spectrum of substituted fluorene
*** fluorescence spectrum of pyrene

Chapter 6 Air Particulate and Diesel Exhaust Particulate Samples

6.1 Introduction

The primary focus of this work was the development of analytical methods suitable for the analysis of both atmospheric particulates and diesel exhaust particulates. Specifically, methods were developed to allow accurate identification and quantification of the sixteen priority PAHs, as well as the following nitro-PAH components, 2-nitrofluorene, 9-nitroanthracene, 3-nitrofluoranthene, 1-nitropyrene, 6-nitrochrysene, 7-nitrobenz[*a*]anthracene, and 6-nitrobenzo[*a*]pyrene.

This chapter is organized according to the following steps in method development: extraction of particulate samples, comparison of stationary phases for a LC cleanup separation of the particulate samples, LC reversed phase separation for the priority PAHs, GC/MS separation for PAHs, SFC separation of the priority PAHs, reversed phase LC C18 analysis for the amino-PAHs, and an SFC separation for the amino-PAHs. Finally, a quantitative comparison of the PAHs and the nitro-PAHs levels will be given for the Environment Canada diesel exhaust filters and several air particulate samples that were collected in-house.

Two possible analytical methodologies were investigated for the quantification of nitro-PAHs in particulate samples. Nitro-PAHs do not fluoresce well. However, amino-PAHs do tend to exhibit good fluorescence. The reduction of nitro-PAHs to the corresponding amino-PAHs allows the use of fluorescence detection to monitor these compounds. The first method developed for the analysis of the amino-PAHs used two-dimensional LC chromatography coupled with fluorescence detection. The first

chromatographic dimension was a DNBS column described earlier in the oil studies. This was used to fractionate the particulate extracts into classes and remove polar interferences. The nitro-PAHs were then reduced and analyzed as amines using a reversed phase separation as the second dimension. The second method developed used a one-dimensional SFC separation with the aminopropyl stationary phase. In this case an off-line reduction was performed to produce the corresponding amine before the SFC separation and detection using laser excited fluorescence.

The priority PAHs in the diesel exhaust particulates were quantified using one of three possible two-dimensional chromatographic procedures. In each case the LC-DNBS normal phase clean up separation was used as the first dimension to remove the larger more polar species that may interfere with analysis. The second or analytical dimension consisted of one of a reversed phase C18 separation, a SFC separation using an aminopropyl column described in chapter 3, or a capillary GC separation using mass spectrometric detection. Laser excited fluorescence detection was used for both the SFC and the reversed phase LC separations.

6.2 Experimental

6.2.1 Apparatus

A pressurized fluid extraction (PFE) system was designed and built in house. A schematic of this system is shown in Figure 6.1. The system consisted of a Shimadzu LC-

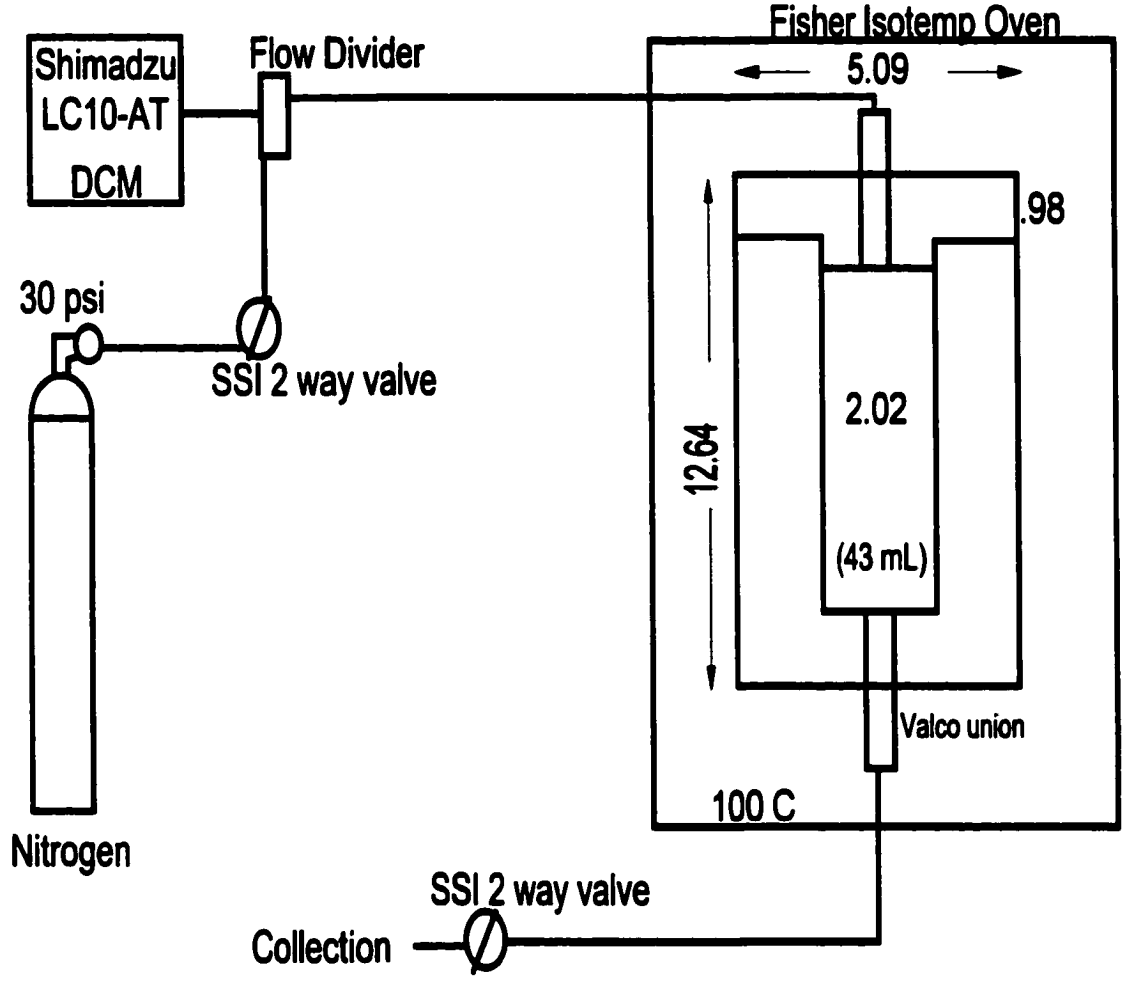

Figure 6.1: A schematic of the pressurized fluid extraction apparatus used to perform the extractions on the particulate samples.

10AT HPLC pump, Valco Tee (shown as 1), a nitrogen gas cylinder, 2 SSI two-way shut off valves (shown as 2 and 3), Fisher Isotemp oven Model 106G, extraction cell (12.64 cm x 5.09 cm, 43 mL volume) fabricated in-house, and a collection flask. Valve 2 was used to prevent solvent from expanding back into the nitrogen pressure regulator during extraction. Valve 3 was used to seal the exit of the extraction vessel and opened to collect the extract. The extraction cell was machined from a cylindrical piece of solid stainless steel stock. Valco unions were milled and silver soldered into each of the ends to allow the use of standard 1/16'' HPLC fittings and 1/16'' tubing (0.002 mm diameter). A groove was cut into the top of the cell to accommodate a Teflon® O ring used to seal the cover of the cell.

The GC/MS system used for the analysis of the priority PAHs in the particulate samples was described in chapter 4. The LC-DNBS separation that was used as a first dimension fractionation for the PAHs and nitro-PAHs consisted of an Agilent model 1100 quaternary pump, a Rheodyne 7725 injection valve with a 200 microliter sample loop, Keystone aminopropyl column (25 cm x 4.6 mm, 5 μ particles) derivatized as described in chapter 2, an Agilent 1100 oven, an Agilent 1100 diode array detector, and an Agilent 1100 fluorescence detector. The LC system used for priority PAH analysis consisted of an Agilent model 1100 quaternary pump, a Rheodyne 7725i injection valve with a 20 microliter sample loop, Supelco PAH column (15 cm x 4.6 mm, 3 μ particles) and a Supelco PAH column (5 cm x 4.6 mm, 3 μ particles) coupled in series, an Agilent 1100 oven, an Agilent 1100 diode array, and an Agilent 1100 fluorescence detector.

The reversed phase amine separation used an Agilent 1100 quaternary HPLC pump, a Rheodyne 7725i injection valve with either a 20, 200 or 1000 uL sample loop, in-house packed zinc powder column, a Rheodyne 7000 switching valve, a Supelco (25 cm x 4.6 mm,

5 μ particle) deactivated C18 column, and either an Agilent 1100 fluorescence detector or the laser excited fluorescence detector described in chapter 2. A schematic representation of this system is shown in Figure 6.2

The SFC system for the analysis of the PAHs and nitro-PAHs in the particulate samples was as described in chapter 3 using the Keystone aminopropyl column and laser excited fluorescence detector with the high-pressure flow cell.

6.2.2 Chemicals

The standards SRM 1649d, SRM 1647a, SRM 1650a, and SRM 1587 were provided through NIST. Dichloromethane, hexane, methanol and acetonitrile solvents were Optima grade provided by Fisher Scientific and used without further purification. Diesel particulate combustion solids were supplied by Syncrude Canada. Diesel exhaust particulate samples were collected from the exhausts of Ontario Transit buses by Environment Canada and shipped to Halifax for analysis. Ambient air particulate samples were collected in Halifax with a low volume active ambient air sampler.

6.2.3 Procedures

Three separate solvent systems were investigated for the extraction of the particulate matter with pressurized fluid extraction (PFE): methanol, acetonitrile, and dichloromethane. Particulate samples were weighed with an analytical balance to 0.1 mg, and then introduced into a cellulose thimble (Whatman International Ltd. 10 mm x 50 mm), covered with a glass

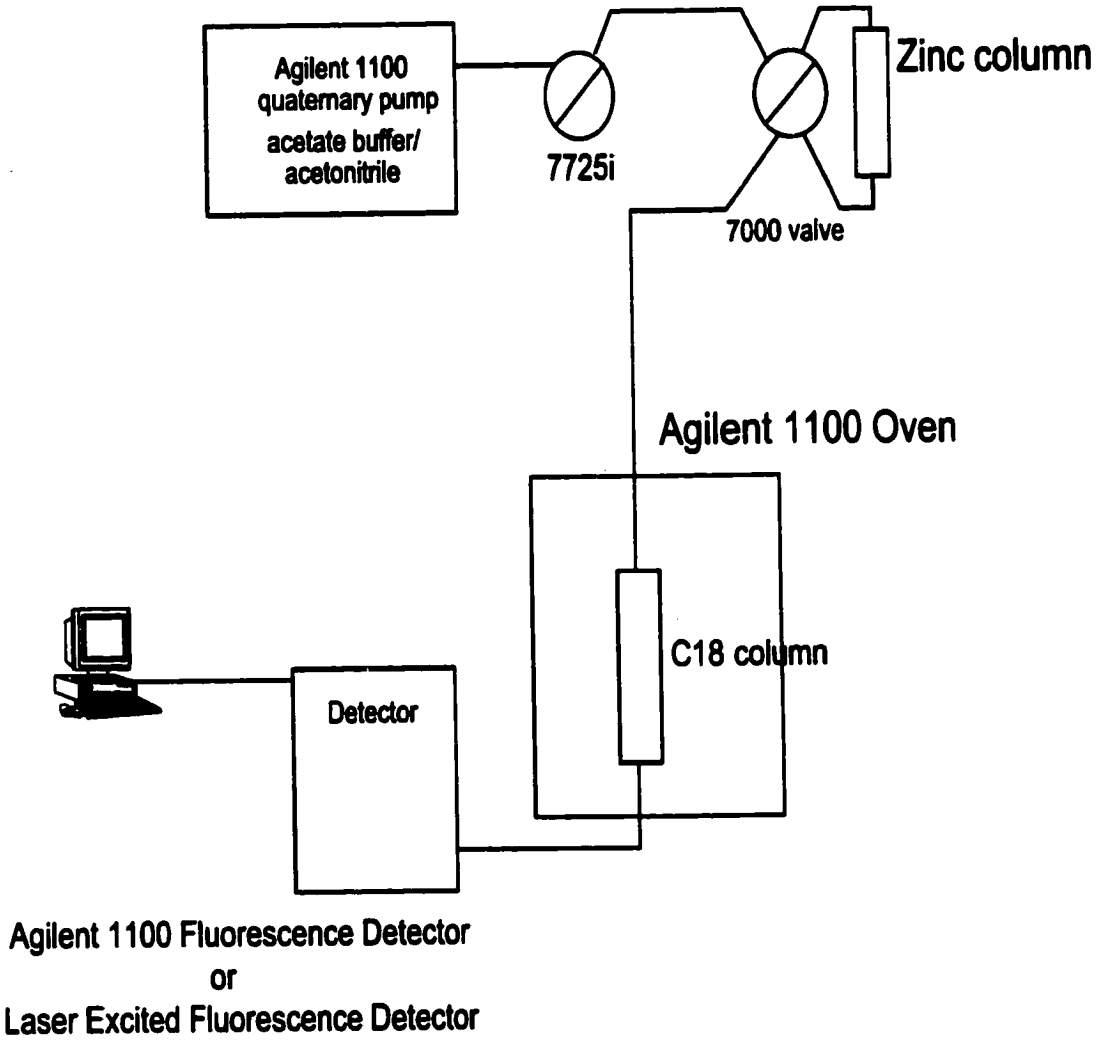

Figure 6.2: A schematic of the on-line reduction apparatus with the C18 column and fluorescence detectors.

wool plug and placed into the PFE cell. The cell was then filled with solvent at ambient temperature and pressurized to between 200 and 250 bar. Next, the cell was heated to the appropriate temperature after being placed into the oven. The temperature was set to 100 °C for the dichloromethane extractions. The methanol and acetonitrile extractions were done using a temperature of 140 °C. All extractions were performed under static conditions. Both the methanol and acetonitrile extractions utilized three cycles. The first extraction was performed for 20 minutes. The remaining cycles lasted 10 minutes each. The dichloromethane extractions were performed using 2 cycles, 20 minutes for the first cycle followed by a final 10 minute static cycle. Between the extraction cycles, the extraction cell was purged using nitrogen at a pressure of 30 to 50 pounds per square inch (psi). Extracts were collected in a 150 mL round bottom flask containing 10 mL of the extraction solvent. The tubing from the extraction vessel was submersed in solvent as an added trapping measure. Samples were then pre-concentrated using a rotary evaporator to near dryness and then reconstituted with hexane to approximately 1-2 mL total volume for subsequent analysis. The volume was calculated by weighing the extracts with an analytical balance.

An LC-DNBS separation was used as a cleanup for the particulate samples. Two hundred microliter samples of a standard containing the priority PAHs and several nitro-PAHs were injected onto the DNBS column and monitored using the diode array and the 1100 fluorescence detector in series. The diode array detector was set to monitor wavelengths at 220 nm and 254 nm whereas the fluorescence detector used excitation at 260 nm and monitored the fluorescence emission at 430 nm. Three injections were performed to establish a fraction or collection region that contained both the PAHs and nitro-PAHs but not the larger and more polar constituents. The replicate injections also served to establish the

precision of the separation, after which the detectors were switched off and particulate extracts were injected. Collections were based upon the times observed from the standard chromatograms. Injections were repeated until roughly one half of the sample had been fractionated. The collected region of interest was taken to near dryness using a rotary evaporator and reconstituted to approximately 1 mL with acetonitrile for reversed phase LC analysis of the priority PAHs or nitro-PAHs. The remainder of the raw extract was treated in a similar way, except that the sample was spiked with a deuterated PAH standard and reconstituted with hexane for GC analysis of the priority PAHs or SFC analysis of the nitro-PAHs and priority PAHs.

Analysis of the priority PAHs was facilitated through the use of three methods. The first method used a reversed phase LC separation. Twenty microliters of reconstituted particulate sample dissolved in acetonitrile was injected onto the two Supelco C18 columns in series and monitored using the laser excited fluorescence detector with the 266 nm laser. The columns were thermostated at 25 C using the Agilent 1100 oven. A water/acetonitrile gradient that started at 60% water/40% acetonitrile and increased linearly to 100% acetonitrile over 10 minutes, remaining constant for 10 minutes, was used to elute the priority PAHs. The flow rate was set to 1.5 mL/min.

The second analytical method used a capillary GC separation to perform the analysis. Samples were eluted from the GC into the mass spectrometer using a temperature program shown in Table 6.1. Helium was used as the carrier gas at a flow rate of 2.0 mL/min. Two microliter splitless injections were performed into the GC inlet set to 325 C. The mass spectrometer was operated using retention windows for selected masses. The parameters are shown in Table 6.2. The source and the transfer line were set to 320 C.

Table 6.1: Temperature program conditions for GC separation of priority PAHs

Time (min)	Temperature (°C)
0	50
12.5	250
16.5	250
21	320
24	320

Table 6.2: Retention windows and masses used for the detection of the priority PAHs with GC-MS.

Mass	Dwell Time (seconds)	Retention Window
128.1	0.05	0-12.50 minutes
152.1	0.05	
154.1	0.05	
164.1	0.05	
165.1	0.05	
178.1	0.10	12.60-16.50 minutes
188.1	0.10	
202.1	0.10	
228.1	0.15	16.60-20.00 minutes
240.1	0.15	
252.1	0.20	20.10-24.00 minutes
264.1	0.20	
276.1	0.20	24.10-28.00 minutes
278.1	0.20	
292.1	0.10	

The third method was a SFC analysis of the priority PAHs using the aminopropyl column. This separation was performed as described in chapter 3.Analysis of the nitro-PAHs was examined using two methods. The first method was a reversed phase LC separation that used a pre-separation on-line reduction of the nitro-PAHs to the corresponding amino-PAHs. A deactivated Supelco C18 column thermostated to 35 C was used for the separation. Gradient conditions for the separation are shown in Table 6.3. This separation required the use of an aqueous 100 mM acetate buffer. The buffer was prepared as follows. One liter of 0.1 M acetic acid was prepared by diluting 5.75 mL of glacial acetic acid with one liter of distilled water. 8.2 grams of solid anhydrous sodium acetate was dissolved in the 0.1 M acetic acid. To this solution 0.85 grams of copper(II) chloride was added to improve reduction efficiency. A small Supelco HPLC guard column (1cm x 4.6 mm) was sacrificed and repacked with zinc powder and used as the reducing agent for the nitro-PAHs. Twenty microliters of sample were injected, passed through the zinc column and then onto the

Table 6.3: Gradient conditions for reversed phase separation of aromatic amines

Time (min)	% Aqueous Buffer	% acetonitrile
0	70	30
10	10	90
15	0	100
20	0	100

analytical column. After 2 minutes the zinc column was switched out of the eluent stream to prevent excess zinc salts from being passed onto the analytical column. The amino-PAHs were detected using either the Agilent 1100 fluorescence detector set to excite at 260 nm and monitored at 315, 366, 430, and 525 nm or the laser excited fluorescence detector using the 266 nm laser.

A second method was investigated for the analysis of nitro-PAHs present in particulate samples. This method used the Keystone aminopropyl column in a SFC separation. Two hundred microliters of sample was injected onto the zinc column, batch reduced and eluted with the aqueous buffer. This procedure was repeated until 1 mL of extract was processed. The products of the reduction were collected, combined and then evaporated to dryness and reconstituted with hexane. Twenty five microliters of this sample were then injected onto the aminopropyl column using the Alcott auto sampler. The aromatic amines were separated with a constant organic modifier concentration of 16 %. The organic modifier was a mixture of 2.5% propylamine in acetonitrile. The pressure of the mobile phase was maintained at 250 bar. Flow rate was set at 1.0 mL/min. Oven temperature was maintained at 60 °C. The eluent was monitored using the laser excited fluorescence detector with excitation using the 266 nm laser.

6.3 Results and Discussion

6.3.1 Extraction of the Particulate Matter

The particulate samples presented a different challenge than the light gas oils studied

in previous chapters. The focus here was to obtain quantitative results on samples with much lower concentrations of PAHs. The first step was method development of the extraction of the analyte from a solid matrix. Primarily, the single most important factor with such extractions is that they provide a complete and exhaustive removal of the all of the analytes of interest from the particulate matrix. Otherwise, subsequent analysis for the target compounds would produce erroneous results. Typically, Soxhlet extractions have proven popular for such complex matrices. Typical Soxhlet extractions use 200 - 300 mL of solvent and 24 -48 hours, so it was decided to explore methods that use both less time and solvent. Chapter 1 discussed various protocols for the proper validation of extraction methods. For example, spiking experiments tend to produce PAHs more as a 'deposit' instead of in a physically adsorbed state. Deposited PAHs are much more easily extracted because they generally only require solubilization from the surface of the particulate. The goal was to use a standard reference material to test the extraction method and develop a general protocol for diesel exhaust particulates. Pressurized fluid extraction (PFE), sonication and supercritical fluid extraction (SFE) were examined as alternative methods to Soxhlet extraction.

Initial experiments were done using the supercritical fluid chromatograph to simulate the SFE of materials. The test sample was a graphite support (Specpure) spiked with known amounts of acenaphthylene, fluorene, phenanthrene, anthracene, pyrene, benzo[*a*]anthracene, chrysene, benzo[*b*]fluoranthene, benzo[*k*]fluoranthene, benzo[*a*]pyrene, dibenz[*a,h*]anthracene, benzo[*g,h,i*]perylene, and indeno[*1,2,3-c,d*]pyrene. It was observed that even for this sample SFE could not fully extract all of the priority PAHs in a reasonable time period without the aid of an organic modifier such as methanol. Increasing the methanol concentration decreased the time required to extract the PAHs as well as increased the

relative recovery of the PAHs that were spiked onto the graphite. For example, using 10% methanol, the recoveries of the PAHs phenanthrene and benzo[*g,h,i*]perylene were observed to be 84% and 6%, respectively. Increasing the methanol concentration to 20% was found to increase the recovery of phenanthrene to 93% and benzo[*g,h,i*]perylene to 51%.

Additional testing of the SFE extractions was performed with combustion particulates supplied by Syncrude Canada. The particulates were combustion solids deposited on the exhaust walls of an instrument used to measure the cetane number of a diesel fuel. The instrument was operated over a period of 4-6 months before a collection of the combustion solids. It was found that SFE did allow for a much more selective extraction of these particulates. In this case many of the polar interferences could be left behind in the original matrix. In fact, extractions performed with pure CO_2 at low temperature (50 C) and pressure (100 bar) were able to selectively extract the compounds with one to four aromatic rings. However, complete extraction of these compounds could not be confirmed due to the fact that the PAH concentration for these particulates was unknown. Furthermore, trapping the extracts during depressurization presented significant challenges. In addition, restrictor damage became a problem. The pressure (350 bar) and temperature (150 C) limitations of this instrument were below those of commercial SFE instruments. These limitations and the cost of replacement restrictors prevented the use of SFE for further method development.

In terms of equipment and design sonication would seem to be the simplest extraction procedure available. To determine the relative extraction ability of sonication compared to PFE, a comparison was performed using the combustion particulate sample provided by Syncrude Canada. These particulates were ideal because they were a real sample that would better represent the nature of the matrices associated with the Environment Canada exhaust

samples. The chromatograms that result from the reversed phase LC fluorescence of these extracts are shown in Figure 6.3. Each extraction was replicated to ensure that particulate sample inhomogeneity did not skew the comparison. The chromatograms were normalized based upon original particulate mass and final solvent volumes to allow a direct quantitative comparison. This method of comparison was undertaken because of the limited number of standards available during the time of this preliminary study and the fact that procedures had not yet been fully developed to analyze all of the components under investigation. A comparison of the signal intensities shown for each of the chromatograms in Figure 6.3 suggests that slightly more material was extracted (~20% for pyrene) with the pressurized fluid extraction when compared to sonication. However, recent literature reported that sonication offered complete extraction from diesel exhaust particulates using an acetone/dichloromethane solvent mixture [152]. However, lengthy extraction times of several hours were required to achieve these results. The sonication extraction tested in this work used dichloromethane as the solvent and an extraction time of 60 minutes. The PFE method used methanol as the solvent. A typical PFE experiment required 35 minutes to complete. Sonication extractions when performed with methanol extracted less material than when performed with dichloromethane.

PFE was found to offer a more exhaustive extraction of the PAHs from the Syncrude particulates compared to sonication. In addition, PFE was found to extract the PAHs in less time than either sonication or Soxhlet. PFE was selected as the extraction method of choice. Once selected, the PFE was subjected to a rigorous validation by extracting the standard reference materials Urban Dust 1649a and Diesel Particulate Matter 1650a supplied by NIST and comparing our measured values with certified values.

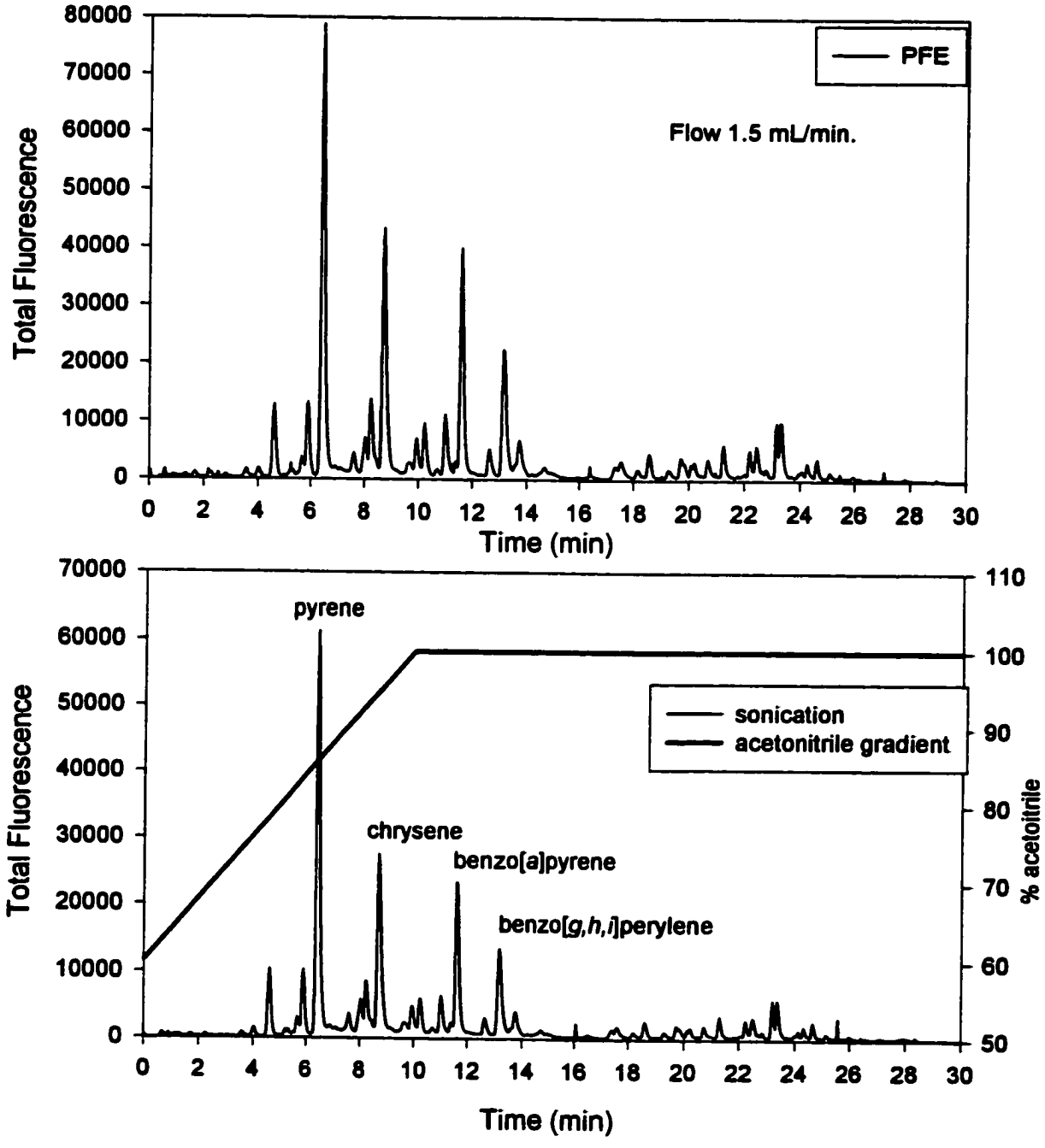

Figure 6.3: Reversed phase C18 chromatograms of diesel particulate extracts monitored using the laser excited fluorescence system and the 266 nm laser. Upper chromatogram results from the use of pressurized fluid extraction with methanol at 100 °C and 250 bar of the Syncrude diesel particulates. The lower chromatogram results from the extraction of Syncrude diesel particulates with sonication for one hour with dichloromethane. Chromatographic conditions are shown in the figure.

Each static extraction cycle required 35-40 mL of solvent to fill the extraction cell and 5 mL to purge the cell. Increasing the number of extraction cycles may increase the total amount of material extracted but also increases the total volume of extract that must be preconcentrated before instrumental analysis. It would be beneficial to extract the analytes from the matrix with a minimum volume of solvent. In order to test the number of static extraction cycles that were required for exhaustive extraction of the PAHs from the standard reference materials, the extract from each static cycle was analyzed individually. Figure 6.4 shows the chromatograms that result from each of the individual extracts using methanol. Exhaustive extraction for the priority PAHs was achieved after 3 static cycles using methanol as the solvent. The total volume of solvent required for each extraction under these circumstances was between 120 -140 mL. This represents a considerable volume of solvent to remove before further sample preparation commences. A more practical solvent was investigated in an attempt to lessen the total extract volume through reduced extraction cycles.

Acetonitrile and dichloromethane were examined as alternative solvents to methanol in an attempt to reduce the total extract volume through a reduction of the number of static cycles required for exhaustive extraction. Three cycles were found to be sufficient for complete extraction of the sample matrix using acetonitrile. This provided little benefit in terms of solvent reduction but extraction efficiencies for compounds such as benzo[*b*]fluoranthene, benzo[*k*]fluoranthene, and benzo[*a*]pyrene were enhanced with acetonitrile as compared to methanol. Table 6.4 summarizes the recoveries of the Priority PAHs from standard reference materials NIST 1649a urban dust and NIST 1650a diesel exhaust particulates using each of the three solvent choices, methanol, acetonitrile, and

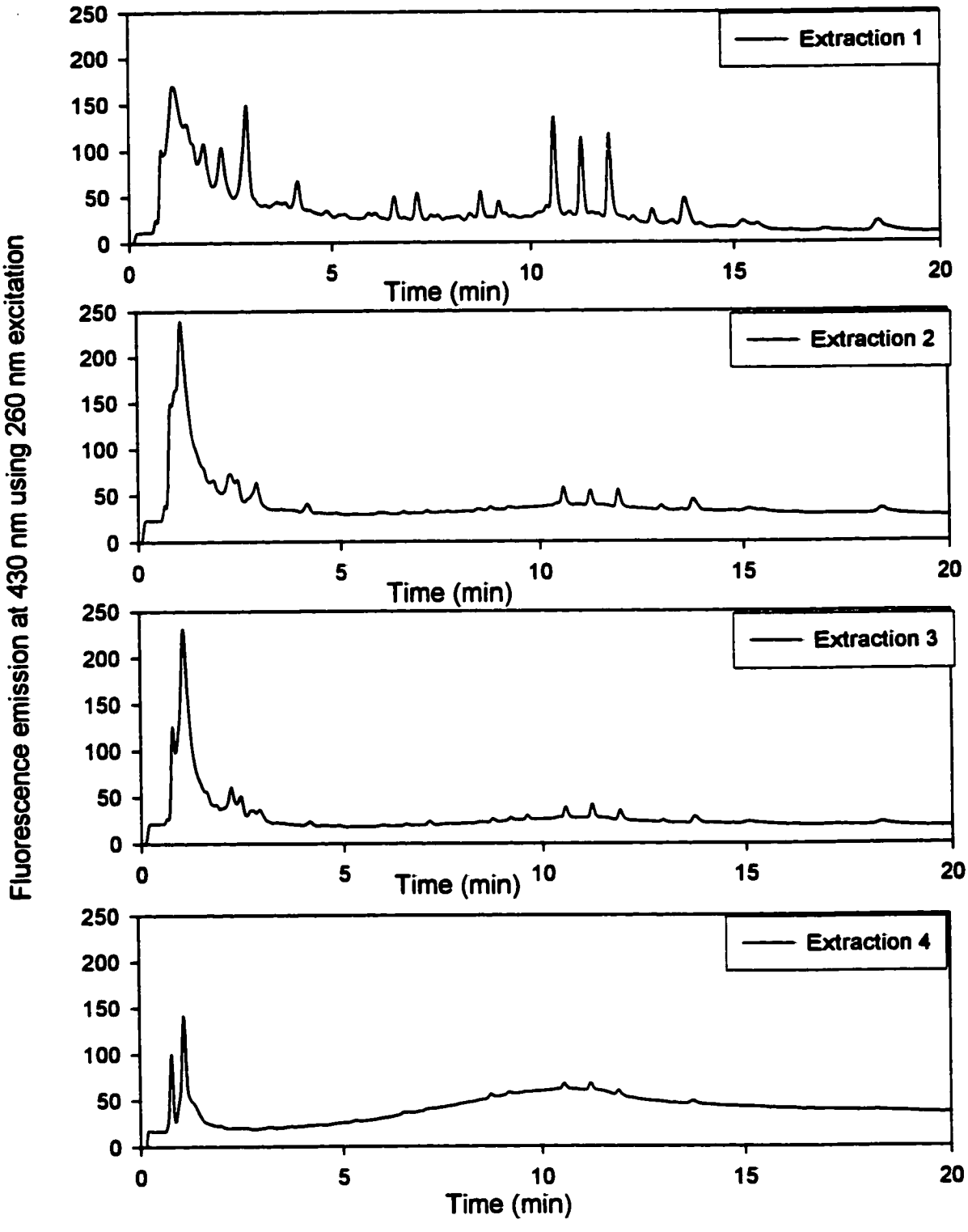

Figure 6.4: Chromatograms of individual extracts from a single Urban Dust (1649d) sample separated on a reveresed phase C18 column using Agilent fluorescence detection. Methanol (140°C) was used as the extraction solvent. Extracts were injected without prior cleanup.

dichloromethane. As well, the recovery of 1-nitropyrene was documented for NIST 1650a.

Several of the priority PAHs, naphthalene, acenaphthene, acenaphthylene, and fluorene were

Table 6.4: Data for the extractions of the priority PAHs from NIST 1649a and NIST1650a using methanol (140°C), acetonitrile (140°C), and dichloromethane (100°C). Values in brackets represent NIST certified values.

Compound	Methanol NIST1649a	MeCN NIST1649a	DCM NIST1649a	DCM NIST1650a
Phenanthrene	4.05±0.16 (4.14±0.37)	3.89±0.16 (4.14±0.37)	3.81±0.11 (4.14±0.37)	61.5±9.2 (68.4±8.5)
Anthracene	0.40±0.02 (0.43±.08)	0.40±0.02 (0.43±.08)	0.39±0.01 (0.43±.08)	**NP
Fluoranthene	6.44±0.26 (6.45±0.18)	6.77±0.27 (6.45±0.18)	6.12±0.25 (6.45±0.18)	44.9±3.5 (49.9±2.7)
Pyrene	5.18±0.21 (5.26±0.5)	5.34±0.27 (5.26±0.5)	5.13±0.21 (5.26±0.5)	43.7±3.9 (47.5±2.7)
Benz[*a*]anthracence	1.90±0.06 (2.21±.073)	2.08±0.02 (2.21±.073)	2.07±0.02 (2.21±.073)	5.95±0.30 (6.33±0.77)
Chrysene	2.77±0.11 (3.049±.60)	3.23±0.20 (3.049±.60)	3.23±0.19 (3.049±.60)	13.88±1.1 (14.5±0.8)
Benzo[*b*]fluoranthene	5.54±0.22 (6.45±0.64)	5.86±0.12 (6.45±0.64)	5.86±0.12 (6.45±0.64)	7.90±0.95 (8.81±0.6)
Benzo[*k*]fluoranthene	1.57±0.05 (1.91±.031)	1.76±0.02 (1.91±.031)	1.76±0.02 (1.91±.031)	2.40±0.84 (2.64±0.61)
Benzo[*a*]pyrene	2.21±.09 (2.51±.087)	2.28±0.07 (2.51±.087)	2.36±0.07 (2.51±.087)	1.21±0.56 (1.33±0.35)
Dibenz[*a,h*]anthracence	*NA (0.29±.023)	*NA (0.29±.023)	*NA (0.29±.023)	*NA
Benzo[*g,h,i*]perylene	3.05±0.09 (4.01±0.91)	3.61±0.14 (4.01±0.91)	3.76±0.11 (4.01±0.91)	5.2±0.73 (6.5±0.94)
Indeno[*1,2,3-c,d*]pyrene	2.99±0.18 (3.18±0.71)	3.37±0.24 (3.18±0.71)	2.89±0.32 (3.18±0.71)	4.89±0.44 (5.62±0.53)
1-nitropyrene	**NP	**NP	**NP	17.9±3.8 (19±2)

Values in parenthesis represent NIST certified values
All values in ug/g of particulate
*Not done
**Not present or below detection limit

omitted from this table because NIST does not provide certification for these compounds. Dichloromethane was found to produce the most efficient extraction with only two static cycles required for complete extraction of the PAHs from the particulates. These numbers, however, reflect the total procedure of extraction cleanup, and instrumental analysis. Typical recoveries were 91-98% for the urban dust and 80-96% for the diesel particulates. All of the recoveries were within the 95% confidence limits specified by NIST except for dibenz[*a,h*]anthracene and benzo[*a*]pyrene.

The use of dichloromethane represented the smallest volume of extract to evaporate or pre-concentrate. Furthermore, the relatively low boiling point of this solvent compared to acetonitrile and methanol allowed more efficient removal of the solvent at low temperature using a rotary evaporator. This minimizes the loss of some of the more volatile PAHs such as naphthalene during the pre-concentration of the extract. Dichloromethane also has the added advantage of being more compatible with the analytical methods. For example, the cleanup procedure that was used prior to instrumental analysis was normal phase chromatography with hexane and dichloromethane eluents. Furthermore, polar solvents result in peak fronting when used in conjunction with a HP-5ms capillary GC column. Acetonitrile was found to be incompatible with the normal phase separations. Poor resolution and precision were observed with the chromatograms that used acetonitrile in the injection solvent. Therefore, the use of acetonitrile as an extraction solvent required an additional step in sample preparation as the initial extract had to be taken to near dryness and solvent exchanged to a compatible solvent. This presents an added risk of contamination or sample loss. Although no notable loss was observed for components with molecular weights greater than phenanthrene, the possibility of loss of more volatile species such naphthalene may

occur. In addition, extraction with acetonitrile produced a precipitate that was believed to result from extracted silicates from the urban dust. This was not observed with the dichloromethane extracts. The precipitate that formed after extraction with acetonitrile may occlude some of the PAHs affecting accurate quantification. In order to prevent such errors the precipitate would have to be completely resolubilized. This presented difficulties as the precipitate required an acidic aqueous solvent for dissolution. Such solvents were not compatible with the sample workup procedure. Dichloromethane was chosen as the primary solvent for performing the extractions of the Environment Canada filter samples. Extra care must be taken with such chlorinated solvents as they pose a greater risk of human exposure due to elevated vapor pressures at room temperature.

6.3.2 Characterization of the Cleanup Separation for the Air Particulate and Diesel Exhaust Particulate Samples

Preliminary analysis of the NIST urban dust extracts (chromatogram shown in Figure 6.10b) suggested that a cleanup or fractionation of the raw extracted sample was required for accurate quantification of the priority PAHs using reversed phase chromatography. More importantly, preliminary studies of the diesel exhaust filter extracts separated using reversed phase chromatography revealed very complex chromatograms with many unresolved peaks resulting in poor quantification of the PAHs. The sub fractionation of the PAHs present in such a sample may provide less complex reversed phase chromatograms resulting in better quantification. Three stationary phases were investigated as possible candidates for this purpose. A silica, an aminopropyl and a DNBS column were each characterized with a simple standard mixture that contained both the priority PAHs and selected nitro-PAH compounds

The nitro-PAHs in the standard were 1-nitronaphthalene, 2-nitrofluorene, 9-nitroanthracene, 2-nitrobiphenyl, 3-nitrofluoranthene, 1-nitropyrene, and 6-nitrochrysene. A diesel exhaust particulate sample was injected onto each column to establish the usefulness of each separation. Figure 6.5 shows the results of this characterization for the preparative silica column. The chromatogram of the PAH standards and nitro-PAH standards in this figure suggest that a fractionation between these regions may be possible. However, as the chromatogram suggests there is insufficient resolution to enable a fractionation of the priority PAHs in the Environmental Canada sample according to the number of aromatic rings present. Diesel exhaust samples are often similar to light gas oils in that they contain alkylated PAHs as well as the parent PAHs. It was hoped that a cleanup separation would permit both a PAH fractionation based upon the number of aromatic rings and removal of late eluting compounds. The silica column had the largest capacity with 400 microliter injection volumes as long as the injection plug was comprised almost entirely of hexane. The addition of dichloromethane or acetonitrile to the injection solvent degraded chromatography to the point that considerable overlap was observed between regions. However, overlap between the high molecular weight PAHs and the nitro-PAHs was not of primary concern as they are well separated (*vide infra*) in reversed phase chromatography. It was found, however, that polar compounds interfere with the reversed phase separation of the amino-PAHs. An example of this is shown later in this chapter in Figure 6.28. The silica column was unable to provide sufficient resolution to retain these polar compounds and separate them from the nitro-PAHs. Furthermore, the silica column required large quantities of solvent (~90-100 mL) to cleanup a reasonable amount of sample. The silica column was not used in further experiments.

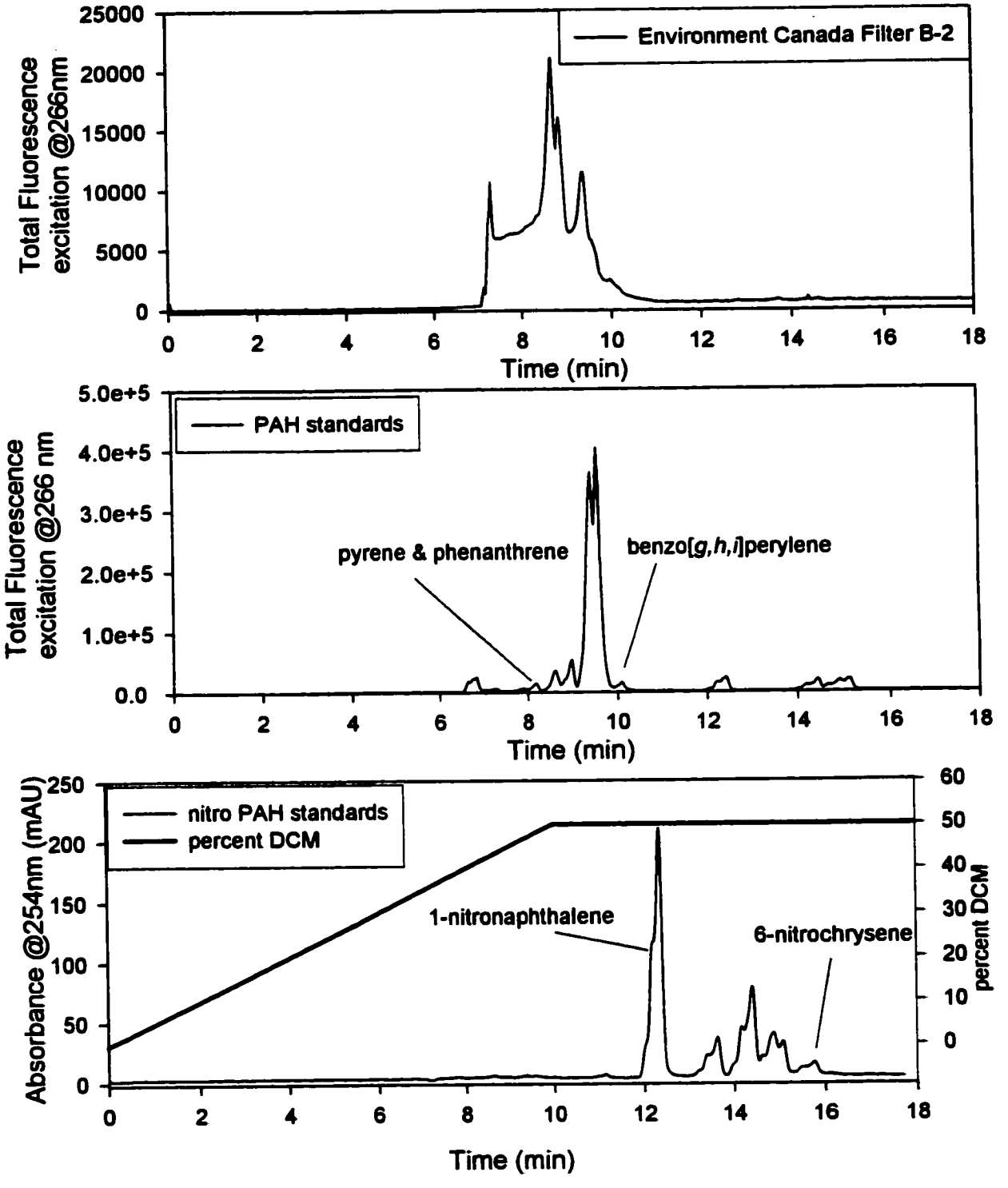

Figure 6.5: Chromatograms of Enviroment Canada's diesel exhaust filter sample B-2 separated on the silica column. Flow rate was 3.0 mL/min. A hexane/dichloromethane gradient was used as the eluent. A standard PAH and nitro PAH mixture was used to characterize the separation. The PAHs were monitored with the fluorescence detector while the nitro-PAHs were detected using a diode array detector set to record absorbance at 254 nm.

The Keystone aminopropyl column was investigated next and was characterized in the same manner as the silica column. The chromatograms are shown in Figure 6.6. As with the silica column, insufficient resolution was present within the PAH region to allow for the fractionation of the compounds. As well, poor peak shapes were observed for this separation. This was found to be a result of injection solvent composition. Similar to the silica column, the efficiency of the aminopropyl column was susceptible to small quantities of dichloromethane and acetonitrile. Closer inspection of the priority and nitro-PAH regions indicates that significant overlap exists for these compound classes. The greatest difficulty with this separation was the capacity of the aminopropyl column. The maximum injection volume was limited to 20 microliters. This makes the cleanup of the particulate sample extract of 1-2 mL impractical. A larger column may offer more capacity and more reasonable results. However, the resolving capability of this column with the diesel samples did not appear to warrant the expense of purchasing a larger column. An alternative was to use a more powerful stationary phase such as the DNBS, in lieu of a larger column.

The final separation examined for the cleanup of the particulate samples used a DNBS stationary phase derived from a commercial Keystone aminopropyl column. The DNBS column offered excellent capacity and could easily handle 200 microliter injection volumes despite that fact that it had the same column dimensions as the aminopropyl column. In addition, this column was much less prone to losses in column efficiency due to injection solvent composition when compared to the silica and aminopropyl columns. The chromatograms of an Environment Canada filter sample with the priority and nitro-PAHs are shown in Figure 6.7. The separation observed within the priority PAH region of this chromatogram suggests that the collection of sub-fractions may be viable. An overlap was

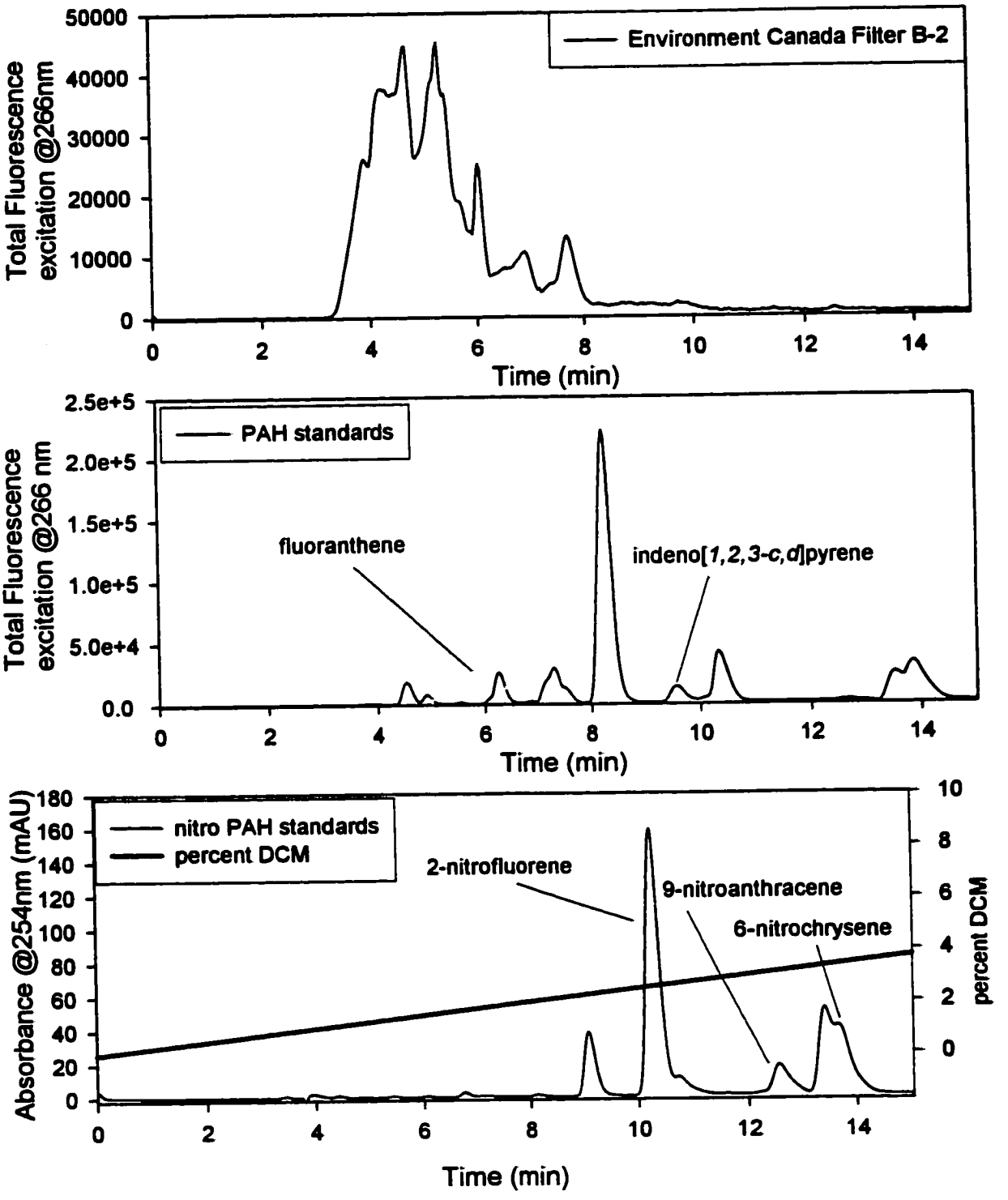

Figure 6.6: Chromatograms of Environment Canada's diesel exhaust filter sample B-2 separated on the aminopropyl column. Flow rate was 1.0 mL/min. A hexane/dichloromethane gradient was used as the eluent. A standard PAH and nitro-PAH mixture was used to characterize the separation. The PAHs were monitored with the fluorescence detector while the nitro-PAHs were detected using a diode array dector set to record absorbance at 254 nm.

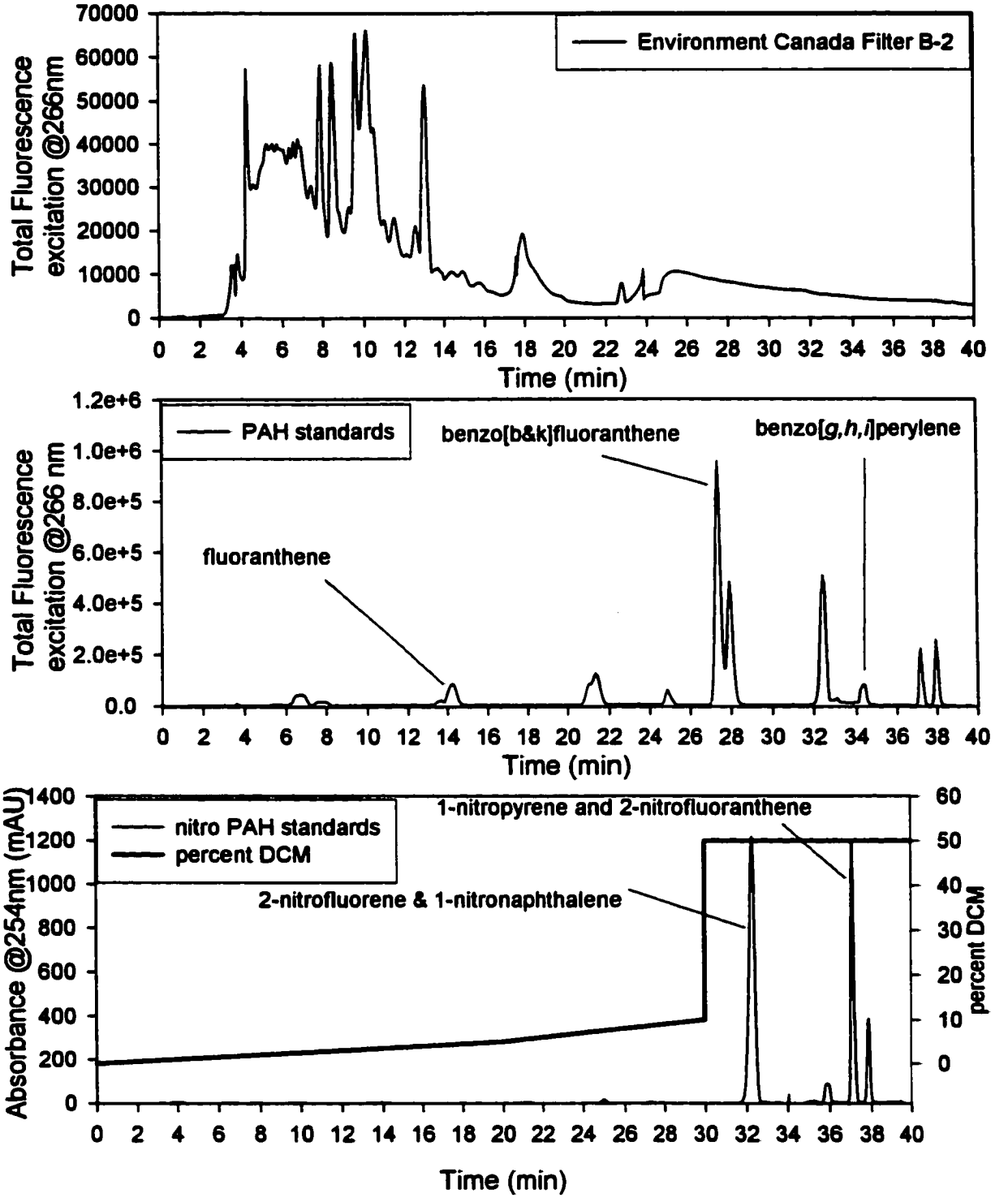

Figure 6.7: Chromatograms of Enviroment Canada's diesel exhaust filter sample B-2 separated on the DNBS column. Flow rate was 1.0 mL/min. A hexane/dichloromethane gradient was used as the eluent. A standard PAH and nitro-PAH mixture was used to characterize the separation. The PAHs were monitored with the fluorescence detector while the nitro-PAHs were detected using a diode array dector set to record absorbance at 254 nm.

observed between the priority and nitro-PAHs. However, the polar compounds that interfere with the analysis of the amino-PAHs were well retained by this stationary phase. The conditions in Figure 6.7 lend themselves to the greatest resolution they also generate extended analysis times. Since multiple injections were required to clean up an entire sample a faster gradient was examined with a slight loss of resolution. The results are shown in Figure 6.8. Examination of the chromatograms generated by the PAH and nitro-PAH standards in Figures 6.7 and 6.8 suggest that indeed a reduction was observed for the retention times of the priority and nitro-PAHs. However, this reduction in analysis time was not evident with the particulate samples from the Environment Canada filter B-2 and the NIST diesel exhaust particulate SRM 1650a. In Figure 6.8, the methoxy-PAHs as well as the large polars that were found to prevent accurate quantification of the nitro-PAHs and some priority PAHs are clearly shown. These compounds appear less prevalent in the chromatogram of the Environment Canada filter (B-2) extract shown in Figure 6.7. This was due to differences between the two samples and increased retention on the DNBS column due to weaker eluent concentrations used during the separation of SRM 1650a. The preliminary studies with reduced eluent concentrations required flushing with 100% dichloromethane to remove polar compounds from the column. There were differences in the relative PAH distribution between the two samples as observed through the chromatograms in Figure 6.7 and Figure 6.8. The SRM 1650a displayed an increased concentration of PAHs with a number of aromatic rings greater than pyrene compared to the B-2 filter. In fact, the B-2 filter appeared to have greatest percentage of the PAHs eluting before fluoranthene and pyrene. These differences will be examined in greater detail later in this chapter.

Since many of the priority PAHs such as benzo[*a*]pyrene were sensitive to

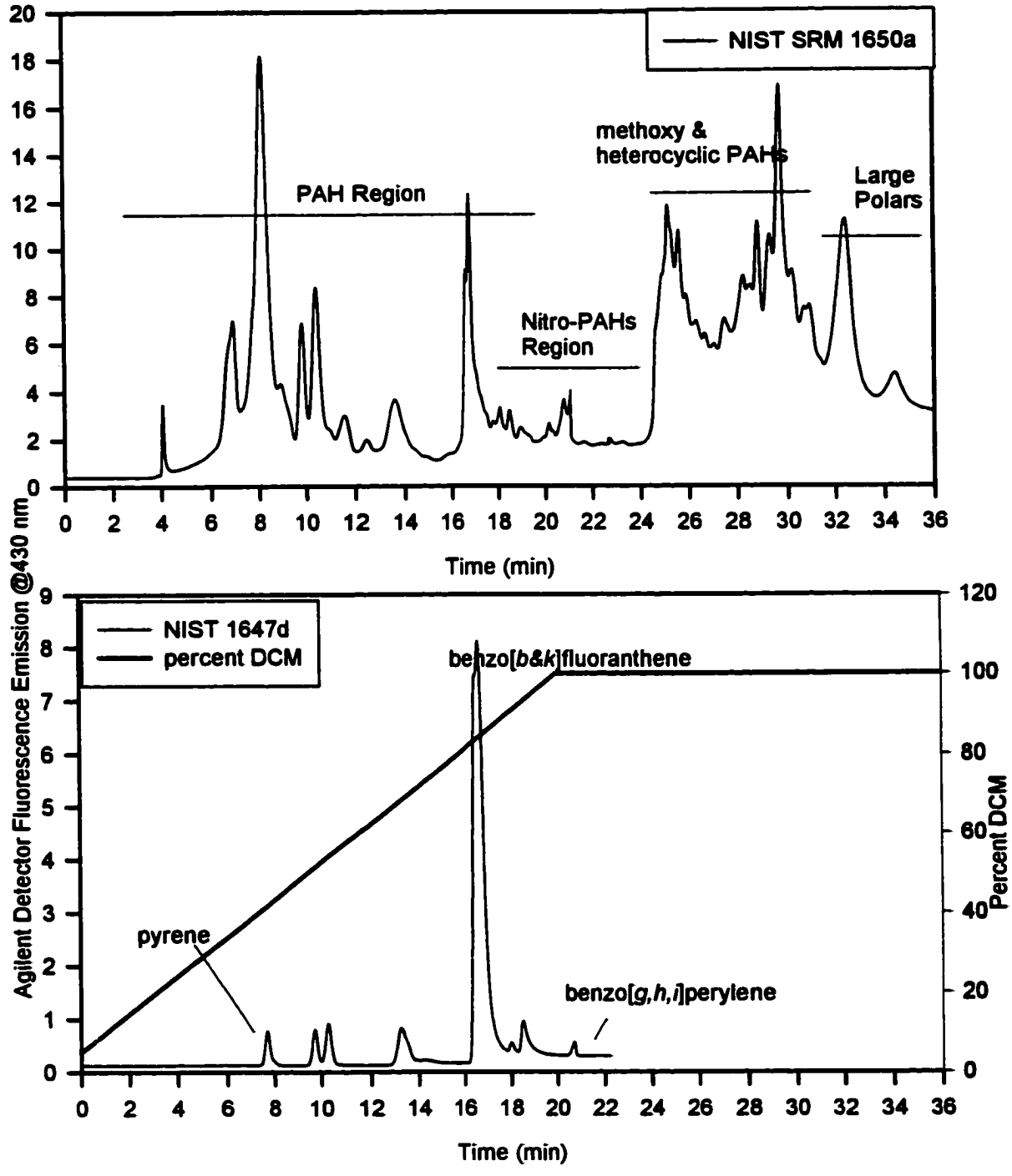

Figure 6.8: LC chromatograms of diesel exhaust particulates and priority PAH standards separated on the DNBS column with the Agilent 1100 fluorescence detector. Fluorescence emission provided by excitation at 260 nm. Flow rate was set to 1.0 mL/min.

photodegradation, it was decided that the cleanup separation would have to be performed with the fluorescence excitation light source turned off. Otherwise, photodegradation may occur causing inaccurate quantification. Hence, there was a need to establish the precision of the separation so as to ensure the correct collection of each fraction. Figure 6.9 shows three replicate injections of the standard reference material NIST 1650a using the same chromatographic conditions as in Figure 6.8. From the three chromatograms there is good inherent precision in retention times with the DNBS separation. A separate study, done by Kathleen Duggan looked at the recovery of a PAH standard using the same separation [153]. The results suggested that complete recovery for all of the priority PAHs was observed with the exception of naphthalene and fluorene. It was believed that the volatility of these compounds resulted in losses during the rotary evaporation of the solvent. Otherwise the DNBS cleanup provided an ideal separation for the cleanup of urban dust and diesel exhaust particulate samples after extraction with the PFE system. The majority of the quantification experiments described later, used a collected fraction that consisted of the Priority PAHs and the nitro-PAHs. This fraction represents between 3 to 23 minutes of the chromatogram shown in Figure 6.9. Although, the DNBS separation displayed sufficient resolution to enable some fractionation of the priority PAHs (according to the number of aromatic rings) in diesel exhaust filter samples, in practice this was less successful for two reasons. First, it was difficult to collect specific regions relatively close in retention times without the aid of a detector. Second, the fractions that were examined from the DNBS column based upon aromatic group size still presented complex chromatograms on the reversed phase columns due to large numbers of alkylated PAHs. This observation was most prominent for the diesel particulate samples from Environment Canada and to a lesser extent with the NIST SRM

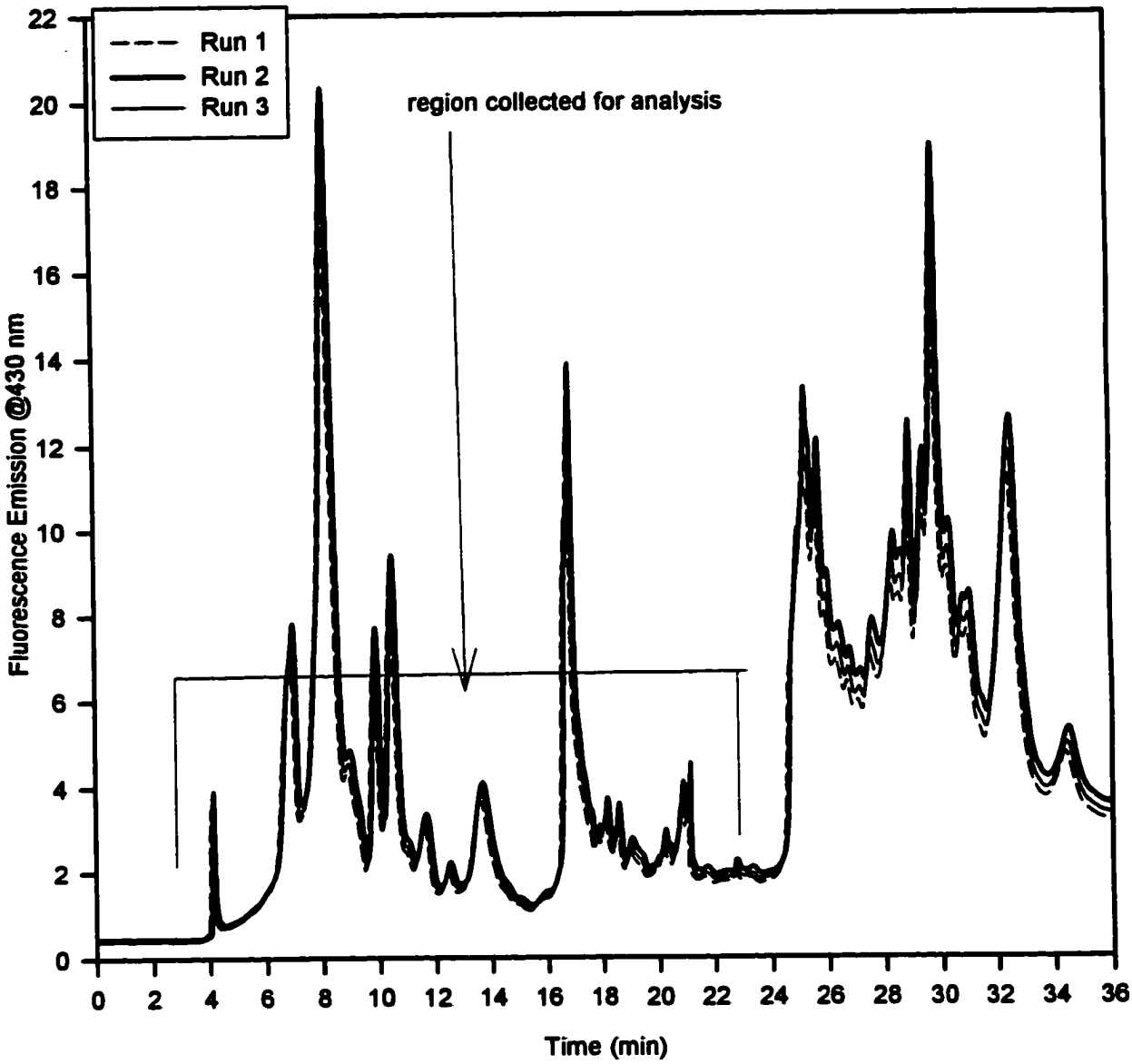

Figure 6.9: Three replicate injection of the standard reference material NIST 1650a separated on the DNBS column using the Agilent 1100 fluorescence detector with excitation at 260 nm. The chromatographic conditions are given in Figure 6.8.

1650a. As a result, there was little benefit to collect fractions within the PAHs based upon the number of aromatic rings as opposed to a single region that contained all of the PAHs as well as the nitro-PAHs.

6.3.3 Reversed Phase LC Analysis of the Priority PAHs

Preliminary quantitative experiments attempted to analyze the priority PAHs directly without prior sample cleanup because multi-dimensional chromatographic operations add complexity to the analysis. Initial studies used the Agilent 1100 commercial fluorescence detector because of the higher sensitivity associated with this detector when compared to the laser excited fluorescence detector. The Agilent system used a larger bandpass (20 nm) that lowered the spectral resolution. The laser excited fluorescence detector developed in-house provided better spectral resolution but initially the system was much less sensitive than the Agilent detector. However, several modifications were performed to the laser system to enhance the sensitivity of this detector. Specifically, a 1 mW 266 nm laser was replaced with a 43 mW output 266 nm laser and a single fiber optic was replaced with two smaller fiber optic bundles. Table 6.5 shows the detection limits for each detector. The detection limits were estimated by extrapolation from calibration data as 3 times the standard deviation of baseline noise. With the increase in sensitivity, it was believed that the laser excited fluorescence detector might offer much better selectivity through spectral resolution compared to the Agilent detector and thereby allow quantification of the priority PAHs using a reversed phase separation without a cleanup procedure. The results for the standard reference material NIST 1649a separated on the C18 columns before and after cleanup are

Table 6.5: Detection limits for the analysis of the priority PAHs and the amino-PAHs.

Compound	Priority PAHs			
	LC-Agilent	LC-Laser 43 mW	GC-MS	SFC-laser 43 mW
Naphthalene	0.7	2.3	1.1	6.7
Acenaphthene	Not done	1.3	1.2	3.7
Acenaphthylene	Not done	1.3	1.5	3.9
Fluorene	0.1	0.2	0.5	0.6
Phenanthrene	0.4	2	0.4	5.6
Anthracene	0.1	11	0.5	>32
Fluoranthene	0.6	0.4	0.8	1.1
Pyrene	0.5	0.3	0.7	0.8
Benz[*a*]anthracene	0.1	0.2	0.9	0.6
Chrysene	0.1	0.07	0.8	0.2
Benzo[*b*]fluoranthene	0.1	0.3	3.4	0.8
Benzo(*k*]fluoranthene	0.1	0.3	3.9	0.8
Benzo[*a*]pyrene	0.2	0.2	4	0.6
Dibenz[*a,h*]anthracene	0.2	0.3	7	0.9
Benzo[*g,h,i*]perylene	0.1	0.07	7.3	0.2
Indeno[*1,2,3-c,d*]pyrene	0.2	0.4	8.5	1.1

Compound	Amino PAHs		
	LC-Agilent	LC-laser 43 mW	SFC-laser 43 mW
1-aminonaphthalene	0.0018	0.9	2.6
2-aminofluorene	0.0012	1.3	3.8
9-aminoanthracene	0.00009	0.01	0.04
3-aminofluoranthene	not done	0.7	1.9
1-aminopyrene	0.0004	0.07	0.2
6-aminochrysene	not done	1.9	5.4
7-aminobenz[*a*]anthracene	not done	0.8	2.2
6-aminobenzo[*a*]pyrene	not done	0.5	1.3

All Detection Limits in ng/mL

shown in Figure 6.10. The chromatogram of the raw sample indicated that there was polar material that eluted from the column between 0 and 7 minutes. This material was absent from the chromatogram of the cleaned sample. In fact, as the spectra shown in Figure 6.11 suggest, the quantification of phenanthrene was difficult without a cleanup using the DNBS column. Interestingly, the chromatograms in Figure 6.10 for both the raw and cleaned NIST 1649a appear to be very similar beyond 7 minutes. This suggests that the DNBS cleanup procedure offered little benefit for the larger PAHs in the NIST Urban Dust. In fact, this observation was consistent with all of the samples submitted for analysis on the C18 column after DNBS cleanup.

Typically the 266 nm laser was used to excite fluorescence from the sample components because this excitation wavelength was more suited to a broader range of compounds. However, certain compounds such as anthracene and pyrene were more selectively excited using the 325 nm laser. Figure 6.12 shows the Environment Canada diesel exhaust particulate sample B-4 separated on the reversed phase C18 columns after DNBS cleanup using the two excitation wavelengths. The chromatogram that results from the 325 nm laser appears to be less complex than the chromatogram associated with the 266 nm laser. This is due to the selectivity imparted through excitation at 325 nm. Figure 6.13 shows two spectra taken from the chromatogram in Figure 6.12b and two spectra with the same retention times taken from the chromatogram shown in Figure 6.12c. The spectra shown in this figure suggest that the 266 nm laser would provide better excitation for chrysene and benzo[*a*]pyrene. In fact, the spectra that resulted from the 325 nm laser excitation appear to

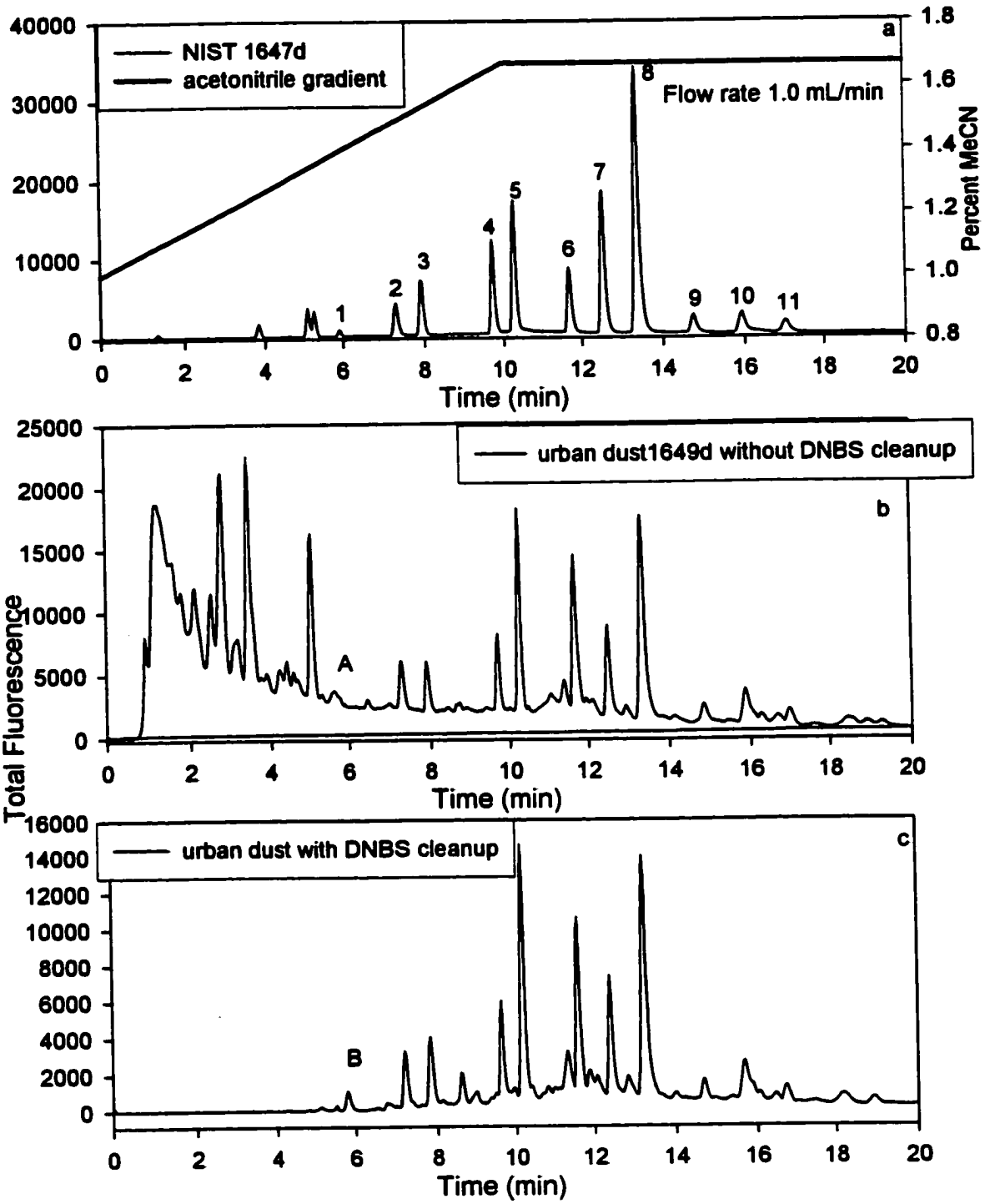

Figure 6.10a-c: Chromatograms of NIST 1649d with and without the DNBS cleanup separation and NIST PAH standard separated using a reversed phase C18 column and laser excited fluorescence detection with 266 nm laser. The chromatographic conditions are listed in the figure.

Peak Identification: 1 phenanthrene, 2 fluoranthene, 3 pyrene, 4 benz[*a*]anthracene, 5 chrysene, 6 benzo[*b*]fluoranthene, 7 benzo[*k*]fluoranthene, 8 benzo[*a*]pyrene, 9 dibenz[*a,h*]anthracene, 10 benzo[*g,h,i*]perrylene, 11 indeno[*1,2,3-c,d*]pyrene

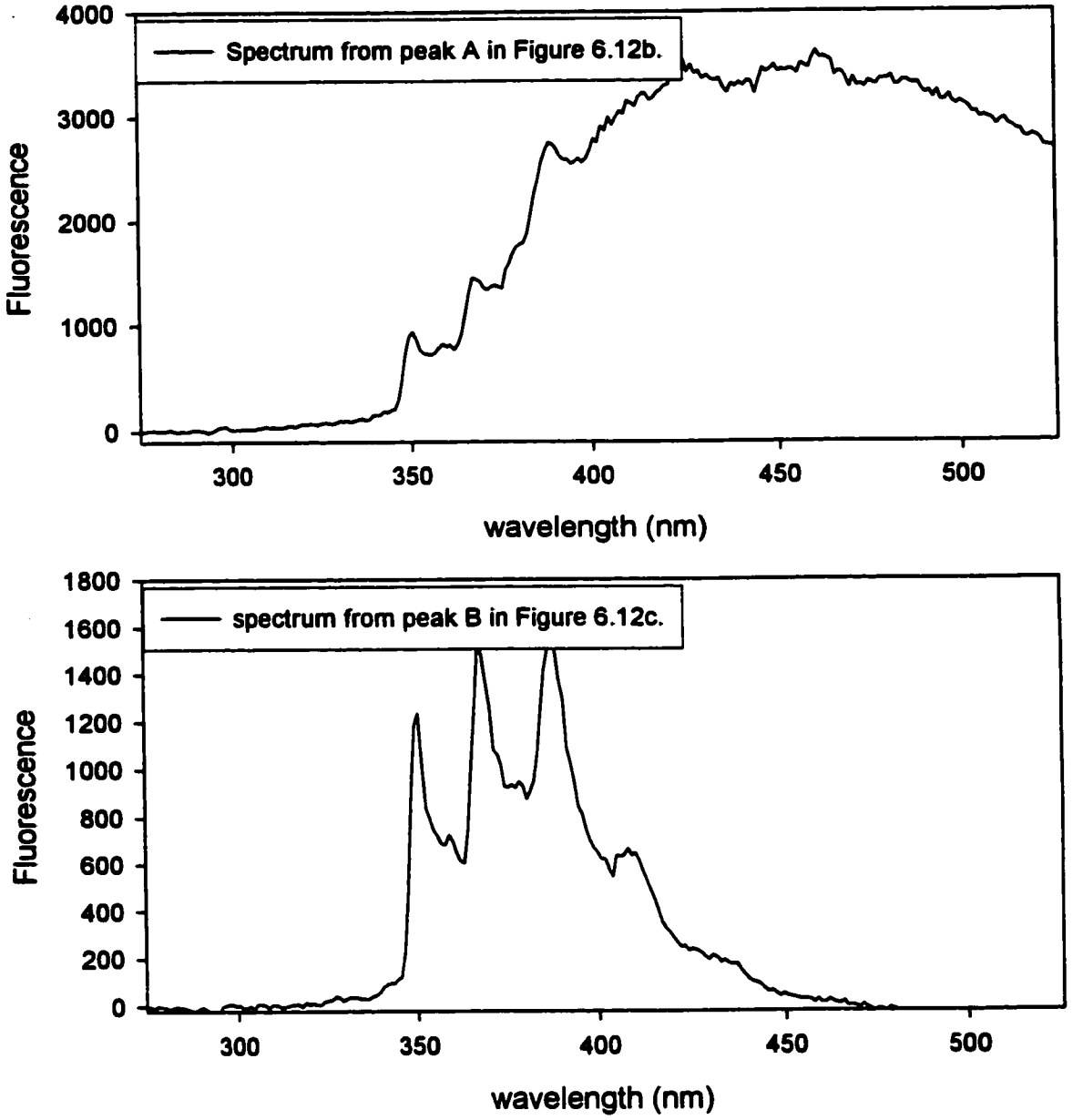

Figure 6.11: Two spectra corresponding to selected peaks in Figure 6.10. Upper chromatogram results from an urban dust (1649d) sample whereas the lower spectrum is for the same retention time in a chromatogram of a dust sample that was fractionated using the DNBS separation.

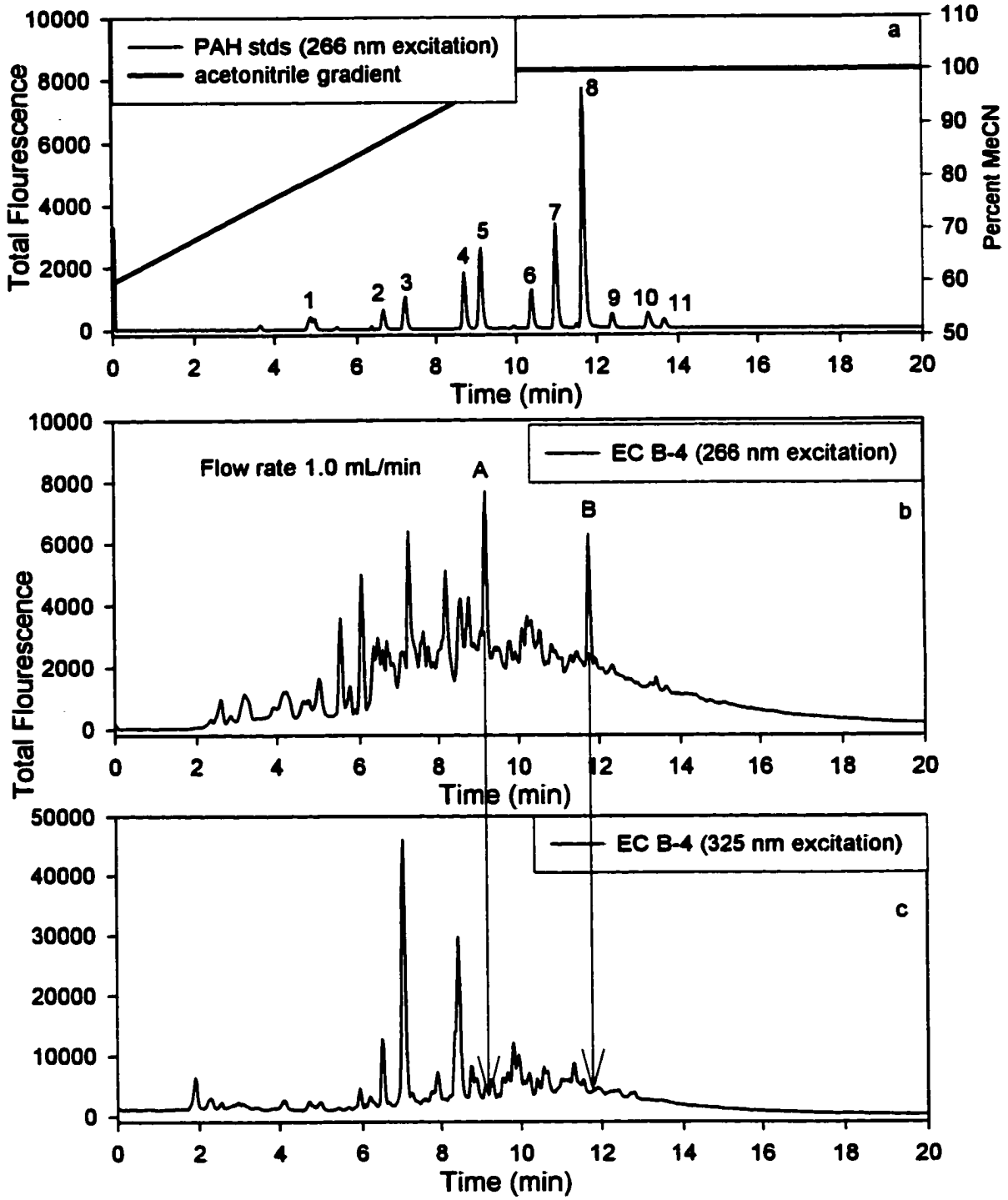

Figure 6.12a-c: Chromatograms of Environment Canada diesel exhaust filter B-4 after DNBS cleanup separation and NIST PAH standard separated using a reversed phase C18 column and laser excited fluorescence detection. The chromatographic conditions listed in the figure.

Peak Identification: 1 phenanthrene, 2 fluoranthene, 3 pyrene, 4 benz[*a*]anthracene, 5 chrysene, 6 benzo[*b*]fluoranthene, 7 benzo[*k*]fluoranthene, 8 benzo[*a*]pyrene, 9 dibenz[*a,h*]anthracene, 10 benzo[*g,h,i*]perrylene, 11 indeno[*1,2,3-c,d*]pyrene

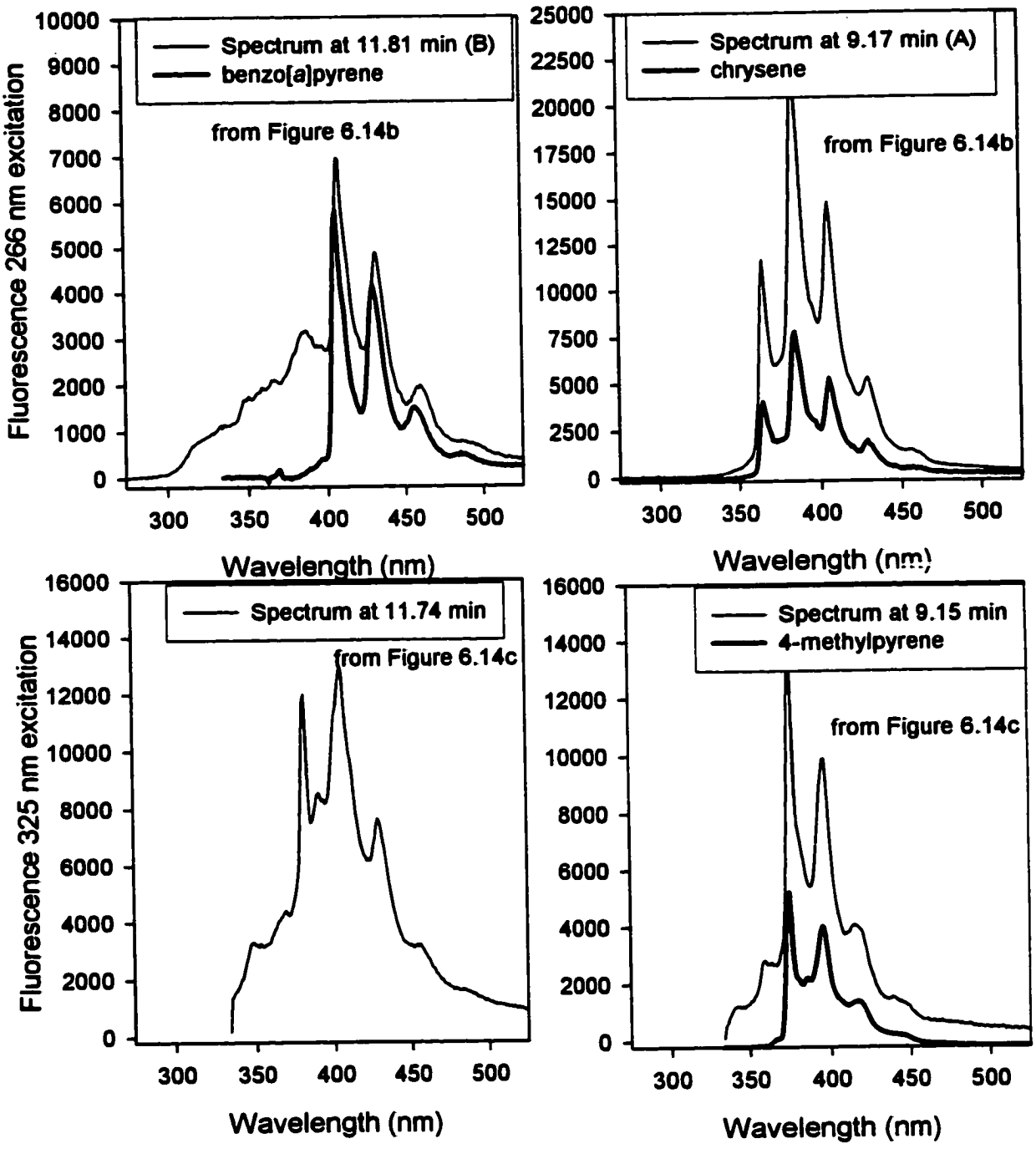

Figure 6.13: Selected spectra from two chromatograms shown in Figure 6.12. The upper left and right spectra result from fluorescence due to excitation with a 266 nm laser. The lower left and right spectra use a 325 nm laser for excitation.

give evidence for an alkyl substituted pyrene co-eluting with chrysene. The major peaks in the chromatogram shown in Figure 6.12c showed spectra suggestive of pyrene and alkylated pyrenes. However, the information presented using the 266 nm laser chromatogram also suggested that phenanthrene and chrysene with various alkyl substituents were present.

There is an interesting comparison to be drawn between the 266 nm chromatograms present in Figure 6.10c for the urban dust and Figure 6.12b with the Environment Canada diesel exhaust sample. Primarily, the reversed phase chromatogram of the diesel exhaust extract seems much more complex than the urban dust with a greater number of partially resolved peaks. Most of the peaks appear at retention times prior to 12 minutes for the B-4 filter suggesting that high molecular weight priority PAHs were present at lower levels in the B-4 diesel exhaust sample than in the urban dust.

Figure 6.14 introduces the reversed phase chromatograms of another Environment Canada diesel exhaust filter E-155. Qualitatively, the chromatograms for this sample look similar to that of the B-4 filter. Each chromatogram in this figure results from the analysis of one half of the filter. In this case each filter half was extracted and processed individually. The filter was processed in this manner to investigate the possibility of dividing the filter paper and analyzing partial filters. This was of interest since the Environment Canada diesel exhaust filter collections were both expensive to purchase and limited in availability. An initial inspection of the two chromatograms in Figure 6.14 suggests that the deposition of particles as well as particle composition appears to be relatively homogenous. A quantitative analysis of each half of the E-155 filter paper was performed to characterize the homogeneity of the deposition of PAHs upon the filter. The results for several selected PAHs are listed in Table 6.6. The data in this table suggest that there was minimal variation between the halves of the

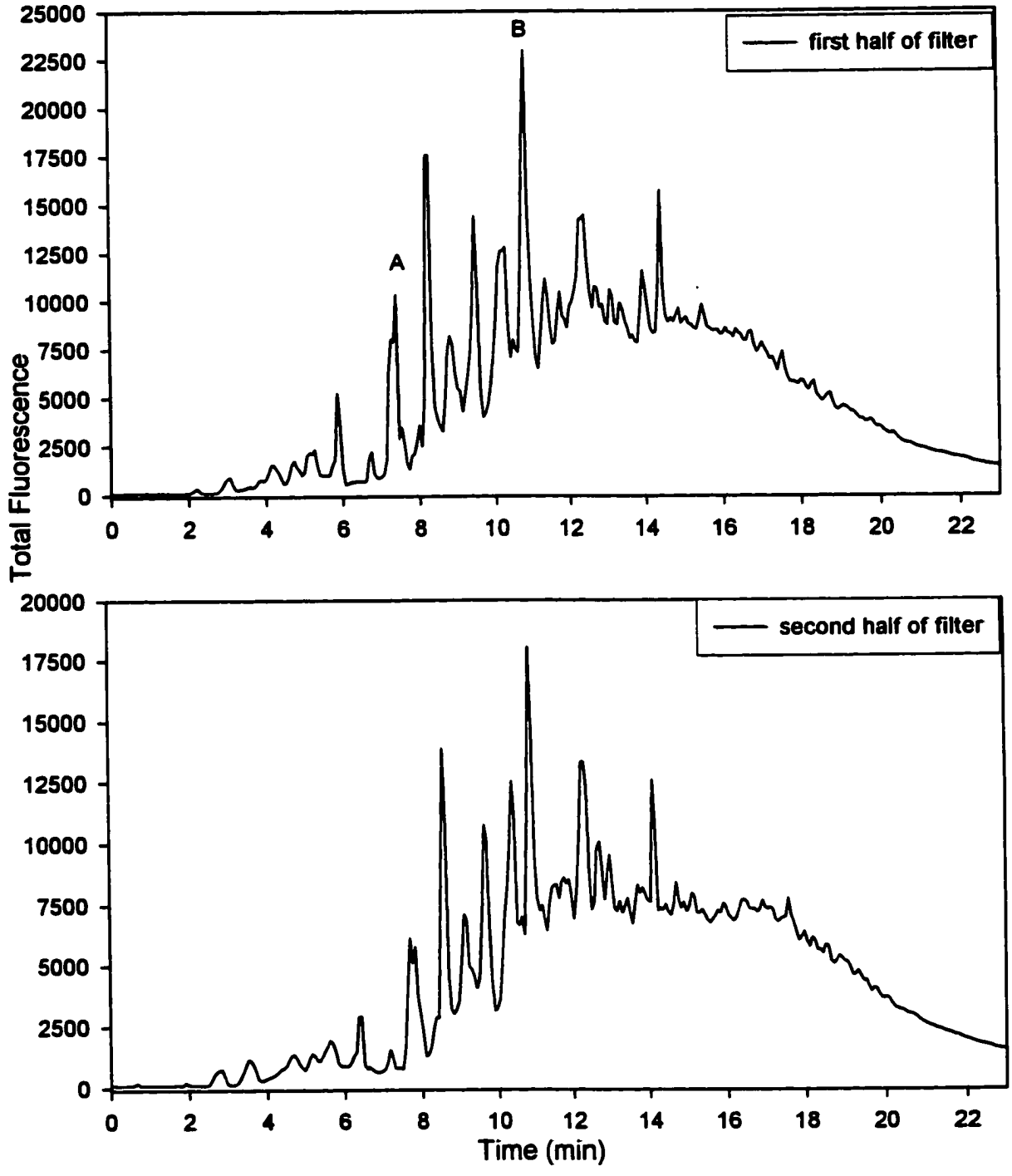

Figure 6.14: Two chromatograms of an Environment Canada diesel exhaust filter E-155 after DNBS cleanup separation. Each chromatogram results from the analysis of a separate half of the filter. Chromatographic conditions are listed in Figure 6.12.

Table 6.6: Total PAHs extracted from Environment Canada Filter E-155

Compound	First Half Mass ug	Second Half Mass ug	Percent Relative Difference
Phenanthrene	0.0607	0.0584	10
Pyrene	0.251	0.309	15
Chrysene	0.0607	0.0739	13
Benzo[*a*]pyrene	0.0170	0.0213	16

filter. The variation associated with pyrene and benzo(*a*)pyrene appeared much larger than for phenanthrene. However, the relative instrumental precision for the analysis of the PAH components was on the order of 6-10 percent. This suggests that there was most likely little difference in composition between each half of the filter.

Accurate quantification requires reproducible chromatography. Initial studies with replicate standard injections on the reversed phase C18 columns found that there was a large variability in the peak shapes of several of the larger PAHs such as benzo[*a*]pyrene. However, temperature control was not used for the initial separations with these columns. Figure 6.15 shows the PAH standard NIST 1647d separated at 15, 25, and 40 C. The chromatograms show a change in peak height for benzo[*a*]pyrene as the solvent strength decreases. This is not the only effect. The number of plates calculated for benzo[*a*]pyrene triples from 30000 plates at 15 C to 109000 plates at 25 C. This is a dramatic change in the column efficiency. For example, increasing column efficiency leads to narrower peaks and increased peak height. A closer look at the elution of peaks 12, 13, and 14 for any two

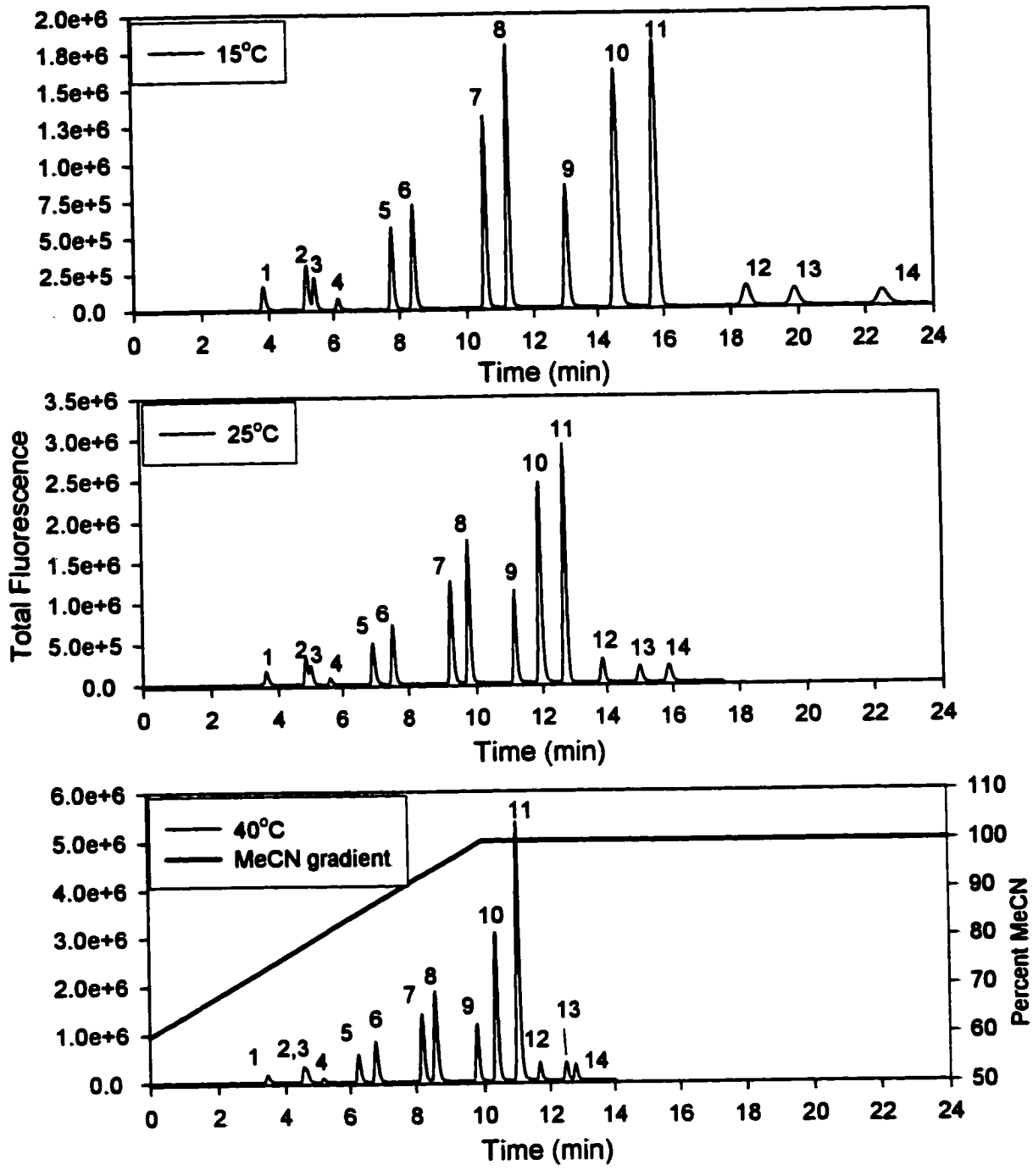

Figure 6.15: Reversed Phase C18 chromatograms of the standard NIST 1647d performed at 15°C, 25°C, and 40 °C. Chromatographic conditions shown in the figure.

Peak Identification: 1 naphthalene, 2 acenaphthene, 3 acenaphthylene, fluorene, 4 phenanthrene, 5 fluoranthene, 6 pyrene, 7 benz[*a*]anthracene, 8 chrysene, 9 benzo[*b*]fluoranthene, 10 benzo[*k*]fluoranthene, 11 benzo[*a*]pyrene, 12 dibenz[*a,h*]anthracene, 13 benzo[*g,h,i*]perylene, 14 indeno[*1,2,3-c,d*]pyrene

temperatures suggests a change in selectivity for these compounds. One possible explanation might be that the temperature affects the ordering of the stationary phase and therefore alters the retention behavior of the column. Once temperature control was set at 25 C the separation was found to be reproducible. Using the background subtracted intensities of the spectra (described in Chapter 3), quantification was possible in Urban Dust (SRM 1649a) and diesel exhaust particulate (SRM 1650a) extracts for each of the priority PAHs except for naphthalene, acenaphthene, acenaphthylene, fluorene, phenanthrene, anthracene, and dibenz[*a,h*]anthracene. Phenanthrene and anthracene could be quantified with a DNBS cleanup. Anthracene was not detected well using the 266 nm laser to excite molecular fluorescence. However, the 325 nm laser provided enough sensitivity to allow quantification in the Urban Dust particulate extracts. Similar results were observed with the extracts from the Environment Canada diesel exhaust filter extracts. However, the analysis was less successful with the quantification of larger PAHs such as benzo[*g,h,i*]perylene and indeno[*1,2,3-c,d*]pyrene. This was most likely due to low concentrations of these components in the samples as well as the presence of interferences.

6.3.4 Analysis of the Priority PAHs using GC-MS

Quantitative methods that use a mass spectrometer as the detector require additional care during analysis compared to methods that utilize typical spectrophotometric detectors such as a diode array. For example, changes in the MS source due to compound deposition upon the electronic lenses will alter the focus of the ions moving through to the mass analyzer. In addition, variations in the number of electrons that leave the ionizing filament

will create differences in the number of molecules of analyte that are ionized. Each of these variations could have the effect of altering the response factor for the analyte and decreasing the accuracy of the analysis. For this reason, most quantitative work with a mass spectrometer involves the use of at least one internal standard. In addition, significant error can be associated with manual injections onto a capillary GC. In order to characterize the precision of the GC-MS analysis, a NIST 1647d PAH standard was spiked with the following deuterated compounds, d_{10} acenaphthylene, d_{10} phenanthrene, d_{12} chrysene, and d_{12} perylene. Ratios of the areas for each of the deuterated PAHs to the priority PAHs in close proximity were calculated according to the following relationship, where 1 and 2 represent different runs,

$$\text{Ratio} = (\text{area1}_{is}/\text{area2}_{is})/(\text{area1}_{PAH}/\text{area2}_{PAH}) \qquad [6\text{-}1]$$

Ratios that have a value close to unity would suggest that biases such as instrument response and injection volume were accurately corrected using the appropriate internal standard. Table 6.7 shows these ratios for selected PAHs resulting from two consecutive injections onto the GC. The internal standard for each PAH was selected by choosing an internal standard that eluted as close as possible to the analyte. For example, using deuterated chrysene (t_r=15.12 min.) and chrysene (t_r=15.18 min.) provided a good correction(ratio=1.05) due to their similar retention times. On the other hand, the use of deuterated acenaphthene (t_r=8.02 min.) with chrysene results in much poorer ratios (1.66) that would introduce significant error into the analysis. Good agreement was achieved as long as the priority PAH was within 2 minutes in retention to the deuterated internal standard. Outside of this interval poorer correction

Table 6.7 Calculated correction ratios between multiple injections of the SRM 1649d spiked with deuterated internal standards.

Compound	Peak Area Run 1	Peak Area Run 2	Correction Ratio
Naphthalene	32115	30212	0.95 (with #1)
Phenanthrene	3105	2662	0.99 (with #2)
Pyrene	5357	4473	1.02 (with #2)
Chrysene	614	902	1.05 (with #3) 1.66 (with #1)
Benzo[*a*]pyrene	791	847	0.96 (with #4)
Benzo[*g,h,i*]perylene	294	385	0.78 (with #4)
Indeno[*1,2,3-c,d*]pyrene	412	578	0.73 (with #4)
#1 d_{10} acenaphthene	863	768	
#2 d_{10} phenanthrene	1084	919	
#3 d_{12} chrysene	491	507	
#4 d_{12} perylene	269	276	

resulted. As the data in this table suggests poor correction was observed for benzo[*g,h,i*]perylene (t_r=21.80 min.), and indeno[*1,2,3-c,d*]pyrene (t_r=22.20 min.). This was because the retention time of the closest deuterated compound (d_{12} perylene t_r=19.51 min.) was eluted too early to permit accurate correction. The addition of deuterated dibenz[*a,h*]anthracene was found to solve this difficulty and provide correction for both of these compounds. This underscores the need for multiple internal standards because the

variation suggests that the response of the mass spectrometer was variable during the chromatogram.

As a complementary technique to the reversed-phase, laser-excited fluorescence analysis of the priority PAHs, capillary GC/MS was investigated. Initial studies were performed to test the requirement for a cleanup procedure. Experiments were designed using the NIST urban dust standard reference material with triplicate analysis of three extractions using the GC-MS. A portion of each extraction was cleaned using the DNBS column. The remainder was analyzed directly using the GC-MS in single ion mode. Figure 6.16 shows two chromatograms of the urban dust, with and without a cleanup. The raw dust sample showed lower signal intensities but it appeared to be similar in complexity to the cleaned sample with the exception of several additional peaks between 9 and 13 minutes. However, a comparison of the NIST certified concentrations of PAHs to the values obtained from the analysis suggested that the raw sample produced consistently high (>100%) values for phenanthrene, anthracene, pyrene, and chrysene as indicated by the values in Table 6.8. The erroneous values most likely resulted from fragment ions (with the correct unit mass) from compounds co-eluting with the PAH of interest. The Quattro mass spectrometer did not have the capability to allow more accurate mass detection. The values for the larger PAHs were similar for the raw sample and the cleaned sample with the exception of chrysene. However, the baseline noise was reduced for the cleaned sample compared to the raw extract. This improved the detection limit for the larger PAHs and provided better signals for quantification. This was particularly important because a lower sensitivity was observed for these compounds. Similarly, accurate quantification of the NIST SRM 1650a was not possible without a cleanup of the raw extract on the DNBS column. As a result all samples

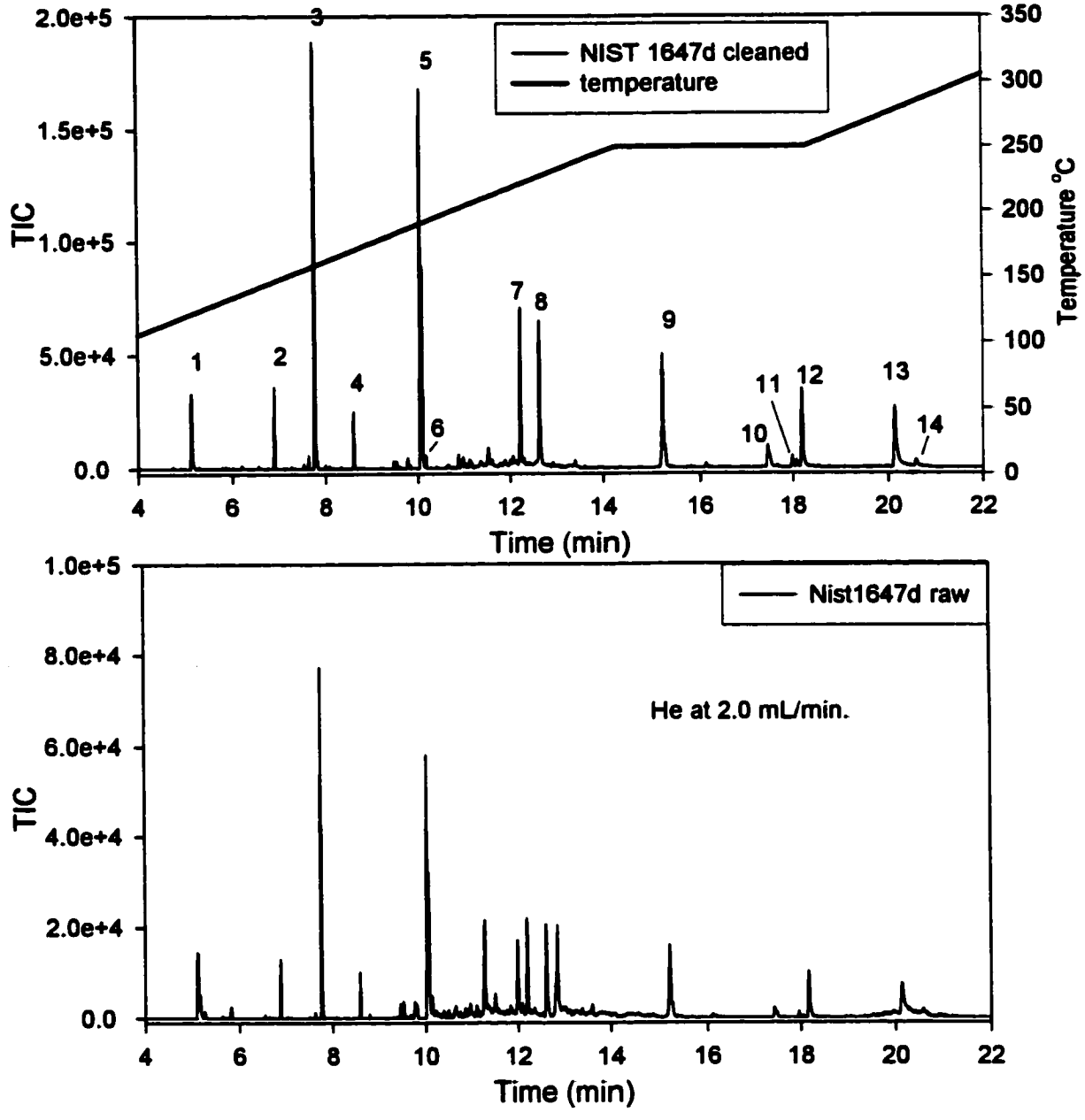

Figure 6.16: GC-MS chromatograms of standard reference material NIST1647d before and after DNBS separation cleanup. Mass spectrometer operated in SIR mode. Two microliter injections were performed.

Peak Identification: 1 naphthalene, 2 acenaphthene, 3 acenaphthylene, d_8-acenaphthylene, 4 fluorene, 5 phenathrene, d_{10}-phenathrene, 6 anthracene, 7 fluoranthene, 8 pyrene, 9 benz[*a*]anthracene, d_{12}-chrysene, chrysene, 10 benzo[*b*]fluoranthene, benzo[*k*]fluoranthene, 11 benzo[*a*]pyrene, 12 d_{12}-perylene, 13 d_{14}-dibenz[*a,h*]anthracene, 14 dibenz[*a,h*]anthracene, benzo[*g,h,i*]perylene, indeno[*1,2,3-c,d*]pyrene

Table 6.8: Comparison of the values from this work to NIST certified values of the Urban Dust SRM 1649a using GC-MS. The values in the table result from the direct analysis of the raw extracts without prior sample cleanup. Dichloromethane was used as the extraction solvent (PFE 100°C).

Compound	DCM NIST1649a Percent Recovery
Phenanthrene	114
Anthracene	124
Fluoranthene	105
Pyrene	125
Benz(*a*)anthracence	89
Chrysene	174
Benzo(*b&k*)fluoranthene	113
Benzo(*a*)pyrene	93
Dibenz(*a,h*)anthracence	256
Benzo(*g,h,i*)perylene	88
Indeno(*1,2,3-c,d*)pyrene	91

were subjected to a cleanup separation using the DNBS column before analysis on the GC. The difficulty observed with the quantification of chrysene was still present after the cleanup procedure. The problem with chrysene was believed to arise as a result of the co-elution of this compound with triphenylene. Figure 6.17 shows the standards chrysene and triphenylene injected separately on the GC. The co-elution of these compounds is evident. Furthermore, the mass spectrometer was not able to discriminate between these compounds because they

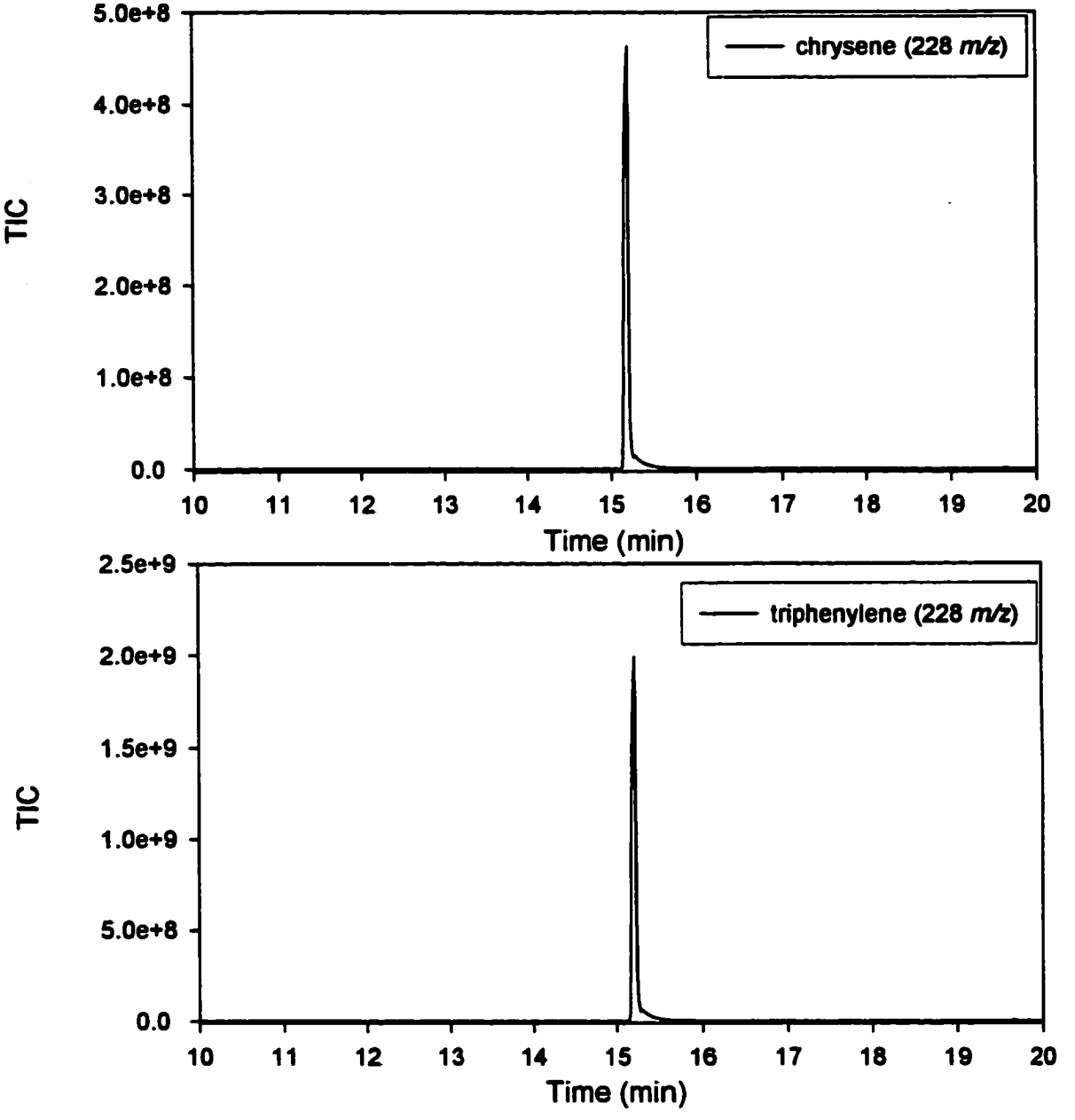

Figure 6.17: GC-MS chromatograms of chrysene and triphenylene
The mass spectrometer was operated in SIR mode for each run.
The chromatographic conditions are given in Figure 6.16.

each have the same molar mass. Accurate quantification of chrysene was not possible using GC-MS. Figure 6.18 shows a GC-MS chromatogram of an Environment Canada diesel exhaust filter E-175 with a PAH standard mixture as well as saturated hydrocarbon standards. The chromatogram of the filter sample suggested that many compounds were present on the particulates. The chromatogram in this figure results from data collection with the mass spectrometer in scan mode (40:400 amu) that enabled the mass spectrum of each peak to be analyzed. A comparison of the chromatogram for the saturated standard mixture and the filter sample suggests the possibility of saturates on the particulates. This is further suggested with the mass spectra shown in Figure 6.19 for the peak at 20.73 minutes and the standard spectra of triacontane. The mass spectrum does not provide unambiguous evidence for the presence of triacontane since the mass spectra of such large saturated compounds are similar as indicated by the mass spectrum of dodecane. Instead, the general presence of saturated compounds is suggested. The collection of saturated compounds may result from inefficient combustion inside the diesel engine. The unburned fuel may escape in the diesel exhaust where it adsorbs onto particulate matter and is subsequently collected on the filter.

The priority PAHs with masses greater than chrysene were either present at extremely low levels or below the detection limit in the Environment Canada diesel exhaust filter extracts. Detection of the larger PAHs may have been made more difficult due to the low sensitivity for these compounds on the GC-MS system. Table 6.5 listed the detection limits for the GC-MS separation as well as the reversed phase fluorescence separation. Although the mass spectrometer was found to have sensitivity comparable to fluorescence detection for

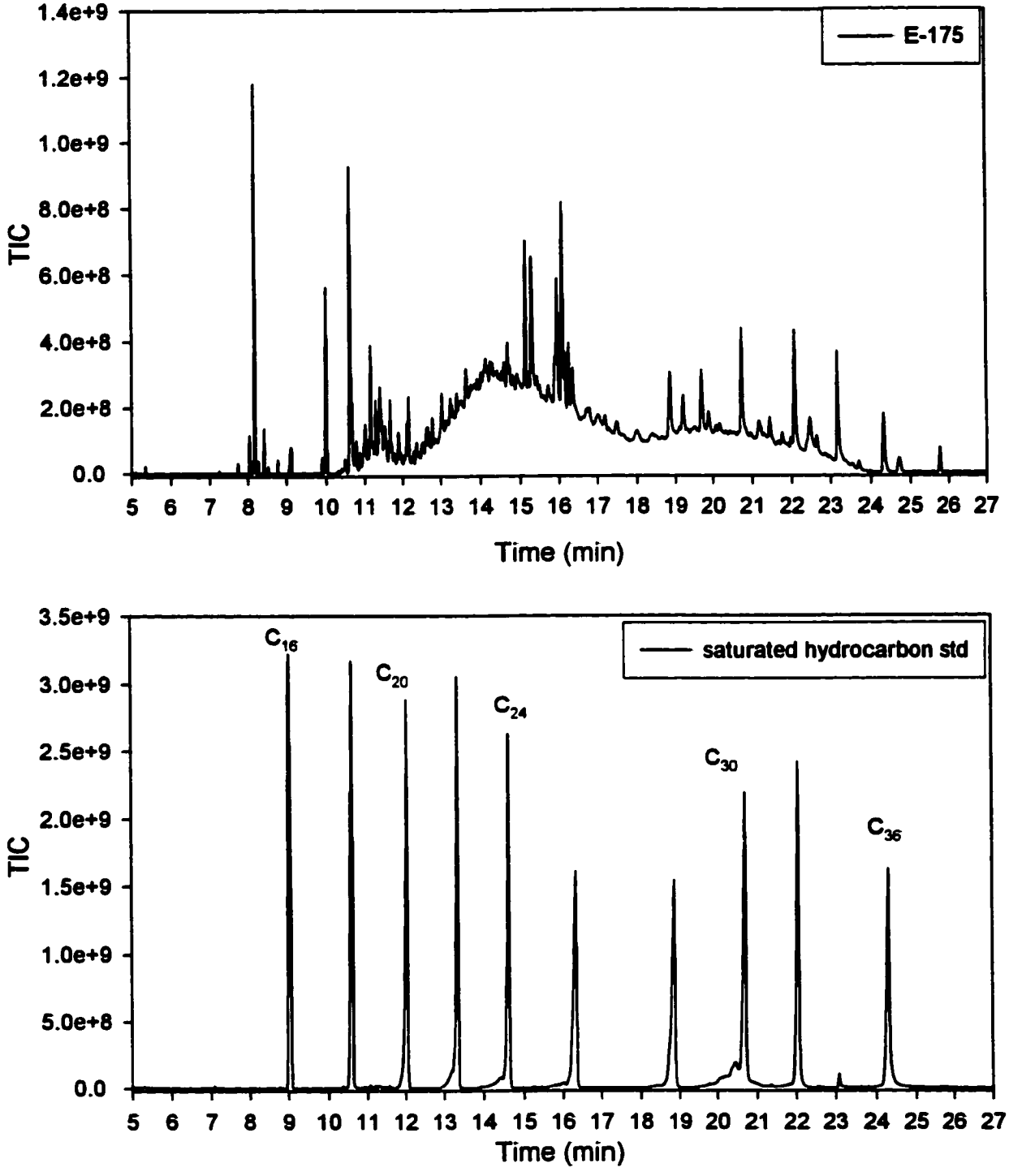

Figure 6.18: GC-MS separation of environment Canada filter E-175 with standards. The chromatographic conditions are shown in Figure 6.16.

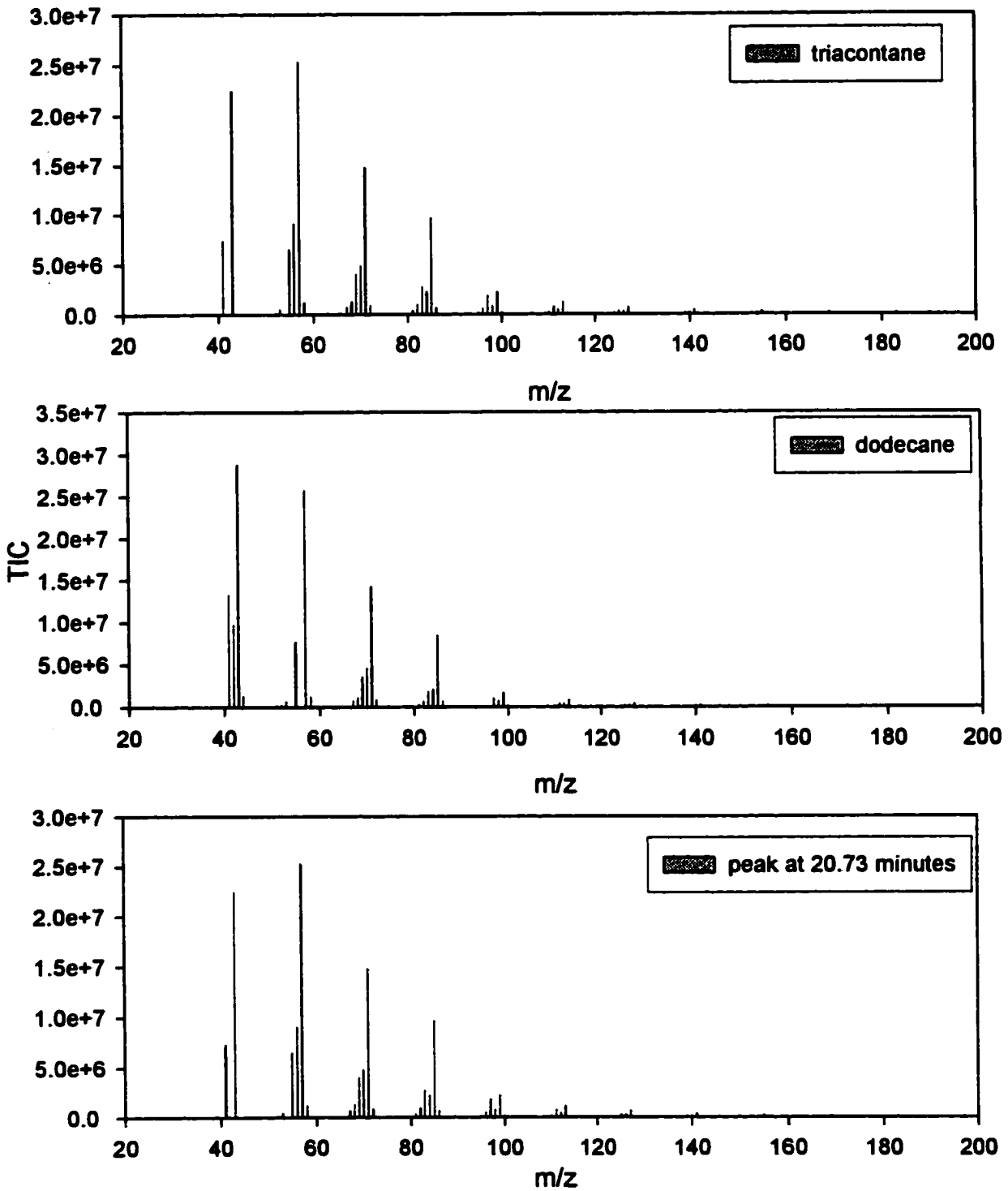

Figure 6.19: The mass spectrum from a peak at 20.73 minutes of GC-MS separation of E-175 filter with mass spectra of triacontane and dodecane. The chromatograms from which each spectrum originates are shown in Figure 6.18.

the smaller PAHs, a loss in sensitivity was observed for the larger PAHs.

In real samples, GC-MS was more successful than LC-fluorescence for the determination of both light and heavy PAHs in the diesel exhaust particulates. LC-fluorescence was less reliable than GC-MS for the quantification of compounds above chrysene due to background interferences present in the reversed phase chromatogram even though detection limits were better than those observed for standard compounds with the GC-MS. Accurate quantification of chrysene was not possible using the GC-MS due to co-elution with triphenylene.

6.3.5 Analysis of the Priority PAHs using SFC and Laser Excited Fluorescence Detection.

Chapter 3 discussed the possibility of using the Keystone aminopropyl column as an SFC separation to analyze and quantify the priority PAHs extracted from diesel exhaust and air particulate samples. This section will examine the application of this separation to several real samples. The samples studied were a diesel combustion solids sample provided by Syncrude Canada and an air particulate sample collected using a high volume sampler and Environment Canada diesel exhaust particulate. Figures 6.20, Figure 6.21, and Figure 6.22 show the chromatograms that result for each of the samples, respectively. The three chromatograms were presented in this manner to illustrate the differences between samples.

The chromatogram in Figure 6.20 for the Syncrude Canada sample appears to be less complex than either the air particulate sample or the diesel exhaust filter E-175. The fact that the chromatograms for E-175 and the Syncrude diesel particulates were dissimilar may reflect differences in the collection processes for each sample. The Environment Canada filter was

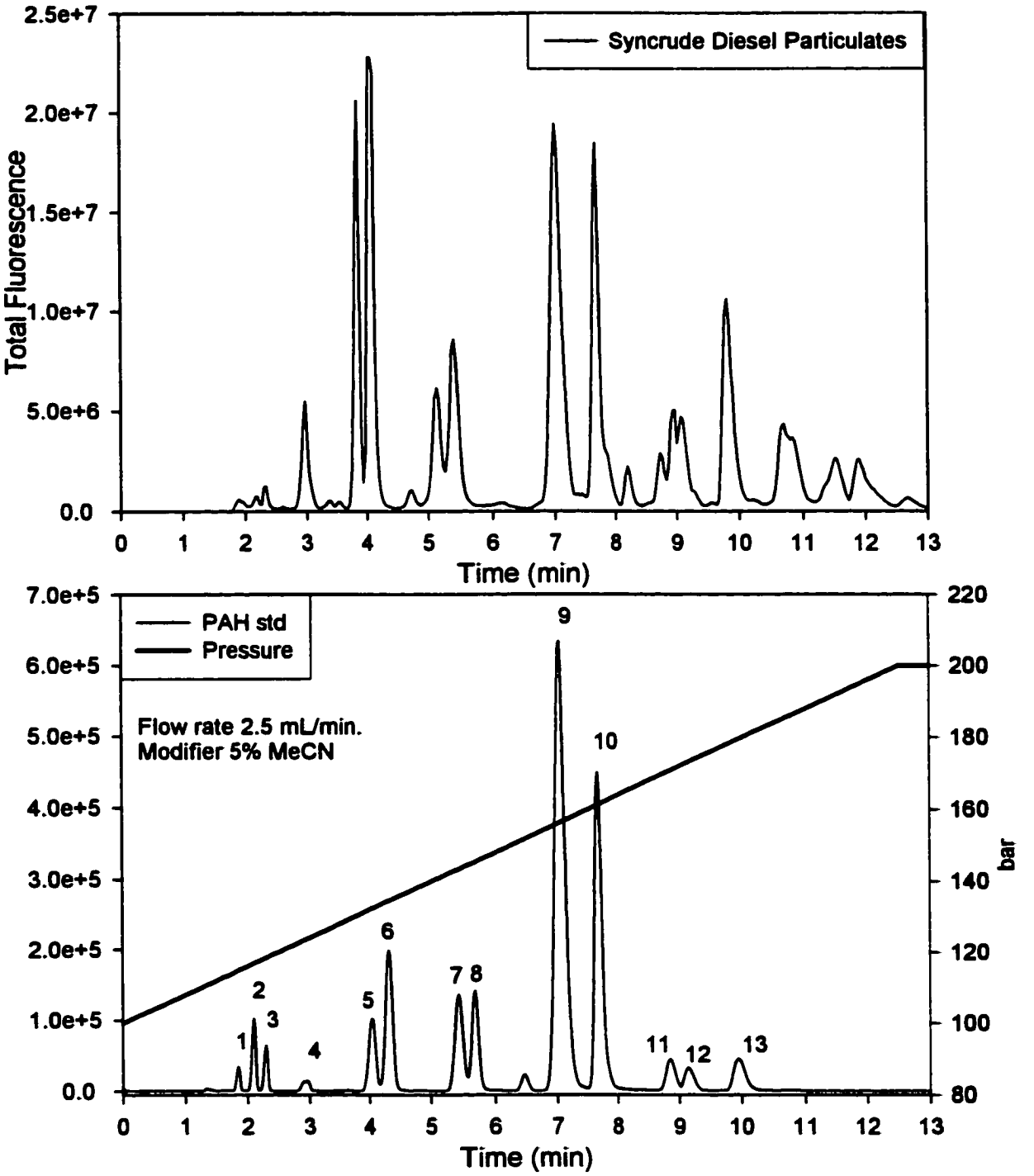

Figure 6.20: SFC of Syncrude diesel combustion solids separated using the Keystone aminopropyl column. The compounds were detected using the laser excited fluorescence detector with the 266 nm laser.

Peak Identification: 1 naphthalene, 2 acenaphthene, 3 acenaphthylene, fluorene, 4 phenanthrene, 5 fluoranthene, 6 pyrene, 7 benz[*a*]anthracene, 8 chrysene, 9 benz[*b*]fluoranthene, benzo[*k*]fluoranthene, 10 benzo[a]pyrene, 11dibenz[*a,h*]-anthracene, 12 indeno[*1,2,3-c,d*]pyrene, 13 benzo[*g,h,i*]perylene

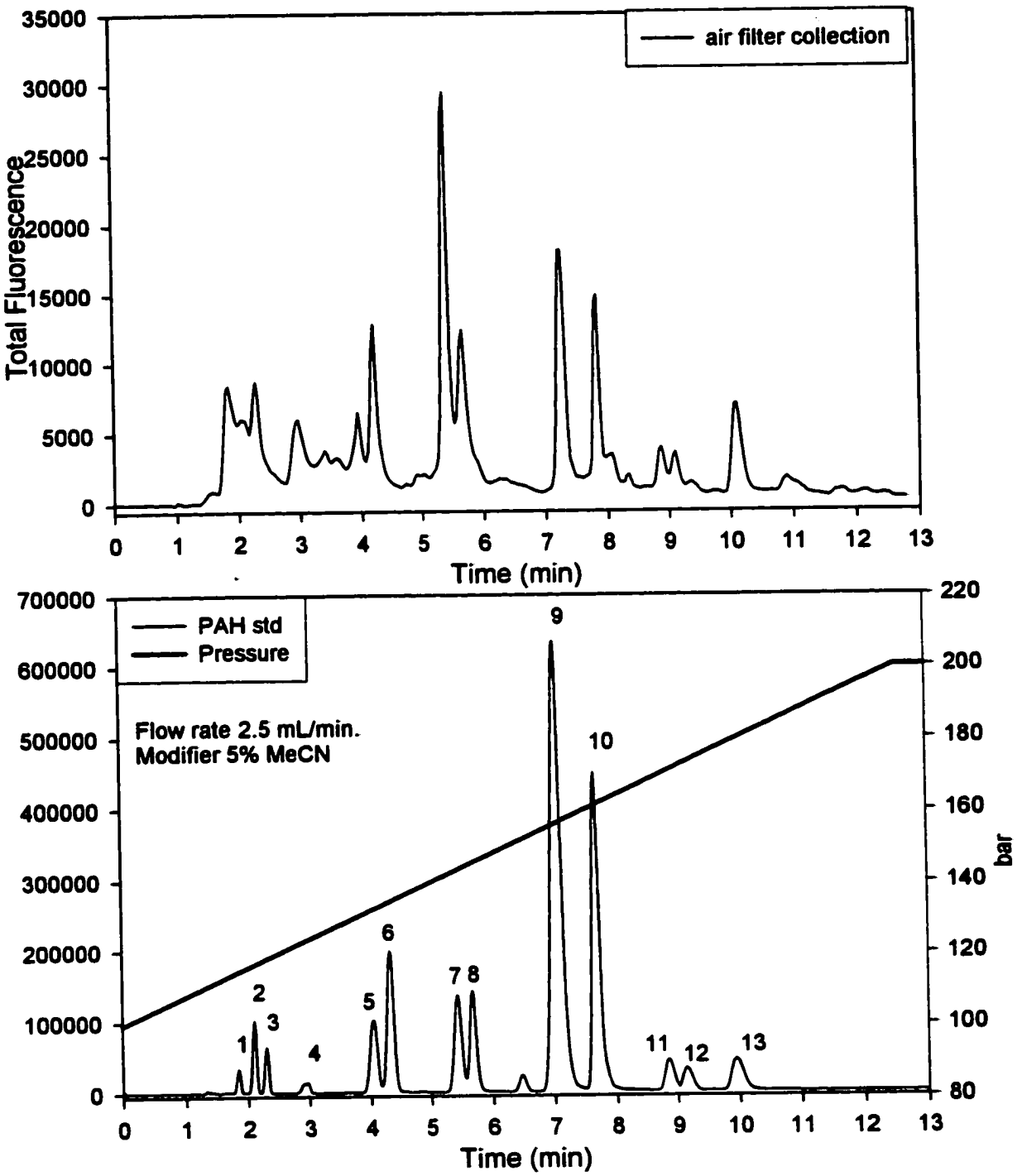

Figure 6.21: SFC of an air particulate filter separated using the Keystone aminopropyl column. The compounds were detected using the laser excited fluorescence detector with the 266 nm laser.

Peak Identification: 1 naphthalene, 2 acenaphthene, 3 acenaphthylene, fluorene, 4 phenanthrene, 5 fluoranthene, 6 pyrene, 7 benz[*a*]anthracene, 8 chrysene, 9 benzo[*b*]fluoranthene, benzo[*k*]fluoranthene, 10 benzo[a]pyrene, 11dibenz[*a,h*]-anthracene, 12 indeno[*1,2,3-c,d*]pyrene, 13 benzo[*g,h,i*]perylene

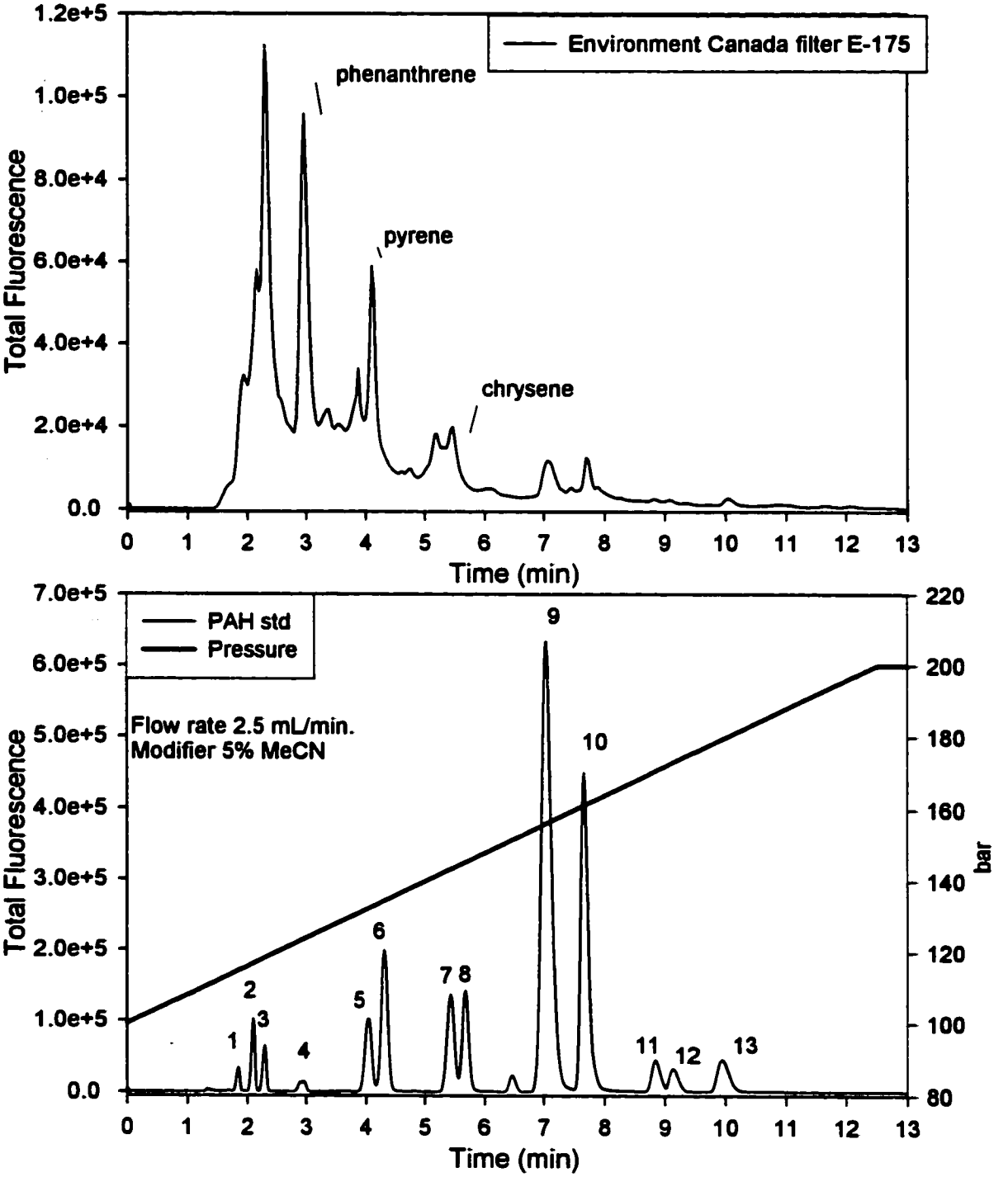

Figure 6.22: SFC ofan Environment Canada filter E-175 separated using the Keystone aminopropyl column. Compounds were detected using the laser excited fluorescence detector with the 266 nm laser.

Peak Identification: 1 naphthalene, 2 acenaphthene, 3 acenaphthylene, fluorene, 4 phenanthrene, 5 fluoranthene, 6 pyrene, 7 benz[*a*]anthracene, 8 chrysene, 9 benz[*b*]fluoranthene, benzo[*k*]fluoranthene, 10 benzo[*a*]pyrene, 11dibenz[*a,h*]-anthracene, 12 indeno[*1,2,3-c,d*]pyrene, 13 benzo[*g,h,i*]perylene

collected from the exhaust pipe of a bus, stored, and then sent directly for analysis. On the other hand, the Syncrude particulates were allowed to aggregate for several months and then scraped from the exhaust pipe. As a result the Environment Canada sample contained a much greater level of naphthalene, fluorene, phenanthrene and pyrene as well as their corresponding methyl substituted components. By contrast, the Syncrude particulates displayed an increase in the non-substituted PAHs as well as the larger PAHs. The chromatogram of the air particulates in Figure 6.21 was intermediate between the two diesel exhaust samples. Quantification of the priority PAHs in both the air and Syncrude diesel particulates was possible. The Environment Canada diesel exhaust particulate extracts contained elevated levels of alkylated components that presented additional difficulty. For example, the concentration calculated for phenanthrene using this method was almost double the concentration calculated using either the reversed phase C18 separation or the GC-MS separation for the filter E-175. The difficulty arises due to the lack of resolution of this stationary phase to separate a methyl-substituted phenanthrene from phenanthrene. Furthermore, the similarity of the fluorescence spectra for these two compounds would make spectral resolution difficult particularly when superimposed upon each other.

Smaller collection regions using the DNBS cleanup may allow phenanthrene to be fractionated from its methyl substituents since the DNBS phase was capable of resolving these compounds. This may allow the subsequent quantification of phenanthrene using the aminopropyl SFC separation but provides little benefit compared to the reversed phase fluorescence analysis on the C18 columns. For example, Figure 6.23 compares the chromatographic ability of the aminopropyl SFC separation to the reversed phase C18 separation for an air particulate sample collected near a busy intersection. The SFC

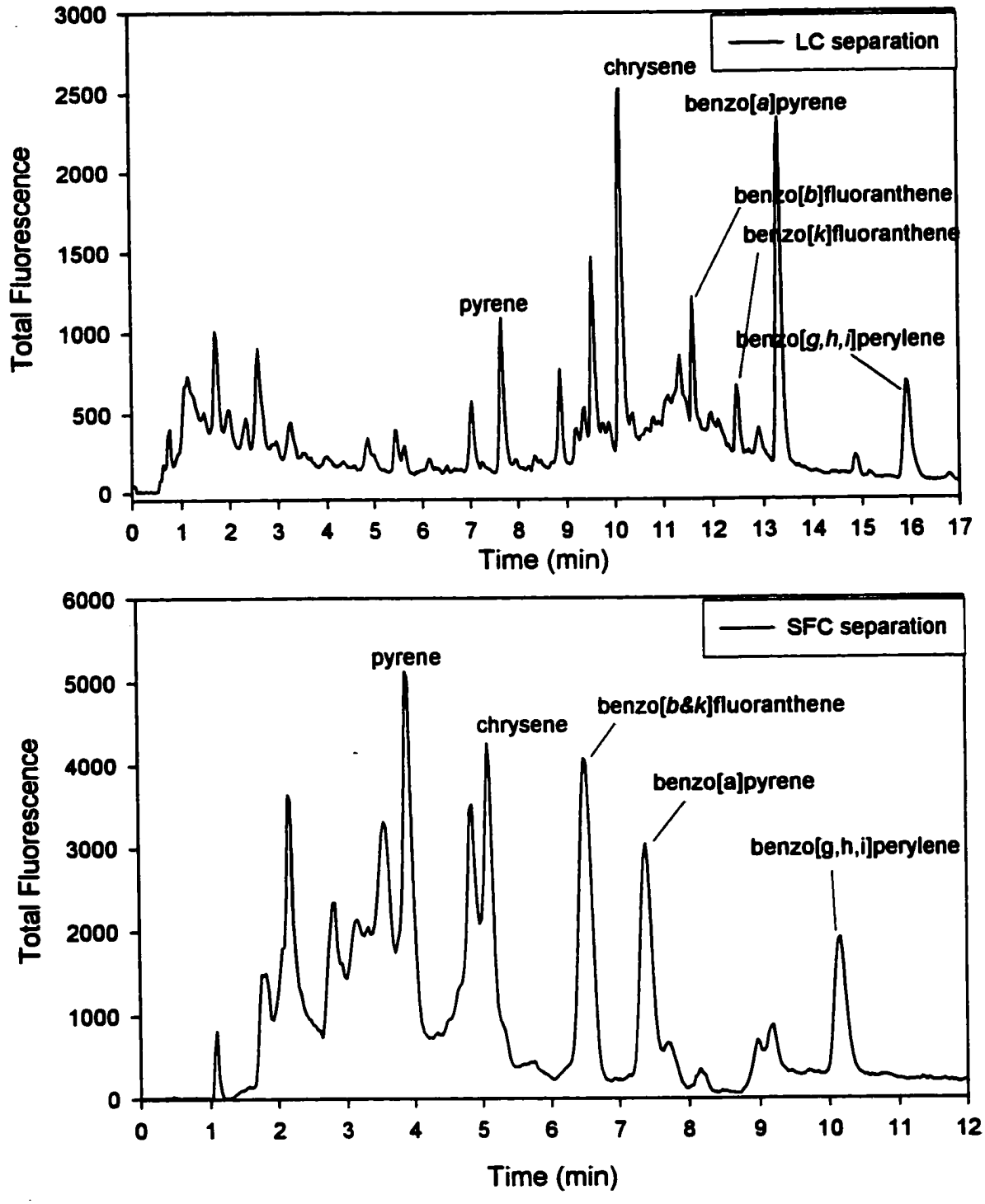

Figure 6.23: Upper chromatogram is of an air particulate sample separated using a reversed phase C18 column while the lower chromatogram results from a SFC separation with an aminopropyl column. Both separations used fluorescence detection with excitation from the 266 nm laser.

separation displays a poorer ability to resolve all of the priority PAHs compared to the C18 column. In addition, a three-fold decrease in sensitivity was observed with the high-pressure cell required to withstand the pressures associated with SFC conditions.

6.3.6 Analytical Separation of Aromatic Amines using a reversed Phase C18 Column and Fluorescence Detection

Two methods were examined for the analysis of nitro-PAHs present in diesel exhaust and air particulate samples. The first method used a reversed phase C18 separation whereas the second method was a SFC separation. The SFC separation will be discussed in the next section. Since the nitro-PAHs were present at trace concentrations a more sensitive detector than a typical diode array was required. Primarily, fluorescence detection was used for aromatic amines. Nitro-PAHs are weakly fluorescent but the corresponding aromatic amines fluoresce strongly. The reduction of the nitro-PAHs was done using a column packed with zinc powder and an acetate buffer set to pH 4.7. Copper(II) chloride was spiked into the buffer to increase the reduction efficiency.

Since the reduction column could be placed on-line, two possible scenarios were available for the analysis, pre- and post-column reduction of the nitro-compounds to the amines. In the first case, the nitro-PAHs would be reduced to the corresponding amino-PAHs and then separated as the amines on the C18 column. This required that the mobile phase be suitably buffered to maintain the proper pH on the column. In the second case, since reduction would take place post separation then the actual nitro-PAH components would be separated on the C18 column. Under these circumstances the mobile phase would not be buffered, therefore, a make-up stream of acetate buffer would need to be added prior to the

reduction column. It was observed that poor reduction efficiencies occurred when no buffer was present. Two chromatograms of a nitro-PAH standard mixture are shown in Figure 6.24, the upper chromatogram results from using pre-column reduction whereas the lower chromatogram used post-column reduction. The pre-column reduction shows that each of the six amino-PAHs were resolved. The post-column chromatogram on the other hand, was not able to resolve all of the compounds. The zinc column when used in conjunction with post-column reduction caused dramatic losses in chromatographic efficiency. For this reason, a pre-column reduction was investigated as the primary means to perform this analysis. It should be mentioned that extended used of the reduction column could also cause losses in chromatographic resolution. This is due to the consumption of zinc causing void volumes in the reduction column. This did not present a problem for two reasons, the zinc column was repacked weekly and low modifier concentrations during the start of the chromatogram pre-concentrated the amines at the head of the chromatographic column.

Initial studies with pre-column reduction of the nitro-PAHs suggested that by using high buffer concentrations (90%) at the start of the separation gradient, large injection volumes could be performed without compromising the separation of the aromatic amines. In this manner, the large injection volume (5 mL) could be viewed as an on-line pre-concentration of the sample before analysis. However, the use of high buffer concentrations produced elevated and variable backgrounds that complicated the analysis of the aromatic amines. Figure 6.25a shows a blank chromatogram that was representative of the typical interferences that were observed. The data in this figure suggest that the interference peaks in the background may have resulted from the buffer solution (100 mM). A less concentrated buffer (10 mM) was used to investigate the effect of buffer on the production of background

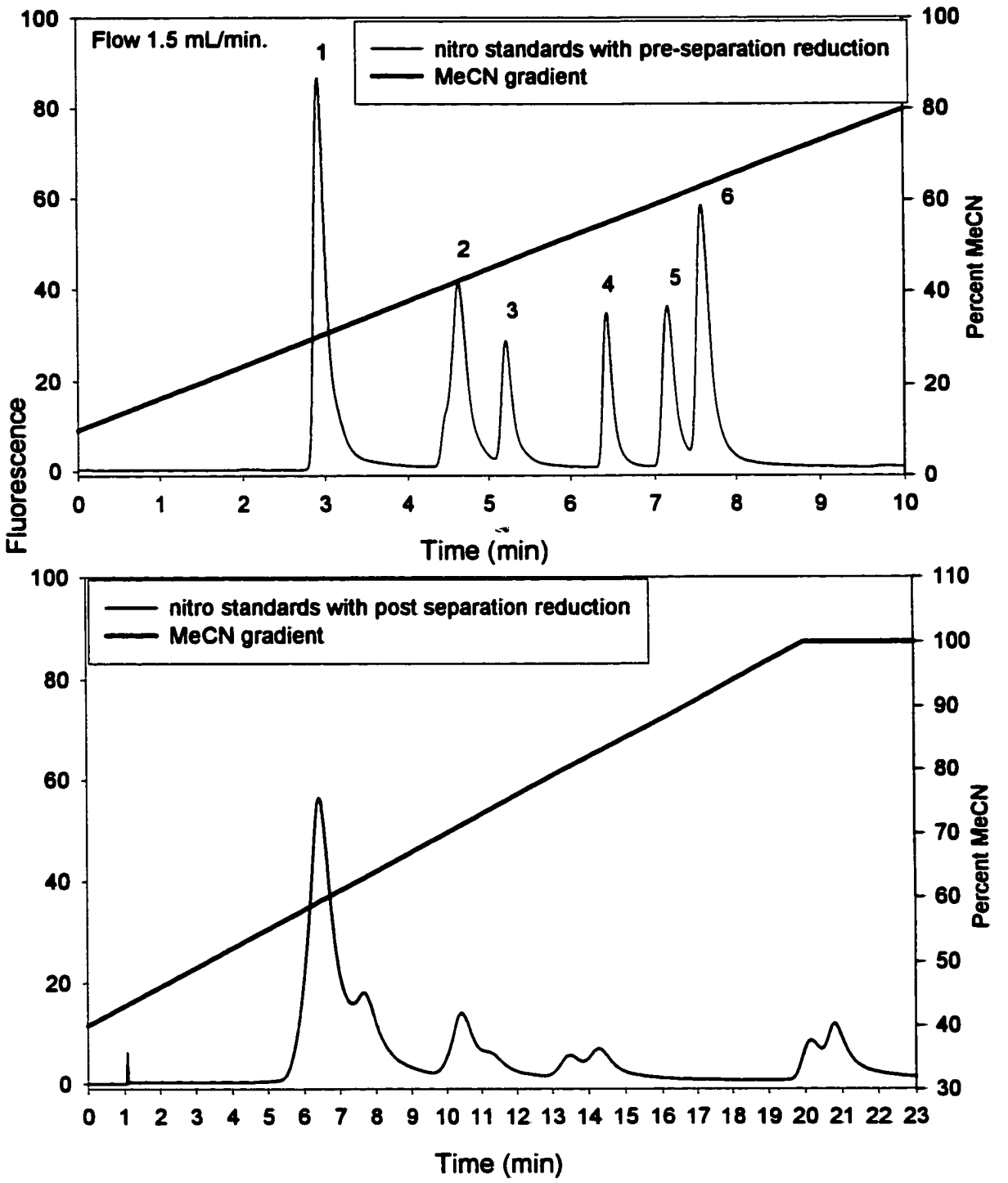

Figure 6.24: The reversed phase separation of nitro-PAH standards with pre-column reduction and post column reduction.

Peak Identification: 1 1-aminonaphthalene, 2 2-aminofluorene, 3 2-aminobiphenyl, 4 2-aminoanthracene, 5 2-aminofluoranthene, 6 1-aminopyrene

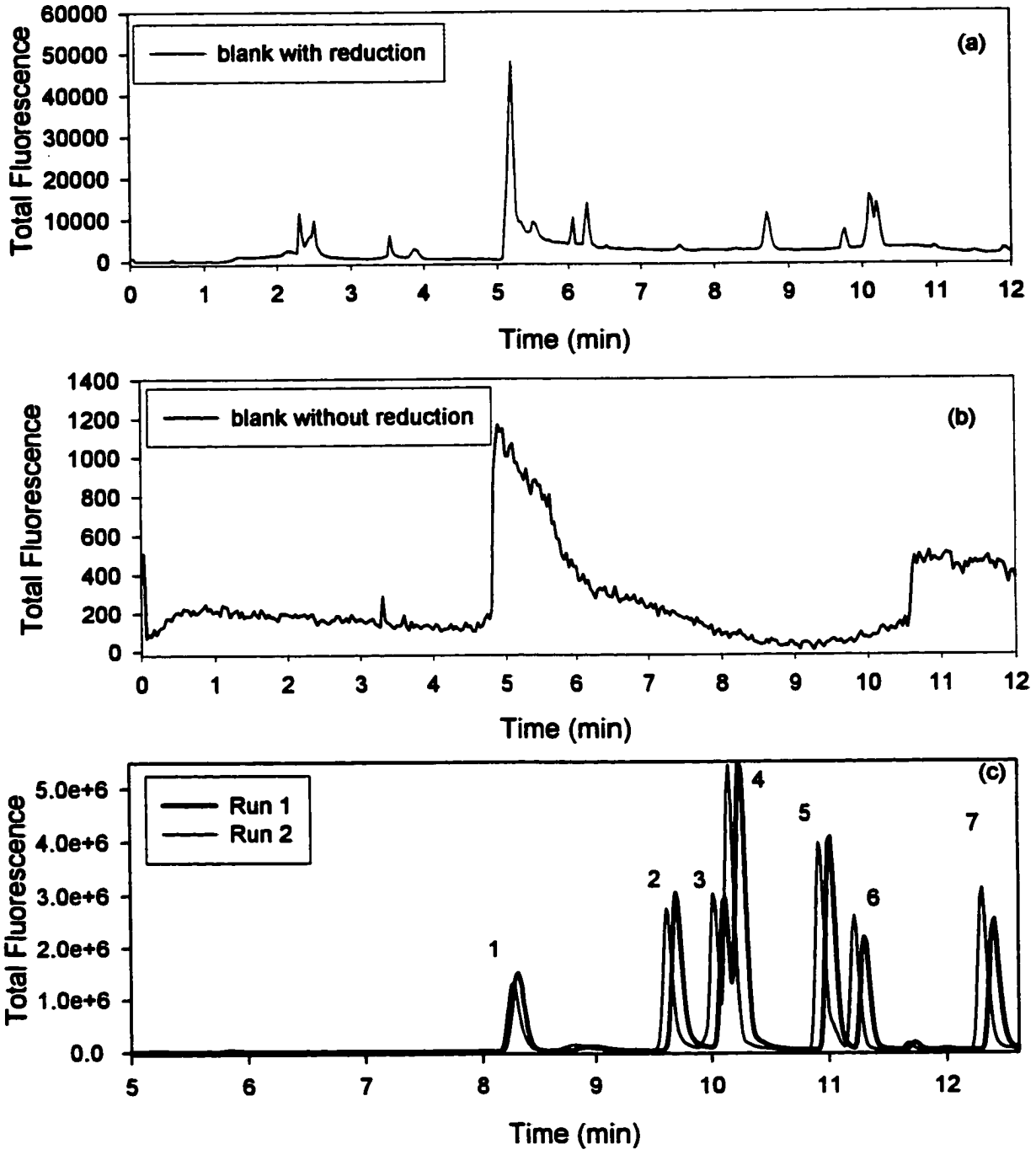

Figure 6.25: Upper figures show blanks of the reversed phase separation with (a) and without reduction buffer (b). Reversed phase separation of nitro PAH standard mixture using the pre-separation reduction. Two replicate injections of a reduced nitro-PAHs standard is shown as (c). The 266 nm laser was used to excite fluorescence. The experiental conditions are given in Figure 6.24.

Peak Identification: 1 2-aminofluorene, 2 9-aminoanthracene, 3 2-amino-fluoranthene, 4 1-aminopyrene, 5 6-aminochrysene, 6 7-aminobenz[*a*]-anthracene, 7 6-aminobenzo[*a*]pyrene

peaks.

However, severe peak broadening was observed with the chromatography. It was believed that due to the lowered buffer capacity the pH could increase above pH 4.7 as the zinc consumed some of the acid as it was oxidized. Switching the zinc column out of the eluent stream after reduction restored the chromatographic peak shapes. However, the number and variability of the background peaks was only slightly reduced. The two chromatograms for a nitro-PAH standard are shown in Figure 6.25c. These chromatograms indicate good peak heights but variable retention times.

This method of quantification, a reduction of the analyte, involves the chemical transformation of the parent compound. The success of many chemical reactions often depends upon such variables such as temperature and reactant concentration. Initially, such factors were not considered important since both the standard and the unknown sample were treated in the same manner, it could be expected that, if there was less than quantitative reduction of the nitro-PAH to the amine, then the same error would apply to both the standard and the unknown. This would effectively cancel the resulting error in the calculation for the nitro-PAHs in the sample. However, since it could be expected that there would be differences between the concentrations of the nitro-PAHs in both the standard mixture and the particulate extract, it was decided that the effect of concentration upon the reduction efficiency should be investigated. In this experiment, the following aromatic amine standards, 1-aminonaphthalene, 2-aminofluorene, 9-aminoanthracene, 2-aminofluoranthene, and 1-aminopyrene were analyzed for their fluorescence response using concentrations that ranged between 10 ng/mL to 5 ug/mL. The corresponding nitro-PAHs were then reduced on-line and analyzed over a similar concentration range. Quantitative reduction was observed for

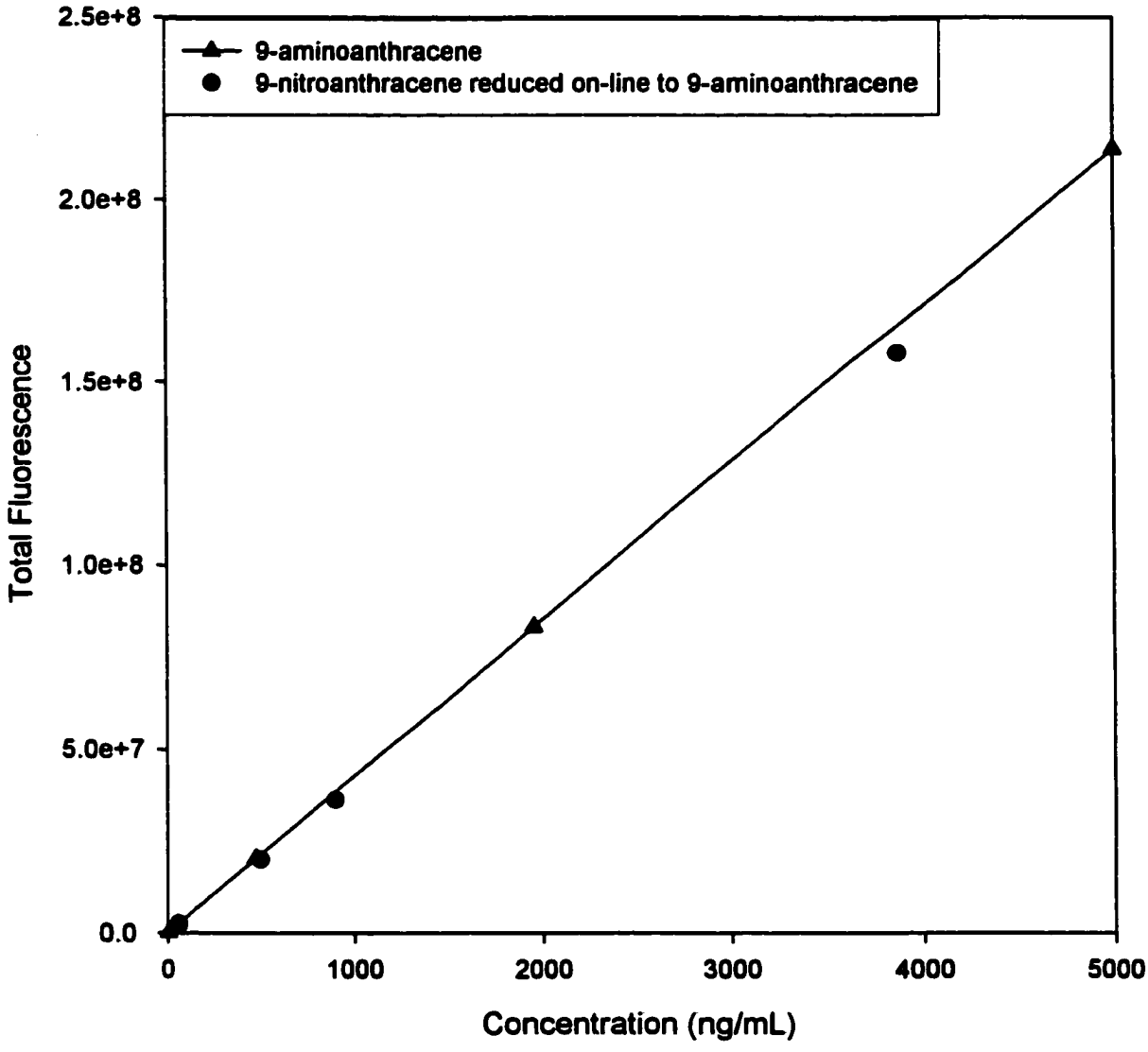

Figure 6.26: A calibration curve for the response of 9-aminoanthracene separated on the reversed phase column using the 266 nm laser to excite molecular fluorescence. Circles superimposed on the curve correspond to on-line reduction of 9-nitroanthracene and then separated using the C18 column.

each of the nitro-PAHs. Figure 6.26 shows a calibration curve for 9-aminoanthracene. In this figure the data points represent various concentrations of 9-nitroanthracene that were reduced and then analyzed for response. The best agreement with the standard 9-aminoanthracene occurs when the concentration of 9-nitroanthracene was below 500 ng/mL. As a result, the nitro-PAHs in the particulate sample were quantitated with nitro-PAH standards as close as possible in concentration to the unknown sample.

Figure 6.27 shows the separation of a standard mixture of the priority PAHs spiked with selected nitro-PAH compounds analyzed using pre-column reduction on the reversed phase C18 column. This chromatogram suggests that the PAHs were well resolved from the amino-PAHs. As a result, the priority PAHs need not be fractionated from the nitro-PAHs as either could be analyzed independently, without interference. On the other hand, polar compounds were removed prior to analysis because they presented interferences that prevented detection of the amino-PAHs. It was mentioned earlier that the cleanup separation was not successful using the silica column. Figure 6.28 shows the separation of a fraction from the silica column (Syncrude combustion particulates) that would contain the nitro-PAHs separated on the reversed phase C18 column after pre-separation reduction and again without reduction. The resulting chromatograms on the C18 column contain multiple peaks that eluted over a range of retention times that might have corresponded to aromatic amines. The fact that the compounds fluoresced without reduction suggests that they did not correspond to nitro-PAHs and were most likely interfering compounds such as methoxy-PAHs. As a result fractionation or cleanup of this particulate sample using the silica column was not able to provide quantitative information for the nitro-PAHs. Figure 6.29 shows similar chromatograms of the Syncrude particulate sample fractionated using the DNBS column.

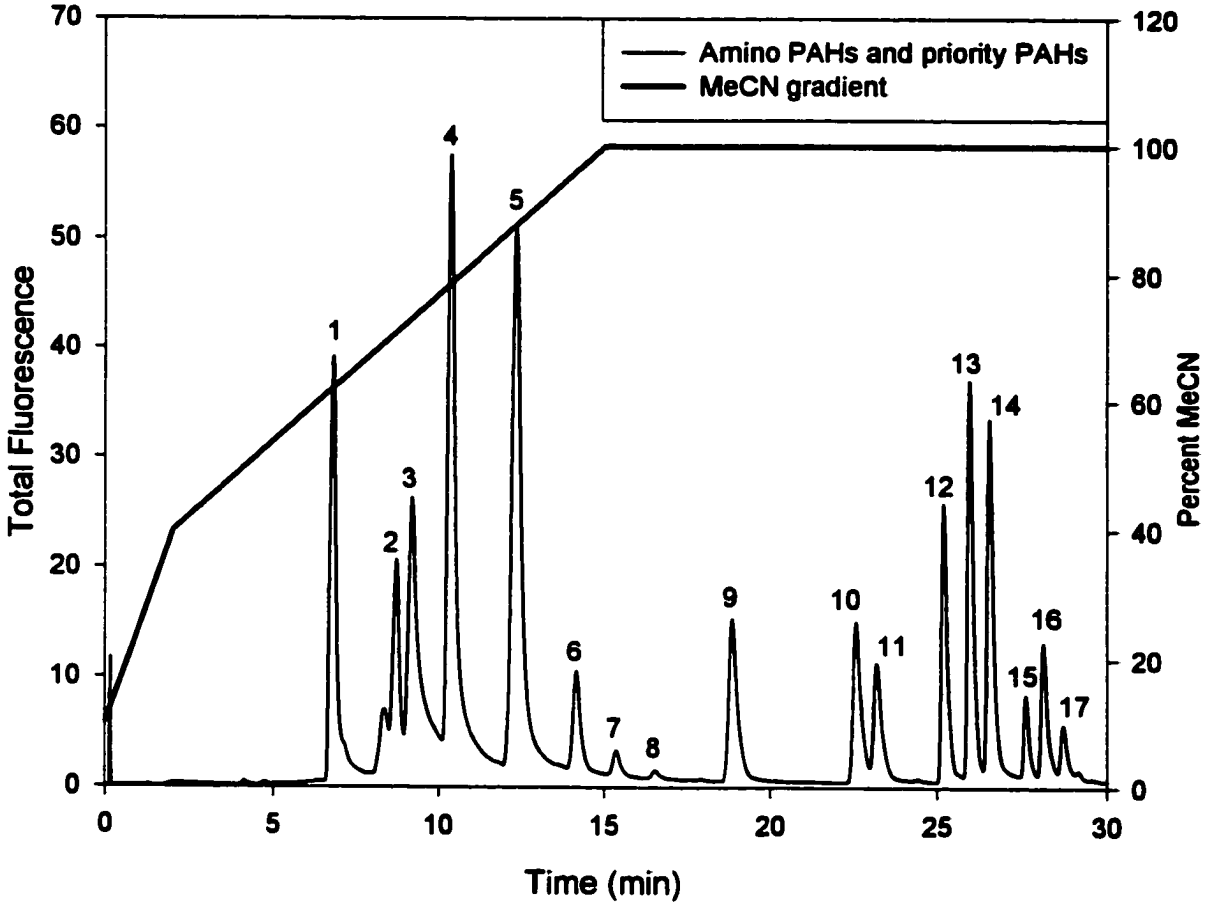

Figure 6.27: A reversed phase separation of the amino and priority PAHs on 5 cm C18 Supelco column. Agilent 1100 fluoescence detetor (excitation 260 nm) was used to monitor the eluent. Flow rate 1.0 mL/min.

Peak Identification: 1 1-aminonaphthalene, 2 2-aminofluorene,
3 2-aminobiphenyl, 4 2-aminoanthracene, 5 2-aminofluoranthene,
1-aminopyrene, 6 6-aminochrysene, 7 7-aminobenz[*a*]anthracene,
8 phenanthrene, 9 fluoranthene, pyrene, 10 benz[*a*]anthracene,
11 chrysene, 12 benzo[*b*]fluoranthene, 13 benzo[*k*]fluoranthene,
14 benzo[*a*]pyrene, 15 dibenz[*a,h*]anthracene, 16 benzo[*g,h,i*]perylene,
17 indeno[*1,2,3-c,d*]pyrene

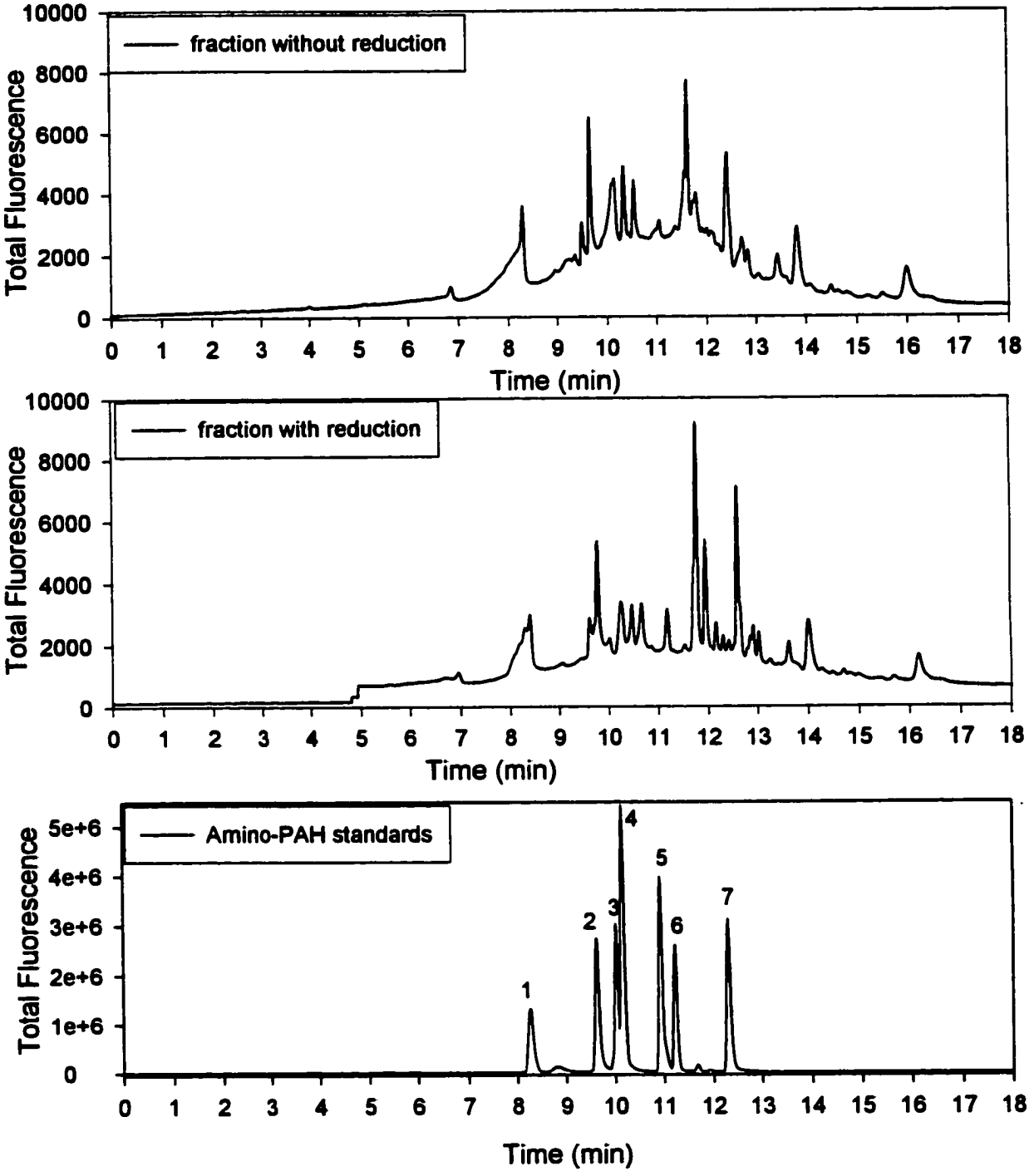

Figure 6.28: The eversed phase separation of the nitro-PAH fraction from silica column (Syncrude particulates) using pre-separation reduction and no reduction on the same sample. The 266 nm laser was used to excite fluorescence.
The experimental conditions are shown in Figure 6.27.

Peak Identification: 1 2-aminofluorene, 2 9-aminoanthracene, 3 2-amino-fluoranthene, 4 1-aminopyrene, 5 6-aminochrysene, 6 7-aminobenz[*a*]-anthracene, 7 6-aminobenzo[*a*]pyrene

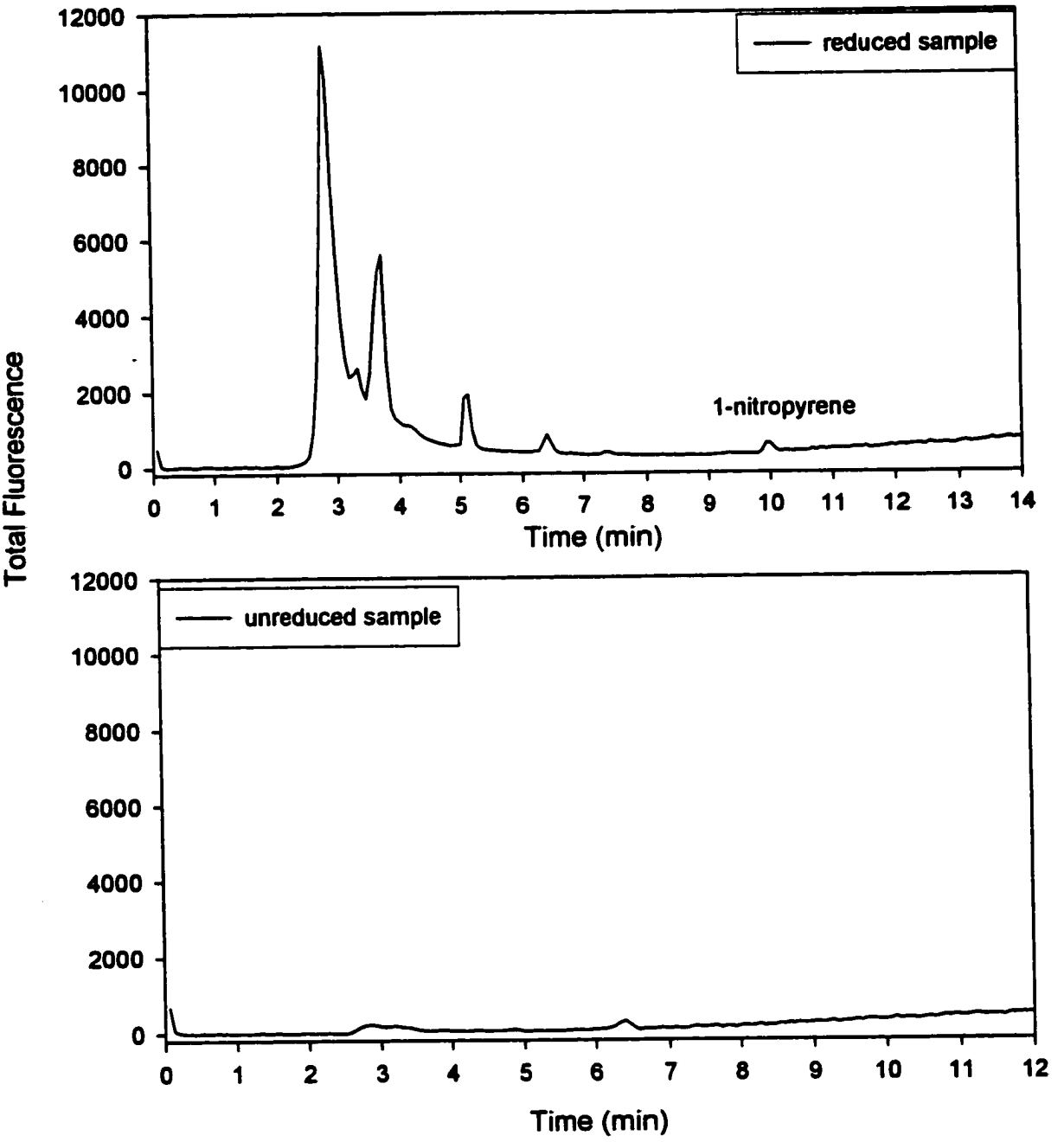

Figure 6.29: Reversed phase separations of the nitro-PAH fraction resulting from the separation of Sycrude combustion solids on the DNBS column. The upper figure used the zinc column reduction and the lower used no reduction. The experimental conditions are given in Figure 6.27.

Peak Identification: 1 2-aminofluorene, 2 9-aminoanthracene, 3 2-amino-fluoranthene, 4 1-aminopyrene, 5 6-aminochrysene, 6 7-aminobenz[*a*]-anthracene, 7 6-aminobenzo[*a*]pyrene

The unreduced nitro-PAH fraction produced a chromatogram without peaks. After reduction, several peaks were present. Many of the earlier peaks were not identified but were believed to result from background interferences. The presence of 1-nitropyrene was identified in the Syncrude particulates. Furthermore, the reversed phase chromatograms from the nitro-PAH fraction on the DNBS column did not contain any of the peaks that were observed for the silica separation. This suggests that the DNBS column provided a better separation compared to the silica phase between the nitro-PAHs and other polar compounds.

Figure 6.30 shows the nitro-fraction (from DNBS column) of an Environment Canada diesel exhaust bus filter (E-170) separated using a reversed phase C18 column with reduction. This chromatogram displays many additional peaks compared to the Syncrude particulate sample. Several of these peaks were not identified and believed due to the background from the reduction procedure and sample matrix. However, 2-aminofluorene, 1-aminopyrene and 6-aminochrysene were identified and quantified in this sample. The laser excited fluorescence detector was used to identify compounds from this chromatogram. Since spectra of the amino-PAHs have less fine structure compared to PAHs the spectral resolution of the laser excited fluorescence array detector was not required. The Agilent 1100 fluorescence detector was investigated because of its higher sensitivity. In practice, the laser system was still more beneficial compared to the Agilent detector to distinguish between the amino-PAHs and background interference peaks.

6.3.7 Analysis of Nitro-PAHs using SFC and Fluorescence Detection

A second method of analysis for the amino-PAHs was a SFC separation using the

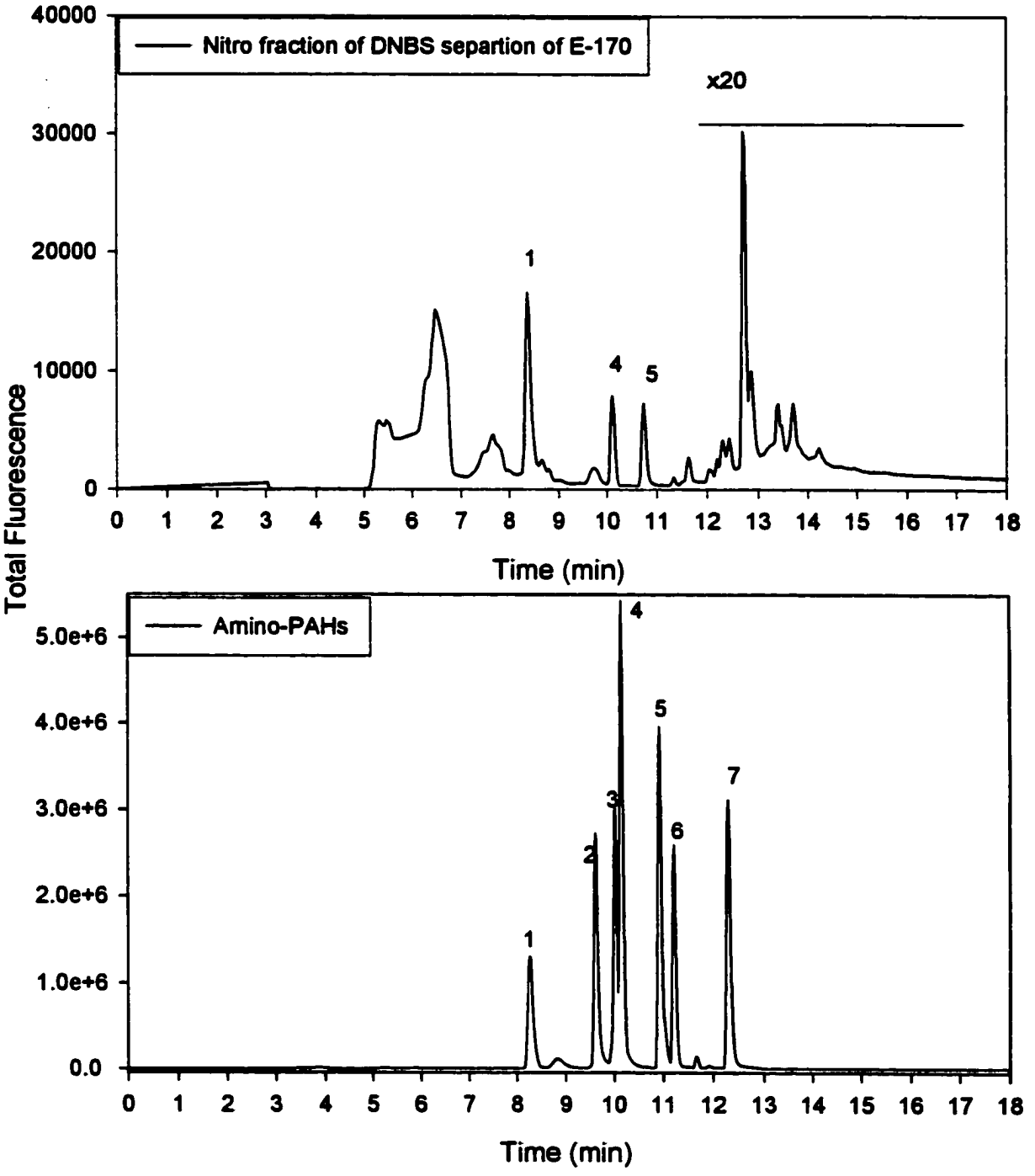

Figure 6.30: Reversed phase separations of nitro-PAH standard mixture and nitro region from DNBS column of filter sample E-170 using pre-separation reduction. The 266 nm laser was used to excite fluorescence. The experimental conditions are shown in Figure 6.27.

Peak Identification: 1 2-aminofluorene, 2 9-aminoanthracene, 3 2-amino-fluoranthene, 4 1-aminopyrene, 5 6-aminochrysene, 6 7-aminobenz[*a*]-anthracene, 7 6-aminobenzo[*a*]pyrene

aminopropyl stationary phase. The on-line pre-separation reduction of the nitro-PAHs used with the LC separation was a convenient means to introduce the sample on the column for analysis. Although such an on-line operation was possible using the SFC configuration, there was concern about the possible precipitation of salts in the restrictor. As a result, an off-line reduction was performed using the zinc column and apparatus from the LC reduction procedure. The reduced extract was collected on a Sep-pak® C18 column and eluted with hexane before injection with the Alcott autosampler.

It was previously shown that the presence of interference or background peaks observed during the LC analysis of the amino-PAHs presented some concerns. Some of the interferences were due to the reduction process and some were due to the actual sample matrix. It was hoped that the SFC analysis would provide a cleaner separation and an alternate selectivity with the aminopropyl stationary phase. The aromatic amines interacted strongly with the basic nature of the stationary phase. As a result, separation of the amines on the aminopropyl column required high modifier concentrations. In addition, the modifier had to be doped with a basic additive to compete with the active sites on the stationary phase. Under these conditions, the priority PAHs, as well as some of the more polar material would tend to elute at earlier retention times than the amino-PAHs. Figure 6.31 shows the chromatograms of a PAH standard mixture and nitro-PAH standards analyzed on the aminopropyl column after an off-line reduction. As this chromatogram suggests, the PAHs were resolved from the amino-PAHs. However, incomplete chromatographic resolution was observed for 3-aminofluoranthene and 1-aminopyrene. This does not present a problem since these two compounds are well resolved spectrally at 430 nm and 520 nm. The use of selective wavelength monitoring allows the accurate quantification of these two compounds.

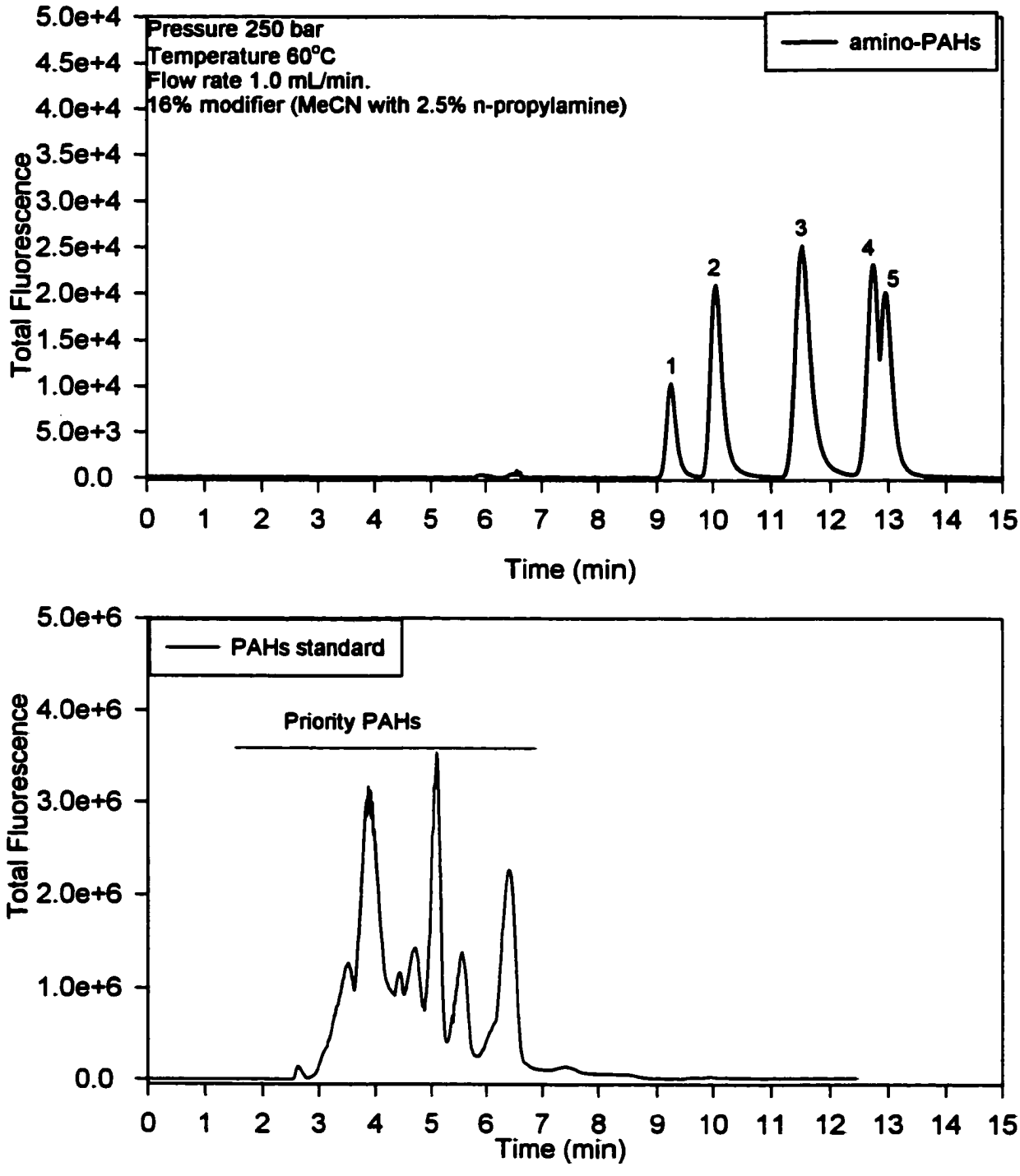

Figure 6.31: SFC using the aminopropyl column to separate standards mixtures of the priority PAHs and amino-PAHs.

Peak Identification: 1 1-aminonaphthalene, 2 2-aminofluorene, 3 2-amino-anthracene, 4 2-aminofluorene, 5 1-aminopyrene

Figure 6.32 illustrates the effectiveness of selective wavelength programming for these components. As mentioned in section 6.5.1 the spectra of the aromatic amines was somewhat ill-defined so it was important to determine the variation associated with the retention times for these compounds on the aminopropyl column as the spectra were less reliable for identification purposes compared to the priority PAHs. Figure 6.33 shows replicate injections of a nitro-PAH standard after reduction as well as replicate injections of an aromatic amine standard. In each case reasonable precision was observed. However, these experiments were performed with the same batch of modifier. Significant variations in the retention times and peak resolution were observed between batches of modifier. This most likely results from small variations in the amount of n-propylamine spiked into the organic modifier acetonitrile. This was avoided by mixing large batches of modifier solution.

Figure 6.31 showed that the priority PAHs were resolved from the amino-PAHs on the Keystone aminopropyl column. This was further exemplified with the Environment Canada diesel exhaust sample B-6. The chromatogram of this sample is shown in Figure 6.34. From this chromatogram, it would appear that the nitro-PAHs were present at lower concentrations compared to the PAHs in this sample. This is as expected from a typical diesel particulate sample. The lower two chromatograms in this figure have been scaled to emphasize the amino-PAHs. As well, selective wavelengths (430 nm and 520 nm) have been used to resolve the compounds present. There appears to be evidence for 9-aminoanthracene, 3-aminofluoranthene, 1-aminopyrene, and 6-aminochrysene within this sample. Multiple injections were found to return good instrumental precision with relative peak area errors less than 7-8 percent. However, what appears most significant with respect to the SFC separation of the standard amino-PAHs as well as the particulate samples was the absence of the

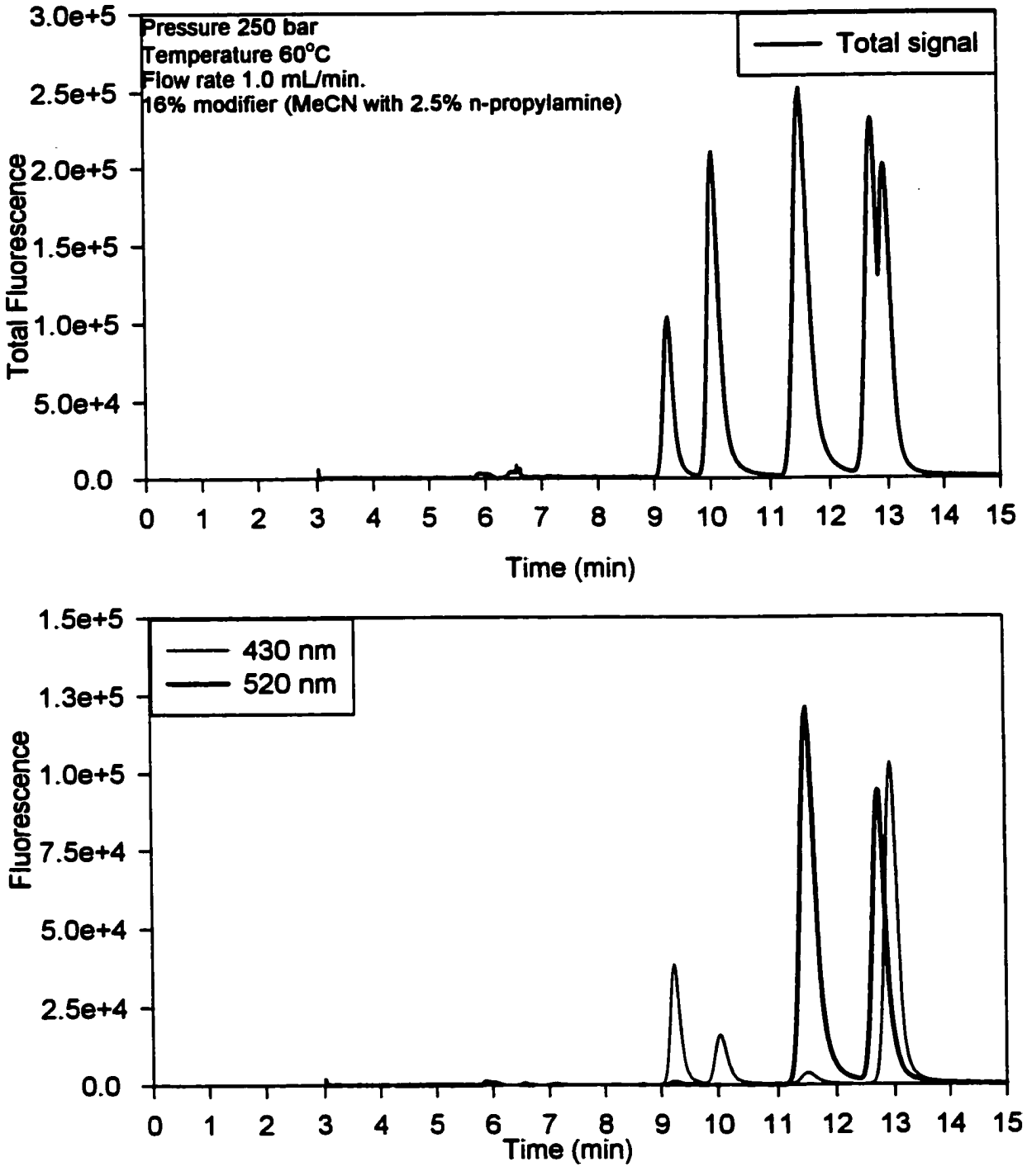

Figure 6.32: SFCs of a standard mixture of aromatic amines separated on the aminopropyl column. Upper chromatogram results from TOTAL FLUORESCENCE. Lower chromatograms result from fluorescence emission at 430 nm and 520 nm.

Peak Identification: 1 1-aminonaphthalene, 2 2-aminofluorene, 3 2-amino-anthracene, 4 2-aminofluorene, 5 1-aminopyrene

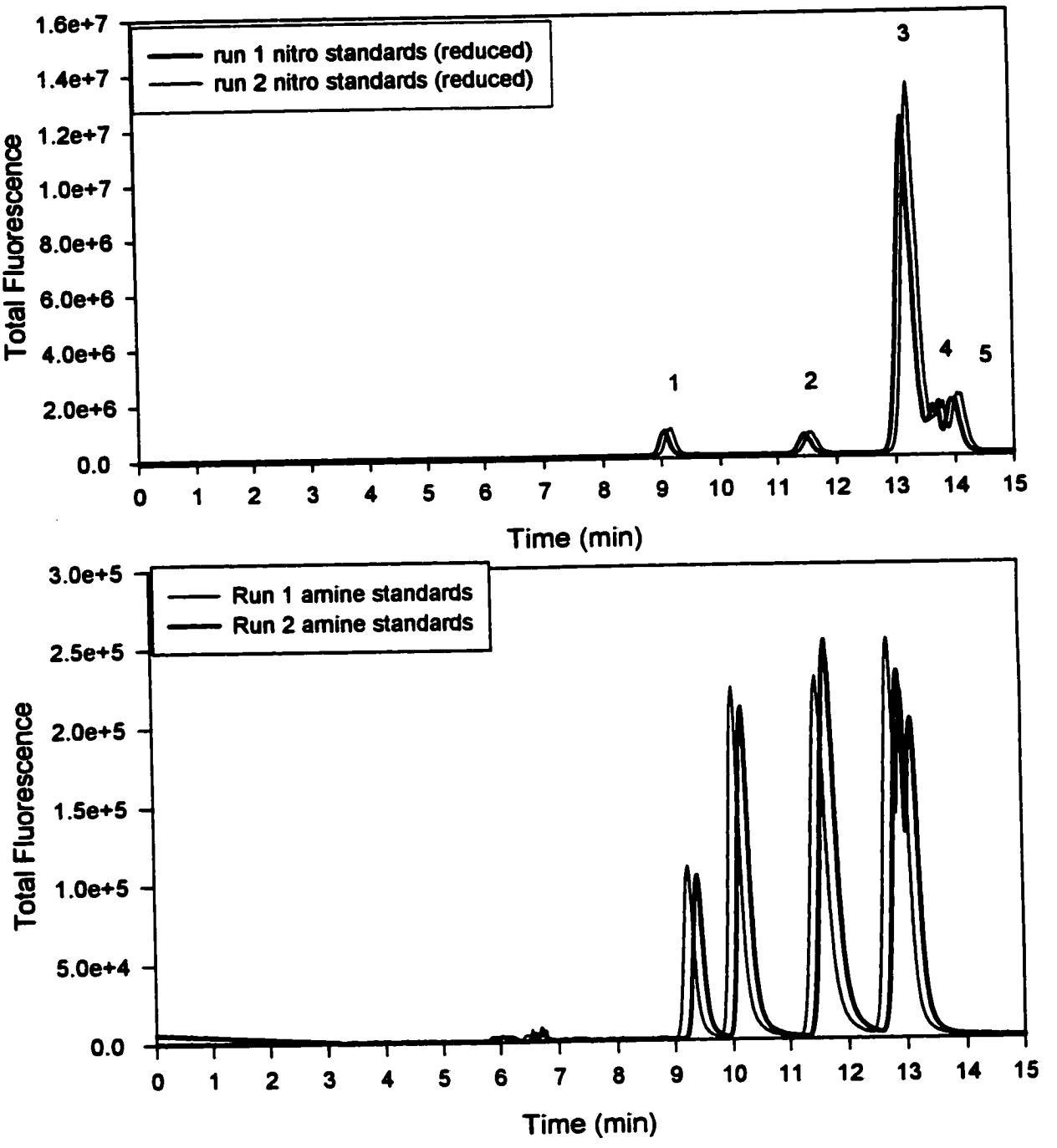

Figure 6.33: Replicate chromatograms of amino-PAHs and nitro-PAHs (reduced) on SFC aminopropyl column. The exerimental conditions are shown in Figure 6.32.

Peak Identification: 1 1-aminonaphthalene, 2 9-aminoanthracene, 3 3-aminofluoranthene, 1-aminopyrene, 4 6-aminochrysene, 5 7-benz[*a*]anthracene, 6-aminobenz[*a*]pyrene

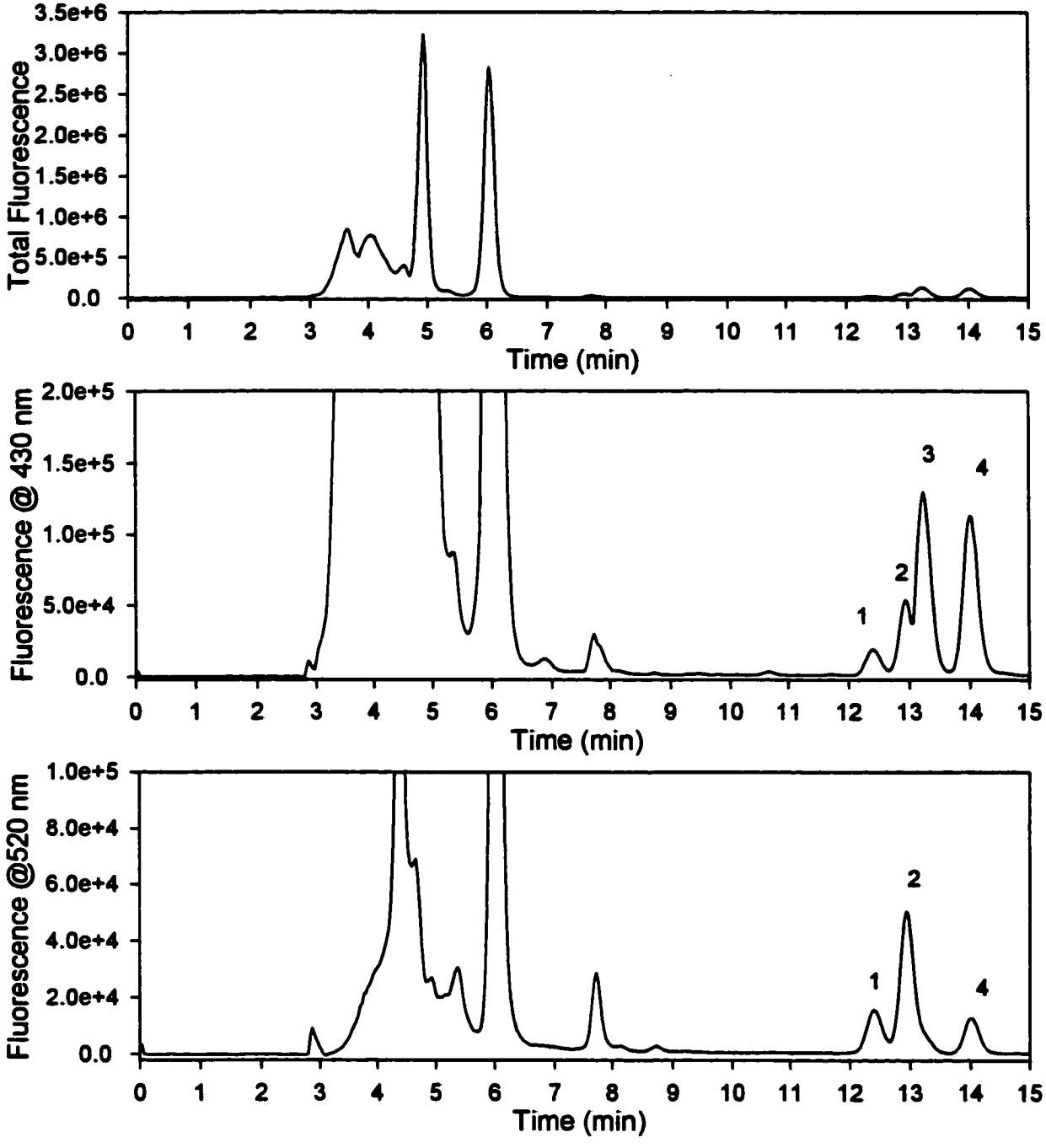

Figure 6.34: Environment Canada diesel exhaust filter collection B-6 separated on the aminopropyl column. The upper chromatgram uses total fluorescence. The center and lower chromatograms use specific emission wavelengths. These two chromatograms have ben scaled to emphasize the amino-PAHs. The experimental conditions are given in Figure 6.32.

Peak Identification: 1 9-aminoanthracene, 2 3-aminofluorene, 3 1-aminopyrene, 4 6-aminochrysene

background and interference peaks that were observed with the LC analysis.

The SFC analysis using the aminopropyl column represented the second dimension of a two-dimensional chromatographic analysis. The first chromatographic dimension was the DNBS cleanup separation that removed polar compounds from the sample matrix. This was required for the reversed phase C18 analysis of the nitro-PAHs. However, if the DNBS cleanup separation could be removed then the nitro-PAH analysis would be performed with a single chromatographic dimension. Figure 6.35 shows the chromatogram of an Environment Canada diesel exhaust sample B-2 separated on the aminopropyl column without prior sample cleanup. This chromatogram suggests that the Keystone aminopropyl column operating under SFC conditions was capable of analyzing the aromatic amines directly without prior sample cleanup. This has important implications with respect to analysis speed, simplicity, and possible accuracy.

6.3.8 Quantitative Comparison of the Components Identified on the Diesel Exhaust Particulate Samples and the Air Particulate Samples.

The final section in this chapter compares the relative amounts of target compounds found on several of Environment Canada's diesel exhaust filter samples and air particulate samples that were collected in-house. Each of these samples wase characterized for the levels of priority PAHs and selected nitro-PAHs. Several analytical methodologies were examined earlier in this chapter to accomplish this task. Phenanthrene, anthracene, fluoranthene, pyrene, benz[*a*]anthracene, benzo[*b*]fluoranthene, benzo[*k*]fluoranthene, benzo[*g,h,i*]perylene, and indeno[1,*2,3-c,d*]pyrene were quantified using GC/MS. Reversed

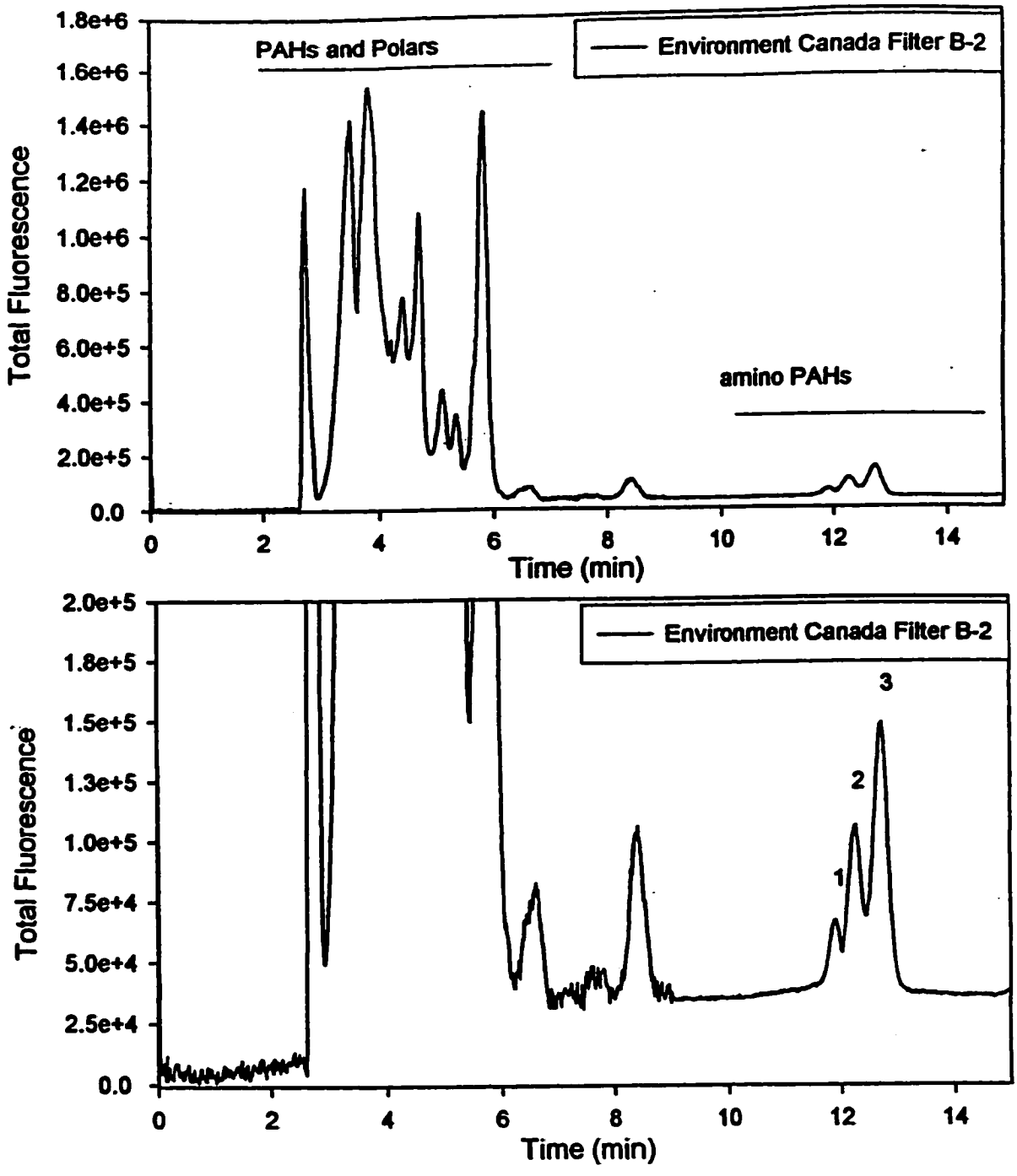

Figure 6.35: SFC separations of Environment Canada's diesel exhaust filter B-2 after off-line reduction process. Separation was achieved using aminopropyl column with the chromatographic conditions shown in Figure 6.32. The lower chromatogram has been scaled to emphasize the amino-PAHs. Sample was not treated with a cleanup prior to analysis.

Peak Identification: 1 3-aminofluoranthene 2 1-aminopyrene 3 6-aminochrysene

phase LC coupled with laser excited fluorescence detection was used to quantify chrysene. The most favorable analysis for the nitro compounds was found to result from the use of a SFC separation and the aminopropyl column. Initially, it was hoped that the level of alkylated PAHs could be estimated. In practice, this proved more difficult that expected. Two problems were observed. First, the GC chromatograms of the diesel particulate samples were complex and the co-elution of interference peaks was observed. Second, the lack of adequate standards made it impossible to identify structural isomers between different aromatic compounds. For example, there was no way to distinguish between a dimethylfluoranthene and a dimethylpyrene species. Since such alkylated standards were not available at the time of this experiment, the quantification of alkylated PAHs was not performed.

The levels of targeted compounds found on both the air filter collections as well as the diesel exhaust filter collection from the Ottawa transit buses are summarized in Table 6.9. Unfortunately very little was known about the actual collection and sampling process of the Environment Canada samples as this information was not provided when the filters were delivered. This makes it difficult to draw any comparisons with respect to the different filters. In fact, the only way to report the levels of target compounds was in terms of mass of PAH per filter paper. This was because the mass of the particulates on each filter was not known. This is contrary to the accepted convention to report concentration in terms of mass of PAH per gram of particulate or volume of air sampled. It should be mentioned at this point the values reported for naphthalene, acenaphthylene, acenaphthene, and fluorene are most likely low. As it was discussed earlier such volatile compounds were subject to losses during rotary evaporation. In fact, NIST does not provide certification for these samples in their SRM 1650a (diesel particulates) and 1649d (urban dust). The values reported in Table 6.9

Table 6.9: Summary of the levels of compounds quantified on the Environment Canada diesel exhaust filters and the in-house collections of air particulate samples.

Compound	E170	E155	B2	B4	E177	E175	B6	Air1	Air2	Air3
Naphthalene	98	34	51	31	69	89	54	NA	NA	NA
Acenaphthene	27	106	44	40	34	24	16	NA	NA	NA
Acenaphthylene	14	4	7	2	1	1	1	NA	NA	NA
Fluorene	54	28	36	114	143	126	153	1.4	1.1	1.8
Phenanthrene	663	566	635	587	535	188	755	3.3	1.1	1.8
Anthracene	100	40	97	58	62	12	69	NA	NA	NA
Fluoranthene	745	302	255	258	270	215	273	.52	.50	1.0
Pyrene	1089	442	295	329	312	251	348	.27	.28	.68
Benz(*a*)anthracene	122	40	39	34	44	29	89	.11	.02	.03
Chrysene	222	62	59	46	29	8	75	.11	.07	.14
Benzo[*b&k*]fluoranthene	264	74	62	74	145	0	150	.13	.08	.14
Benzo[*a*]pyrene	55	16	7	17	21	2	22	.06	.03	.05
Dibenz[*a,h*]anthracene	0	0	0	1	20	0	9	0	0	0
Benzo[*g,h,i*]perylene	67	18	13	27	2	7	10	.05	.05	.07
Indeno[*1,2,3-c,d*]pyrene	96	24	12	29	0	0	23	.04	.04	.04
nitrofluorene					3	6	5	NA	NA	NA
nitroanthracene					0.5	2	2	NA	NA	NA
nitrofluoanthene					0	0	11	NA	NA	NA
nitropyrene					2	1	22	NA	NA	NA
nitrochrysene					10	8	32	NA	NA	NA
nitrobenzo[*a*]pyrene					1	0	8	NA	NA	NA

NA not available or not done

All diesel particulate values in ng/filter; All air particulate values in ng/m^3

Air1, Air2, Air3, refer to in-house sample collection performed on 10/26/2001,10/27/2001, and 10/28/2001 respectively

these four compounds were estimates.

A survey of the data collected for each of the Environment Canada filters suggests that there were a number of similarities that exist between filters as far as the priority PAHs are concerned. For example, the level of phenanthrene found on each of the filters was relatively consistent except for the filter E-175. Similarly, the levels of pyrene and fluoranthene were found to be consistent except for the filter E-170. These outliers are difficult to explain without knowing the complete circumstances of sample collection.

Three of the Environment Canada diesel exhaust filter samples were analyzed for the levels of nitro compounds present on the filters. Evidence for six nitro-PAHs was confirmed. For the most part, the levels of these compounds were much lower than the levels of priority PAHs such as phenanthrene and pyrene. The levels of nitro-PAHs on different diesel exhaust filters appeared to be much more variable than the corresponding priority PAHs. For instance, a comparison of the amount of 1-nitropyrene on filters E-177 and B-6 indicates that the filter B-6 contained ten times the level as that reported on E-177 even though B-6 contained only a slightly elevated level of pyrene compared to the filter E-177. Similarly, chrysene was present at roughly the same concentration for each of these filters and again, the B-6 filter showed a threefold increase in the relative amounts of 6-nitrochrysene between the filters. Although the experimental sampling parameters were unknown, one may be able to surmise that these observations may be indicative of changing engine conditions such as operating temperature resulting in the observed differences in PAH nitration.

The three air particulate samples included in Table 6.9 result from collection with a high volume sampler located 500 m from a busy intersection at a residential location. These samples were analyzed for the priority PAHs using reversed phase LC coupled with laser

excited fluorescence detection. These samples were collected as part of a parallel study to monitor air quality in Nova Scotia. Air1, Air2, and Air3 in this table are air collections performed on three sequential days. Initial inspection of the data for these samples suggests that the levels of the priority PAHs remains relatively consistent over these three days. A more interesting comparison may be drawn between the air samples and the diesel exhaust particulate samples. The data from Table 6.9 are shown graphically in Figure 6.36, including the PAH concentrations calculated from the NIST SRM 1650a and 1649d. The values reported in this figure represent the fraction of a particular PAH with respect to the entire mass of PAHs present in the sample. This allows the relative distribution of the priority PAHs to be examined for each type of sample regardless of the manner in which the concentrations of the priority PAHs were reported. A comparison of the samples in Figure 6.36 provides some rather interesting observations. The SRM 1649a that corresponds to a typical urban dust sample seems to show a shift in the distribution of the priority PAHs compared to the other three samples. Specifically, the urban dust contains a much larger percentage of high molecular weight priority PAHs such as benzo[*g,h,i*]perylene compared to smaller PAHs such as phenanthrene. In fact the relative distributions of the priority PAHs for the E-177 sample and the Air2 sample appear to follow a similar distribution observed with the SRM 1650a that is supposed to be representative of a diesel exhaust particulate sample. In this case a much higher distribution of low molecular weight PAHs was favored over the larger PAHs. The similarity of the distribution patterns for the Environment Canada sample to the NIST diesel exhaust standard reference material was understandable as they both were collected from the exhausts of diesel engines. The fact that the distribution of an air particulate sample bears

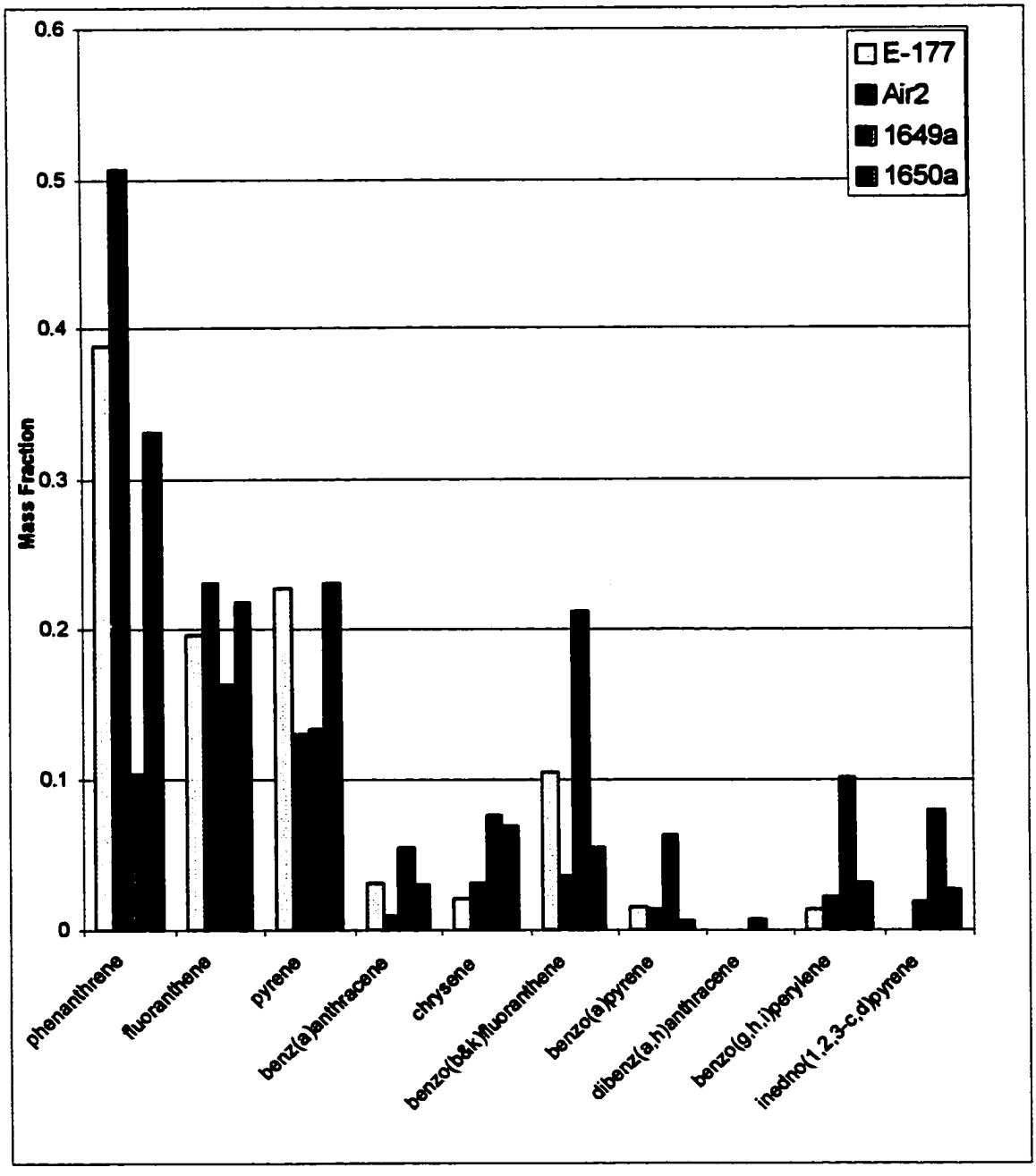

Figure 6.36: The relative distribution of PAHs in the Environment Canada diesel exhaust E-177, the air particulate sample collected on 10/27-28/2001, and the two standard reference materials, 1649d and 1650a.

such a similarity to that of a diesel exhaust sample is at first quite perplexing, particularly since there were no diesel engines operated within the vicinity of the air sampler. One possible explanation may be that the observed distribution of the priority PAHs contained within the air filter sample results from emissions of home heating devices such as domestic furnaces. In general, these devices burn either furnace or stove oil. This oil is quite close in composition to diesel fuel resulting in a similarity in the resulting emission products between diesel engines and domestic heating furnaces.

In closing, it should be mentioned that the sample composition determined the complexity of the analytical procedures required. For example, the air particulate samples could be quantified using standard reversed phase chromatography and fluorescence detection without a prior cleanup separation. In fact, pressurized fluid extraction was found to offer no benefits compared to sonication with acetonitrile. Under these circumstances the air particulate samples were both easier and faster to analyze. The Environment Canada filters required a much more complex methodology to obtain accurate quantitative information. Much of the increased complexity of these samples was believed to result from the presence of raw or un-combusted fuel condensing on the particulate matter. As a result, the Environment Canada diesel exhaust filters as well as the SRM 1650a were the more taxing samples to analyze compared to either the air particulates or the SRM 1649a.

Chapter 7 Conclusions

The first phase of this research was concerned with the development of qualitative methods for the determination of PAHs in light gas oils. A DNBS column was used to fractionate a light gas oil that had been subjected to a hydrotreating process at Sycrude Canada. Eight fractions were collected in total for off-line characterization with two-dimensional and three-dimensional chromatography. Additional dimensionality was added through selective detection. Two-dimensional LC(DNBS)-GC/MS provided a means to identify the aromatic class through the use of UV and fluorescence detection (LC-DNBS) and characterize the amount of aliphatic substitution (GC-MS). The oil MB13B was found to contain benzenes, naphthalenes, biphenyls, fluorenes, phenanthrenes, and pyrenes. The analysis of the fractions containing the larger aromatic classes (fluorenes to pyrenes, fractions 4-8) was more reliable than the earlier fractions. This was because of the large number of unresolved compounds observed in the LC-DNBS and GC-MS separations of fractions 1 to 3. Also, higher levels of alkyl substitution with the earlier fractions made the compounds more prone to fragmentation in the mass spectrometer. As a result, compound identification remained tentative for these fractions and were reported solely in terms of double bond equivalents.

The goal of the first chromatographic dimension was to separate the oil by aromatic class or ring number. The DNBS column was found to offer the best fractionation compared to other stationary phases examined in this research. The DNBS separation was still prone to overlap between aromatic classes when these were substituted with alkyl groups. This was most evident with the larger classes (3 and 4 aromatic rings). Two-dimensional studies involving LC(DNBS)-SFC(DNBS) suggested

that an improvement with class separation was observed when the DNBS column was operated under SFC conditions.

Three-dimensional LC(DNBS)-RP(monomeric C18)-(polymeric C18 or NP-TCP)) was investigated as an alternative to the two-dimensional procedures. Although, each of the LC separations was observed to have low peak capacity when compared to capillary GC, the combination of three LC separations showed a peak capacity to comparable to GC. The geometric selectivity of the Vydac and TCP columns provided structural information that aided with a tentative assignment of substitution patterns on several phenanthrene species.

Evidence was observed for a series of PAHs with aliphatic rings attached for pyrene and phenanthrene. A logical source for these compounds was from the hydrotreating process. Since crude feed products contain much larger aromatic classes (ie. chrysene, benzo[*g,h,i*]perylene), it stands to reason that the reduction of a single aromatic ring on chrysene could produce a phenanthrene species. The presence of aromatic compounds (phenanthrene and pyrene) with an aliphatic ring attached may indicate relative inefficiencies with respect to the processing parameters involved with the hydrotreating process. Additional oils were investigated that resulted from a variation in temperature control during hydrotreating. The levels of phenanthrenes and pyrenes observed in the product were dependent upon the temperature at which the hydrotreating was performed.

The second phase of this research was concerned with the development of quantitative methods for the analysis of priority PAHs and nitro-PAHs in diesel exhaust and air particulate samples. A PFE extraction procedure using dichloromethane was

found to provide quantitative extraction from a NIST SRM 1650a (diesel particulates) and 1649d (urban dust).

Sample cleanup was required to remove polar material before analysis for the priority PAHs. This was accomplished with a DNBS column. This column provided a better separation between polar compounds resulting in lower background during analysis. Three separations were investigated for the quantification of the priority PAHs, a reversed phase LC-fluorescence, SFC(aminopropyl)-fluorescence, and a GC-MS. The SFC method had the least resolution and highest detection limits of the three methods. GC-MS was found to provide the best data. All of the priority PAHs except for naphthalene, acenaphthene, acenaphthylene, fluorene, chrysene, and were analyzed with this method. The smaller priority PAHs (naphthalene-fluorene) were not quantified because NIST did not provide certification for these compounds in the standard reference materials. Chrysene had to be quantified with the LC-fluorescence separation due to co-elution with triphenylene in the GC separation. Although the detection limits of the larger PAHs (benzo[*b*]fluoranthene-indeno[*1,2,3-c,d*]pyrene) were higher for GC-MS when compared to LC-fluorescence for standards, background interferences with real samples made the LC separation less useful for these compounds.

Two methods were investigated for the analysis of nitro-PAHs. The first was a SFC separation that required off-line reduction to the amine for fluorescence detection. The second was a in-line RP-LC separation with fluorescence detection. The detection limits were higher (~3 times) for the SFC method due to the design of the high-pressure flow cell. The LC method had higher backgrounds and more interference peaks that made quantification more difficult. The SFC method was used to quantify 2-

nitrofluorene, 9-nitroanthracene 3-nitrofluoranthene, 1-nitropyrene, and 6-nitrochrysene in several of the diesel exhaust filters.

Several exhaust filters were characterized for priority PAHs and nitro-PAHs. Differences in the absolute levels of PAHs and nitro-PAHs but similarity in the relative distribution of PAHs was observed between filters. The difference may be due to collection artifacts or may be engine related. Since the filters were supplied by an external agency (no experimental conditions) it is difficult to speculate on an exact cause of the differences. However, the general distribution of the priority PAHs on the diesel exhaust filter was very different from that of a typical urban dust sample. The urban dust contained a much greater percentage of large PAHs while the diesel particulates showed evidence of larger concentration of smaller aromatics (below pyrene). These differences may allow the fingerprinting of emissions to indicate the sources of diesel fuels.

References

1 Sok Yui, Keng H. Chung, Oil and Gas Journal, Vol. Pp, No. 1, 46-53, 2001.

2 M. Zander, Polycyclic Aromatic Hydrocarbons, Vol. 7, 209-221, 1995.

3 Alastair Lewis, Sarah A. Askey, Krystyna M. Holden, Keith D. Bartle, and Michael J. Pilling, Journal of High Resolution Chromatography, Vol. 20, 109-114, February, 1997.

4 Selim Senkan and Marco Castaldi, Combustion and Flame, Vol. 107, 141-150, 1996.

5 H.Y. Tong and F.W. Karasek, Analytical Chemistry, Vol. 56, 2129-2134, 1984.

6 T. Watanabe, S. Ishida, M. Kishiji, Y. Takahaashi, A. Furuta, T. Kasai, K. Wakabayashi, and T. Hirayama, Journal of Chromatography A, Vol. 839, 41-48, 1999.

7 Jurgen Jacob, Mahmoud Alawi, and Gernot Grimmer, Polycyclic Aromatic Compounds, Vol. 2, 13-17, 1991.

8 Z. Aizenshtat, Geochimica et Cosmochimica Acta, Vol. 37, 559-567, 1973.

9 M. Radojevic, Chemistry in Britain, December, 29-31, 1998.

10 Phillip M. Fine, Glen R. Cass, and Bernd R. T. Simoneit, Environmental Science and Technology, Vol. 35, 2665-2675, 2001.

11 Environment Canada, Environmental Leaders 3 Voluntary Action on Toxic Substances, A Progress Report, Minister of Public Works and Government Services Canada, Ottawa, 1999.

12 Ana M. Mastral and Maria S. Callen, Environmental Science and Technology, Vol. 34, 3051-3057, 2000.

13 James J. Schauer, Michael J. Kleeman, Glen R. Cass, and Bernd R.T. Simoneit, Environmental Science and Technology, Vol. 33, 1566-1577, 1999.

15 Anders Dyermark, Roger Westerholm, Eva Overik, and Jan-ake Gustavsson, Atmospheric Environment, Vol. 29, No. 13, 1553-1558, 1995.

16 Jurgen Zuhlke, Dietmar Knopp, and Reinhard Nieber, Journal of Chromatography A, Vol. 807, 209-217, 1998.

17 Anders Fieldberg, Morten W. B. Poulsen, Torben Nielsen, and Henrik Skov, Atmospheric Environment, Vol. 35, 353-366, 2001.

18 R. Atkinson and J. Arey, Environmental Health Perspectives, Vol. 102, 117-126, 1994.

19 Angelo Cecinato, Fabio Marino, Patrizia Di Filippo, Luca Lepore, and Massimilano Possanzini, Journal of Chromatography A, Vol. 846, 255-264, 1999.

20 Eva Leotz-Gartziandia, Veronique Tatry, and Patrick Carlier, Environmental Monitoring and Assessment, Vol. 65, 155-163, 2000.

21 Anders Fielberg and Torben Nielsen, Environmental Science and Technology, Vol34, 789-797, 2000.

22 Ronald G. Harvey (Ed.), Polycyclic Aromatic Hydrocarbons, New: John Wiley and Sons, 1997.

23 Phillip Garrigues, Marie-Pierre, Marniesse, Stephen A. Wise, Jacqueline Bellocq, and Marc Ewald, Analytical Chemistry, Vol. 59, 1695-1700, 1987.

24 S. E. Manahan (Ed.), Toxicology Chemistry: A guide to Toxic Substances in Chemistry, Michigan: Lewis Publishers Inc., 1989.

25 James J. Schauer, Michael J. Kleeman, Glen R. Cass, and Bernd R.T. Simoneit, Environmental Science and Technology, Vol. 33, 1578-1587, 1999.

26 Linsey C. Marr, Thomas W. Kirchstetter, Robert A. Harley, Antonio H. Miguel, Susanne V. Hering, and S. Katherine Hammond, Environmental Science and Technology, Vol. 33, 3091-3099.

27 Peter C. Van Metre, Barbara J. Mahler, and Edward T. Furlong, Environmental Science and Technology, Vol. 34, 4064-4070, 2000.

28 Stephanie S. Buehler, Ilora Basu, and Ronald A. Hites, Environmental Science and Technology, Vol. 35, 2417-2422, 2001.

29 K.H. Chung, C. Xu, M. Gray, Y.Zhao, L. Kotlyar, and B. Sparks, Reviews in Process Chemistry and Engineering, Vol. 1, 41-79, 1998.

30 James A. Kent (Ed.), Riegel's Handbook of Industrial Chemistry, New York: Van Nostrand Reinhold Company, 1974.

31 Sok Yui, Nobukazu Matsumoto, and Yoichi Sasaki, Oil and Gas Journal, 43-51, Jan. 19, 1998.

32 Kuangnan Qian and Chang S. Hsu, Analytical Chemistry, Vol. 64, No. 20, 2327-2933, October 15, 1992.

33 Environment Canada, PSL Assessment Report-Respirable Particulate Matter, Minister of Public Works and Government Services Canada, Ottawa, 2000.

34 J. O. Allen, N. M. Dookeran, K. Taghizadeh, A. L. Lafleur, K. A. Smith, and A. F. Sarofim, Environmental Science and Technology, Vol. 31, No. 7, 2064-2070, 1997.

35 Antanio H. Miguel, Thomas W. Kirchstetter, Robert A. Harley, and Susanne V. Hering, Environmental Science and Technology, Vol. 32, 450-455, 1998.

36 Satoko Ishii, Yoshiharu Hisamatsu, Koji Inazu, Morio Kadoi, and Ken-Ichi Aika, Environmental Science and Technology, Vol. 34, 1893-1899, 2000.

37 Jurgen Schnelle-Kreis, Istvan Gebefugi, Gerhard Welzl, Thomas Jaensch, and Antonius Kettrup, Atmospheric Environment, Vol. 35, Supplement No. 1, S71-S81, 2001.

38 T. Romanowski, W. Funcke, J. Konig, and E. Balfanz, Analytical Chemistry, Vol. 54, 1285-1287, 1982.

39 Miriam L. Diamond, Sarah E. Gingrich, Kirsten Fertuck, Brian E. Mccarry, Gary A. Stern, Brian Billeck, Bert Grift, Deborah Brooker, and Thomas D. Yager, Environmental Science and Technology, Vol. 34, 2900-2908, 2000.

40 Ortech Corporation, CPPI Report No. 94-7, ISBN 1-896063-06-3, June, 1994.

41 Alastair C. Lewis, Dorota Kupiszewska, Keith D. Bsrtle, and Michael J. Pilling, Atmospheric Environment, Vol. 29, No. 13, 1531-1542, 1995.

42 Pilar Fernandez and Josep M. Bayona, Journal of Chromatography, Vol. 625, 141-149, 1992.

43 J.D. Berset, R. Holzer, and H. Hani, Journal of Chromatogrphy A, Vol. 823, 179-187, 1998.

44 Nguyen Thi Kim Oanh, Lars Betz Reutergardh, and Nghiem Trung Dung, Environmental Science and Technology, Vol. 33, 2703-2709, 1999.

45 Chih-Shan Li and Yu-Sun Ro, Atmospheric Environment, Vol. 34, 611-620, 2000.

46 T. Letzel, E. Rosenberg, R. Wissiack, M. Grasserbauer, and R. Niessner, Journal of Chromatography A, Vol. 855, 501-514, 1999.

47 Glenn S. Frysinger and Richard B. Gaines, Journal of High Resolution Chromatography, Vol. 22, No. 5, 2511-255, 1999.

48 Russell M. Kinghorn and Phillip J. Marriott, Journal of High Resolution Chromatography, Vol. 21, 32-38, January, 1998.

49 Phillip Marriott and Russell Kinghorn, Journal of Chromatography A, Vol. 866, 203-212, 2000.

50 Phillip Marriott and Russell Kinghorn, Analytical Chemistry, Vol. 69, 2582-2588, 1997.

51 K. Akiyama, Chromatographia Supplement, Vol. 53, S340-S344, 2001.

52 Stephen A. Wise, Laurence R. Hilpert, Gary D. Byrd, and Willie E. May, Polycyclic Aromatic Hydrocarbons, Vol. 1, No. 1&2, 81-98,1990.

53 Grant W. Kelly, Keith D. Bartle, Anthony A. Clifford, and Danny Scammells, Journal of Chromatographic Science, Vol. 31, 73-76, March, 1993.

54 Tuulia Hyotylainen and Marja-Liisa Riekkola, Journal of Chromatography A, Vol. 819, 13-24, 1998.

55 Jan Blomberg, Paul C. de Groot, Henk C.A. Brandt, Jan J.B. van der Does, and Peter J. Schoenmakers, Journal of Chromatography A, Vol. 849, 483-494, 1999.

56 A. Trisciani, and F. Munari, Journal of High Resolution Chromatography, Vol. 17, 452-456, June, 1994.

57 Tao Jiang and Yafeng Guan, Journal of Chromatographic Science, Vol. 37, 255-262, July, 1999.

58 Robert Pal, Miklos Juhasz, and Arpad Stumpf, Journal of Chromatography A, Vol. 819, 249-257, 1998.

59 R. Fuoco, A. Ceccarini, M. Onor, and L. Marrara, Journal of Chrmatography A, Vol. 846, 387-393, 1999.

60 Stephen A. Wise, Angela Diessler, and Lane C. Sander, Polycyclic Aromatic Hydrocarbons, Vol. 3, 169-184. 1993.

61 Winston K. Robbins, Journal of Chromatographic Science, Vol. 36, 457-466, September, 1998.

62 Willie E. May and Stephen A. Wise, Analytical Chemistry, Vol. 56, No. 2, February, 225-231, 1984.

63 Thomas V. Alfredson, Journal of Chromatography, Vol. 218, 715-728, 715-728.

64 A. Kurganov, K.K. Unger, and F. Eisenbeib, Chromatographia, Vol. 39, No. 3/4, 175-179, August, 1994.

65 W.J. Sonnefeld, W.H. Zoller, W.E> May, and, S.A. Wise, Analytical Chemistry, Vol. 54, 723-727, 1982.

66 Milan Popl, Vladimir Dolansky, and Jiri Mostecky, Journal of Chromatography, Vol. 117, 117-127, 1976.

67 Q.H. Wan, L. Ramaley, and R. Guy, Chromatographia, Vol. 48, No. 7/8, 523-528, 1998.

68 A.P. Kohne, U. Dornberger, and T. Welsch, Chromatographia, Vol. 48, No. 1/2, 9-16, July, 1998.

69 S. A. Wise, S. N. Chesler, H. S. Hertz, L. R. Hilpert, and W. E. May, Analytical Chemistry Vol. 49, No. 14, December, 2306-2309, 1977.

70 Mieczyslaw M. Boduszynski, Robert J. Hurtubise, Todd W. Allen, and Howard F. Silver, Analytical Chemistry, Vol. 55, 225-231, 1983.

71 U. Pyell, S. Schober, and G. Stork, Fresenius Journal of Analytical Chemistry, Vol. 359, 538-541, 1997.

72 U. Pyell and G. Stork, Fresenius Journal of Analytical Chemistry, Vol. 342, 376-380, 1992.

73 Jan Chmielowwiec, Albert E. George, Analytical Chemistry, Vol. 52, No. 7, 1154-1157, 1980.

74 K. Jinno, T. Nagoshi, N. Tanaka, M. Okamoto, J. C. Fetzer, and W. C. Biggs, Journal of Chromatography, Vol. 392 75-82, 1987.

75 W. Holstein, Chromatographia, Vol. 14, No. 8, 468-477, 1981.

76 Lane Sander and Stephen A. Wise, Analytical Chemistry, Vol. 67, 3284-3292, 1995.

77 Lane Sander and Stephen A. Wise, Analytical Chemistry, Vol. 61, 1749-1754, 1989.

78 Stephen A. Wise, Wendy J. Bonnett, Franklin R. Guenther, and Willie E. May, Journal of Chromatographic Science, Vol. 19, 457-465, September, 1981.

79 Stephen A. Wise and L.C. Sander, Journal of High resolution Chromatography & Chromatography Communications, Vol. 8, 248-255, May, 1985.

80 Mauri Makela and Lauri Pye, Journal of Chroamtography A, Vol. 699, 4-57, 1995.

81 J.C. Fetzer and W.R. Biggs, Journal of Chromatography, Vol. 322, 275-286, 1985.

82 Kiyokatsu Jinno, Shigeru Shimura, John C. Fetzer, and Wilton R. Biggs, Polycyclic Aromatic Hydrocarbons, Vol. 1, No. 3, 151-159, 1990.

83 Kiyotasu Jinno, Chisa Okumura, Mitsuyo Harada, Yoshihiro Saito, and Mitsuyoshi Okamoto, Journal of Liquid Chromatography and Related Technology, Vol. 19, No. 17&18, 2883-2899, 1996.

84 Gavin F. Shilstone, Mark W. Raynor, Keith D. Bartle, Anthony A. Clifford, Ilona L. Davies, and SAAD A. Jafar, Polycyclic Aromatic Hydrocarbons, Vol. 1, 99-108, 1990.

85 J. M. Levy and W. M. Ritchey, Journal of Chromatographic Science, Vol. 24, June, 242-248, 1986.

86 Rodger M. Smith, Journal of Chromatography A, Vol. 856, 83-115, 1999.

87 R. Holzhauser, Gilson Chromatography, Applications, Vol. 5, No. 3, 1-2.

88 Bruce E. Richter, Brian A. Jones, John L. Ezzell, Nathan L. Porter, Nebojsa Avdalovic, and Chris Pohl, Analytical Chemistry, Vol. 68, 1033-1039, 1996.

89 A. Venter, E.R. Rohwer, and A.E. Laubscher, Journal of Chromatography A, Vol. 847, 309-321, 1999.

90 Roger M. Smith, Orapin Chienthavorn, Nicholas Danks, and Ian D. Wilson, Journal of Chromatography A, Vol. 798, 203-206, 1998.

91 M. T. Combs, M. Ashraf-Khorassani, L. T. Taylor, and E. M. Fujinari, Analytical Chemistry, Vol. 69, 3044-3048, 1997.

92 Iulia M. Lazar, Milton L. Lee, and Edgar D. Lee, Analytical Chemistry, Vol. 68, 1924-1932, 1996.

93 J. David Pinkston and Thomas L. Chester, Analytical Chemistry, 650-656, November 1, 1995.

94 Patrick J. Arpino and J. Cousin, Rapid Communications in Mass Spectrometry, Vol. 1, No. 2, 28-32, 1987.

95 Darren Thomas, P. Greig Sim, Frank M. Benoit, Rapid Communications in Mass Spectrometry, Vol. 8, 105-110, 1994.

96 J. F. Anacleto, L. Ramaley, R. K. Boyd, S. Pleasance, M. A. Quilliam, P. G. Sim, and F. M. Benoit, Rapid Communications in Mass Spectrometry, Vol. 5, 149-155, 1991.

97 Sheryl A. Tucker, William E. Acree Jr., John C. Fetzer, and Jurgen Jacob, Polycyclic Aromatic Hydrocarbons, Vol. 3, 1-10, 1992.

98 J.R. Kershaw and J.C. Fetzer, Polycyclic Aromatic Hydrocarbons, Vol. 7, 253-268, 1995.

99 W.R. Biggs and J.C. Fetzer, Trends inn Analytical Chemistry, Vol. 15, No. 4, 196-206, 1996.

100 F. Morgan, Ph. Garrigues, M. Lamotte, annd J.C. Fetzer, Polycyclic Aromatic Hydrocarbons, Vol. 2, 141-153, 1991.

101 J. Rima, T.J. Rizk, P. Garrigues, and M. Lamotte, Polycyclic Aromatic Hydrocarbons, Vol. 1, No. 3, 161-169, 1990.

102 A.D. Campiglia, D.M. Hueber, and T. Vo-Dinh, Polycyclic Aromatic Compounds, Vol. 8, 117-128, 1996.

103 William E. Acree Jr., Sheryl A. Tucker, and John C. Fetzer, Polycyclic Aromatic Copounds, Vol. 2, 75-105, 1991.

104 N. Selvarajan, M.M. Panicker, S. Vaidyanathan, and V. Ramakrishnan, Indian Journal of Chemistry, Vol. 18A, 23-26, July, 1979.

105 A. G. Davidson, and O. E. Faridan, Analyst,Vol. 113, 533, 1988

106 J. C. Fetzer, Polycyclic Aromatic Compounds, Vol. 7, 269-274, 1995.

107 Robert M. Garrett, Chantal C. Guenette, Cooper E. Haith, and Rodger C. Prince, Environmental Science and Technology, Vol. 34, 1934-1937, 2000.

108 Zhendi Wang, Merv Fingas, Michael Landriault, Lise Sigouin, Bill Castle, David Hostetter, Dachung Zhang, and Brad Spencer, Journal of High Resolution Chromatography, Vol. 21, No. 7, 383-395, 1998.

109 Maria P. Elizalde-Gonzalez, Markus Hutlieb, and Kurt Hedden, Journal of High Resolution Chromatography, Vol. 19, 345-352, June, 1996.

110 Chang S. Hsu, M. A. McLean, K. Qian, T. Aczel, S. C. Blum, W. N. Olmstead, L. H. Kaplan. W. K. Robbins, and W. W. Schulz, Energy & Fuels, Vol. 5, 395-398, 1991.

111 Eric C. Huang, Timothy Wachs, James J. Conboy, and Jack D. Henion, Analytical Chemistry, Vol. 62 No. 13, July 1, 1990.

112 Joseph F. Anacleto, Louis Ramaley, Frank M. Beniot, Robert K. Boyd, and Michael A. Quilliam, Analytical Chemistry, Vol. 67, 4145-4154, 1995.

113 D.S. Millington, D.A. Yorke, and P. Burns, Advances in Mass Spectrometry, Vol. 8b, 1819-1825, 1980.

114 Daniel Waterman, Brian Horsfield, Franz Leistner, Keith Hall, and Steve Smith, Analytical Chemistry, Vol. 72, 3563-3567, 2000.

115 Ivan Viden and Vaclav Janda, Journal of High Resolution Chromatography, Vol. 20, March, 181-182, 1997.

116 Oliver P. Haefliger, Thomas D. Bucheli, and Renato Zenobi, Environmental Science and Technology, Vol. 34, 2184-2189, 2000.

117 Turlough F. Guerin, Journal of Environmental Monitoring and Assessment, Vol. 1, 63-67, 1999.

118 L. Morselli, L. Setti, A. Iannuccilli, S. Maly, G. Dinelli, and G. Quattroni, Journal of Chromatography A, Vol. 845, 357-363, 1999.

119 Mark D. Burford, Steven B. Hawthorne, and David J. Miller, Analytical Chemistry, Vol. 65, 1497-1505, 1993.

120 John J. Langenfeld, Steven B. Hawthorne, David J. Miller, and Janusz Pawliszyn, Analytical Chemistry, Vol. 66, 909-916, 1994.

121 John J. Langenfeld, Steven B. Hawthorne, David J. Miller, and Janusz Pawliszyn, Analytical Chemistry, Vol. 65, 338-344, 1993.

122 T.L. Chester, J.D. Pinkston, and D.E. Raynie, Analytical Chemistry, Vol. 70, 301R-319R, 1998.

123 Mark A. Stone and Larry T. Taylor, Analytical Chemistry, Vol. 72, 12268-1274, 2000.

124 David J. Miller, Steven B. Hawthorne, and Mary Ellen P. McNally, Analytical Chemistry, Vol. 65, 1038-1042, 1993.

125 Sarah L. Cresswell and Stephen J. Haswell, Analyst, Vol. 1224, 1361-1366, 1999.

126 John R. Dean, Analytical Communications, Vol. 33, June, 191-192, 1996.

127 Bruce E. Richter, Brian A. Jones, John L. Ezzell, Nathan L. Porter, Nebojsa Avdalovic, and Chris Pohl, Analytical Chemistry, Vol. 68, 1033-1039, 1996.

128 Katie M. Meney, Christine M. Davidson, David Littlejohn, Nichols J. Cotton, and Bernard Fields, Analytical Communications, Vol. 35, 173-175, June, 1998.

129 Michele M. Schantz, John C. Nicols, and Stephen A. Wise, Analytical Chemistry, Vol. 69, 4210-4219, 1997.

130 Colin F. Poole and Salwa K. Poole, Analytical Communications, Vol. 33, 11H-14H, July, 1996.

131 Erland Bjorklund, Tobias Nilsson, and Soren Bowadt, Trends in Analytical Chemistry, Vol. 19, No. 5, 434-445, 2000.

132 Dawit Z. Bezabeh, Todd M. Allen, Eileen M. McCauley, Peter B. Kelly, and A. Daniel Jones, Journal of the American Society for Mass Spectrometry, Vol. 8, 630-636, 1997.

133 Marco Vincenti, Claudio Minero, Ezio Pelizzetti, Marco Fontana, and Roberta De Maria, Journal of the American Society for Mass Spectrometry, Vol. 7, 1255-1265, 1996.

134 Sophie Nicole, Jose Dugay, and Marie-Claire Hennion, Journal of Separation Science, Vol. 24, 451-458, 2001.

135 Marwan Dimashki, Stuart Harrad, and Roy M. Harrison, Atmospheric Environment, Vol. 34, 2459-2469, 2000.

136 W.A. Korfmacher, L.G. Rushing, J. Arey, B. Zielinski, and J.N. Pitts Jr., Journal of High Resolution Chromatography & Chromatography Communications, Vol. 10, 641-647, Decemberr, 1987.

137 Xu Jinhui and Frank S.C. Lee, Chemosphere, Vol. 42, 245-250, 2001.

138 .Xu Jinhui and Frank S.C. Lee, Analytica Chimica Acta, Vol. 416, 111-115, 2000

139 Josef Cvacka, Jiri Barek, Arnold G. Fogg, Josino C. Moreira, and Jiri Zima, Analyst, Vol. 123, 9R-18R, 1998.

140 E. Veigl, W. Posh, W. Linder, P. Tritthart, Chromatographia, Vol. 38, No. 3/4, February, 199-206,1994.

141 Tsuyoshi Murahashi and Kazuichi Hayakawa, Analytica Chimica Acta, Vol. 343, 251-257, 1997.

142 Kaoru Hanaya, Takashi Muramatsu, Hideaki Kudo, Yuan L. Chow, Journal of the American Chemical Society, 2409-2410, 1979.

143 G. William Chase Jr. and Brian Thompson, Journal of AOAC International, Vol. 83, No. 2, 407-410, 2000.

144 Lloyd A. Kaplan, Communications to the Editor, Vol. 50, 740-741, 1964.

145 Hang Li, Roger Westerholm, Journal of Chromatography A, Vol. 664, 177-182, 1994.

146 Kenneth W. Sigvardson and John W. Birks, Journal of Chromatography, Vol. 316, 507-518, 1984.

147 L. Bonfanti, M. Careri, A. Mangia, P. Manini, and M. Maspero, Journal of Chromatography A, Vol. 728, 359-369, 1996.

148 Tamika T. J. Williams and H. Perreault, Rapid Communications in Mass Spectrometry, Vol. 14, 1474-1481, 2000.

149 L. Nondek, Journal of Chromatography, Vol. 373, No. 1, 61-80, 1986.

150 Akira Nomura, Joseph Yamada, Takaghi Yarita, Tsuneaki Maeda, Journal of Supercritical Fluids, Vol. 8, No. 4, 329-333, 1995.

151 Turlough F. Guerin, Journal of Environmental Monitoring, Vol. 1, No. 1, 63-67, 1999.

152 Louis Ramaley and J. Larry Campbell, Instrumentation Science and Technology, Vol. 28, No. 3, 189-204, 2000.

153 Kathleen Duggan, The Analysis of Particulate and Vapor Phase Polycyclic Aromatic Hydrocarbons In Atmospheric Samples Using Liquid Chromatography With Fluorescence Detection and Gas Chromatography With Mass Spectrometric Detection, MSc. Thesis, Dalhousie University, 2001.

154 Genvieve Mercier, The use of Supercritical Fluid Chromatography Coupled with Mass Spectrometry and Gas Chromatography for the Analysis of Polycyclic Aromatic Hydrocarbons, MSc. Thesis, Dalhousie University, 2001.